UNIVERSITE BRETAGNE LOIRE

Politechnika Łódzka

UNIVERSITÉ DE NANTES

Thèse de Doctorat

Katarzyna M. ROMEK

Mémoire présenté en vue de l'obtention du
grade de Docteur de l'Université de Nantes
sous le sceau de l'Université Bretagne Loire
grade de Docteur de Lodz University of Technology

École doctorale : *« 3MPL Matière, Molécules, Matériaux en Pays de la Loire »*

Discipline : *Chimie*
Spécialité : *Chimie analytique*
Unité de recherche : *CEISAM; Université de Nantes*
Unité de recherche : *Institute of Applied Radiation Chemistry ; Lodz University of Technology*
Soutenue le *09 Decembre 2016*
Thèse N° :

Studies of isotopic fractionation of ^{13}C during biosynthesis and enzymatic reactions

JURY

Président :	**Gérald REMAUD**, Professeur, Université de Nantes
Rapporteurs :	**Jaleh GHASHGAIE**, Professeur, Université de Paris XI **Roland WERNER**, Ingénieur de Recherche, ETH Zurich
Examinateurs :	**Michael DE WAARD,** Directeur de Recherche, Université de Nantes **Agnieszka DYBAŁA-DEFRATYKA,** Dr. hab**,** Lodz University of Technology **Małgorzata SZYNKOWSKA,** Proffeseur, Lodz University of Technology **Beata KOLESIŃSKA,** Dr. hab**,** Lodz University of Technology
Directeur de Thèse :	**Richard ROBINS**, Directeur de Recherche, Université de Nantes
Co-Directeur de Thèse :	**Piotr PANETH**, Proffeseur, Lodz University of Technology
Co-encadrant de Thèse :	**Pierrick NUN**, Maître de Conférences, Université de Nantes

Acknowledgments

This work has been carried out in two teams – the EBSI (Elucidation of Biosynthesis by Isotopic Spectrometries) group of the CEISAM (Chemistry and Interdisciplinarity: Synthesis, Analysis and Modelling) laboratory (University of Nantes, France) and the LIES (Laboratory of Isotope Effects Studies) group in the Chemistry Department (Lodz University of Technology, Poland).

I thank the French embassy in Warsaw for a Bursary from the French Government that partially financed this thesis studies.

I would like to warmly thank my supervisor Dr Richard J. Robins, first for his patience and an ocean of support through all the years that I have had the pleasure to work with him, secondly for his substantive and moral feedback at every level and last but not least for his great sense of humour and belief in me.

I would like to express my appreciation to my supervisor Prof Piotr Paneth for giving me the opportunity of working on the computational chemistry field and broaden my horizons.

I would also thank to my co-supervisor Dr Pierrick Nun for being there when the chemistry get complicated.

A huge thank-you goes to Virginie Silvestre, who spent numerous hours on giving me training on irm^{13}C-NMR and her valuable advices. Also to Benoit Charrier for making sure that I knew how not to break the spectrometers!

I would like to thank to Prof Gérald Remaud for his precious comments on my work and his help with interpretation of the results, as well as to Serge Akoka, who made NMR understandable.

For keeping irm-EA/MS measurements enjoyable I want to thank Mathilde Grand, Anne-Marie Schiphorst and Ingrid Antheaume.

Great thanks to Denis Loquet for help with the GC and HPLC analyses.

To the EBSI team (whose composition was changing within the time) – thank you for your constant support through all the years and putting up with my temper. Special thanks to Dr Maxime Julien who always had time for discussion, either scientific or not, and never refused his help. To Dr MBaye Diaw Dioum who, on rainy days always managed to bring a smile with him and cheer me up. To Dr Rémi Vanel for finding solutions when thought that the light at the end of the tunnel had already gone. To Laetitia Rouger for her kindness and feminine touch in the team. To Boris Gouilleux for having 'sharp' jokes exchange. To Valentin Joubert for the peaceful atmosphere at the office when it was needed and great Saturday nights parties. To Tangi Jezequel for coping with my bad temper.

I would like to thank to Dr Kathy Chen who was always having good and positive vibrations that kept me in a positive thinking mode, especially during the past few months before my defence.

To the LIES team – thank you for taking me under your theoreticians' wings and making the impossible – possible. Special thanks to Agnieszka Krzemińska-Kowalska without whom theoretical calculations will still be in the area of the dark arts, who spent numerous days on explanations and was the best companion for life outside the laboratory. To Dr Agnieszka Dybała-Defratyka for her comments and support. To Dr Anna Grzybkowska who always had the time to help me along.

For her huge support (day and night) I would like to thank Roxana Vasilescu, who always knew how and when to scold me over a few glasses at Chateaulain Wednesdays.

The list of people who were standing by my side and to whom I am very grateful for their presence is possibly longer than this dissertation, so I would like to say thank you to all the members of CEISAM laboratory for making this place friendly, safe and almost like home. I would also like to thank to all of the people who never had anything to do with chemistry and they still are my friends and whom support I felt through thick and thin.

Last but not least I want to thank my entire family for their constant support, optimism and enormous dose of patience during my thesis.

For keeping me calm and sane as well as supporting me on my way I want to thank to Antoine Mazel.

Table of contents

Terms and Definitions

Isotopes are variants of a particular chemical element which differ in neutron number, although all isotopes of a given element have the same number of protons and electrons in each atom.

Isotopic fractionation is the selection of one isotopologue versus another during a physical or (bio)chemical process which leads to a non-statistical distribution of isotopes in the population of isotopologues within the final product and the residual substrate.

Isotopologues are molecules that differ only in their isotopic composition. Simply, the isotopologue of a chemical species has at least one atom with a different number of neutrons than the parent.

Isotopomers are isotopologues having the same number of each isotope of each element but differing in their positions.

Global carbon isotope ratio for a target molecule, $\delta^{13}C_g$ (‰) is calculated from:

$$\delta^{13}C_g(‰) = \left(\left(\frac{R_s}{R_{V-PDB}}\right) - 1\right) \cdot 1000$$

where the value of $R_{V\text{-}PDB}$ is 0.0111802. Since the V-PDB standard possess a relatively high ^{13}C content, most samples coming from biomass have negative $\delta^{13}C$ values.

The position-specific-carbon isotope ratio for a target molecule $\delta^{13}C_g$ (‰) is calculated from:

$$\delta^{13}C_i = \left(\left(\frac{R_i}{R_{V-PDB}}\right) - 1\right) \cdot 1000$$

(See section 2.1.3. for details).

Abbreviations

abbreviation	*explanation*
Acetyl-CoA	Acetyl coenzyme A
AdoHcy	*S*-Adenosyl-L-homoserine
AdoMet	*S*-Adenosyl-L-methionine
AMBER FF	Assisted Model Building with Energy Refinement Force Field
Arg	Arginine
Asp	Aspartic acid
ATP	Adenosine triphosphate
CAM	Crassulacean acid metabolism
Cr(acac)$_3$	chromium (III) acetyloacetonate
^{13}C EIE	Equilibrium isotope effect in carbon isotope fractionation
^{13}C KIE	Kinetic isotope effect in carbon isotope fractionation
COMT	Catechol-*O*-methyl transferase
DFT	Density Functional Theory
DHAP	Dihydroxyacetone phosphate
DMSO	Dimethyl sulfoxide
EA	Elemental analyser
EC	Enzyme code
EIE	Thermodynamic ('equilibrium') isotope effect
GC	Gas chromatography
Glu	Glutamate
G3P	Glyceraldehyde-3-phosphate
Hcy	L-Homocysteine
Homo-Ser	homoserine
IRC	Intrinsic Reaction Coordinate
irm	Isotope ratio monitoring
irm-NMR	Isotope ratio monitoring by nuclear magnetic resonance
Jr	Coupling constant
KIE	Non-equilibrium ('kinetic') isotope effect
MD	Molecular dynamics
Met	L-Methionine
MLEV	Composite pulse sequence
MS	Mass spectrometry
Mtases	Methyl transferases
NAMD	Nanoscale Molecular Dynamics
NOE	Nuclear Overhauser Effect
NVT	Canonical ensemble; N – amount of substance, V – volume, T - temperature
OPH	*O*-Phosphohomoserine
Orn	Ornithine
PCR	Polymerase chain reaction
PDH	Pyruvate dehydrogenase
PEP	Phospho*enol*pyruvate
PEPc	Phospho*enol*pyruvate carboxylase (EC 4.1.1.31)

pK	Acid dissociation constant
PLP	Pyridoxal phosphate
PM3	Semi-empirical calculation using the PM3 Hamiltonian
PM6	Semi-empirical calculation using the PM6 Hamiltonian
Pi	Orthophosphate
PPi	Pyrophosphate
Pro	Proline
QM/MM	Quantum mechanics/molecular mechanics
RCSB PDB	Research Collaboratory for Structural Bioinformatics Protein Data Bank
RF	Resonance frequency
RMSD	Root-mean-square deviation of atomic positions
RuBisCO	Ribulose bisphosphate carboxylase-oxygenase (EC 4.1.1.39)
S/N	Signal-to-Noise ratio
THF	Tetrahydrofolate
TMSCl	trimethyl chlorosilane
Trp	Tryptophan
WALTZ	Pulse sequence

1 Chapter I - Objectives of the Study and Summary of the Results

1.1 Objectives

To investigate the causes of intramolecular isotopic fractionation in a range of specialised plant products.

1) The particular interest has been focused on understanding intramolecular isotope fractionation in L-methionine metabolism in relation to its role as a methyl group donor. The hypothesis that was put forward is that isotope depletion in the *S*-methyl group occurs during methionine biosynthesis and is thus conserved in all compounds that contain Met-derived methyl groups.

2) To evaluate the extent to which intramolecular isotopic variation can be related to biochemical pathways of specialized product formation. In particular, to probe the use of observed intramolecular isotopic fractionation to predict unknown pathways of specialised products.

1.2 Methods

The principal method that has been used to collect the data was isotopic ratio monitoring by nuclear magnetic resonance spectrometry. This also required back-up with isotopic ratio monitoring by mass spectrometry. Both methods required specific sample treatment to adjust the molecular properties to the analytical procedure.

1.3 Results

1) The development and exploitation of a general protocol for determining the intramolecular distribution of ^{13}C in amino acids was achieved. Using this, it was possible to deduce aspects of intramolecular isotope fractionation during amino acid biosynthesis.

2) Evidence was obtained by irm-^{13}C NMR that the *S*-methyl group of methionine is strongly depleted in ^{13}C relative to the rest of the molecule, by about 20‰.

3) By conducting theoretical calculations to obtain the probable reaction mechanism of the enzyme methionine synthase (cobalamin-independent) it was shown that fractionation against ^{13}C during the transfer of Me from Me-THF to L-homocysteine occurs.

4) Measurements of the intramolecular isotope fractionation in the biosynthetically-related alkaloids nicotine and tropine indicated common isotope fractionation in the common steps and different fractionation in the unique steps. It also allowed deductions as to the interpretation of data for their known and unknown biochemistry.

5) Measurements of the intramolecular isotope fractionation in the newly-discovered alkaloid tramadol made possible the prediction of a possible biochemistry biosynthetic pathway based on the interpretation of this fractionation.

1.4 Conclusions

Intramolecular isotope fractionation can give insight into metabolic pathways and common features of metabolism can be described. The overall project also showed that hints as to probable biochemistry can be obtained by interpreting observed intramolecular isotope fractionation in relation to known isotope effects.

2 Chapter II - Introduction

2.1 Isotopic fractionation in natural products

2.1.1 Definition and occurrence of isotopes

Isotopes are the different forms of the same element with the same atomic number that vary only in the number of neutrons, which causes the differences in the molecular mass. We can distinguish two main groups: stable and radioactive. In nature, carbon possess three isotopes, two stable – ^{12}C and ^{13}C – and one radioactive – ^{14}C, which is widely used for radiocarbon dating of the fossils. Carbon also has a number of un-natural short-lived isotopes of which ^{11}C is the longest living ($T_{½}$ ~20 min). For hydrogen there are also two stable isotopes – ^{1}H and ^{2}H (deuterium) and one radioactive – ^{3}H (tritium). Each element of the periodic table consists of at least one isotope, but some elements (e.g. phosphorous) exist as only one isotope (^{31}P) in nature. Due to their nature (identical chemical properties) they cannot be separated by chemical methods but it is possible to make a distinction between individual isotopes through mass separation.

Main building blocks of natural products contain in their structures H, C, N, O, S, which all have at least one stable heavy isotope, and P which is monoisotopic. In all cases, the stable isotope exists at low abundance relative to the lighter one. In these elements, the range is between ~0.02% for ^{2}H and ~4.25% for ^{34}S.[1]

The isotopic content of the heavy and light isotope of the same element is expressed as *R* and is defined by the equation below:

$$R = \frac{heavy}{light} \qquad \textit{Equation 1.}$$

The isotopic abundance, *A*, is a molar fraction of the element with its heavy isotope added and is defined by:

$$A = \frac{heavy}{heavy + light} \qquad \textit{Equation 2.}$$

2.1.2 Definition and causes of isotopic fractionation

Isotope fractionation is the degree of selection of one isotope for another and, in the example of carbon, causes variation in the $^{13}C/^{12}C$ ratios. Isotopic fractionation occurs most prevalently in open systems under natural conditions. Overall, biological systems can be described as open and irreversible. Defined unidirectional processes and reactions are the basis of irreversibility. Hence, isotopic fractionation can substantially contribute to the formation of isotopic patterns and the degree of variation will reflect the processes involved. It takes an incomplete or branched substrate conversion to cause an isotope discrimination *in vivo*. To maintain an isotop-

[1] E. Roth, '*Critical evaluation of the use and analysis of stable isotopes*', Pure and Applied Chemistry, 69, (1997), 1753-1828

ic balance, the isotope shifts in the products need to be mutually counteractive, i.e. to be opposed and to be in relation to their chemical yields. However, isotope discrimination *in vivo* will not be manifest by a non-branched and quantitative process, despite the fact that the reaction by which the process is carried out (e.g. an enzyme), may indicate *in vitro* isotope effects.

The most common classification of isotope effects is division into kinetic or thermodynamic but the real distinction begins between non-equilibrium (KIE) and equilibrium (EIE) situations. The balance of two kinetic effects at chemical equilibrium is represented by thermodynamic effects, which are generally smaller than individual kinetic effects. Unequal distribution of isotope species among phases in a system is the best example of a thermodynamic effect. Thermodynamic and kinetic isotope effects are temperature dependent.[2]

^{13}C KIEs are expressed during the formation and fission of bonds that involve a carbon atom. Other processes such as diffusion or volatilisation are also affected by mass. As an example of a non-reactional kinetic effect the difference between the binary diffusivity of $^{13}CO_2$ and that of $^{12}CO_2$ in air can be given. This has a major impact on the $^{13}C/^{12}C$ ratio of natural metabolites from different plant species. As an example of a reaction-related kinetic effect, the difference between the kinetic constants for the reaction of $^{12}CO_2$ and $^{13}CO_2$ with ribulose bisphosphate carboxylase-oxygenase (RuBisCO, EC 4.1.1.39) can be cited.[3] Both of these processes under-privilege the heavier isotope, and therefore show so called 'normal' kinetic isotope effects. The impact of this on the $^{13}C/^{12}C$ ratios of plant metabolites will be developed in section 2.1.4.

There are several different mechanisms with different inherent KIEs[3] through which hydrogen atom transfers can occur. This is manifest in such situations as the typical alternating ^{2}H depletion of fatty acids[4]. For carbon, a similar alternating ^{13}C patterns was deduced from partial degradation.[5] This appears to be caused by the KIE of the pyruvate dehydrogenase (PDH, EC 1.8.1.4)[6] reaction and is consistent with the bulk relative ^{13}C depletion of fatty acids. This observed variations in the CH_2-chains of alternating hydrogen and carbon isotope patterns are inconsistent with a thermodynamic order. Similarly, in specialised metabolites such as terpenes[7]

---

[2] G. D. Farquhar *et al.*, '*Carbon Isotope Fractionation and Plant Water-Use Efficiency*', Stable Isotopes in Ecological Research, (Springer New York, 1989), pp. 21–40

[3] H-L. Schmidt *et al.* , '*Systematics of ^{2}H Patterns in Natural Compounds and Its Importance for the Elucidation of Biosynthetic Pathways*', Phytochemistry Reviews, 2.1–2 (2003), 61–85

[4] I. Billault *et al.*, '*Natural Deuterium Distribution in Long-Chain Fatty Acids Is Nonstatistical: A Site-Specific Study by Quantitative ^{2}H NMR Spectroscopy*', ChemBioChem, 2.6 (2001), 425–31.

[5] K. D. Monson and J. M. Hayes, '*Carbon Isotopic Fractionation in the Biosynthesis of Bacterial Fatty Acids. Ozonolysis of Unsaturated Fatty Acids as a Means of Determining the Intramolecular Distribution of Carbon Isotopes*', Geochimica et Cosmochimica Acta, 46.2 (1982), 139–49 ; K. D. Monson and J. M. Hayes, '*Biosynthetic Control of the Natural Abundance of Carbon 13 at Specific Positions within Fatty Acids in Escherichia Coli. Evidence Regarding the Coupling of Fatty Acid and Phospholipid Synthesis*.', Journal of Biological Chemistry, 255.23 (1980), 11435–41.

[6] E. Melzer and H-L. Schmidt, '*Carbon Isotope Effects on the Decarboxylation of Carboxylic Acids. Comparison of the Lactate Oxidase Reaction and the Degradation of Pyruvate by H_2O_2*', The Biochemical Journal, 252.3 (1988), 913–15.

[7] G. J. Martin *et al.*, '*The Fellowship of Natural Abundance ^{2}H-Isotopomers of Monoterpenes*', Phytochemistry, 65.20 (2004), 2815–31; S. M. Gerdov and others, '*Quantitative ^{2}H NMR Spectroscopy 2. "H/D-Isotope Portraits" of Cyclic Monoterpenes and Discrimination of Their Biosynthetic Pathways*', Russian Chemical Bulletin, 54.5 (2005), 1258–65.

and phenylpropanoids,[8] pathway-dependent ^{2}H and ^{13}C patterns are observed, yet thermodynamic considerations require for these pathways of synthesis an absolute independence of isotopic patterns. Reaction mechanisms and KIEs are thus combining to create a reproducible and potentially predictable 'order' in metabolism.

The *in vivo* impact of KIEs is highly dependent on pool sizes and actual metabolic conditions. Water, atmospheric O_2 and CO_2 (extrinsic pools) are the infinite sources of primary precursors and precondition for constant and maximum isotope discrimination. On the other hand, NADPH and intermediates (intrinsic pools) are finite and variable and their metabolism may well lead to relatively limited or variable isotope discriminations.

Overall, then, the final isotope content and pattern is the sum of the contribution of the unidirectional secondary processes, while metabolite isotopic patterns of 'transient' molecules (intermediates) are often preserved in 'permanent' (sink) products. The result of the existence of alternative pathways can lead to different patterns of the same product. A parallel relative depletion of the heavy isotopes for carbon and hydrogen is not necessarily observed in metabolic steps or chains. This effect occurs only occasionally, because the involved reactions and kinetic isotope effects strongly differ from each other.

Extrinsic (pools of primary precursors, temperature, and pressure) and intrinsic factors (metabolite pools, alternative pathways, turnover rates) are modulating the *in vivo* effectiveness of thermodynamic and kinetic isotope effects on enzyme-catalysed reactions (expressed as isotope discrimination). The assignment of alternative/competing biochemical pathways can be achieved through a proper understanding of the *in vivo* isotope discrimination and application of this knowledge to the intrinsic and extrinsic conditions of biosynthetic origin of natural products.[9] In the enzyme-catalysed reactions involved in metabolism, the KIEs can only manifest themselves as an isotopic fractionation (*in vivo*) in cases of incomplete substrate conversion. Thus, when the substrate is converted into two or more products by metabolic branching [10] then the substrate can become enriched or depleted in the heavier isotopomer by a dominant branching route: as a result, the isotopic shifts values are inverted in the other branch, as required to maintain an isotopic balance.

As already noted, the primary pools of basic precursors for biological molecules - atmospheric CO_2 and O_2 and oceanic water - can be considered as infinite. To take as an example atmospheric CO_2, the starting material for photosynthesis, its isotopic characteristic can be taken as constant (but see 2.1.5.1). The majority of carbon in the atmosphere and living organisms is ^{12}C (98.9%) with 1.1% of ^{13}C isotope. Since the isotopic distribution within different compounds

---

[8] H-L. Schmidt *et al.*, '*The Prediction of Isotopic Patterns in Phenylpropanoids from Their Precursors and the Mechanism of the NIH-Shift: Basis of the Isotopic Characteristics of Natural Aromatic Compounds*', Phytochemistry, 67.11 (2006), 1094–1103

[9] H-L. Schmidt, '*Fundamentals and Systematics of the Non-Statistical Distributions of Isotopes in Natural Compounds*', Naturwissenschaften, 90.12 (2003), 537–52

[10] J. M. Hayes, *'Isotopic Order, Biogeochemical Processes, and Earth History: Goldschmidt Lecture, Davos, Switzerland, August 2002*', Geochimica et Cosmochimica Acta, 68.8 (2004), 1691–1700; J. M. Hayes, '*Fractionation of Carbon and Hydrogen Isotopes in Biosynthetic Processes*', Reviews in Mineralogy and Geochemistry, 43.1 (2001), 225–77; H. L. Schmidt and H. Kexel, '*Metabolite Pools and Metabolic Branching as Factors of in-Vivo Isotope Discriminations by Kinetic Isotope Effects*', Isotopes in Environmental and Health Studies, 33.1–2 (1997), 19–30.

is non-statistical, fractionation can give data about all the processes that are involved into carbon transformations. The overall abundance of ^{13}C in atmospheric carbon dioxide is greater than in plant tissues, which gives an indication that carbon isotope discrimination occurs in the incorporation of CO_2 into plant biomass. This has been amply proven and countless attempts of understanding the carbon isotope discrimination have been made since this area was extensively studied by O'Leary:[11] this will be developed below. Due to the stability of isotopes, the inherent information in the ratios of carbon isotopes (presented by convention as $^{13}C/^{12}C$) is constant as long as carbon is not lost.

Oceanic water is the largest primary pool for forming 'organic' hydrogen and oxygen. A small amount of O is introduced by oxygenases that introduce O from O_2. The isotope ratios are defined by the international reference standard mean ocean water – V-SMOW.[12] All terrestrial water pools such as lakes; rivers and the ice of glaciers originate as clouds from the sea. Isotopic fractionation accompanies all the phase transitions in the water cycle and it does not necessary always leads to isotopic equilibrium, which depends on temperature and pressure. Depletion of heavy water isotopologues in the vapour above the sea is a result of evaporation. Relative ^{2}H and ^{18}O enrichment of precipitated water causes a further depletion of heavy isotopes in the remaining vapour is caused by condensation. The continental effect defines the last rain, which is falling far away from the sea, as the 'lightest' one. Influences of altitude, temperature and amount are superimposed on this general scheme. Geographical origin of meteoric water is the reason of its isotopic composition. The 'Meteoric water line' indicates the correlation between the values of the $\delta^{2}H$ and $\delta^{18}O$ of precipitation water from the same geographical origin.[13] The source water is taken up by the plants and as a result of transpiration, enrich again in heavy isotopes. Plant intrinsic parameters are dominating the correlation of the ^{2}H and ^{18}O enrichment, which is different than that for meteoric water. Thus, the biosynthesis of organic matter[14] should be correlated with the 'supply' of plant leaf water, which is enriched in ^{2}H and ^{18}O, since this serves as the primary source of any hydrogen and most oxygen. Several processes that impact on the composition of the cell water of animals can be identified, such as oxidation of nicotinamide adenine dinucleotide or reduced form (NADH) in the respiratory chain.[15] It also should be underlined that the biggest impact is caused by the local drinking water, oxygen and hydrogen atoms are related to dietary habits. Isotopic fractionation occurs through evaporation via sweat and exhalation of CO_2 in the breath (largely enriched in ^{18}O in relation to water).[16] It has been

[11] M. H. O'Leary, *'Carbon Isotope Fractionation in Plants*', Phytochemistry, 20.4 (1981), 553–67.
[12] R. Gonfiantini *et al., 'Standards and intercomparison materials for stable isotopes of light elements'*, vol. IAEA-Techdoc-825 (pp. 159), (1995). Vienna: IAEA.
[13] H. Craig, '*Isotopic Variations in Meteoric Waters*', Science, 133.3465 (1961), 1702–3
[14] J. W. C. White, '*Stable Hydrogen Isotope Ratios in Plants: A Review of Current Theory and Some Potential Applications', in Stable Isotopes in Ecological Research*, ed. by P. W. Rundel, J. R. Ehleringer, and K. A. Nagy, Ecological Studies, 68 (Springer New York, 1989), pp. 142–62; M. M. Barbour, '*Stable Oxygen Isotope Composition of Plant Tissue: A Review*', Functional Plant Biology, 34.2 (2007), 83.
[15] M. J. Kohn, '*Predicting Animal $\delta^{18}O$: Accounting for Diet and Physiological Adaptation*', Geochimica et Cosmochimica Acta, 60.23 (1996), 4811–29; D. W. Podlesak *et al.*, '*$\delta^{2}H$ and $\delta^{18}O$ of Human Body Water: A GIS Model to Distinguish Residents from Non-Residents in the Contiguous USA*', Isotopes in Environmental and Health Studies, 48.2 (2012), 259–79.
[16] N. Krivachy *et al.*, '*Potentials and Caveats with Oxygen and Sulfur Stable Isotope Analyses in Authenticity and Origin Checks of Food and Food Commodities*', Food Control, Recent Advances of Food Analysis, 48 (2015), 143–50 .

observed in microorganisms that the intracellular water can temporarily originate predominantly from metabolism[17], indicating that bulk water may not represent water available for cellular use.

In summary, isotope discriminations coupled with irreversible or unidirectional processes permit kinetic isotope effects to come into play and this leads to isotopic fractionation. When the isotope shifts in the products are following an isotopic balance (e.g. incomplete turnover or metabolic branching events) kinetic isotope effects linked with them can become effective *in vivo*. Variations in isotope distributions occur as a consequence of changes in metabolic fluxes. If from a common precursor pool, several reactions are competing with each other, as a result none of them achieve *in vivo* isotope discrimination, irrespective of their *in vitro* kinetic isotope effects. Taking into account the overall contribution of the kinetic isotope effects to the formation of sink products isotope patterns, major significance should be credited to flavoprotein-catalysed hydrogen transfers for hydrogen, to the pyruvate dehydrogenase reaction for carbon, the GOGAT reaction for nitrogen, and to monooxygenase reactions for oxygen, since these key reactions have been identified as having an important role in regulating isotopic distribution in general metabolism.

2.1.3 Expressing Isotopic fractionation

Isotopic abundance in the environment, then, can vary dependent on isotopic fractionation which occurs during physicochemical and/or enzymatic processes. Isotopic fractionation can be expressed in a number of ways.

The isotopic fractionation (α) can be defined in the most general sense as the enrichment in one isotope of a given sample relative to another sample. Frequently, these samples are related by a defined process which is affecting the relative abundance of isotopes. Then:

$$\alpha = \frac{R_{substrate}}{R_{product}} \qquad \textit{Equation 3.}$$

where $R_{substrate}$ and $R_{product}$ are the isotopic contents of starting material and final product, respectively. These may be directly linked, such as the substrate and product of an enzyme, or distal, such as the starting point of a pathway (e.g. glucose) and an end product (e.g. ethanol). To give a specific example: an α factor has been defined as the quotient of the isotope ratios of the source R_{CO2} relative to that of the product R_{Leaf}. Since $R_{substrate}$ is usually enriched relative to $R_{product}$, this relationship gives positive values of isotopic fractionation between these pools.

The apparent or total isotope discrimination Δ (for carbon, $\Delta^{13}C$) is defined as its deviation from unity[18], because in practice the dried whole leaf plant matter is analysed in the laboratory:

[17] H. W. Kreuzer-Martin *et al.*, '*Oxygen Isotopes Indicate Most Intracellular Water in Log-Phase Escherichia Coli Is Derived from Metabolism*', Proceedings of the National Academy of Sciences of the United States of America, 102.48 (2005), 17337–41.

[18] G. D. Farquhar and J. Lloyd, '*Carbon and Oxygen Isotope Effects in the Exchange of Carbon Dioxide between Terrestrial Plants and the Atmosphere*', Stable Isotopes and Plant Carbon-Water Relations (Elsevier, 1993), pp. 47–70.

$$\Delta^{13}C = \alpha - 1 = \frac{R_{CO_2}}{R_{Leaf}} - 1 \qquad \textit{Equation 4.}$$

If we take the correlations of R to the corresponding δ values ($\delta^{13}C_{Sample}=R_{Sample}/R_{V\text{-}PDB}-1$) and establish that the equation is independent from $R_{V\text{-}PDB}$ with $\delta^{13}C_{Leaf} << 1$, the equation will take the form presented below:

$$\Delta^{13}C = \frac{(\delta^{13}C_{CO_2} - {}^{13}C_{Leaf})}{(1 - {}^{13}C_{Leaf})} \cong (\delta^{13}C_{CO_2} - {}^{13}C_{Leaf}) \qquad \textit{Equation 5.}$$

Fractionation factors, which are also denoted by α, are the isotope effects that result in fractionations of isotopes. Here they are defined as the ratio of carbon isotope ratios in reactant and product:

$$\alpha = \frac{Rr}{Rp} \qquad \textit{Equation 6.}$$

where, respectively, R_r and R_p are $^{13}C/^{12}C$ molar ratios of reactant and product. Defined in this manner, a kinetic isotope effect can be seen as the ratio of the rate constant for ^{13}C and ^{12}C containing substrates, k^{13} and k^{12}, respectively. Therefore,

$$\alpha_{kinetic} = \frac{k^{12}}{k^{13}} \qquad \textit{Equation 7.}$$

Delta terminology is a means of expressing all isotope ratios for a given element versus a universal calibrated standard. Considering carbon, the global value for the whole molecule, $\delta^{13}C_g$ [‰], is the deviation of the carbon isotopic ratio R_s relative to that of the international standard Vienna Pee Dee Belemnite, (V-PDB), $R_{v\text{-}PDB}$. It is calculated from:

$$\delta^{13}\mathrm{C_g}\ [‰] = \left(\frac{\mathrm{R_S}}{\mathrm{R_{V-PDB}}} - 1 \right) \qquad \textit{Equation 8.}$$

where, the value of $R_{V\text{-}PDB}$ is 0.0111802.[19] Since the V-PDB standard possess a relatively high ^{13}C content, most samples coming from biomass have negative $\delta^{13}C$ values. Also, values aretypically multiplied by 1000 and expressed in ‰ to give easier numbers.

$$R_{V-PDB} = \frac{0.0111802}{1 - 0.0111802} \qquad \textit{Equation 9.}$$

$$R_i = \frac{A_i}{1 - A_i} \qquad \textit{Equation 10.}$$

$$A_i = \frac{f_i}{F_i} \cdot A_g \qquad \textit{Equation 11.}$$

[19] R. A. Werner and W. A. Brand, '*Referencing Strategies and Techniques in Stable Isotope Ratio Analysis*', Rapid Communications in Mass Spectrometry: RCM, 15.7 (2001), 501–19.

$$A_g = \frac{R_g}{R_g + 1}$$ *Equation 12.*

$$R_g = \left(\left(\frac{\delta_g}{1000} + 1\right)\right) \cdot R_{V-PDB}$$ *Equation 13.*

where, δ_g is the global value obtained by measurements with irm-EA/MS.

$$\frac{f_i}{F_i} = \frac{^{13}C\ mole\ fraction}{^{13}C\ statistical\ mole\ fraction}$$ *Equation 14.*

$$f_i = \frac{Area_{(corr)}}{\Sigma Area_{(corr)}}$$ *Equation 15.*

$$Area_{(corr)} = Area\ under\ the\ peak \cdot (1 + n \cdot 0.011)$$ *Equation 16.*

Where, *n* is the number of carbon atoms that are bonded with the carbon atom which is considered.

Table 1. Parameters for calculating $\delta^{13}C_i$ [‰] -the position-specific carbon isotope ratio.

Symbol (unit)	Meaning
$\delta^{13}C$ [‰]	Carbon isotope composition: deviation of the carbon isotopic ratio relative to the international standard (Vienna Pee Dee Belemnite, V-PDB)
$\delta^{13}C_g$ [‰]	Average isotope composition of the whole molecule (see equation above)
$\delta^{13}C_i$ [‰]	Specific isotope composition of the carbon position *i*
***f_i* (dl)[1]**	^{13}C mole fraction for a carbon position *i* measured by ^{13}C NMR: area of the peak corresponding to the carbon position *i* divided by the sum of all the carbon sites of the molecule ($f_i = S_i / \sum_n S_i$)
***F_i* (dl)**	Statistical mole fraction for a carbon site *i*: molar fraction for the carbon position *i* in case of a homogeneous ^{13}C-distribution within the molecule. (for example: F_i = 1/6 for glucose)
A_i [%]	Isotopic abundance for a carbon site *i*
A_g [%]	Isotopic abundance of a whole molecule

[1]dl, dimensionless

2.1.4 Fractionation associated with primary carbon fixation

Isotope effects on primary enzymatic CO_2 fixation lead to the most important carbon isotopic fractionation in plant metabolism. Isotopic fractionation in C_3 plants is caused by the RuBisCO reaction and in C_4 plants is dominated by the phospho*enol*pyruvate (PEP) carboxylase (EC 4.1.1.31) reaction. Substrate differences (CO_2 and HCO_3^-, respectively) result in different $^{13}C/^{12}C$ ratios in the fixed substrate, which are overlaid by mechanistic differences. In addition, the isotopic fractionation is affected by CO_2 diffusion, which is common to both fixation mechanisms. Such differences lead to different bulk $\delta^{13}C$ values for C_3 plants (-28 ± 2‰ V-PDB) and C_4 plants (-10 ± 2‰ V-PDB), while plants adapted to the use of Crassulacean acid metabolism (CAM) have $\delta^{13}C$ values between these two ranges.[20]

The primary source of carbon is atmospheric carbon dioxide with $\delta^{13}C$ = -8‰ V-PDB. (Note that due to the Suess effect[21] - the mobilisation of fossil carbon - the $\delta^{13}C$ value is continuously decreasing). In aquatic systems CO_2 sources (deviating from $\delta^{13}C$ value) can be HCO_3^- or CO_2 , while in some specialised habitats, such as forest canopies, a significant amount of recycled carbon in coming from (photo)respiration[22]) can be present. By means of a 'Keeling plot' [23] this extraordinary $\delta^{13}C$ value for this CO_2 can be identified from the mixture with the background CO_2.

2.1.4.1 Fractionation effects due to diffusion

The internal CO_2 concentration in the leaf causes variations of isotope fractionation. It was first suggested by Farqhuar et al. in 1982[24] that in terrestrial C_3 plants the isotope fractionation would vary as the internal CO_2 concentration in the leaf also varied. The equation below describes isotope fractionation in C_3 plants:

$$\Delta\delta = [a + \frac{(b-a)P_{int}}{P_{atm}} - d] \qquad \textit{Equation 17.}$$

where a is the discrimination due to diffusion (3.4-4‰), b is the RuBisCO discrimination (30‰ when corrected for the equilibrium effect on CO_2 dissolution), P_{int} is the internal gas-phase pressure of CO_2, and P_{atm} is the external CO_2 pressure. Along with the internal CO_2 concentration variations, the isotope fractionation will also vary or to put differently, the isotope fractionation will fluctuate as the relative resistivities of stomatal diffusion and carboxylation will change.

The term *d* involves contribution from several different, poorly-defined factors such as respiration, fixation in C_3 plants by PEP carboxylase and a whole range of others.

---

[20] M. O'Leary and C. B. Osmond, '*Diffusional Contribution to Carbon Isotope Fractionation during Dark CO_2 Fixation in CAM Plants 1*', Plant Physiology, 66.5 (1980), 931–34.

[21] H. E. Suess, '*Radiocarbon Concentration in Modern Wood*', Science, 122.3166 (1955), 415–17.

[22] J. D. Marshall *et al.*, '*Sources of Variation in the Stable Isotopic Composition of Plants*', Stable Isotopes in Ecology and Environmental Science, ed. by Robert Michener and Kate Lajtha (Blackwell Publishing Ltd, 2007), pp. 22–60 .

[23] D. E. Pataki *et al.*, '*The Application and Interpretation of Keeling Plots in Terrestrial Carbon Cycle Research*', Global Biogeochemical Cycles, 17.1 (2003), 1022.

[24] G. Farquhar *et al.*, "*On the Relationship between Carbon Isotope Discrimination and the Intercellular Carbon Dioxide Concentration in Leaves*.", Australian Journal of Plant Physiology, 9 (2) 1982 121-137.

Another correlation that has been shown in number of studies[25] is the relationship of the fractionation with internal CO_2 partial pressure, and therefore, with water-use efficiency. Field studies conducted by more traditional methods can be superseded with an accurate isotopic studies.[26]

2.1.4.2 Fractionation in terrestrial C_3 plants

Substantial isotope fractionation is shown in terrestrial C_3 plants. It reflects the large fractionation correlated with the ribulose bisphosphate carboxylase-oxygenase (RuBisCO, EC 4.1.1.39) mechanism and a small fractionation related to diffusion and the internal CO_2 concentration in the leaf. The isotope fractionation caused by RuBisCO was discerned early on as a probable cause of the large isotope fractionation reported in C_3 plants.[27] Combustion analysis[28] of this fractionation, by specific analysis of individual carbon atoms in substrate and product[29] has been measured by several researchers. They have also analysed the remaining CO_2 during the carboxylation.[30] The isotope fractionation associated with this reaction at 25°C, pH 8 is 29‰, with an uncertainty of less than 1‰.[31] At present there is no evidence against the assumption that RuBisCO from miscellaneous higher plants introduce essentially similar isotope fractionations.[32] However, it should be taken into account that the number of species that have been studied is relatively small and the possibility of small variations in fractionation is still questionable.

2.1.4.3 Fractionation in C_4 plants

A smaller isotope fractionation is observed in C_4 plants. These plants are distinguished by using a double-fixation strategy: an initial fixation by PEP carboxylase followed by a second fixation by RuBisCO. The key feature of C_4 plants is that the RuBisCO activity takes place in an elevated $p[CO_2]$ environment, thus avoiding the oxygenase activity and eliminating photorespiration.

Numerous researchers have conducted measurements of the fractionation associated with the first step in carbon fixation in C_4 plants photosynthesis, catalysed by PEP carboxylase

---

[25] G. D. Farquhar *et al.*, *'Carbon Isotope Discrimination and Photosynthesis*', Annual Review of Plant Physiology and Plant Molecular Biology, 40.1 (1989), 503–37.

[26] M. H. O'leary *et al.*, '*Physical and Chemical Basis of Carbon Isotope Fractionation in Plants*', Plant, Cell & Environment, 15.9 (1992), 1099–1104.

[27] R. Park and S. Epstein, '*Carbon Isotope Fractionation during Photosynthesis*', Geochimica et Cosmochimica Acta, 21.1 (1960), 110–26.

[28] W. A. Laing and J. T. Christeller, '*A Model for the Kinetics of Activation and Catalysis of Ribulose 1, 5-Bisphosphate Carboxylase*', Biochemical Journal, 159.3 (1976), 563–570.

[29] C. A. Roeske and M. H. O'Leary, '*Carbon Isotope Effects on Enzyme-Catalyzed Carboxylation of Ribulose Bisphosphafte*', Biochemistry, 23.25 (1984), 6275–6284.

[30] H-L. Schmidt *et al.*, '*^{13}C-Kinetic Isotope Effects in Photosynthetic Carboxylation Reactions and δ^{13}C-Values of Plant Material*', Israel Journal of Chemistry, 17 (3) 223-224, (1978).

[31] C. Roeske and M. H. O'Leary, '*Carbon isotope effects on enzyme-catalyzed carboxylation of ribulose bisphosphate.*' Biochemistry, 23, (1984), 6275–6284.

[32] G. G. B. Tcherkez *et al.*, '*Despite Slow Catalysis and Confused Substrate Specificity, All Ribulose Bisphosphate Carboxylases May Be Nearly Perfectly Optimized*', Proceedings of the National Academy of Sciences, 103.19 (2006), 7246–51.

using methods of substrate depletion and products analysis.[33,34] The general consensus is that the isotope fractionation for this reaction is only 2‰. However, it should be born in mind that the value of 2‰ applies to the enzyme-dependent fractionation, where HCO_3^- is considered to be the starting state. Models which are used to predict the overall isotope fractionation relative to atmospheric CO_2 must include hydration of CO_2 to form HCO_3^- This is achievable by combining four factors: isotope fractionation, equilibrium isotope fractionation for CO_2, dissolution and hydration. Then with reference to gaseous CO_2 the isotope fractionation becomes -5.7‰ and in most modelling this value is included.

Hypothesis, which was put forward - that the isotope fractionation by PEP carboxylase is independent of environment and species - is supported to the great extent by experimental data. Some virtual complications in the case of the phosphorylation of PEP carboxylase (it occurs *in* vivo) and the proteolysis may occur during purification.[35] Aptly, the isotope fractionation for the enzyme coming from maize is independent of both processes.

2.1.4.4 Fractionation in Crassulacean acid metabolism plants

Plants that exploit Crassulacean acid metabolism (CAM) are adapted to harsh environmental conditions in which water conservation is crucial. The strategy allows the stomata to be kept closed during the day. As with C_4 plants, RuBisCO functions in an elevated p[CO_2] environment, which leads to $\delta^{13}C$ values between these two ranges.[36]

At night, extensive CO_2 fixation by PEPc takes place, which allows production of malate that is stored in the vacuole. Due to this process, the characterization of CAM plants can be expressed by a marked diurnal variation in titratable acidity. At night, when the evaporative demand is lower, stomata are open and there is a usage of stored carbohydrate to produce PEP. In the opposite situation (during the day) when the evaporative demand is high, stomata close and previously produced malic acid is decarboxylated to obtain CO_2, which afterwards is fixed by the normal PCR cycle.

When decarboxylation is occurring and the stomata are closed (during the day) the CO_2 concentration in the leaf can rise to considerably high levels. The CO_2 concentration can range from 0.08% to 2.5%, as was established through sampling of the internal gas phase in numerous CAM plants.[37]

CAM plants are capable of carrying out normal C_3 photosynthesis if they are growing under reasonable moisture levels. This process occurs at the end of the day when de-

---

[33] M. H. O'Leary *et al.*, '*Kinetic and Isotope Effect Studies of Maize Phosphoenolpyruvate Carboxylase*', Biochemistry, 20.25 (1981), 7308–7314.

[34] T. Whelan *et al.*, '*Enzymatic Fractionation of Carbon Isotopes by Phosphoenolpyruvate Carboxylase from C_4 Plants 1*', Plant Physiology, 51.6 (1973), 1051–54.

[35] J. Jiao and R. Chollet, '*Posttranslational Regulation of Phosphoenolpyruvate Carboxylase in C_4 and Crassulacean Acid Metabolism Plants 1*', Plant Physiology, 95.4 (1991), 981–85.

[36] M. H. O'Leary and C. B. Osmond, '*Diffusional contribution to carbon isotope fractionation during dark CO_2 fixation in CAM plants',* Plant. Physiol. 66 (1980), 931-934.

[37] W. Cockburn *et al.*, '*Relationships between Stomatal Behavior and Internal Carbon Dioxide Concentration in Crassulacean Acid Metabolism Plants*', Plant Physiology, 63.6 (1979), 1029–32; M. H. Spalding *et al.*, '*Crassulacean Acid Metabolism and Diurnal Variations of Internal CO_2 and O_2 Concentrations in Sedum Praealtum DC*', Australian Journal of Plant Physiology, 1979.

acidification is complete. The post-illumination burst can be observed during this phase (photosynthesis is sensitive to O_2). If all these conditions are fulfilled, then photorespiration in CAM plants is similar to that occurring in C_3 plants. Even though there are several superficial similarities to C_3 plants in the potential capacity for photorespiration, it should be noted that normally this capacity is supressed due to the elevated CO_2 concentration that predominates in the light during photosynthesis.[38]

This process for carbon fixation leads to values of $\delta^{13}C$ that are intermediate between normal C_3 photosynthesis and C_4 photosynthesis, in the range of 12 to 20‰.

2.1.5 Fractionation in carbon associated with post-photosynthetic metabolism

In natural organic compounds the backbone is a chain of carbon atoms. The formation and fission of carbon-carbon bonds are the major processes that are occurring during anabolic and catabolic reactions in plants. Another group of reactions of great importance is those that participate in carbon-hydrogen bond creation/breaking. The last product of a (reductive) synthesis chain is most commonly the one which is the most depleted in heavy atoms of carbon and hydrogen taking into consideration the assumption that kinetic isotope effects are implicated in the steps in the biosynthesis, and that this is associated with metabolic branching. Within the degree of reduction from carbon dioxide via carbohydrates to aromatic compounds and lipids to methane, values of $\delta^{13}C$ and $\delta^{2}H$ usually get increasingly more negative (Figure 1).[39]

[38] T. G. Owens, '*Plant Physiology, Biochemistry and Molecular Biology*'; D. T. Dennis and D. H. Turpin', *The Quarterly Review of Biology*, 67.1 (1992), 61–61.

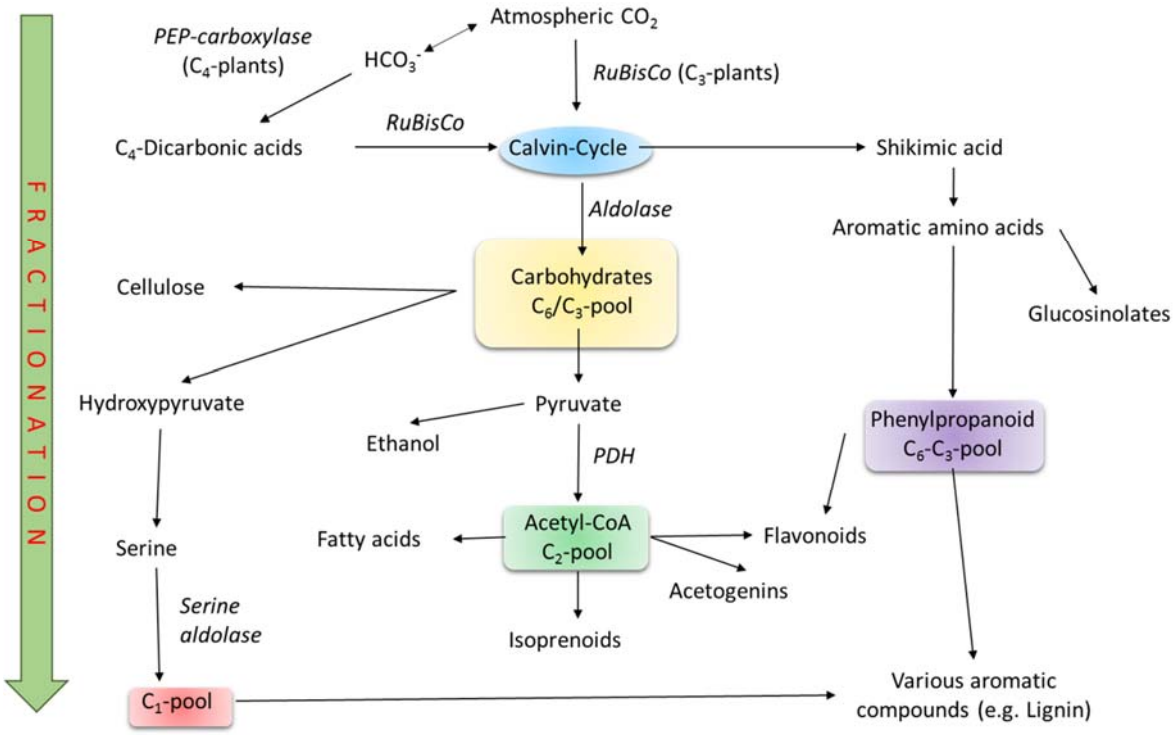

Figure 1. Pathway of carbon in primary and specialised plant metabolism and possible sites for enzyme catalysed reactions with kinetic isotope effects. Scheme redrawn from Schmidt and Gleixner 1998[39]

In general, due to isotopic fractionation in plant metabolism, the ^{13}C content of metabolites tend to decrease as the compound becomes more distal to primary carbon fixation: carbohydrates > proteins > lignin > lipids.[40] In a given plant, the differences from the bulk mean δ value between organs can frequently be a result of different contents of these main components. Isotope patterns can be defined by the differences in $\delta^{13}C$ values between different metabolites, because at branching points the isotopic fractionations in specialised metabolism are occurring to variable extents.

Isotopic fractionation is clearly visible also at the molecular level, and early studies identified specific characteristics for some functional groups and parts of molecules. In a groundbreaking experiment, Abelson and Hoering[41] reported a general relative ^{13}C enrichment in the carboxyl groups of all amino acids coming from the same source. It was nearly 2 decades later

[39] H.-L. Schmidt and G. Gleixner, '*Carbon isotope effects on key reactions in plant metabolism and ^{13}C-patterns in natural compounds*'. Stable Isotopes. Integration of Biological, Ecological and Geochemical Processes 13-25 (BIOS Scientific, Oxford, 1998).

[40] L. A. Kodina, '*Carbon Isotope Fractionation in Various Forms of Biogenic Organic Matter: I. Partitioning of Carbon Isotopes between the Main Polymers of Higher Plant Biomass*', Geochemistry International, 48.12 (2010), 1157–65.

[41] P. H. Abelson and T. C. Hoering, '*Carbon isotope fractionation in formation of amino acids by photosynthetic organisms*', Proceedings of the National Academy of Sciences of the United States of America, 47.5 (1961), 623–32.

that a further key feature was demonstrated when Monson and Hayes showed that fatty acids retained an alternating pattern in their carbon backbone, derived from acetate.[42]

More than a decade later, the objective of measuring all position-specific $^{13}C/^{12}C$ ratios in a target molecule was brought closer by the work of Rossmann and Schmidt[43] who showed that the individual $\delta^{13}C_i$ values in glucose differed one from another. Considering the central position of glucose in metabolism, this discovery opened the way to a new concept of observing isotope fractionation in metabolic pathways. They used isotope ratio monitoring by mass spectrometry (irm-MS) (see section 2.2.1) on fragments of glucose that were obtained by partial or complete degradation (chemical and/or biochemical). In this paper it is clearly shown that the carbon isotopic ratio distribution in natural glucose is non-statistical. Unfortunately this approach has 2 major draw-backs: (i) the methodology has to be developed for each target molecule, and (ii) not all positions are measured directly but some have to be obtained by difference.

Being equipped with the knowledge of the ^{13}C isotope pattern in glucose,[43] permitted the prediction of expected patterns for several compounds, including ethanol and acetic acid, malic and citric acids, and several amino acids. Subsequently, distributions predicted in this way were confirmed experimentally with an substantial degree of agreement. Notably, the ^{13}C-enrichment in both malic and citric acids extracted from citrus fruits showed a good comparison to values predicted from glucose. It should also be noted that these acids in citrus fruit represent end-product accumulation, and values from central metabolism may be radically different. This might in part explain why the pattern was qualitatively, but not always quantitatively as expected.

All of these studies involved the tedious degradation or partial degradation of the target molecule and the analysis of products by irm-MS. Since the 1980's, however, the development of the alternative technique of isotope ratio monitoring by nuclear magnetic resonance spectrometry (irm-NMR) has allowed the direct measurement of isotope ratios in a range of natural products. First developed for ^{2}H, it has now been applied successfully to advance our understanding of the isotopic variation of ^{13}C. There are a number of important parameters that need to be carefully controlled in order to apply this technique successfully: these are detailed in Section 2.2.2.

Gilbert *et. al.*[44] developed an irm-^{13}C NMR technique adapted for glucose, a key metabolite in most biological systems. Gilbert's studies confirmed by direct analysis that natural glucose shows a non-statistical isotope distribution and that the internal $^{13}C/^{12}C$ profiles in glucose can be dependent on the photosynthetic pathway involved (C_3 and C_4 plants). This was also shown by examining ethanol made by fermentation from C_3-, C_4-, or CAM-derived glucose.[45] In ethanol

---

[42] K. D. Monson and J. M. Hayes, '*Carbon isotopic fractionation in the biosynthesis of bacterial fatty acids. Ozonolysis of unsaturated fatty acids as a means of determining the intramolecular distribution of carbon isotopes',* Geochimica et Cosmochimica Acta, 46 (2), (1982) 139-149

[43] A. Rossmann *et al.*, '*Evidence for a Nonstatistical Carbon Isotope Distribution in Natural Glucose*', Plant Physiology, 96.2 (1991), 609–14.

[44] A. Gilbert *et al.*, '*Accurate Quantitative Isotopic ^{13}C NMR Spectroscopy for the Determination of the Intramolecular Distribution of ^{13}C in Glucose at Natural Abundance*', Analytical Chemistry, 81.21 (2009), 8978–85.

[45] E. P. Botosoa *et al.*, '*Unexpected Fractionation in Site-Specific ^{13}C Isotopic Distribution Detected by Quantitative ^{13}C NMR at Natural Abundance*', Journal of the American Chemical Society, 130.2 (2008), 414–15.

the $^{13}C/^{12}C$ ratios of methyl and ethyl groups were inverted in C_4 plants relative to that in C_3 plants (the methylene site is ^{13}C-enriched in comparison to the methyl).

One of the questions that can be put forward is: is there a consistent intramolecular pattern in glucose? The agreement between the data from irm-MS and irm-^{13}C NMR is in a good agreement, although the C1 position is found to be more ^{13}C-enriched when measured by ^{13}C NMR. The pattern has been confirmed in ethanol produced from fermentation is in agreement with that in glucose and sucrose.[46] Comparing C_3, C_4 and CAM plants, the isotope patterns in glucose show similarities between C_3 and C_4 with the exception at C4 position of sucrose, which shows a 3.5‰ enrichment in sugar beet (C_3). It had already been reported[47] that the C4 atom was 1.2‰ more enriched in glucose of C_3 plants than in C_4 plants. It appears that the C1 atom of the glycosyl moiety is also more ^{13}C-enriched in C_4 sucrose, while the C6 position is somewhat more enrichment than the C5 position. The explanation of such differences seems to lie in the involvement of photorespiration in C_3 plants, in which there is a much great photorespiratory flux.

In a further study, it was shown that the fructosyl moiety of sucrose had ^{13}C-isotope ratios at C1 and C2 inverse to those in the glucosyl moiety.[48] In order to investigate the cause of this isotope fractionation, the site-specific ^{13}C-isotope fractionations associated with the activities glucose isomerase and invertase were measured *in vitro*.[49] It was found that site-specific kinetic and thermodynamic isotope effects were accompanying glucose isomerization. The isomerisation of glucose to fructose tends to enrich in ^{13}C the C1 position in glucose and the C2 in fructose, which is in agreement both with the profiles observed in sucrose and with thermodynamic potentials and explains the systematic enrichment in carbonyl in comparison to the hydroxyl groups.

The technique has subsequently been applied to a number of compounds with a great success for determining the site-specific ratios (denoted as $\delta^{13}C_i$ [‰]). A study of the position-specific ^{13}C distribution in vanillin showed that this was related to the source from which the molecule was obtained. Furthermore, it proved possible to provide supporting evidence for the proposed chain-shortening reaction by combining experimental and theoretical analysis of the biotransformation of ferulic acid to vanillin.[50]

Numerous commonly-used beverages such as coffee, tea and cocoa contain the natural xanthines, caffeine, theobromine and theophylline. In the light of authenticity regulations their

---

[46] A. Gilbert *et al.*, '*Biochemical and Physiological Determinants of Intramolecular Isotope Patterns in Sucrose from C_3, C_4 and CAM Plants Accessed by Isotopic ^{13}C NMR Spectrometry: A Viewpoint*', Natural Product Reports, 29.4 (2012), 476–86.

[47] A. Rossmann *et al.*, '*Evidence for a nonstatistical carbon isotope distribution in natural glucose',* Plant Physiology, 96 (2), (1991), 609-614

[48] A. Gilbert *et al.*, '*A ^{13}C NMR spectrometric method to determine the intramolecular $\delta^{13}C$ values in fructose from plant sucrose samples.*' New Phytol. 191 (2011) 579–588

[49] A. Gilbert *et al.*, '*Intramolecular ^{13}C Pattern in Hexoses from Autotrophic and Heterotrophic C_3 Plant Tissues*', Proceedings of the National Academy of Sciences of the United States of America, 109.44 (2012), 18204–9.

[50] E. P. Botosoa *et al*., '*Quantitative isotopic ^{13}C nuclear magnetic resonance at natural abundance to probe enzyme reaction mechanisms via site-specific isotope fractionation: The case of the chain-shortening reaction for the bioconversion of ferulic acid to vanillin.*' Analytical Biochemistry 393, (2009), 182-188.

origin needs to be certified and for this purpose irm-MS is being used. However, this technique is very limited. Diomande *et al.* developed a methodology for this range of compounds that exploits the power of irm-^{13}C NMR and chemical modification of xanthines, that enables high precision in the determination of positional intramolecular $^{13}C/^{12}C$ ratios.[51] Due to the poor solubility of theobromine and theophylline compared with caffeine, several difficulties were faced during their measurement. To solve this issue and make collection of the spectra more feasible, the other xanthines were *N*-methylated to caffeine. The method shows good repeatability of the $\delta^{13}C_i$ values in caffeine and is confirmed as robust. It was shown that the occurrence of isotope fractionation during the *N*-methylation is negligible and the original positional $\delta^{13}C_i$ values are preserved. The application of this method is mainly focused on using the position-specific variations of the $^{13}C/^{12}C$ distribution in the xanthines to indicate differences coming from their geographical origin. However, distinct dissimilarities between ^{13}C patterns of theobromine coming from cocoa and caffeine from tea were seen, which may indicate variation in the underlying biochemistry.

In all of these publication the strong evidence of the power of irm-^{13}C NMR technique is shown. The elucidation and interpretation of variations in isotopic patterns and continuation of this work is one of the major objectives of this thesis (see chapters IV and V).

2.1.6 How the fractionation is happening: thermodynamic considerations

Galimov was systematically investigating inter- and intramolecular carbon isotope distributions. He put forward a postulate about the existence of a general 'thermodynamic order' inside and between natural organic molecules.[52] The proposition of the usage of the thermodynamic isotope factor β (ratio between the partition function of two isotopomers) was advanced by Galimov when he applied Urey's theory on isotopic exchange equilibria[53] to organic molecules, with the assumption of the existence of an isotopic equilibrium for the carbon isotopes within and between organic molecules. For the positional carbon equilibrium within a molecule it takes the form of β_i, while for the one in between molecules - β_Σ. Dependence of the numeric β_i values lies in the binding of a given C-atom and are consisting of the increases for C=O, C-O, C≡N, C=N, C-N, C≡C, C=C, C-C, C-H bindings.

In some cases and under steady-state conditions of metabolism, reversible reactions can come to isotopic equilibrium and meet the criteria for thermodynamic order. Reduced isotopic partition functions (β factors) calculations are in agreement with isotope distributions for this type of reaction. On the other hand, if these reactions are under conditions of unidirectional processes, their influence on isotope distributions goes through kinetic isotope effects. Then, only general guide lines can be given by an observed correlation of isotope patterns with isotopic β factors on the possible metabolic conditions which are dominating during the biosynthesis.

---

[51] D. G. Diomande *et al*., '*Position-specific isotope analysis of xanthines: a ^{13}C Nuclear Magnetic Resonance method to determine the ^{13}C intramolecular composition at natural abundance.*' Analytical Chemistry 87, (2015), 6600-6606.

[52] E. Galimov, '*The Biological Fractionation of Isotopes*', Elsevier (2012), pp 212.

[53] H. C. Urey and L. J. Greiff, '*Isotopic Exchange Equilibria*', Journal of the American Chemical Society, 57.2 (1935), 321–27.

An essential principle of thermodynamic approach can be defined in a way that the final state of a process is uninfluenced by the pathway by means of which it was attained. This statement is true also for the isotope patterns of natural compounds with the assumption that they are dominated by thermodynamic principles. Classification of natural compounds can be divided into two classes of products: 'transient' and 'permanent'. The first category involves monosaccharides, organic acids and amino acids, intermediates engaged in energy metabolism or playing a role in the creation of precursors for other products. They are part of the fast anabolic and catabolic turnover and can attain thermodynamic order. The second class of products – permanent – brings together compounds such as polymers, cellulose, lignin, starch, proteins and nucleic acids. Also many small molecules are included in this group, such as certain lipids or alkaloids, all of which are part of synthetic metabolism. These do not obey thermodynamic principles. By the secondary turnover reactions they will gain additional pattern characteristics. Nevertheless, they still preserve completely or in parts the isotope patterns of their forerunners. This will be further developed in Chapter 5.

2.1.7 Exploitation of isotopic fractionation to probe enzyme mechanisms

The phenomenon of isotope effects is one of the most powerful tools by which to study enzyme mechanisms.[54] Substitution of a heavy isotope for the normal lighter one is the cause of these effects. They can be divided into equilibrium isotope effects (an effect on equilibrium constants) and kinetic isotope effects (an effect on rates). The ratio of the equilibrium constants is defined as an *equilibrium* or *thermodynamic isotope* effect (EIE). In a given reaction the ratio of the rate constants is defined as the *kinetic isotope effect* (KIE). In enzyme-catalysed reactions this definition refers to the *rate-limiting step.* The strength of kinetic isotope effects is based on the stiffness of bonding in the substrate and the transition state, while equilibrium isotope effects are determined by the relative stiffness of bonding of the isotopic atom in substrate and product (the heavy isotope becomes enriched in the position of the stiffer bond). In the so-called primary isotope effects, bonds are made or broken. They can show very strong discrimination against the heavy isotope – described as the 'normal' isotope effect (>1) – or in some cases the presence of the heavier isotope helps the reaction mechanism, leading to an 'inverse' isotope effect (<1).[55]

Fast and reversible formation of an enzyme-substrate complex, which is commonly accompanied by a conformational change in the enzyme precedes an enzyme-catalysed reaction. The kinetically *rate-determining* step (sometimes irreversible) is the major reason for the occurrence of the overall kinetic isotope effect, even though the rates of other steps can also be sensitive to isotope substitutions.[56]

For any enzyme that has been isolated and characterized in terms of its physical properties the most sought-after information is the reaction mechanism. This is crucial for knowing and understanding the processes which the enzyme undergoes under a given set of reactant condi-

[54] P. F. Cook, '*Enzyme Mechanism from Isotope Effects.*' (pp. 500). Boca Raton: CRC Press, (1991).
[55] W. W. Cleland, *'The Use of Isotope Effects to Determine Enzyme Mechanisms'*, Archives of Biochemistry and Biophysics, 433.1 (2005), 2–12.
[56] H-L. Schmidt, 'Fundamentals and Systematics of the Non-Statistical Distributions of Isotopes in Natural Compounds', Naturwissenschaften*,* 90**,** (12), (2003), 537-552..

tions. The functional groups important for reaction such as the affinity for other reactants and cofactors, pK values of enzyme general acids, bases, nucleophiles and electrophiles may change due to their dependence on the active sites of enzymes. It also helps understand how enzymes carry out reactions under 'green chemistry' conditions (aqueous solution, low temperature, etc.)

The reaction mechanisms of enzyme-catalysed reactions can be studied by qualitative and quantitative analyses. Determining the order of addition of reactants to the enzyme active site and release of the products from it gives a qualitative description of the reaction pathway. This allows the study of the initial velocity in the absence/presence of product and dead-end inhibitors.[57] However, other techniques needs to be evoked because this type of studies is inconclusive and usually insufficient to clearly identify the kinetic mechanism. More informative techniques include (they are not limited only to these parameters), isotope exchange at equilibrium[58], isotope partitioning,[59] positional isotope exchange[60], and rapid or pre-steady-state kinetics.[61]

The rate constants for individual steps of the reaction pathway such as: reactant adsorption, enzyme conformational changes, chemical interconversion, and product release can be estimated through the quantitative aspects of the kinetic analysis of the reaction mechanism. Notwithstanding, it is almost impossible to obtain the absolute values of microscopic rate constants, but the general idea from initial velocity studies (slow steps are present along the reaction pathway) can be achieved. Obviously there are some exception like Theorell-Chance mechanism, which includes limitation of the overall reaction by the release of the last products, or the rapid equilibrium random mechanism where interconversion of the enzyme complexes with all reactants bound is slow.[62]

The ability to obtain both qualitative and quantitative information for kinetic reaction mechanisms was made possible by the application of isotope effects to enzyme-catalysed reactions.[63] Moreover, isotope effects are also used for obtaining information on the regulatory kinetic mechanism of enzymes (chemical interconversion, reactant release, etc.).[64]

---

[57] W. W. Cleland, '*The Kinetics of Enzyme-Catalyzed Reactions with Two or More Substrates or Products'*, Biochimica et Biophysica Acta (BBA), 67 (1963), 104–37 .

[58] D. L. Purich and R. D. Allison, '*Isotope Exchange Methods for Elucidating Enzymic Catalysis*', Methods in Enzymology, Enzyme Kinetics and Mechanism - Part B: Isotopic Probes and Complex Enzyme Systems (Academic Press, 1980), LXIV, 3–46 .

[59] I. A. Rose, '*The Isotope Trapping Method: Desorption Rates of Productive E.S Complexes*', Methods in Enzymology, 64 (1980), 47–59.

[60] F. M. Raushel and J. J. Villafranca, '*Positional Isotope Exchange*', Critical Reviews in Biochemistry, 23.1 (1988), 1–26.

[61] D. G. Herries, '*Enzyme Structure and Mechanism (Second Edition)*', Pp 475, (1984), ISBN 0–7167–1614–3 *Biochemical Education*, 13.3 (1985), 146–146.

[62] E. F. Armstrong, *'Enzymes',* By J.B.S. Haldane, M.A. Monographs on Biochemistry. Pp. vii, 235. London: Longmans, Green & Co., (1930) , *Journal of the Society of Chemical Industry*, 49.44 (1930), 919–20.

[63] W. W. Cleland, *'Mechanistic Deductions from Isotope Effects in Multi Reactant Enzyme Mechanisms*', Biochemistry, (1981), 1790-1796; N. Ahn and J. P. Klinman, '*Mechanism of Modulation of Dopamine Beta-Monooxygenase by pH and Fumarate as Deduced from Initial Rate and Primary Deuterium Isotope Effect Studies*', Biochemistry, 22.13 (1983), 3096–3106.

[64] P. F. Cook, '*Kinetic Studies to Determine the Mechanism of Regulation of Bovine Liver Glutamate Dehydrogenase by Nucleotide Effectors*', Biochemistry, 21.1 (1982), 113–16.

The concentration of product in the reaction mixture affects the isotope effects which means, that this effect will be mechanism dependent. The product dependence of isotope effects on V, V/K_a and V/K_b (**V** – maximal velocity (Michaelis-Menten constant), **K** – equilibrium constant defined by the free-energy difference between the transition state and the reactants, **a** – proton as the reference isotope, **b** - deuterium as the reference isotope) minimal mechanism is considered more complex than for the substrate dependence of isotope effects. Mechanisms depending on product isotope effects also needs to take into account the reversal of the reaction that occurs upon the addition of product. However, it allows for a more complete picture of isotope effects than substrate isotope effect dependant mechanisms.

Isotope effect studies are one of the most powerful tools in for enzymology research. By making use of the substrate and product dependence of isotope effects the complete description of the kinetic mechanism of an enzyme can be acquired. There are two possibilities of obtaining the information; basing on the order of addition of reactants and release of the products or by locating the slow steps along the reaction pathway (it allows values or ratios of rate constants to be determined). The effect of modifiers on the rate processes can be examined through the determination of isotope effects in the absence/presence of allosteric modifiers. This can lead to significant simplification of the elucidation of kinetic mechanism for enzymes, where they are applicable.[65]

A complementary approach to obtaining isotope effect data is to carry out studies involving theoretical calculations (this is used to obtain significant aid in terms of isotopic effects during the methionine production reaction from homocysteine with the usage of methionine synthase: see section 4.6). A pre-requisite to conducting this kind of calculations is the necessity of obtaining a good 3D structure of the protein from an X-ray crystallographic analysis of the atomic array. As the calculation depends on having the atoms correctly positioned in relationship one to another, the higher the resolution of the X-ray-derived atomic structure the better. A minimum of about 1.8 to 2.25Å is needed, although working with lower resolution is possible. It should be noted that the structures obtained from the data bases (RCSB PDB Protein Data Bank in this case) are missing hydrogens in their structure and need to be optimized for a proper geometry. It is also advantageous if a crystal structure with the substrate product or an analogue present in the active site is available.

The approach generally taken, as in this case, to reduce the amount of time necessary for the optimization and simplification of the model, is to work on a pre-optimized model obtained by molecular dynamics: typically dynamics of 1ns are conducted (see section 4.6.1.1.). This provides the stabilized structure and the proper geometry for further investigation (modelling the reaction mechanism). A range of calculation modes are now available, and the choice depends on the level of stringency required, as well as the time required to perform the calculations. The model presented in this thesis was performed with the relatively low stringency PM3 method, which is semi-empirical. The most desirable and recognizable in the theoretical chemistry world is taking the calculations to the higher level of theory within PM6, which allows a better potential energy profile to be obtained (i.e. values are closer to the real ones). Nevertheless, even though the PM3 level typically serves as the starting point for further calculations, it can

[65] P. F. Cook, *Enzyme Mechanism from Isotope Effects* (CRC Press, 1991).

also be used for isotopic calculations (isotope effects on the individual atoms), elucidation of the reaction mechanism, energy profile, determining the rate-limiting step and overall geometry of the reaction pathway.

The main disadvantages of this method are the relatively long time required for the calculations (between 1-3 months depending on the power of the computer used), the need for manual optimization of the starting structure, and proper parametrization of the metal ion in the active site of an enzyme (zinc in this case) that coordinates the reactants.

2.2 Methods of measurements

The data required to monitor isotope ratios is classically obtained by Mass Spectrometry.[66] Special mass spectrometers which can be tuned to collect a small number of discrete masses are available by which appropriate ions can be quantified (see section 2.2.1). More recently Infra-Red spectroscopy has been developed for irm determination.[67] Both these techniques require that the analyte is either a gas or is pre-combusted to give gases. An alternative technique is to use NMR spectrometry, which allows the isotope ratio at each resolved position to be measured (see section 2.2.2).

2.2.1 Isotope ratio monitoring by MS

The problematic issue that arose when it was required to analyse a range of different organic sample types for their stable isotope content at natural abundance found its solution with the development of the continuous flow online linkage of an elemental analyser to an isotope-ratio monitoring mass spectrometer irm-EA/MS). This technique, which utilizes He gas as a carrier permits a faster and more simplified analysis than an off-line system. Unification of the sample preparation process, gas purification along with on-line mass spectrometry notably increased the capacity of acquiring large amounts of stable isotopic data. For nitrogen and carbon this improvement was adapted initially due to difficulties that conventional methods had for samples with low N- and C-contents. Consequently, this technique became widely accepted for the routine analysis of $^{15}N/^{14}N$ and $^{13}C/^{12}C$ ratios. Subsequently, isotopic analysis by irm-EA/MS was developed for other elements, H, O and S.[68]

2.2.1.1 Overall scheme of the machine and protocol of measurements

irm-MS instruments are specifically designed to measure precisely small differences in the abundances of isotopes such as $^{2}H/^{1}H$, $^{13}C/^{12}C$, $^{15}N/^{14}N$, $^{18}O/^{16}O$, and $^{34}S/^{32}S$. To allow the analysis of organic samples (liquid or solid) they need to be transformed into simple gasses: H_2 (H), CO_2 (for C), N_2 (for N), CO (for O), or SO_2 (for S). The choice depends on the composition of the material and which isotopes are to be analysed. Subsequently, the machine measures the quantity of the ions that correspond to the different isotopomers of these gases. If we consider the analysis

[66] W. A. Brand, '*High Precision Isotope Ratio Monitoring Techniques in Mass Spectrometry',* Journal of Mass Spectrometry, 31, 225-235 (1996)

[67] R. N. Zare *et al.*, '*High-precision optical measurements of $^{13}C/^{12}C$ isotope ratios in organic compounds at natural abundance',* Proceedings of the National Academy of Sciences, 106(27), (2009), 10928-10932.

[68] N. V. Grassineau, *'High-Precision EA-IRMS Analysis of S and C Isotopes in Geological Materials'*, Applied Geochemistry, Frontiers in Analytical Geochemistry–An IGC 2004 Perspective, 21.5 (2006), 756–65.

of carbon isotope ratios, the mass spectrometer separates ions with mass to charge ratios (*m/z*) of 44, 45, 46 which corresponds to the ions obtained from CO_2 molecules that contains ^{12}C, ^{13}C, ^{16}O and ^{18}O in different combinations.

Instrumental variation requires that, for comparison between samples of different origins and from different analyses, a relative scale needs to be defined. This is achieved thanks to the international standards (primary materials)[69] in accordance to which the isotope ratios at natural abundance level are measured. It is extremely important to use well-characterized international standards to which the samples of unknown composition can be related either directly, or via a laboratory standard[70] for which the isotope ratios have already been determined against the primary materials.

The order of the analysis can be shown in four steps:

1. Within the elemental analyser the sample undergoes combustion or thermal conversion;
2. The evolved gases are carried in a stream of He gas and introduced into the ion source of the mass spectrometer through the interface;
3. The gas molecules are ionised, accelerated, separated on the basis of their mass, and detected in the form of ions by the Faraday cages in the mass spectrometer;
4. Raw data is evaluated and used to calculate the isotope ratio.

This general scheme allows a wide range of materials to be analysed by irm-EA/MS. For solid substances as well as for non-volatile liquids the tin (for C/N analysis) or silver (for O/H) capsules can be used to introduce the samples into the elemental analyser system. In the case of liquids, those with limited viscosity can be directly injected using a liquid inlet system.

The system in the analyser typically consists of a two-reactor system:

1. 'combustion' reactor
2. 'reduction' rector

even though both can be combined in the single tube. They are follow by a water-separation device and a packed GC column for gas separation (in the case of C and N analysis, this separates CO_2 and N_2). The scheme of the overall system is shown in Figure 2.

[69] https://nucleus.iaea.org/rpst/ReferenceProducts/ReferenceMaterials/Stable_Isotopes/index.htm
[70] In the EBSI laboratory, we use glutamic acid.

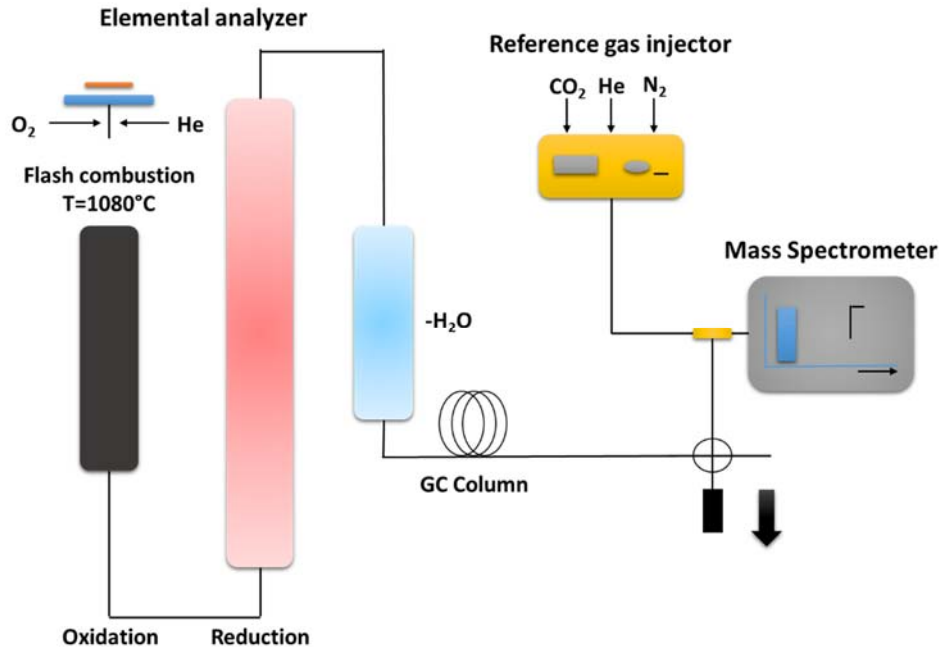

Figure 2. Overall scheme of working principle of irm-EA/MS for C and N isotope analysis

To produce CO_2, NO_x and H_2O the combustion is taking place in a quartz reactor under oxygen. To bind sulphur and halogens, typically the reactor is containing Cr_2O_3 and Co_3O_4+Ag, notwithstanding it should be mentioned that different variations can be used (and are recommended) for specific applications. Typically the temperature of the reactor is held between 900°-1050°C, but the combustion temperature of tin capsules usually is raising the overall temperature up to about 1080°C. To avoid removing the reactor each time it is filled, usage of ash crucibles (quartz inserts) to collect the ash and residue from samples and tin capsules is recommended.

In a second quartz reactor at 650°C removal of excess oxygen and reduction of the NO_x to N_2 takes place. Typically it is packed with high purity Cu.

Magnesium perchlorate ($Mg(ClO_4)_2$), commonly called Anhydrone™, is used in a 'water trap'. For nitrogen isotope ratio analysis only, it is very convenient to remove CO_2 from the gas stream, either with a chemical trap that contains soda lime (Ascarite™ or Carbosorb™), or with a switching valve post-GC column. Reagent can be placed before or after the water trap depending on the specificity of the sample. In the final step the N_2 and CO_2 are separated via an isothermal packed GC column.

Through the interaction with the electron beam (electron ionisation) gas molecules are ionized. The process takes place in the ion source of the mass spectrometer. After the ions leave the source, they are focused and accelerated through a high voltage. After passing through the magnetic field, the ions reach the Faraday cup detectors ions. The trajectory of the ions is determined by the strength of the magnetic field and accelerating voltage and this is tuned to determine which ions will enter the Faraday cups. Simultaneous measurement of ion intensity ratios with a contemporary negation of the fluctuations in the intensity of the ions beam is achieved by the usage of multiple collectors.

Three collectors are necessary for nitrogen and carbon ratio measurements, which are specifically spaced to collect *m/z* 28 and 29 or m/z 44, 45 and 46, respectively. Another solution is the universal triple collector in which the outer cups are wide with respect to the dispersion of the ion beam. In the case of oxygen isotope ratio measurements, which are based on CO that is isobaric with N_2, the same set of collectors can be used. The machine provided by SERCON (outside view) is presented on Figure 3.

Figure 3.SERCON irm-EA/MS instrument

Conventional extraction methods for the determination of C- and S- isotope ratios in samples are slowly repressed by the continuous flow irm-EA/MS technique which significantly improves measurements. One if its main advantages is the small quantity of material used and relatively short time of the analysis. Combined with the simplicity of sample preparation, which doesn't require chemical or complete mechanical mineral phase separation, and rapid sample introduction, irm-EA/MS has become one of the most commonly used techniques. Nevertheless, the technique requires strict compliance with the sample analysis protocol, due to the necessity of controlling a variety of factors needed for high data quality.

The non-linearity effects are minimized by sample weight adjustment for matching the sample and reference peak heights. An accurate calibration is the crucial point of the proper measurements and should be maintain carefully by the usage of standards that have a wide range of isotopic compositions. The ideal situation would be to adjust the analysed samples to both low and high isotopic ratios. To retain accuracy of the calibration, a regular analysis of the laboratory standards should be performed, and a periodic analysis of a calibrated international reference. Monitoring of the calibration equation should be carried out through the run by regular analysis of standards and performance of the Cu-reduction reactor checked to avoid O_2 saturation. Keeping all the above mentioned conditions for analytical detail ensures the measured precision on replicates of isotopic standards around ±0.2 – 0.4‰ for both C and N isotopic analyses.

2.2.2 Isotope ratio monitoring by ^{13}C NMR

The technique of isotope ratio monitoring by ^{13}C NMR spectrometry now serves as a very powerful tool for the analysis the isotopic composition of natural compounds. The data obtained can be exploited in a number of ways, which can lead to the discrimination of biosynthetic schemes and the prediction of reaction mechanisms. This novel approach allows the establishment of isotopic distribution in the tested sample in a relatively short period of time (once the analytical protocol has been established).

2.2.2.1 General aspects of NMR spectroscopy

After the invention of NMR spectroscopy in the late 1940's this technique became the most important tool for structure determination. The range of possibilities that NMR spectroscopy now offers, with various experimental protocols, is a crucial factor in the overall power of this technique. The wide application of NMR spectroscopy comes from the fact that the frequencies of transitions are strongly dependent not only on the magnetic strength, but also on the chemical environment of the nucleus under study. Chemical bonds are essentially the way that electrons are holding the atoms in molecules together, and, depending on the nature and exact environment of those bonds, they produce different magnetic fields. Compared to the external magnetic field they are relatively small. Nevertheless, because different nuclei within a molecule interacts in different ways with the global magnetic fields, thereby they are resonating at different frequencies (local magnetic field + external magnetic field = effective field). This effect is described as a chemical shift due to the differences for the different magnetic fields. Thus:

$$chemical\ shift = \frac{frequency\ of\ nucleus\ under\ study - frequency\ of\ reference}{frequency\ of\ reference} \qquad \textit{Equation 18.}$$

It should be noted that within a molecular framework the influence of a nucleus is not only coming from the local magnetic fields produced by electrons. Other nuclei produce local fields that are the additional factors that have an effect on chemical shift in the NMR spectrum. Adjacent nuclei have a smaller impact than that coming from electrons. This produces a fine splitting of peaks within the spectrum (the so-called 'coupling constant', *J*).

NMR spectroscopy requires magnets that are powerful enough to align spin states in their magnetic fields and make it possible to see differences of the spin states, as mentioned above. Most elements possess an isotope that is magnetically active, but for natural product chemistry there are four basic nuclei of interest: ^{1}H, ^{13}C, ^{15}N and ^{31}P measurements. These nuclei possess nuclear spins of one-half. This means that their magnetic vectors align in an external field either parallel or antiparallel to the field (they behave like very small magnets).

2.2.2.2 Specific aspects of NMR spectrometry applied to isotope ratio monitoring

For the purpose of studying the natural distribution of isotopes in organic molecules, the most powerful technique is isotope ratio monitoring by NMR spectrometry. In comparison to the other spectroscopic methods, irm-NMR spectrometry has a major disadvantage: its intrinsic low sensitivity. This is due to (i) the low abundance of the heavy isotope(s) relative to the light isotope, and (ii) the spin properties of the nuclei under consideration. In contrast, its potential lies

in the possibility of exploring the fingerprints that are produced for a particular compound (unique trace of isotopic composition for the natural products). This makes possible the analysis of the variation in $^{13}C/^{12}C$ within a molecule, which can be exploited in traceability, the elucidation of biosynthetic pathways and the study of reaction mechanisms.

As mentioned earlier, this technique was initially developed for ^{2}H, but for this discussion I shall focus on the more recently developed ^{13}C NMR (irm-^{13}C NMR), as this is the technique exploited in this study. The carbon isotope ^{12}C is the most abundant carbon isotope, but it is not NMR active. Thus, sensitivity is lost because it is possible only to observe 1.1% of the sample: that which is composed of the ^{13}C-isotopomers (similarly for hydrogen, the ^{2}H isotope is at very low abundance and in addition has poor NMR properties.)

The key aspect for ^{13}C is to aim for an error of <1‰, which requires a signal-to-noise (S/N) ratio of >650, the theoretical minimal level required to obtain such a precision.[71] This high level of required trueness and precision (1-2‰ on the δ scale) has been challenging for the application of this technique to the $^{13}C/^{12}C$ isotope ratio. The methodology should have the ability of detection of the signal areas in a range of only 0.2‰. When the absolute value need to be determined the problem of achieve this level of accuracy in a series of repeated measurements over a period of time is especially crucial.

To obtain sufficient precision in irm-^{13}C NMR, a number of parameters (see Table 2) need to be rigorously controlled.

Table 2. Parameters that need to be controlled to perform ^{1}H decoupling (terminology specific for Bruker spectrometers).

Parameter	*Description*
p1	Length of RF pulse
o1p	Frequency in the middle of ^{1}H spectrum
o2p	Frequency in the middle of ^{13}C spectrum
popt	Command that allows optimization of acquisition parameters (**p**arameter **opt**imization)
d1	Value of the longest T_1x10

2.2.2.2.1 ^{1}H decoupling

The most common approach in ^{13}C NMR spectra is to run them in conditions of ^{1}H-decoupling (proton frequencies are saturated). In these conditions, couplings between ^{13}C and ^{1}H are no longer observed, which means that the carbon spectra no longer show quartets, triplets and doublets coming from the adjacent protons but consists of single lines. This approach creates spectra that are more readable and easier to integrate. 'WALTZ-16' is the most commonly used sequence to achieve this. It consists of 16 RF pulses at the centre frequency of the proton spectrum and allows decoupling with a minimal range of RF values and sample heating.

[71] K. Bayle *et al.*, *'Conditions to Obtain Precise and True Measurements of the Intramolecular ^{13}C Distribution in Organic Molecules by Isotopic ^{13}C Nuclear Magnetic Resonance Spectrometry'*, Analytica Chimica Acta, 846 (2014), 1–7.

To obtain compensation of the residual pulse imperfections there is several factors that must be met,[72] such as phase cycle applied during decoupling, a pulse sequence that precedes decoupling sequence and an adiabatic pulse, which performs an inversion of the magnetization over the decoupled bandwidth during the pulse duration (this needs to be short in comparison to the T_2). All of them are responsible for the efficiency of an adiabatic decoupling scheme.[73] Residual heteronuclear splitting (Jr) is a result of an imperfect decoupling; reduction of this value is the aim of decoupling optimization. Line shape reflects its influence, that should be minimal.

There are several limitations, however, that should be considered, such as maximum voltage permitted by the probe (determines ω_2^{max} - which is the maximum amplitude of the RF field) and the RF heating of the sample (these parameters are dependent on the material used for the analysis, duty cycle of the decoupling and the energy deposed on the sample by one RF pulse, determined by the root-mean square-value ω_2^{rms}).

Typically decoupling is exerted in heteronuclear experiments such as carbon-13 detection with proton decoupling. ^{13}C carbon spectral bandwidth is > 100 ppm (< 5 ppm for protons) which makes proton-detected, carbon-decoupled experiment technically one of the most challenging and is the greatest example for discussion of the principles of decoupling. The question is how to decouple wider spectral bandwidth without increasing several factors such as peak, average power and without usage of increasing artefacts. The solution for this problem is the design on broadband inversion pulses. So-called composite RF pulses are the first family of broadband inversion pulses that were implemented for broadband decoupling techniques, they are composed of a number of RF pulses with different nutation angles and relative phases. While the overall rotation during a composite RF pulse is typically much larger than 180°, the final net nutation angle is close to 180° with some insensitivity towards frequency offsets and even towards B_1 inhomogeneity. To compensate the imperfection of a single 180° pulse by under- or over-rotating the magnetization the additional rotations are used. On the basis of MLEV and WALTZ decoupling lies two successful composite pulses which are $90°_x180°_y90°_x$ and $90°_x180°_{-x}270°_x$, respectively.

So called supercycles are used for the purpose of further improvement already greatly improved individual composite RF pulses. Taking as an example WALTZ-4 that is composed of four segments - $R_xR_xR_{-x}R_{-x}$ in which R_x is the original composite pulse – and can be placed inside another supercycle which gave a rise to WALTZ-16 (most commonly used and popular decoupling sequence). The imperfections introduced to the earlier pulses are compensated by the RF pulses in the supercycles. The initial design of composite pulses was based on visual representation of pulse rotation, which means that it is highly limited by human ability to visualize complex rotations. Thanks to the computational optimization of the nutation angle and relative phases of composite pulses several useful decoupling techniques were developed.

---

[72] E. Tenailleau and S. Akoka, *'Adiabatic ^1H Decoupling Scheme for Very Accurate Intensity Measurements in ^{13}C NMR'*, Journal of Magnetic Resonance, 185.1 (2007), 50–58; E. Tenailleau *et al.*, *'NMR Approach to the Quantification of Nonstatistical ^{13}C Distribution in Natural Products: Vanillin'*, Analytical Chemistry, 76.13 (2004), 3818–25.

[73] Ē. Kupce and R. Freeman, *'Stretched Adiabatic Pulses for Broadband Spin Inversion'*, Journal of Magnetic Resonance, Series A, 117.2 (1995), 246–56; M. R. Bendall and T. E. Skinner, *'Calibration of STUD+ Parameters to Achieve Optimally Efficient Broadband Adiabatic Decoupling in a Single Transient'*, Journal of Magnetic Resonance, 134.2 (1998), 331–49.

The application of adiabatic pulses is widely described for heteronuclear broadband decoupling. Even when excitation-free intervals are inserted between successive pulses the superior cyclicity still can be achieved. Due to this phenomenon reduction of sample heating, in comparison with the standard decoupling techniques (involving continuous irradiation), benefits in obtaining low sensitivity to RF. The only parameters that are sufficient for the peak power requirements are the one of the adiabatic pulses used. In general they are corresponding to the power requirements of broadband decoupling by WALTZ-16.[74] However, this is too imperfect to provide quantitative spectra.

Tenailleau and Akoka[75] in their paper presented a novel approach to the previously mentioned problems and were able to make improvements of the adiabatic proton decoupling. The optimization of the parameters was based on the minimum adiabaticity in order to perform quantitative measurements of ^{13}C intensities with high accuracy, close to 1‰.

2.2.2.2.2 Sample preparation

Sample preparation requires the selection of the proper solvent to perform ^{13}C NMR measurements. For each type of the molecule the chosen solvent will differ on the basis of the following points:

1. Solvent with good NMR properties
2. High solubility of the sample
3. Chemical shift of the solvent does not overlap with the peaks coming from the sample
4. Lack of interactions with the compound (solvent needs to be inert towards the sample).

Depending on the size of the molecule the solvents should be of different viscosities. What will be sufficient for small molecules (high viscosity solvents)[76] won't suit the large ones, for which the viscosity needs to be possibly lowest in order to obtain the proper T_1 values for isotopic measurements (see sections 5.1.2.3 and 5.2.4.2. which contain methodological approach in terms of NMR solvents for studied molecules).

It is not always easy to satisfy points N°1 and N°2. For example, all amino acids methyl esters were measured in deuterated DMSO, in which they showed good solubility, hence DMSO has a high viscosity which reduce the T_1 values (see Section 2.2.2.2.3 below).

The importance of point N°4 can be illustrated by two examples. The first involves impurities in the NMR solvent. Solvents used for spectral acquisition that carry some impurities are an additional, unexpected and potentially variable source of error. Slow exchange with hydrogen positions in the analyte can be caused by the traces of deuterated impurities in the solvent. It was found that this can lead to a level of ^{13}C-^{2}H interaction that is not present in the original analyte and an associated chemical shift. In ^{13}C spectra for the hydroxyl chemical function this

[74] Z. Starcuk *et al.*, *'Heteronuclear Broadband Spin-Flip Decoupling with Adiabatic Pulses'*, Journal of Magnetic Resonance, Series A, 107.1 (1994), 24–31.
[75] E. Tenailleau and S. Akoka, *'Adiabatic ^{1}H decoupling scheme for very accurate intensity measurements in ^{13}C NMR'*, Journal of Magnetic Resonance, 1 (185), (2007), 50-58 .
[76] L. A. Luck and C. R. Landis, *'Aprotic, Viscous Solvent Mixtures for Obtaining Large, Negative NOE Enhancements in Small Inorganic and Organic Molecules: Ideal Solvent Systems for Deducing Structures by NMR Techniques',* Organometallics, 11.2 (1992), 1003–5.

phenomenon is well described[77] and in overall view the resonance frequency of the ^{13}C signal from ^{13}C-^{2}H is more shielded. Hence, in cases where the exchange of the hydroxyl group between the OH and O^{2}H forms is slow (in terms of NMR time scale), separate ^{13}C signals coming from C-O^{2}H and C-OH are observable. Their intensities reflect the population of each molecular species. The associated chemical shift change (α shift) is defined as:

$$\Delta^{13}C = \delta^{13}C_{OH} - \delta^{13}C_{O^2H} \qquad \textit{Equation 19.}$$

where $\delta^{13}C$ is the carbon chemical shift (in ppm) in the molecule containing OH and O^{2}H respectively. $\Delta^{13}C$ is largest for the α shift (liked carbon), but can also occur for the β (two bonds) and the γ (three bonds) effect: $\Delta^{2}C(^{2}H)$(or Δβ) and $\Delta^{3}C^{2}H$)(or Δγ), respectively.[78]

A second example of this is given in Chapter III for the O-Me group of methyl esters of amino acids in fully deuterated MeOH. In this case, exchange of the O-Me between ester and solvent caused distortion of the spectral peak (see section 3.3.2.1).

2.2.2.2.3 Intrinsic NMR properties of the target molecule

A crucial parameter for isotopic measurements is the T_1. When the system is endeavouring to reach thermal equilibrium the process is called relaxation and T_1 is the relaxation time, which is defined as a time constant that characterizes the first order processes. T_1 (spin-lattice or longitudinal) relaxation time is a value that quantifies the energy transfer from the nuclear spin system to the adjacent molecules. It is related to restoration of the Boltzmann equilibrium, because the relaxation occurs along the z-axis and is described by:

$$T_2 = \frac{1}{\pi V_{1/2}} \qquad \textit{Equation 20.}$$

where $V_{1/2}$ is the width of the peak at half of its height.

Lack of ways of transferring the NMR energies into thermal energy can make the T_1 values relatively long. For quantitative analysis, it is necessary to allow the nuclear spin system to relax back to the equilibrium before the occurrence of the next pulse.[79] Thus, the T_1 value dictates the recycle delay (time period) between pulses. Relaxation parameters are different for every molecule and for each molecule-solvent combination. For each carbon of the structure, the T_1 will differ, so the adjustments needs to be applied and unified for all of them to assure the proper conditions and clarity of the spectra. If one of the peaks shows a high value for T_1 (long time is consider to be above 1 s) the delay between the pulses is too long in comparison to other

[77] J. Reuben, *'Isotopic Multiplets in the Carbon-13 NMR Spectra of Polyols with Partially Deuterated Hydroxyls. 3. Fingerprints of Molecular Structure and Hydrogen Bonding Effects in the Carbon-13 NMR Spectra of Monosaccharides with Partially Deuterated Hydroxyls'*, Journal of the American Chemical Society, 106.21 (1984), 6180–86; J. Reuben, *'Effects of Solvent and Hydroxyl Deuteration on the Carbon-13 NMR Spectrum of D-Idose: Spectral Assignments, Tautomeric Compositions, and Conformational Equilibria'*, Journal of the American Chemical Society, 107.21 (1985), 5867–70.

[78] A. Gilbert *et al.*, *'Impact of the Deuterium Isotope Effect on the Accuracy of ^{13}C NMR Measurements of Site-Specific Isotope Ratios at Natural Abundance in Glucose'*, Analytical and Bioanalytical Chemistry, 398.5 (2010), 1979–84.

[79] 'University College London - Short Lectures for NMR'.

peaks, making it difficult to achieve complete nuclear relaxation. Some adjustment can be made by modifying acquisition conditions. One of the properties of T_1 is that its values are temperature dependent. Thus, by changing the temperature, better acquisition is possible see Section 4).

Another way to decrease T_1 and to improve the spectral acquisition times is to add a relaxation agent. This has the effect of notably shortening the T_1, as electron-nuclear dipole-dipole relaxation becomes more efficient with increasing concentration. *Tris-acetylacetonatochromium* ($Cr(acac)_3$) is one of the most commonly used relaxation reagent for irm-^{13}C NMR measurements. Its non-labile organic ligand prevents chemical interaction of the chromium (III) with the NMR sample.[80] Its addition allows significant reduction of the acquisition time required for collecting the spectra, which is crucial in irm-^{13}C NMR that requires 5 of high quality (S/N>650) spectra.

All of these influence the quality of the spectra and need to be controlled. can make the measurement impossible for some of compounds. Taking as an example tyrosine methyl ester, which caused several problems, the proper choice of solvent was crucial (see Section 3.3.2.1.).

The nuclear Overhauser effect (NOE) mentioned above is of great importance, for irm-^{13}C NMR. It is defined as a 'change in the integrated nuclear magnetic resonance (NMR) absorption of intensity of a nuclear spin when the NMR absorption of another spin is saturated'.[81] Involved spins can be of different nature: heteronuclear or chemically shifted homonuclear.[82] In both cases, distortion of the quantitative relationship in the spectrum is likely to occur. As a result of the NOE, the intensities of the carbon signals attached to protons are increased, leading to distortions in the relative areas under the peak.

The molecular weight of the compound shouldn't be overlooked. It has a great impact on measurements and their quality. Molecules of higher mass (e.g. Tramadol = 263.4 g/mol) can cause significant difficulties in collecting the spectra, due to the number of carbons observed. This leads to dilution of signal intensity (the equivalent carbons are giving only one peak), as well as the difficulty of overlapping peaks. Larger molecules also tend to have poor NMR properties.

2.2.2.2.4 Spectral treatment

irm-^{13}C NMR requires approximately 1‰ precision for measuring the area under the peak. This demands specialised treatment of the spectrum – more than a standard integration. To obtain the area under the ^{13}C-signal for C-atom in position *i* curve fitting based on a total-line-shape analyses (deconvolution) is carried out with a Lorentzian mathematical model. Most suitable for this purpose is the software supplied by Perch Solutions - PERCH.[83] In this procedure, line-shape parameters are optimized in terms of intensities, frequencies, line-width, line-shape (Gaussian/Lorentzian, phase, asymmetry) by iterative fitted to a minimal residue. All line-fitting should be performed by the same operator. In order to obtain position-specific values ($\delta^{13}C_i$) by irm-^{13}C NMR, it is also necessary to determine $\delta^{13}C_g$ by irm-EA/MS, as will be illustrated below.

---

[80] G. C. Levy and J. D. Cargioli, *'Spin-Lattice Relaxation in Solutions Containing Cr(III) Paramagnetic Relaxation Agents'*, Journal of Magnetic Resonance, 10.2 (1973), 231–34.
[81] J. Noggle, *The Nuclear Overhauser Effect* (Elsevier, 2012).
[82] D. Neuhaus *et al.*, *The Nuclear Overhauser Effect in Structural and Conformational Analysis* (VCH New York, 1989).
[83] Perch^{TM} NMR Software, http://www.perchsolutions.com

3 Chapter III – Isotope distribution in amino acids

3.1 Amino acids - overview

3.1.1 Amino acid pathways and classification

Amino acids contain both an amine group and a carboxyl group. At biological pH (c. 7), both these groups are charged, so they are zwitterionic. They are distinguished by their side chain, (R-group), which confers on each amino acid its specific structure, character and precise chemical properties. They are high-melting, water-soluble, and colourless solids. Due to their basic and acidic functions they each have unique pK_a's, although these all fall within a narrow range of values (with the exception of histidine). Amino acids are best known as the monomer building blocks of proteins, in which 20 amino acids are normally found. However, several of these also perform many other tasks within living cells. Examples include the role of L-arginine as a precursor of polyamines and alkaloids, and L-methionine which acts as methyl group donor (see Chapter IV).

We can also identify a whole range of amino acids that are not incorporated into protein, which possess special functions, many within plants but also in marine organisms and some lower orders. As an example L-canavanine is a highly toxic nonprotein amino acid analogue of L-arginine and has been found in some leguminous seeds such as jack bean (*Canavalia ensiformis*) and alfalfa (*Medicago sativa*).[84] Because of its structural similarity to L-arginine, L-canavanine acts as an antimetabolite.

There are several ways of classifying amino acids into groups or subgroups, but for this research project, the most important and suitable approach is to use a division into families of amino acids based on their biosynthesis, as shown in Figure 4.

[84] S. Natelson, *'Canavanine to Arginine Ratio in Alfalfa (Medicago Sativa), Clover (Trifolium), and the Jack Bean (Canavalia Ensiformis)'*, Journal of Agricultural and Food Chemistry, 33.3 (1985), 413–19.

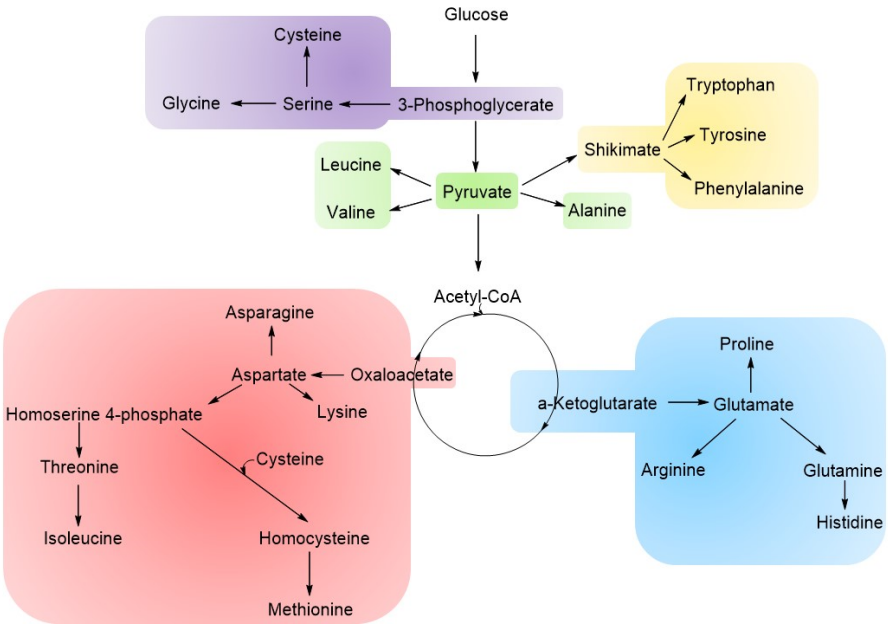

Figure 4. Overall scheme of amino acids families

We can distinguish five main groups that are taking their origin from pyruvate, oxaloacetate, 3-phosphoglutarate, shikimate and *α*-ketoglutarate. In the case of pyruvate there are two subgroups leading to the formation of alanine, leucine and valine. For serine and glycine, in some plants, a significant source of these amino acids are from photorespiration.

From each of these groups, representative amino acids were chosen for study based on their structural features and significance (Figure 5). The representative of the 3-phospho-D-glycerate group is serine. From the pyruvate family, we have studied valine and alanine. From the oxaloacetate family threonine, methionine and lysine were selected (studies of methionine are developed in Chapter IV). From the α-ketoglutarate family, glutamate and glutamine were chosen. This selection was not random. Among these amino acids are examples of those with a functional group possessing a hydroxyl, an amine, a carboxylic acid, a phenolic function and an *S*-methyl function. This wide range of different structural properties allowed us to create a suitable test group for tracking down isotopic variation in relation to biosynthesis. The choice was also partially dictated by the availability of these amino acids from natural sources.

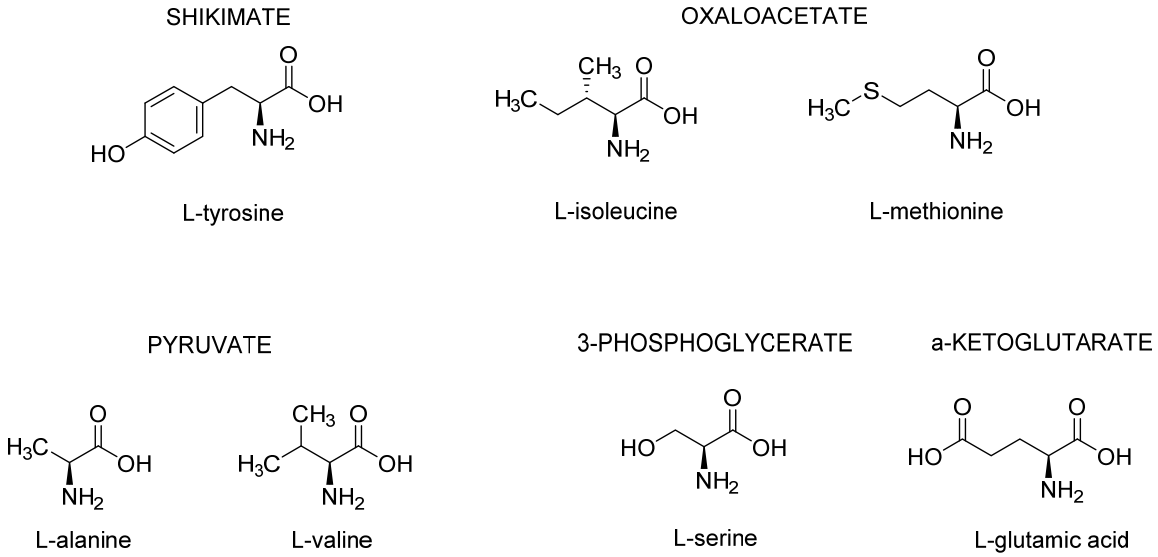

Figure 5. Structures of chosen amino acids from five groups

3.1.2 Prior studies of isotopic fractionation in amino acids

Understanding the causes of intramolecular isotopic fractionation during the overall processes of amino acids metabolism is useful for elucidation of biosynthetic pathways in plants and the methyl transfer phenomenon leading to O-Me and N-Me groups.

3.1.2.1 Global values

Differences in isotope fractionation between plant or plant organs are caused by the different isotope ratios of the same element in relation to the individual components. It has been found by Hobbie and Werner[85] that woody C_3 plants distribute more carbon to ^{13}C-depleted compounds (lignin, lipids) than is done by the herbaceous C_3 or C_4 plants. 'The isotopic heterogeneity of the organs and parts of plant is controlled by carbon isotope composition in biopolymers and their distribution among various parts of the plants'[86] – it can be deduced that physiological or external factors can simulate isotopic fractionation in the whole capacity of the organic matter due to their relative concentrations between or within different tissues or organs under the influence of previously mentioned factors. This can be a reason for misinterpretation of experimental data.

Several studies have focussed on the distribution of ^{13}C within amino acids obtained from photosynthetic organisms. As early as 1961, it was found that the amino acids in protein from photosynthetic microalgae possessed a range of $\delta^{13}C_g$ [‰] values.[87] Since then, similar data has been obtained for higher plants, including a clear indication that fractionation in C_3 and C_4

[85] E. A. Hobbie and R. A. Werner, *'Intramolecular, Compound-Specific, and Bulk Carbon Isotope Patterns in C_3 and C_4 Plants: A Review and Synthesis'*, New Phytologist, 161.2 (2004), 371–85.
[86] L. A. Kodina, *'Carbon isotope fractionation in various forms of biogenic matter: I. Partitioning of carbon isotopes between the main polymers of higher plant biomass*', Geochemistry International, 12 (48), (2010), 1157-1165.
[87] P. H. Abelson and T. C. Hoering, '*Carbon isotope fractionation in formation of amino acids by photosynthetic organisms*', Proceedings of the National Academy of Sciences of the United States of America, 5 (47), (1961), 623-632.

plants is not the same.[88,89] Tissue-specific variation within a plant has also been observed, and also that it differs between leaf and seed of the same plant.[90] Variation in $\delta^{13}C_g$ [‰] within a given amino acid is surprisingly independent of season, but was found to vary within plant groups.[91] In this study the authors were able to show that the $\delta^{13}C_g$ values of amino acids from leaf-protein could to some extent be linked to their biosynthesis and metabolism. It was concluded that the $\delta^{13}C_g$ values are influenced to a greater extent by differential partitioning of metabolic flux at branching points than the fractionation per se associated with de novo biosynthesis.

3.1.2.2 Intra-molecular values

Limited analysis of the positional distribution of ^{13}C within amino acids has been obtained. In the pioneering work of Abelson and Hoering, it was shown that the carboxyl positions of amino acids obtained from the proteins of microalgae were systematically relatively enriched in the carboxyl position.[43] These findings for photosynthetic growth are opposed to those in the organisms grown heterotrophically, where the absence of a major difference between carboxyl carbons of aspartic and glutamic acids and the other carbon of most of the other amino acids is observed. The possibility of carbon entering the protoplasm by other biochemical pathways than ribulose diphosphate was put forward due to the existence of substantial amounts of carbon of different and heavier character in carboxyl carbons during photosynthesis in algae. Savidge and Blair[92] showed that the total amino acid ^{13}C and the carboxyl ^{13}C values varied as might be expected from biosynthetic considerations, and noted that macroalgae had a significantly less enriched carboxyl C fraction than did either C_3 or C_4 vascular plants.[93] This they interpreted as due to their possessing a different β-carboxylation pathway.

Melzer and O'Leary[94] investigated the intramolecular distribution of ^{13}C in Asp in both C_3 and C_4 plants. They showed that the C4 position –COOH was significantly (3-10‰) richer than the mean of the whole molecule. This they interpreted as indicating an important role of PEPc in providing the carbon skeleton of oxaloacetate via the carboxylation of phosphoenolpyruvate. They also noted that the C4 of protein-derived Asp was consistently 5-10‰ richer than that of free Asp although the reason for this is not clear. These effects were more pronounced in C_3 than in C_4 plants. It is therefore not surprising that Asp is mentioned as being generally the 'heaviest' amino acid. From these precursors and their carboxyl groups are formed Asp, Homo-Ser, Trp, Ile and Met. The condensation of oxaloacetate with acetyl-CoA and the first steps of the citric acid cycle lead to α-ketoglutarate, preserving the newly introduced carboxyl group, and

---

[88] M. L. Fogel and N. Tuross, *'Extending the limits of paleodietary studies of humans with compound specific carbon isotope analysis of amino acids.'* Journal of Archaeological Science, 30(5), (2003), 535-545.

[89] T. Larsen *et al.*, '*Stable isotope fingerprinting: a novel method for identifying plant, fungal, or bacterial origins of amino acids.*' Ecology, 90(12), (2009), 3526-3535.

[90] A. H. Lynch *et al.*, *'Liquid chromatography/isotope ratio mass spectrometry measurement of $\delta^{13}C$ of amino acids in plant proteins.'* Rapid Communications in Mass Spectrometry*, 25*(20), (2011), 2981-2988.

[91] A. H. Lynch *et al.*, '*Variability in the carbon isotope composition of individual amino acids in plant proteins from different sources: 1 Leaves.'* Phytochemistry, 125, (2016) 27-34.

[92] W. B. Savidge and N.E. Blair, *'Patterns of Intramolecular Carbon Isotopic Heterogeneity within Amino Acids of Autotrophs and Heterotrophs'*, Oecologia, 139.2 (2004), 178–89.

[93] W. B. Savidge and N. E. Blair, '*Patterns of intramolecular carbon isotopic heterogeneity within amino acids of autotrophs and heterotrophs.'* Oecologia, 139, (2004), 178-189.

[94] E. Melzer and M. H. O'Leary, *'Aspartic-acid synthesis in C_3 plants.*' Planta 185, (1991), 368-371.

providing the carbon skeleton for Glu, Pro, Arg, ornithine, and citruline. It might be expected, therefore, that these related amino acids will also show this common feature.

The aim of this part of the study is to prove a methodology by which access to $\delta^{13}C_i$ values for all carbon positions in an amino acid can be obtained.

3.2 Methodology for methylation

3.2.1 Method development

Amino acids are structurally not readily amenable to irm-^{13}C NMR. Many are poorly soluble in apolar solvents because their zwitterionic character means that they always carry a charge. Therefore, a strategy was developed to derivatize the carboxyl and amine functions, rendering them less polar and more soluble in organic solvents with good properties for NMR spectrometry.

Several techniques were tested. An initial approach used 2,2-dimethoxypropane to methylate the COOH and methylchloroformate to methoxycarbonylate the amine function.[95] But, this method necessitated phase extraction of the derivative under conditions that let to partial degradation of the methyl ester. However, it was useful in indicating that the amine group did not need to be protected, and so subsequent approaches focussed on methylating the carboxyl function only.

Among several different methods of methylation the aim was to find one, which would be suitable for the whole range of amino acids. This was first attempted with thionyl chloride[96] and subsequently with diazomethane (produced in situ from trimethylsilyldiazomethane).[97] However, these methods did not prove reliable for a range of amino acids, giving variable yields and, in some cases, significant quantities of side-products. In terms of accessibility and ease of use the trimethylchlorosilane (TMSCl)/MeOH reaction was chosen. This approach gave good yields (> 90%) of amino acid methyl esters with a number of target amino acids, and was therefore without any introduction of perceptible isotopic fractionation. This method gave high purity compounds suitable for ^{13}C NMR measurements. It was confirmed that the esterification of the carboxyl function enhanced their physicochemical properties, notably solubility in an irm-NMR-compatible solvent (DMSO). The method itself consisted of several steps as described in the protocol below.

3.2.2 Method exploited

0.01 mol of amino acid (purity > 98%) was taken in a flame-dried round bottom flask. Depending on the amino acid, the amounts of reactant and solvent were adjusted separately. Amino acids with only one –COOH group were taken in 10 mL of methanol and stirred. TMSCl (0.02 mol) was added dropwise to the solution, then the flask was closed with a trap containing glass wool and $CaCl_2$ and left stirring between 16 and 48 h at ambient temperature. The reaction

[95] A. Lumbroso *et al.*, *'An Efficient and Scalable Synthesis of N-(Benzyloxycarbonyl)- and N-(Methyloxycarbonyl)-(S)-Vinylglycinol'*, Tetrahedron Letters, 51.24 (2010), 3226–28.
[96] J. Li and Y. Sha, *'A Convenient Synthesis of Amino Acid Methyl Esters'*, Molecules, 13.5 (2008), 1111–19.
[97] V. B. Oza *et al.*, *'Synthesis, Structure, and Activity of Diclofenac Analogues as Transthyretin Amyloid Fibril Formation Inhibitors'*, Journal of Medicinal Chemistry, 45.2 (2002), 321–332.

was monitored with TLC. In the case of compounds containing in their structure two -COOH groups, four equivalents of reagent were introduced (Figure 6).

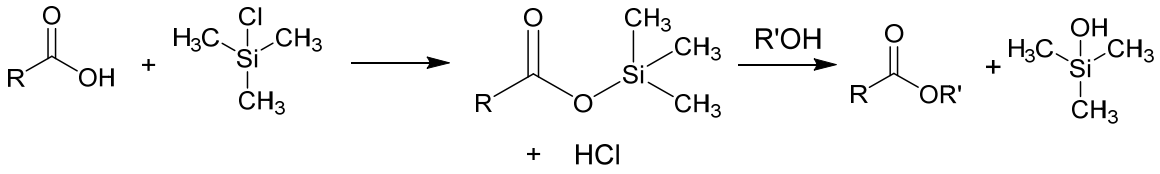

Figure 6. General scheme for the methylation of amino acids with TMSCl

After completion of the reaction, solvent, HCl and excess reagent were removed *in vacuo* and the residue washed several times with MeOH and diethyl ether (evaporation under reduced pressure after each wash). Following further removal of solvent under reduced pressure, the sample was powdered and stored in the fridge. Yields were essentially quantitative, with between 3 and 8% underivatised amino acid present. No attempt was made to remove this, so as to avoid any possible isotopic fractionation.

For a number of amino acids (e.g. L-isoleucine), the derivatisation only reached about 75% with the initial treatment. In such cases, a second cycle of treatment with TMSCl was carried out. This protocol gave yields that were essentially quantitative, with between 3 and 8% underivatised amino acid present. No attempt was made to remove this, so as to avoid any possible isotopic fractionation.

3.3 Methodology for spectral acquisition

3.3.1 Sample preparation

The necessity of making derivatives of amino acids impacts strongly on the sample preparation for irm-^{13}C NMR. Isotopic measurements require several conditions to be fulfil, among which the purity of the sample (>98%) is a major one. It reflects on the quality of the spectra which should not contain any overlap of the peaks that would confuse the overall distribution of the peaks and base line. It also can influence the line-fitting performed with PERCH software for which it's necessary to have spectra with an appropriate signal to noise ratio and a well-phased base-line to make possible the calculation of the dispersion and curve fitting. Purity of the sample also ensures that impurities that can cause additional peaks will not interfere with the analysis.

Another major issues that causes difficulties with proper spectral recording is the variability of the T_1 values for separate peaks (see Section 2.2.2.2.2. for a general discussion of this phenomenon). For complicated amino acids and natural compounds (above 10 carbon atoms) these can vary considerably, which can cause problems with establishing common conditions for spectral acquisition. Taking as an example tyrosine methyl ester, the range of T_1 values for individual peaks is from ~200 msec up to 12 sec. This extremely long T_1 makes it impractical to obtain the desired signal to noise ratio (>650) within a reasonable experimental duration. To solve this problem different approaches were applied, but these had to be adjusted individually for each target amino acid (see Section 3.4 below). To enhance quality of the spectra and shorten the T_1 values, various ploys were tested: varying the temperature of the probe; a mix of different

solvent to lower the viscosity that influences the T_1 values as well as the number of scans, acquisition time and delay values.

The time necessary to obtain single isotopic spectra shouldn't be neglected. While in theory an acquisition duration can be extremely long, this is impractical. In addition, there can be possible changes in the structure of the sample. In accordance with the overall procedure of sample preparation it should be noted that the best results will be obtained from freshly-prepared NMR tubes, thus avoiding degradation. For the amount of material used, see the Appendix.

3.3.2 Acquisition considerations

3.3.2.1 Solvent choice

To illustrate the importance of choosing the most suitable solvent for a given molecule, the example of spectral acquisition for Met methyl ester in MeOH-d_4 is presented in Figure 7. The problem that is visible on this figure occurred due to the initial use of deuterated methanol (MeOH-d_4) as NMR solvent. Five separate sequential spectra were acquired with the acquisition time of 4-5 h each. A slow spontaneous O-Me group exchange occurred between the target analyte and the solvent, which caused a degradation of the peak shape over time. Its width was enlarged, while the height gradually decreased as the analyte increasingly became a mixture of the deuterated and non-deuterated species at the methyl ester group.

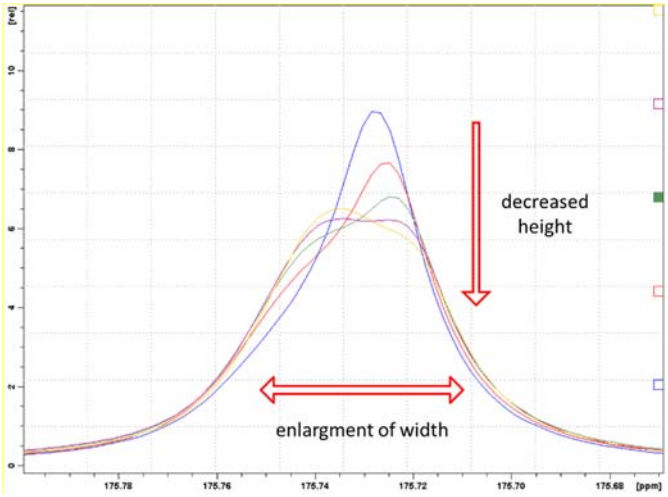

Figure 7. Sequential ^{13}C NMR spectra (5) for methionine methyl ester with the isotopic measurement in MeOH-d_4 showing the exchange effect between O-Me groups and solvent. First spectrum in blue, fifth spectrum in yellow

3.3.2.2 NMR acquisition conditions

Bayle et al[98] have shown that the NMR spectrometer designated CEISAM-400A has an imperfection in the decoupling homogeneity, which can lead to end effects at the extremes of the spectral width for molecules that have a large spectral range. Amino acids, on a 400 MHz

[98] K. Bayle *et al.*, *'Conditions to obtain precise and true measurements of the intramolecular ^{13}C distribution in organic molecules by isotopic ^{13}C nuclear magnetic resonance spectrometry'*, Analytica Chimica Acta, 846, (2014), 1-7.

spectrometer show a spectral range from 2000 to 17000 Hz, due to the presence of the carboxylic acid group and methyl groups.

In order to investigate the influence of this on the values of $\delta^{13}C_i$ [‰] obtained, the same sample of alanine was run on both the CEISAM-400A and CEISAM-400B spectrometers. The latter is considered to give 'truer' values, due to the configuration of the acquisition window, but is less sensitive and therefore less well adapted to running a larger number of samples. A comparison of the 'A' and 'B' spectra showed only small differences in the values of $\delta^{13}C_i$ [‰] obtained, as shown in Table 3.

Table 3. $\delta^{13}C_i$ [‰] values obtained for alanine from two spectrometers – 400A and 400B, with calculated correction factor

Corresponding carbon	***$\delta^{13}C_i$ [‰]***		
	400A	**correction factor**	**400B**
C=O	-20.80	**2.12**	-18.68
CH	-24.02	**-1.32**	-25.34
CH_3	-23.04	**-0.81**	-23.85

This correction in itself can introduce a significant error, compounding that from the spectral acquisition. Therefore, it was decided not to make any systematic correction to the values calculated from the spectra obtained on the CEISAM-400A, but to compare these directly one with another. As the different amino acids were all measured on the same spectrometer under similar conditions, any small deviation from trueness should be comparable within the dataset.

All results presented for amino acids methyl esters in this thesis does not include $\delta^{13}C_i$ values coming from O-Me groups. This approach was taken due to the fact that all the O-Me groups were added through the derivatization procedure (to enhance the solubility of the samples) and does not constitute data of any interest. They have been removed from the presented figures to improve clarity of the presented results and to focus on the other carbon positions studied.

3.4 Results and discussion

3.4.1 Amino acids belonging to the Pyruvate Family

3.4.1.1 Alanine

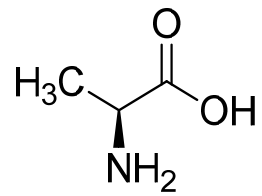

structure of L-alanine

Certificate of Origin Information

Source: Sigma-Aldrich
Origin: synthetic
Product Number: 05129
Product Name: L-Alanine
Quality: BioUltra, ≥ 99.5% NT
Lot Number: BCBM6312V

Origin: Chemical synthesis/chemical transformation.
CAS: 56-41-7

Alanine labelled as 'natural' is not available commercially. Biosynthesis of this amino acid goes through a simple transamination from pyruvate. The sample used in this studies was purchased from Sigma-Aldrich and was obtained by chemical synthesis/chemical transformation.

The values of $\delta^{13}C_i$ for alanine methyl ester (400A CEISAM) are illustrated in Figure 8. Despite its non-natural origin, it shows a profile that is compatible with natural products. As it was expected from data gathered by Abelson and Hoering[99] and Savidge and Blair[100], the C=O group is richer in ^{13}C than the CH group. Thus, the presented range of $\delta^{13}C$ values for the C3 position is compatible with a natural origin from a C_3 plant.

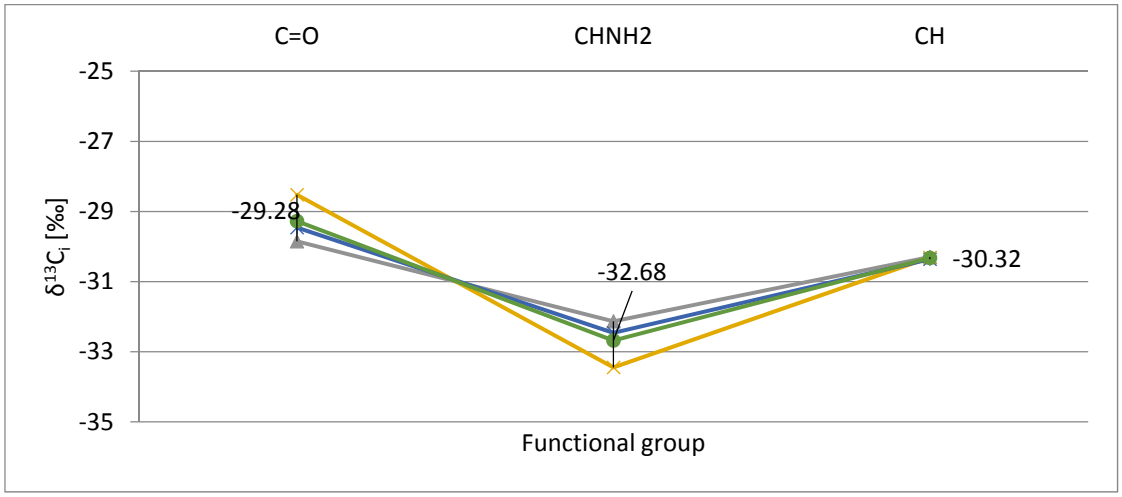

Figure 8. Values of $\delta^{13}C_i$ [‰] for L-alanine in respect to functional group position. The graph shows 3 sequential spectra from one acquisition and the mean values (green)

[99] P. H. Abelson and T. C. Hoering, *'Carbon isotope fractionation in formation of amino acids by photosynthetic organisms',* Proceedings of the National Academy of Sciences of the United States, 47 (5), (1961), 623-632.
[100] W. B. Savidge and N. E. Blair, *'Patterns of Intramolecular Carbon Isotopic Heterogeneity within Amino Acids of Autotrophs and Heterotrophs'*, Oecologia, 139 (2), (2004), 178–89.

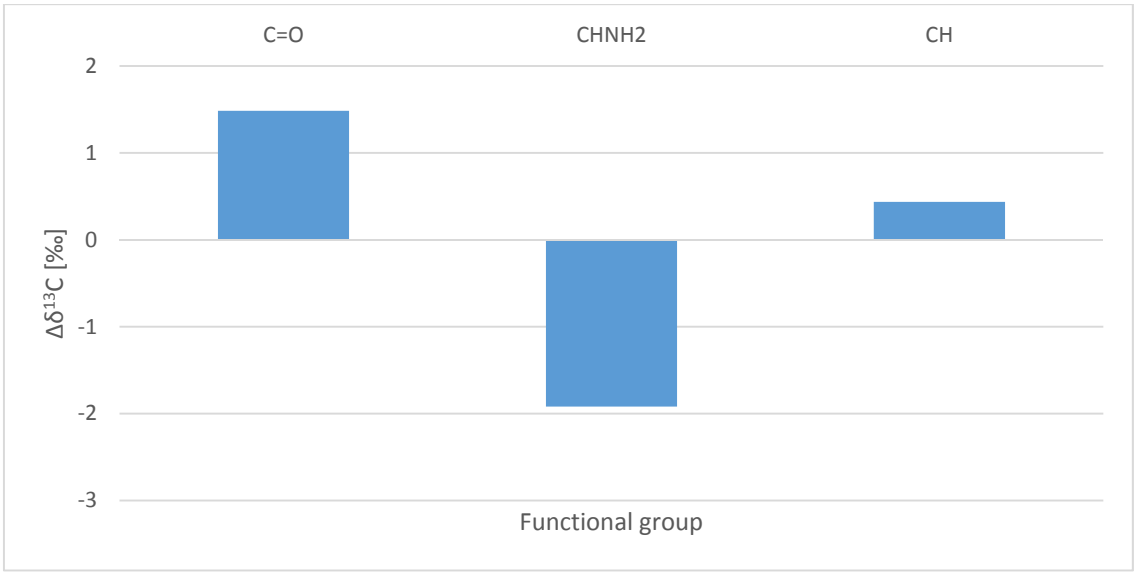

Figure 9. $\Delta\delta^{13}C$ deviation for L-alanine

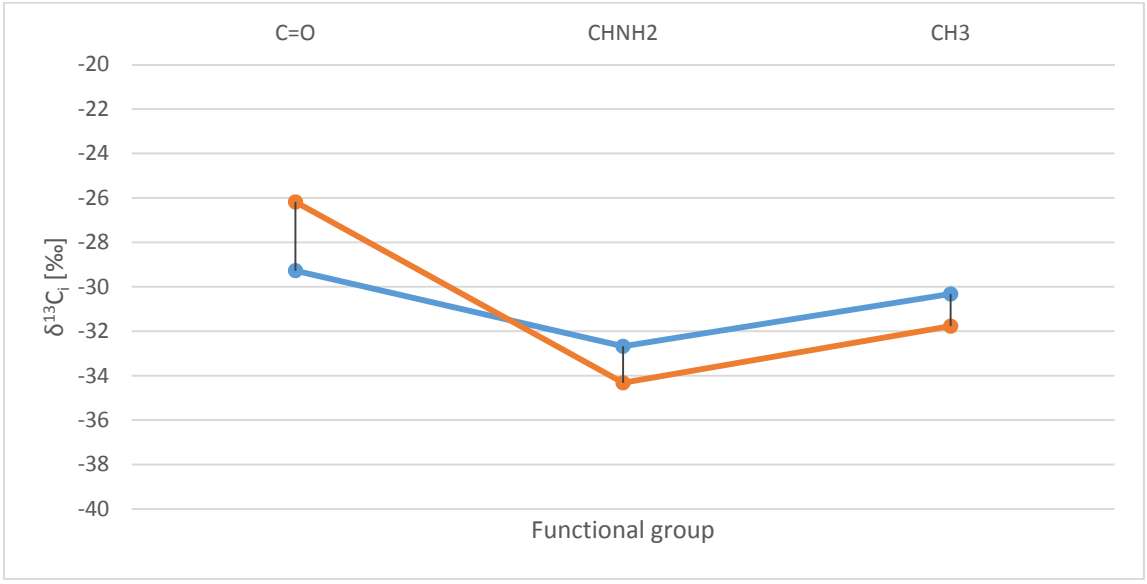

Figure 10. Comparison of obtained $\delta^{13}C_i$ [‰] values obtained for L-alanine by the measurements on two spectrometers – 400A (blue) and 400B (ochre)

It can therefore be tentatively suggested that the synthon is natural, but it has undergone chemical modification. Most commonly used reactions for alanine synthesis are condensation of acetaldehyde with ammonium chloride (in the presence of sodium cyanide), ammonolysis of 2-bromopropanoic acid and the Strecker reaction. These are shown in Figures 11-13 respectively.

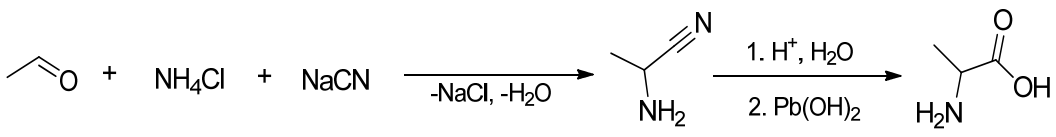

Figure 11. Alanine synthesis reaction scheme by acetaldehyde condensation with ammonium hydrochloride in the presence of sodium cyanide

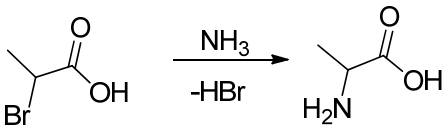

Figure 12. Alanine synthesis reaction scheme by ammonolysis of 2-bromopropanoic acid

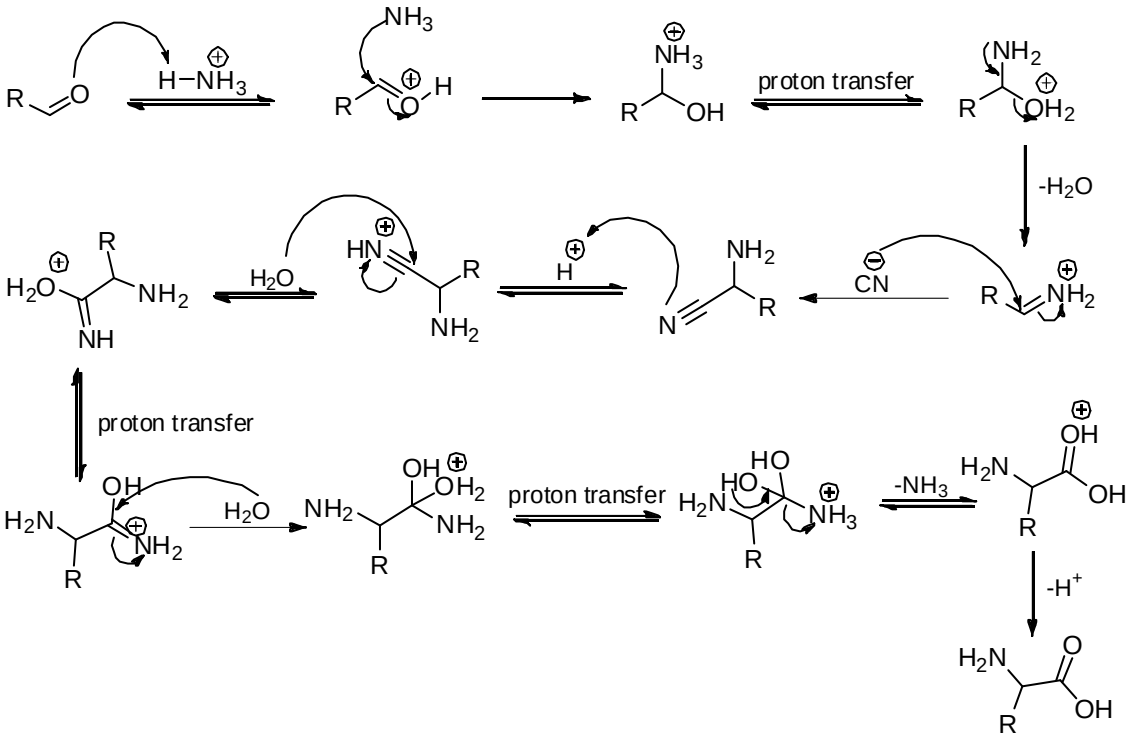

Figure 13. Strecker reaction mechanism for synthesis of amino acids

As none of these reactions involve a product directly obtained from a plant or microbial origin, it must be concluded that this correlation is coincidental. There is a need to isolate alanine from plant source to study its natural profile.

3.4.1.2 Valine

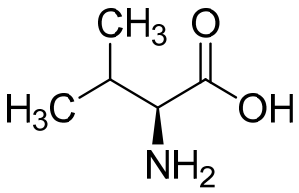

Structure of L-valine

Certificate of Origin Information

Source: Sigma-Aldrich
Origin: natural
Product Number: 94619
Product Name: L-Valine
Quality: BioUltra, ≥ 99.5% NT
Lot Number: BCBM1923V
Origin: Fermentation/ from cell culture
CAS: 72-18-4

Valine has a more complexed structure than alanine but is also derived entirely from pyruvic acid. However, the pathway is much more complex and involves the condensation of 2 molecules of pyruvate, a rearrangement reaction to provide the branched chain, and transami-

nation to insert the amine group (Figure 14). [101] The L-valine used is of natural origin being made by fermentation.

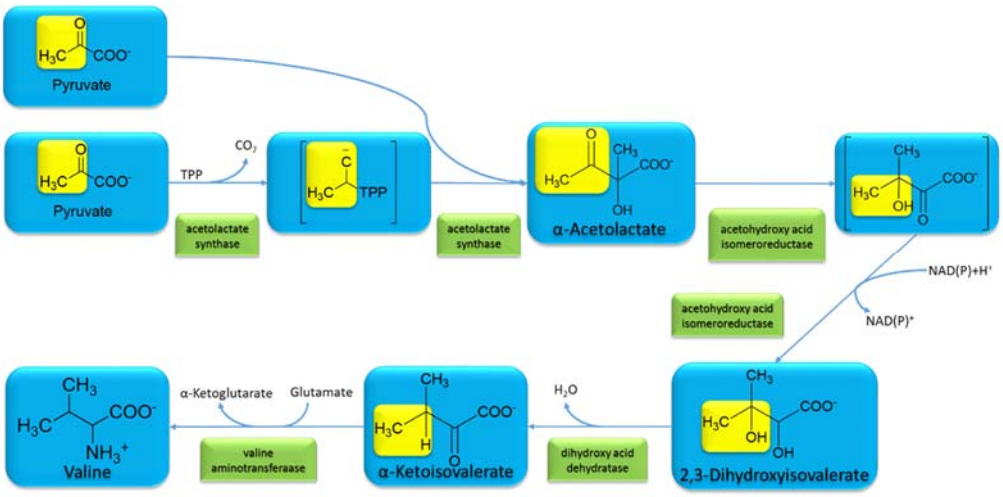

Figure 14. Biosynthetic origin of valine

Position specific $\delta^{13}C_i$ data for L-valine are illustrated in Figure 15. As expected, the range of values fits its natural origin from a C_3 plant source.[102] The $\delta^{13}C_g$ of -32‰ is in the ranges reported for C_3 plants, whereas values around -19‰ for C_4 cereals (seed). In contrast to amino acids from photosynthetic origin, the C=O is considerably depleted in ^{13}C relative to the bulk molecule, as found previously for amino acids of heterotrophic origin. Nonetheless, the value of -54‰ for the C=O indicates a surprisingly high impoverished, in contrast to the general rule indicated by Abelson and Hoering.[103] Further work is required to confirm whether not this is a realistic value. However, it does help to explain why valine from plant sources has an overall low $\delta^{13}C$ value in comparison to other amino acids.

[101] K. Thomazeau *et al.*, '*Structure of Spinach Acetohydroxyacid Isomeroreductase Complexed with Its Reaction Product Dihydroxymethylvalerate, Manganese and (Phospho)-ADP-Ribose'*, Acta Crystallographica. Section D, Biological Crystallography, 56.Pt 4 (2000), 389–97.

[102] A. H. Lynch *et al.*, *'Liquid Chromatography/isotope Ratio Mass Spectrometry Measurement of $\delta^{13}C$ of Amino Acids in Plant Proteins'*, Rapid Communications in Mass Spectrometry, 25.20 (2011);A. H. Lynch *et al.*, '*Variability in the carbon isotope composition of individual amino acids in plant proteins from different sources: 1 Leaves',* Phytochemistry, 125, (2016), 27-34.: T. Larsen *et al.*, '*Tracing carbon sources through aquatic and terrestrial food webs using amino acid stable isotope fingerprinting*',PLOS ONE, 8 (9), (2013), e73441; Absolute values provided as a personal communication

[103] P. H. Abelson and T. C. Hoering, '*Carbon isotope fractionation in formation of amino acids by photosynthetic organisms',* Proceedings of National Academy of Sciences of the United States, 47 (5), (1961), 623-632.

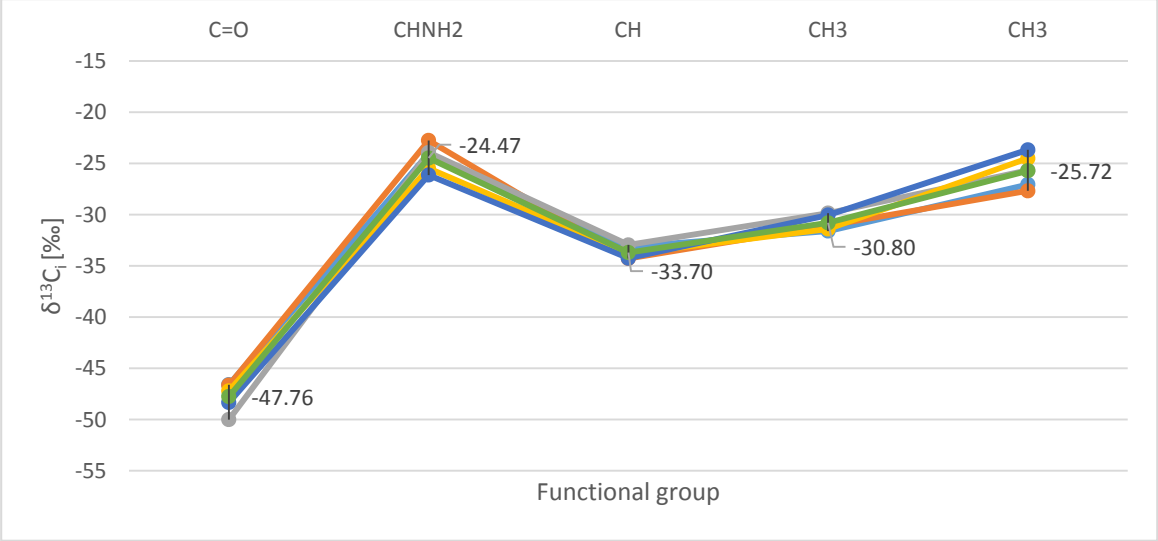

Figure 15. $\delta^{13}C_i$ [‰] values for L-valine corresponding functional groups positions obtained by irm-^{13}C NMR measurements for 5 separate spectral acquisitions; mean values (green line) are displayed on the chart

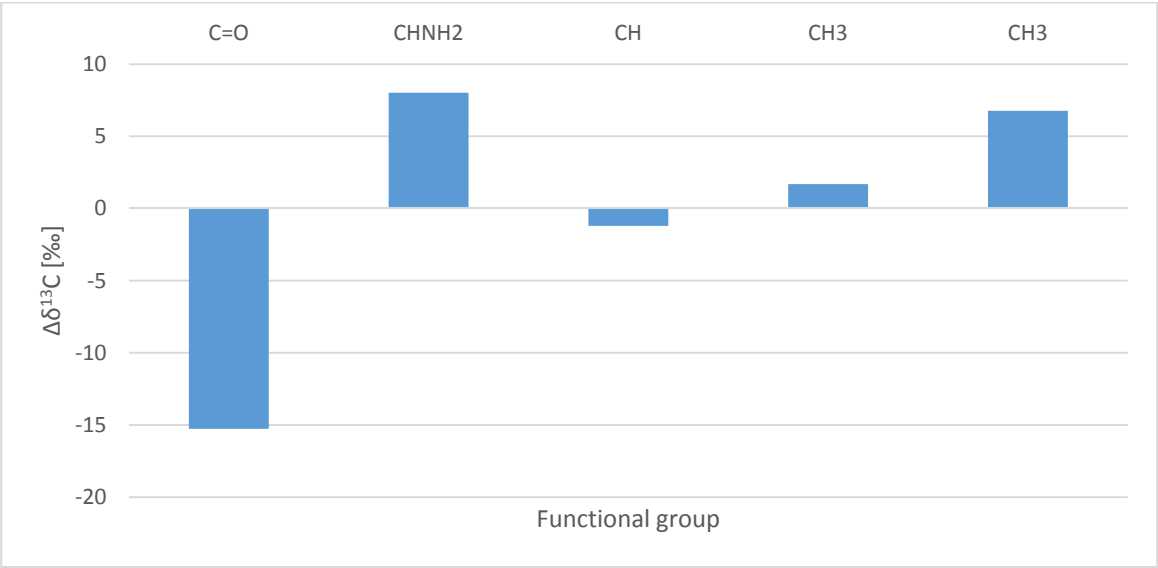

Figure 16. $\Delta\delta^{13}C$ values for L-valine for corresponding functional groups positions

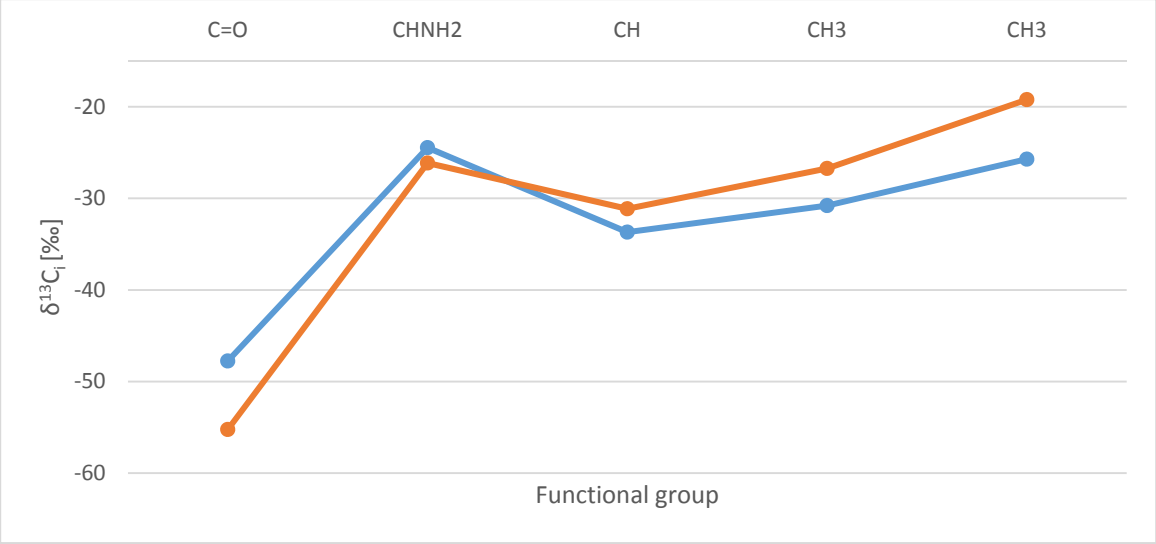

Figure 17. Comparison of results obtained for L-valine between two 400 MHz spectrometers; 400A (blue) vs 400B (ochre)

In the biosynthesis of valine there is a highly unusual methyl transfer reaction carried out by acetohydroxy acid isomeroreductase (Fig. 14). This enzyme has been the subject of considerable attention, it catalyses the shift of the methyl of α-acetolactate to the adjacent carbon nearby forming 2,2-dihydroxyisovalerate.

In this context it is interesting to see that the 2 methyl groups of valine do not show the same $\delta^{13}C$ values, the difference between the two being approximately 9‰. It can be hypothesised that this difference is due to fractionation associated with the vicinal transfer in the shifted group, which undergoes bond cleavage and formation, and a selection against ^{13}C. The other group, in contrast undergoes no such displacement. The mechanism of the enzyme has been carefully investigated (Fig. 18) and the implied breaking of a sp^3 bond followed by the creation of an sp^3 bond would be expected to select against ^{13}C at both events.

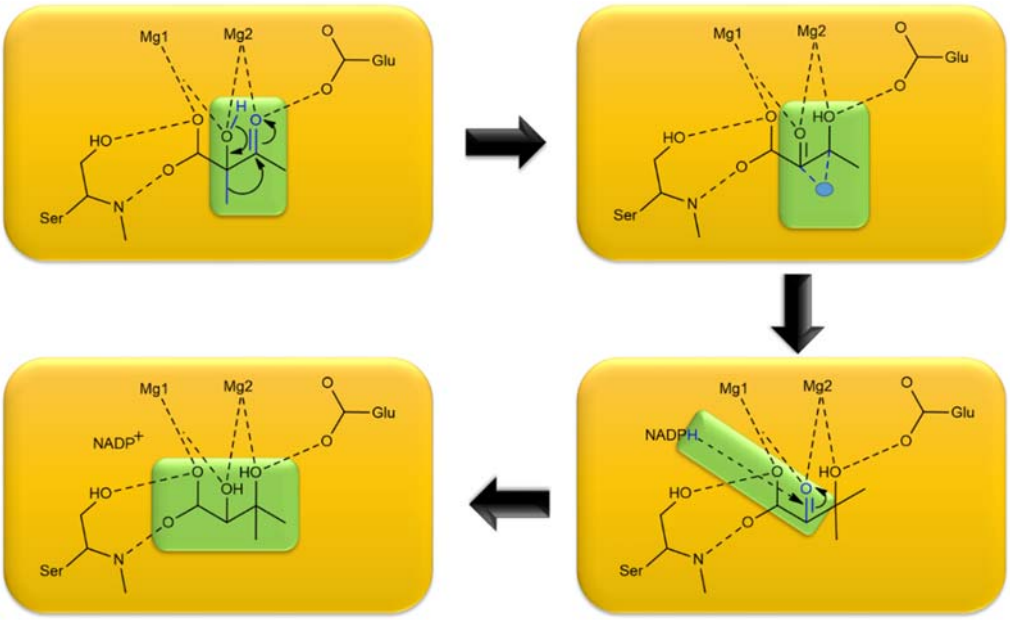

Figure 18. Proposed mechanism of valine synthesis by acetohydroxy acid isomeroreductase

3.4.2 Amino acids belonging to the 3-Phosphoglycerate Family

3.4.2.1 Serine

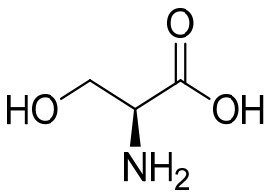

structure of L-serine

Certificate of Origin Information

Source: Sigma-Aldrich
Origin: natural
Product Number: 84959-25G
Product Name: L-Serine
Quality: BioUltra, ≥ 99.5% NT
Lot Number: 1349921V
Origin: Purification/extraction from biological material
CAS: 56-45-1

The L-serine used is of natural origin, being extracted from animal and avian protein. In these animals, L-serine is not an essential amino acid, and therefore it can be considered that this sample is from animal origin. Natural serine that is coming from biological origin shows an overall value of $\delta^{13}C_g$ of -13.5‰, very close to those obtained from legume, wheat or pseudo cereals (C_3 plants), but lower than that from C_4 cereals, as found by Lynch.[104] This indicates that the L-serine analysed probably came from animals fed on a C_3-plant-dominated feedstuff.

The biosynthesis of serine from the glycolytic intermediate 3-phosphoglycerate does not involve the formation or breaking of any of the carbon bonds in this precursor. It consists of three steps with the 3-phosphoglycerate as a starting material, which goes under oxidation at first, then transamination to *O*-phosphoserine that is hydrolysed to form serine in the last step.

Only at the transamination on the C2 position is a carbon atom involved in the reaction. There is a transition sp^2 to sp^3, which could introduce some selectivity in favour of ^{13}C. However, transamination reactions do not, in general fractionate significantly[105], so the values measured should reflect the dietary source.

The range of $\delta^{13}C_i$ values seen are between -7 and -17‰ (Figure 19-20). The relatively high value compared with other amino acids may be due to enrichment by photorespiration, in which depleted CO2 is released.

[104] A. H. Lynch *et al.*, *'Liquid Chromatography/isotope Ratio Mass Spectrometry Measurement of $\delta^{13}C$ of Amino Acids in Plant Proteins'*, Rapid Communications in Mass Spectrometry, 25.20 (2011);A. H. Lynch *et al.*, '*Variability in the carbon isotope composition of individual amino acids in plant proteins from different sources: 1 Leaves',* Phytochemistry, 125, (2016), 27-34; T. Larsen *et al., 'Tracing carbon sources through aquatic and terrestrial food webs using amino acid stable isotope fingerprinting',* PLoS ONE, 8 (9), (2013), e73441.

[105] E. Weiss, *'Transaminase Activity and Other Enzymatic Reactions Involving Pyruvate and Glutamate in Chlamydia (Psittacosis-Trachoma Group)'*, Journal of Bacteriology, 93.1 (1967), 177–84; G. Tcherkez, M. Hodges, *'How Stable Isotopes May Help to Elucidate Primary Nitrogen Metabolism and Its Interaction with (Photo)respiration in C_3 Leaves'*, Journal of Experimental Botany, 59.7 (2008), 1685–93.

Gilbert et al[106] showed that the C1 and C6 of glucose from starch of a C_3 plant depleted relative to the C2 and C5 positions, while the C3 and C4 are the most enriched. This should lead to a pattern in serine of a COOH> $CHNH_2$>CH2OH. No such correlation is seen, indicating that post-ingestion metabolism has dominated over the nutritional source.

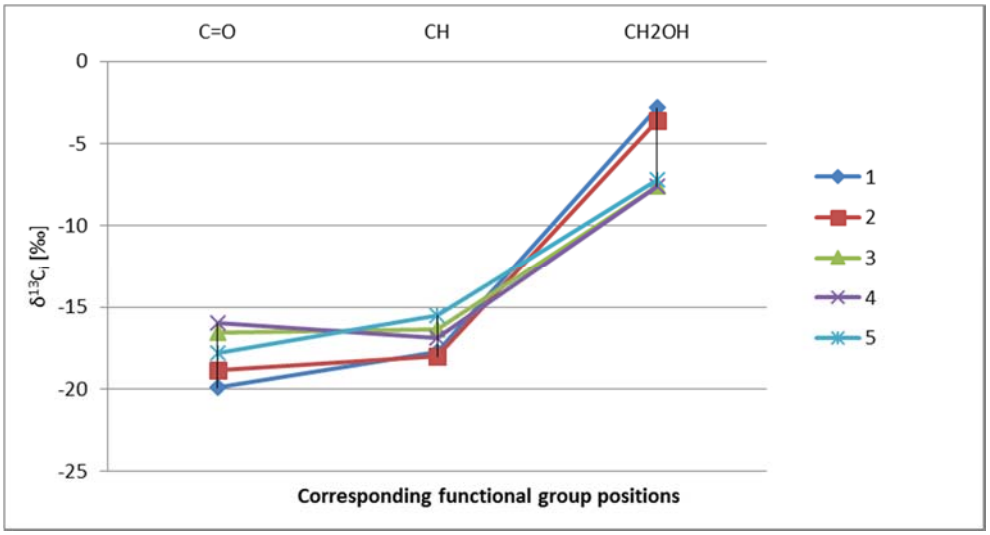

Figure 19. $\delta^{13}C_i$ [‰] values for corresponding functional group positions of L-serine obtained by irm-^{13}C NMR

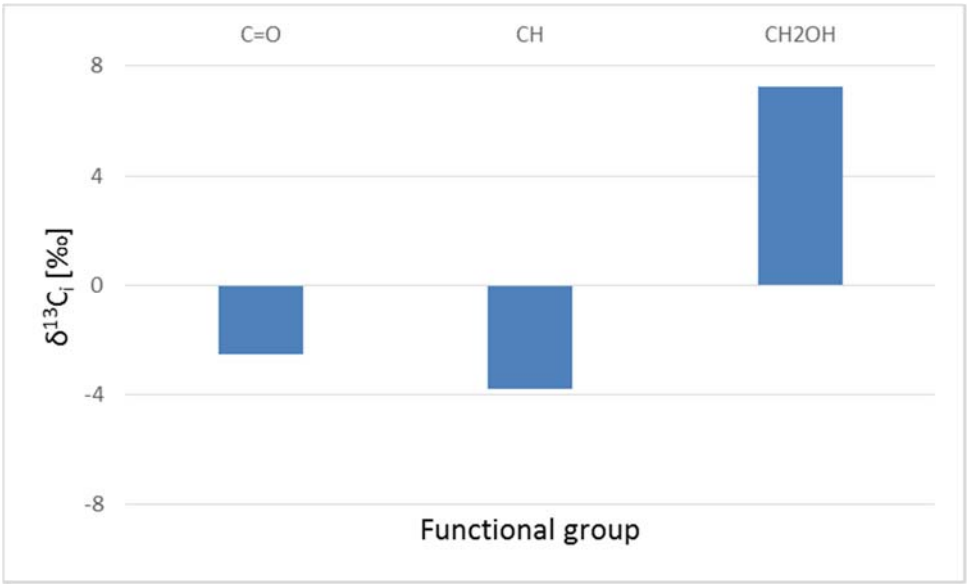

Figure 20. $\Delta\delta^{13}C$ values for L-serine

[106] A. Gilbert *et al., 'Accurate Quantitative Isotopic ^{13}C NMR Spectroscopy for the Determination of the Intramolecular Distribution of ^{13}C in Glucose at Natural Abundance',* Analytical Chemistry, 21 (81), (2009), 8979-8985.

3.4.3 Amino acids belonging to the Oxaloacetate Family

3.4.3.1 Isoleucine

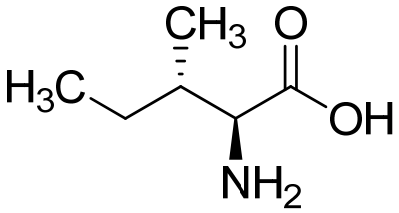

structure of L-isoleucine

Certificate of Origin Information

Source: Sigma-Aldrich
Origin: natural
Product Number: I2752-10G
Product Name: L-Isoleucine
Quality: BioUltra, >= 99.5% NT
Lot Number: SLBJ3502V
Origin: fermentation/microbial
CAS: 73-32-5

The L-isoleucine used is of natural origin being made by fermentation. The fermentation organism is not indicated. The $\delta^{13}C_g$ value of -13.64‰ indicates the use of a C_4 plant derived carbon source, as for serine (see section 3.4.2.1).

Isoleucine is, essentially, the higher homologue of valine, with a methyl group substituted by an ethyl group. This occurs by the second pyruvate molecule being replaced by a molecule of 2-oxobutanoate in the reaction of acetolactate synthase, the product being 2-aceto-2-hydroxybutanoate. As the 2-oxobutanoate unit is derived from threonine, isoleucine tends to be grouped with the other oxaloacetate-derived amino acids, although it could equally well be considered as part of the pyruvate-derived family. In most organisms, the same enzymes are involved in the different transformations (see Figure 4), the pathway thus being strictly parallel for these two amino acids: condensation, rearrangement to provide the branched chain, and transamination to insert the amino group (Figure 14). Mechanistically, the rearrangement by acetohydroxy acid isomeroreductase is identical to the scheme given in Figure 18, with the methyl group substituted by ethyl.

In order to verify that the peaks were correctly assigned, DEPT135 and HSQC spectra were acquired. This made it possible to confirm the assignment of the side-chain carbons in the CH_2, and two CH_3 groups and to confirm the assignments of the *O*-methyl and CH-NH_2. The numbering correlations between the NMR spectral displacements and the IUPAC numbering are:

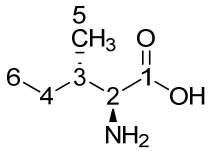

NMR numbering in order of peaks on the spectra numbered from high frequency to low frequency

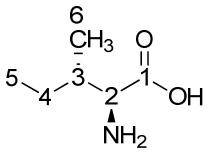

IUPAC numbering

When the $\delta^{13}C_i$ values are determined for natural isoleucine (Figures 21-22), several features are seen that differ markedly from the valine analysed and described above (section 3.4.1.2). First, the carboxyl function is richer than the C2 position by about 5‰, in contrast to that in valine made by fermentation. This might be explained by the different origin of this car-

bon: pyruvate in valine and threonine-derived 2-oxobutanoate in isoleucine. Secondly, the 2 methyl groups of isoleucine differ by about 9‰, as was found for valine. Here, however, a different explanation should be advanced: origins from pyruvate and 2-oxobutanoate. Nonetheless, in both amino acids it is seen that the carbon position which has undergone vicinal transfer – in this case the CH_2 of the ethyl moiety – is substantially impoverished relative to the other carbon positions. Once again, this can be interpreted as due to a fractionation in the shifted group associated with the transfer: the implied breaking of a sp^3 bond followed by the creation of an sp^3 bond would be expected to select against ^{13}C at both events.

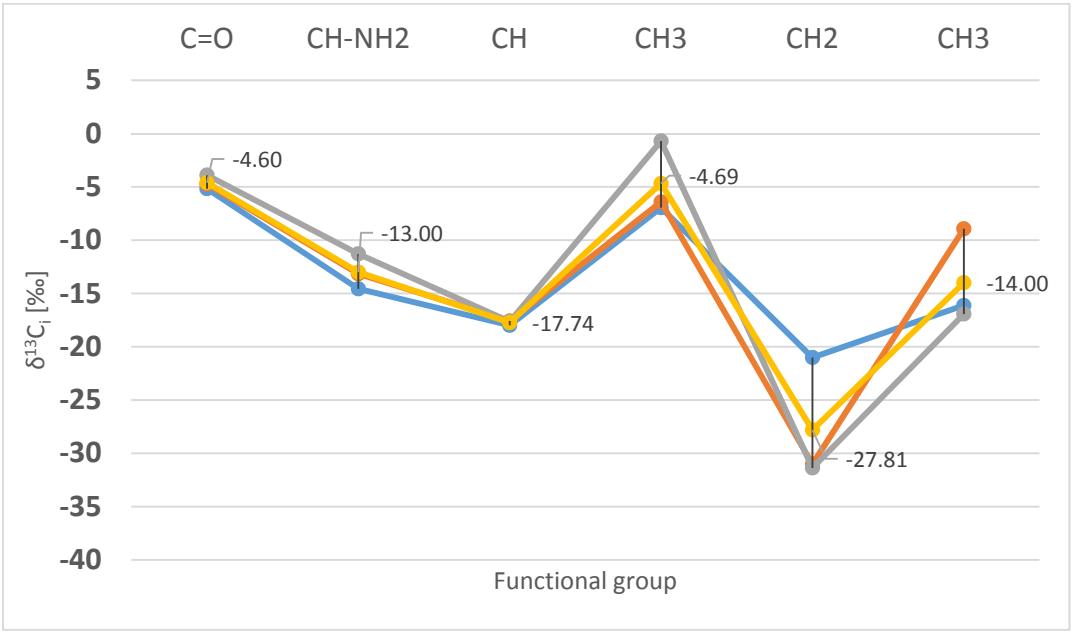

Figure 21. $\delta^{13}C_i$ [‰] values for L-isoleucine with the corresponding functional groups positions obtained by irm-^{13}C NMR measurements; mean values (yellow line) are displayed on the chart

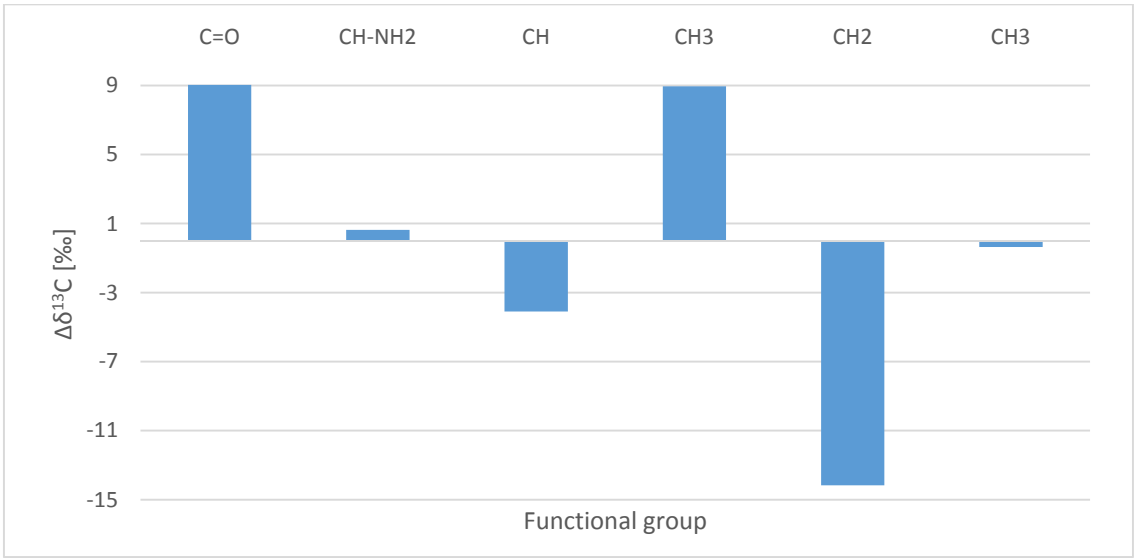

Figure 22. $\Delta\delta^{13}C$ distribution for L-isoleucine with the corresponding functional groups positions obtained by irm-^{13}C NMR measurements

3.4.3.2 Methionine

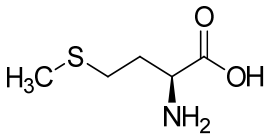

structure of L-methionine

Certificate of origin information

Source: MP biomedicals
Origin: natural
Product Number: 02194707
Product Name: L-Methionine
Quality: >99%
Lot Number: MR31057
Origin: Sheep milk
CAS: 63-68-3

The L-methionine used is of natural origin, being obtained from the hydrolysis of sheep milk proteins. The $\delta^{13}C_g$ value of -25.74‰ indicates the sheep were fed on a C_3 plant-derived carbon source. Although methionine is an essential amino acid in the diet for the majority of mammals, ruminants show a different requirement as their amino-acid complement is derived substantially from rumen microfloral metabolism (see Cantalapiedra-Hijar G., Ortigues-Marty I., Schiphorst A.M., Robins R.J., Tea I., Prache S. 2016 Natural ^{15}N abundance in key amino acids from animal tissues: exploring its new horizon in diet authentication and feed efficiency assessment in ruminants J. Agric. Food Chem. ***64*** *(20), 4058–4067* for a discussion of this).

The interpretation of the distribution observed in the natural methionine will be considered in Chapter IV. Here, only a brief comparison of the natural L-methionine and synthetic DL-methionine will be made. The data obtained from samples of natural L-methionine and synthetic DL-methionine are illustrated in Figure 23. The first feature of note is that the $\delta^{13}C_i$ values differ considerably: -36.2 and -25.7‰ for the synthetic and natural samples, respectively. Thus, only the L-methionine falls within the range of values to be expects for a natural origin, the DL-methionine indicating that some of the carbon atoms are probably of fossil origin. The second is that the $\Delta\delta^{13}C$ for ($\delta^{13}C_1$- $\delta^{13}C_2$) differ, being approx. +5 and -8‰ for the natural and synthetic, respectively. Only the former fits a probable natural origin. The third feature is that they have in common an *S*-methyl group considerably depleted in ^{13}C relative to the other carbon positions of the molecule. For the DL-methionine, this indicates a probable origin from methyl iodide, which has a very impoverished methyl group. The reasons for the depleted *S*-methyl group in the L-methionine will be developed in Chapter IV.

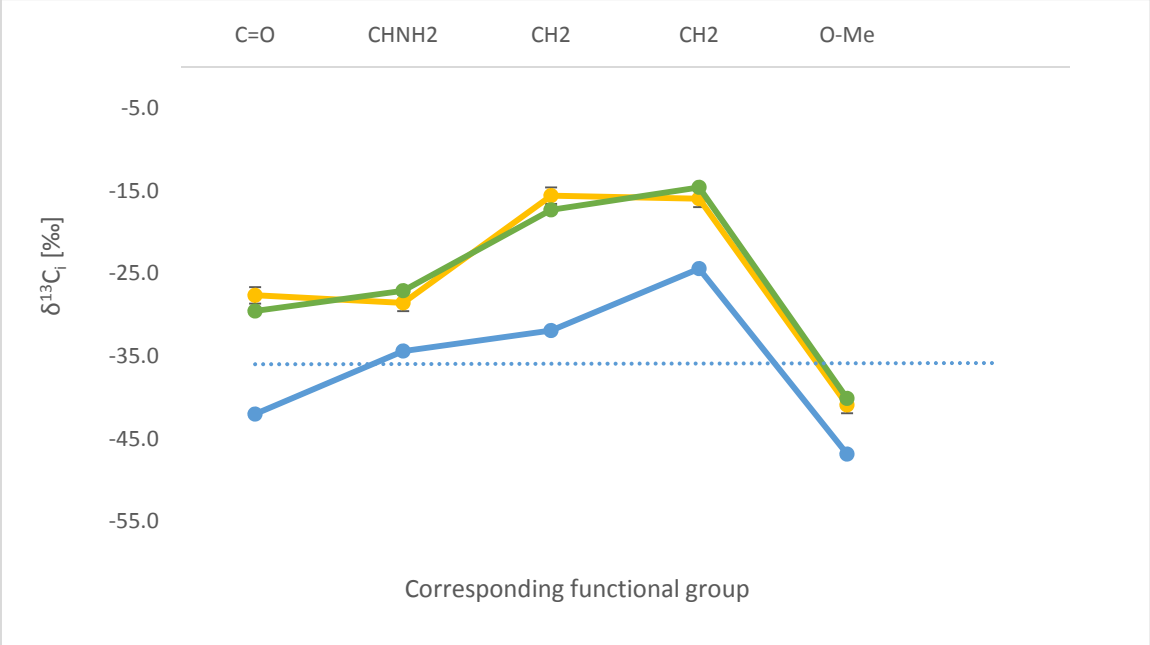

Figure 23. Position-specific $^{13}C/^{12}C$ ratio expressed as $\delta^{13}C_i$ [‰] for natural L-methionine (2 preparations, green/yellow) and for synthetic methionine (blue)

3.4.4 Amino acids belonging to the α-Ketoglutarate Family

3.4.4.1 Glutamic acid

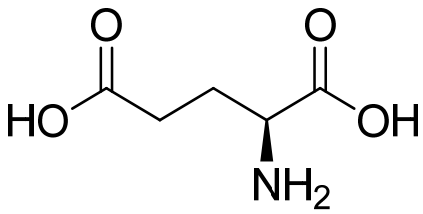

structure of L-glutamic acid

Certificate of Origin Information

Source: Sigma-Aldrich
Origin: natural
Product Number: 49449
Product Name: L-Glutamic acid
Quality: BioUltra, ≥ 99.5% NT
Lot Number: BCBH3883V
Origin: fermentation/cell culture
CAS: 56-86-0

The L-glutamic acid used was of biological origin and was obtained by fermentation. The fermentation organism is not indicated. The $\delta^{13}C_g$ value of -27.25‰ indicates the use of a C_3 plant derived carbon source.

Due to the presence of 2 carboxylic acid groups, 4 mol of TMSCl was used per mol of glutamic acid to make the dimethyl ester. In order to ensure the correct peak assignments – the molecule is of a relatively symmetrical structure – DEPT135, COSY, HSQC and HMBC spectra were acquired (see 8.4. section Additional materials). This made it possible to solve the uncertainties between the C1 and C5 carboxyl groups and the C3 and C4 CH_2 groups.

The numbering correlations between the NMR spectral displacements and the IUPAC numbering are:

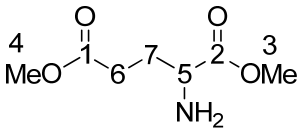

NMR numbering in order of peaks on the spectrum numbered from high frequency to low frequency

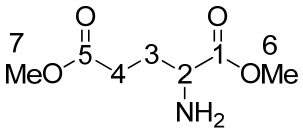

IUPAC numbering

The $\delta^{13}C_i$ [‰] and $\Delta\delta^{13}C$ [‰] values are illustrated in Figures 24 and 25, respectively. As can be seen, the reproducibility of the spectra is poor, but the mean value gives some overall impression of the probable intramolecular position specific distribution of ^{13}C.

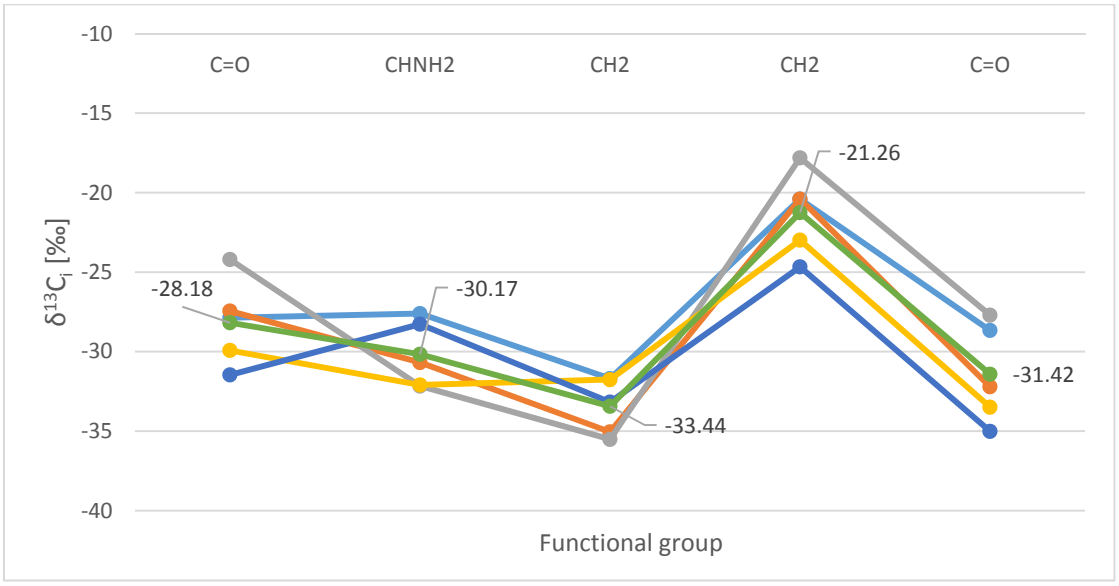

Figure 24. $\delta^{13}C_i$ [‰] values for L-glutamic acid with the corresponding functional groups positions obtained by irm-^{13}C NMR measurements; mean values (green line) are displayed on the chart

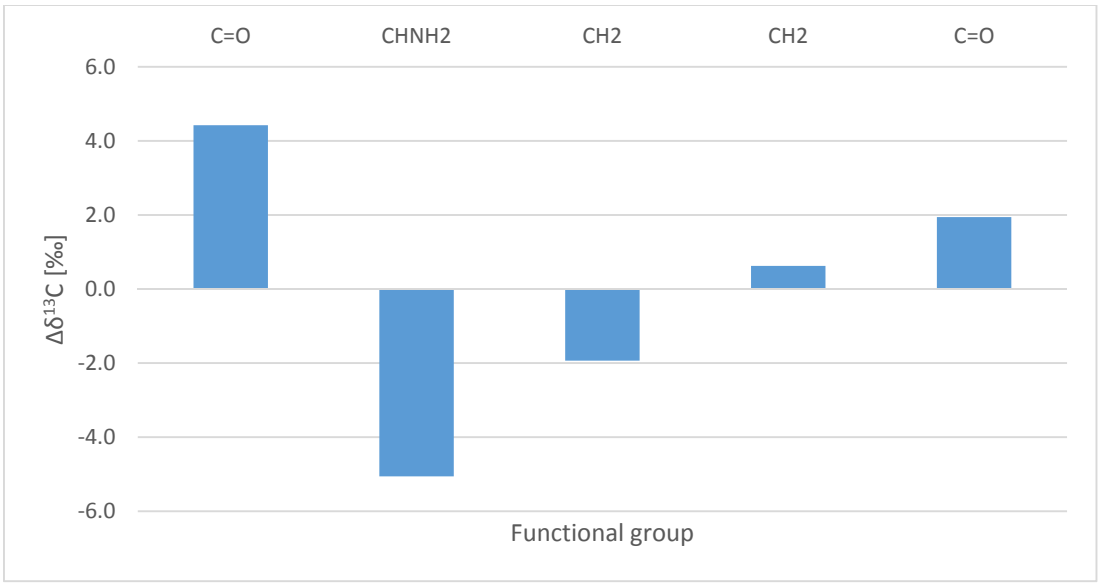

Figure 25. $\Delta\delta^{13}C$ [‰] distribution for L-glutamic acid with the corresponding functional groups positions obtained by irm-^{13}C NMR measurements

Glutamic acid is a key metabolite in that it acts as the donor of amino groups for many other amino acids and as the precursor providing the carbon skeleton for a rather diverse family of amino acids, including arginine, histidine and proline. The interpretation of the ^{13}C distribution within glutamic acid, however, is not straightforward, as it cannot be considered as a dedicated product of a pathway, as is effectively the case for many other amino acids. Further, it is largely derived directly by the transamination of an intermediate of the citric acid cycle, 2-ketoglutaric acid. This compound obtains its carbon atoms from glucose via pyruvate and the incorporation of acetyl-CoA into citric acid. As a result of carbon redistribution in this cycle, considerable scrambling of the carbons takes place. An indirect comparison can be made with citric acid, for which data is available in the literature.[107] The overall pattern fits quite well that observed in citrate, with the carboxyl groups relatively enriched and the C2 position relatively impoverished. As transaminase reactions are not considered to fractionate significantly,[106] this impoverishment is likely largely to be reflecting the isotope pattern present in the precursor.

3.4.5 Amino acids belonging to the the Shikimate pathway Family

3.4.5.1 Tyrosine

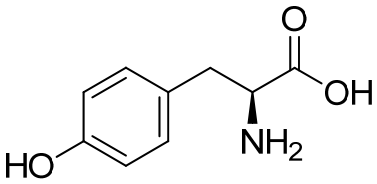

structure of L-tyrosine

Certificate of Origin Information

Source: Sigma-Aldrich
Origin: natural
Product Number: 93829
Product Name: L-Tyrosine
Quality: BioUltra, ≥ 99.0% NT
Lot Number: BCBM5740V
Origin: natural
CAS: 60-18-4

The L-tyrosine acid used was of biological origin but the exact source is not indicated. The $\delta^{13}C_g$ value of -27.34‰ indicates the use of a C_3 plant-derived carbon source. L-Tyrosine is correctly named in UPAC nomenclature as L-2-amino-3-(4-hydroxyphenyl)propanoic acid. The numbering adopted has followed this nomenclature. The numbering correlations between the NMR spectral displacements and the IUPAC numbering are:

[107] H-L. Schmidt *et al.*, '*Non-statistical isotope distribution in natural compounds: mirror of their biosynthesis and key for their origin assignment',* Stable isotopes in the biosphere, edited by E. Wada *et al.,* Kyoto University Press, Japan, (1995), pp. 17-35.

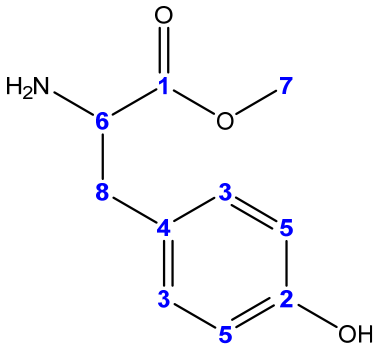

NMR numbering of tyrosine methyl ester in order of peaks on the spectrum numbered from high frequency to low frequency

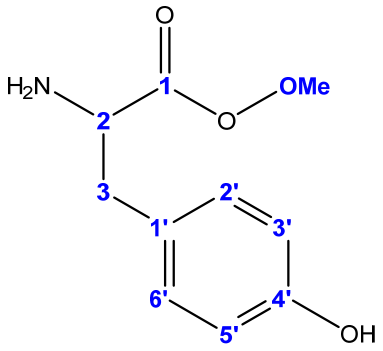

Equivalent IUPAC numbering

The $\delta^{13}C_i$ [‰] values are illustrated in Figures 26 and 27.

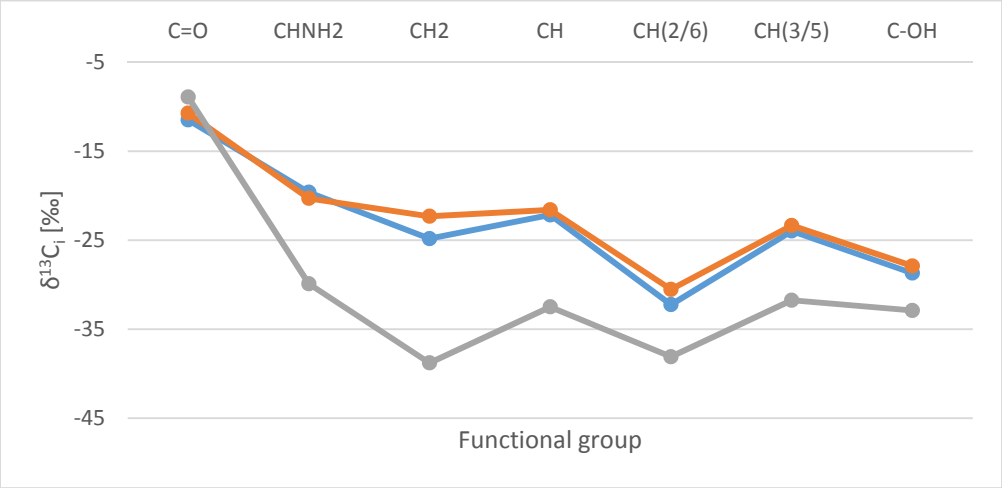

Figure 26. $\delta^{13}C_i$ [‰] values for two preparations of L-tyrosine and for ferulic acid (grey) obtained by irm-^{13}C NMR measurements. Mean from 5 spectra for each of two acquisitions (No. 8 – blue, and 13 - ochre) are given

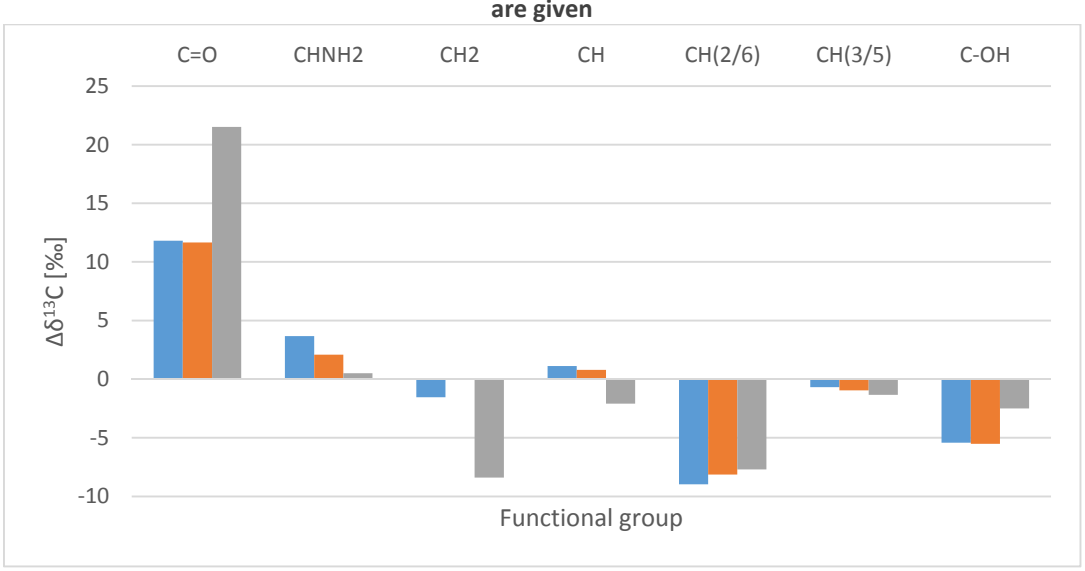

Figure 27. $\Delta\delta^{13}C$ [‰] distribution for two preparations of L-tyrosine (No. 8 – blue, 13 – ochre) and ferulic acid (grey)

Tyrosine is a member of the group of amino acids derived from the shikimate pathway. All three members of this group play important roles in addition to their participation as a component in protein structure. In particular, phenylalanine is the precursor of a large group of compounds that include lignin, flavonoids and a whole range of other 'phenolics'. Tyrosine and phenylalanine also serve as precursor for alkaloid biosynthesis. Their common origin is shikimate, which derives its carbons from one molecule of the pentose phosphate pathway intermediate, D-erythrose-4-phosphate and 1 molecule of phospho*enol*pyruvate (PEP). A further molecule of PEP is added to make chorismate, which undergoes a rearrangement and decarboxylation to form the phenylpropane structure common to phenylalanine and tyrosine (Figure 28).

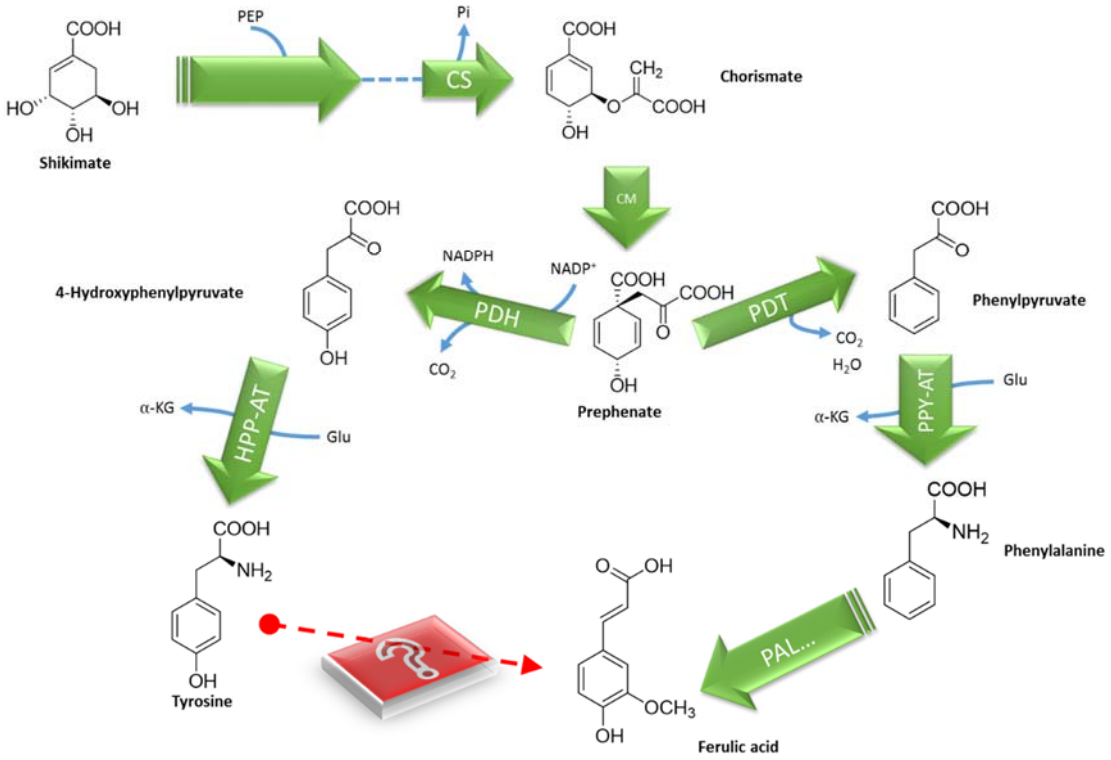

Figure 28. Biosynthesis of tyrosine, phenylalanine and ferulic acid from shikimate[108]

Overall, in L-2-amino-3-(4-hydroxyphenyl)propanoic acid (L-tyrosine) it is found that the carbon atoms derived from a long pathway via shikimate (the 4-hydroxyphenyl moiety) are generally more impoverished in ^{13}C than those introduced from the second molecule of PEP that is combined with shikimate-3-phosphate, and which forms the three carbons of the propanoic acid unit. Considering the 6 positions derived from shikimate, they are all relatively impoverished in ^{13}C but not to the same extent. An interesting pattern is established on the phenolic ring, in which the C1'>C2'<C3'>C4'<C5'>C6'. A detailed interpretation of the causes of this pattern is near-impossible, as all these carbon atoms undergo a detailed series of reactions, including multiple changes of coordination. Within the PEP-derived moiety (the propanoic acid part), a striking difference is seen between the 3 carbons. The C=O (C1) is relatively enriched, by approx. 10 and 12.5‰ relative to the C2 ($CHNH_2$) and C3 (CH_2) positions, respectively.

[108] H. Maeda and N. Dudareva, *'The Shikimate Pathway and Aromatic Amino Acid Biosynthesis in Plants'*, Annual Review of Plant Biology, 63.1, (**2012**), 73–105.

It is also noteworthy that this pattern is very comparable to that observed in natural ferulic acid extracted from rice bran (Figure 26).[109] In this metabolite of phenylalanine, the carboxyl is relatively enriched, as in tyrosine, while the C2 and C3 positions (equivalent to $CHNH_2$ and CH_2, respectively, in tyrosine) show a greater degree of impoverishment, presumably due to the action of phenylalanine ammonia lyase which converts both these sp^3 carbons to sp^2, and which shows a kinetic isotope effect that leads to selection against ^{13}C.[110]

Table 4 contains a data set of the values for all investigate amino acids.

Table 4. Juxtaposition of amino acids carbon groups $\delta^{13}C_i$ [‰] values and their origin. The values for $\delta^{13}C_i$ [‰] are given in Table 7 (Appendix)

Amino acid	Carbon group $\delta^{13}C_i$ [‰] values							**Origin**
L-alanine	C=O	$CHNH_2$	CH					synthetic
	-29.28	-32.68	-30.32					
L-valine	C=O	$CHNH_2$	CH	CH_3	CH_3			natural
	-47.76	-24.47	-33.70	-30.80	-25.72			
L-serine	C=O	CH	CH_2OH					natural
	-16.02	-17.30	-6.25					
L-isoleucine	C=O	$CHNH_2$	CH	CH_3	CH_2	CH_3		natural
	-4.6	-13.0	-17.74	-4.69	-27.81	-14.0		
L-methionine	C=O	$CHNH_2$	CH_2	CH_2	O-Me			natural
	-29.55	-27.10	-17.32	-14.6	-40.12			
D,L-methionine	C=O	$CHNH_2$	CH_2	CH_2	O-Me			synthetic
	-42 01	-34.40	-31.91	-24. 42	-46.84			
L-glutamic acid	C=O	$CHNH_2$	CH_2	CH_2	C=O			natural
	-2.83	-32.31	-29.18	-26.63	-25.31			
L-tyrosine	C=O	$CHNH_2$	CH_2	CH	CH	CH	C-OH	natural
	-10.71	-20.31	-22.31	-21.60	-30.53	-23.35	-27.9	

3.5 General interpretation of the results

This study suffered from two major problems. First, due to a lack of availability of amino acids from natural origins, the study is more limited than desirable. Second, a number of the amino acids that could be obtained from a natural origin (notably glutamine, threonine and lysine) proved intransigent to methylation of the carboxyl function, or produced a mixture of products. Hence, despite of availability of a natural products, data was not obtained.

[109] E. P. Botosoa *et al.*, *'Quantitative Isotopic ^{13}C Nuclear Magnetic Resonance at Natural Abundance to Probe Enzyme Reaction Mechanisms via Site-Specific Isotope Fractionation: The Case of the Chain-Shortening Reaction for the Bioconversion of Ferulic Acid to Vanillin'*, Analytical Biochemistry, 393.2 (2009), 182–88.

[110] H-L. Schmidt and G. Gleixner, 'Carbon Isotope Effects on Key Reactions in Plant Metabolism and ^{13}C-Patterns in Natural Compounds', in *Stable Isotopes*, ed. by H. Griffiths (Oxford: BIOS Scientific Publisher, 1998), pp. 13–25.

Despite these drawbacks, some general conclusions can be made. The first notable feature is that for isoleucine, glutamic acid and tyrosine, the carboxyl function is enriched in ^{13}C in comparison to the C4 CH_2 by approx. 8, 10 and 10‰, respectively. This fits the pattern previously reported by Abelson and Hoering, although generally rather smaller than the range they reported (mean values of 5, 19 and 19‰).[111] In contrast, serine and, even more emphatically valine do not conform to this pattern showing a $\Delta\delta^{13}C$ for ($\delta^{13}C_1$- $\delta^{13}C_2$) of 1 and -23‰, respectively.

Clearly, further analyses are required to determine the range of values from different organisms involving the separation and isotopic characterisation of amino acids from the same biological source.

[111] P. H. Abelson and T. C. Hoering, '*Carbon isotope fractionation in formation of amino acids by photosynthetic organisms*', Proceedings of the National Academy of Science of the US, 47 (5), (1961), 623-632.

4 Chapter IV – Isotope fractionation in methionine metabolism

4.1 Methionine biosynthesis

As the only sulphur-containing amino acid that is essential for mammals, methionine need to be supplied entirely from the diet. In contrast in plants and most microorganisms, methionine is synthesized *de novo*. The initial steps of the synthesis consist of inorganic sulphate assimilation into cysteine via homocysteine. The ensuring metabolic sequence is the conversion of cysteine into methionine and is of the central importance in cellular metabolism. Due to this, the process has been extensively studied and established by John Giovanelli.[112] He noted that in the plant kingdom all the enzymatic reactions that lead to methionine are similar. Methionine along with threonine, isoleucine and lysine are members of the aspartate family of amino acids (Figure 4) in plants as well as in bacteria. There is several specific reasons for prominent attention to be paid to these biosynthetic pathways, especially those that gave rise to essential amino acids. First of all the elucidation of the mechanisms involved in the homeostatic regulation of amino acids in plants involves studying the biochemical and molecular control. This is important because of the deficiency of cereals and legumes in lysine and methionine[113] that limits the nutritional quality of the aforementioned plants (they are included in the diet of human beings and monogastric animals). Last but not least, the inhibition of acetolactate synthase (an enzyme involved in the biosynthesis of amino acids of the aspartate family) by sulfonylureas or imidazolinones is the lethal for plants[114], providing a class of herbicides. In more general terms, all of the key regulatory enzymes of the aspartate-derived amino acid branches are worth a closer look as suitable targets for more productive herbicides.

For a better understanding of the significance of methionine in the plant kingdom it is first necessary to look at its origin. It is possible to distinguish three convergent pathways from which the methionine molecule originates (Figure 29):

1. L-aspartate, which provides the carbon backbone
2. L-cysteine, which provides the sulphur atom
3. L-serine, the 3-carbon which provides the methyl group

[112] J. Giovanelli and S. H. Mudd, *'Synthesis of Homocysteine and Cysteine by Enzyme Extracts of Spinach'*, Biochemical and Biophysical Research Communications, 27.2 (1967), 150–56.
[113] J. Kigel, *Seed Development and Germination* (CRC Press, 1995).
[114] R. A. Azevedo *et al.*, *'The Biosynthesis and Metabolism of the Aspartate Derived Amino Acids in Higher Plants'*, *Phytochemistry*, 46.3 (1997), 395–419.

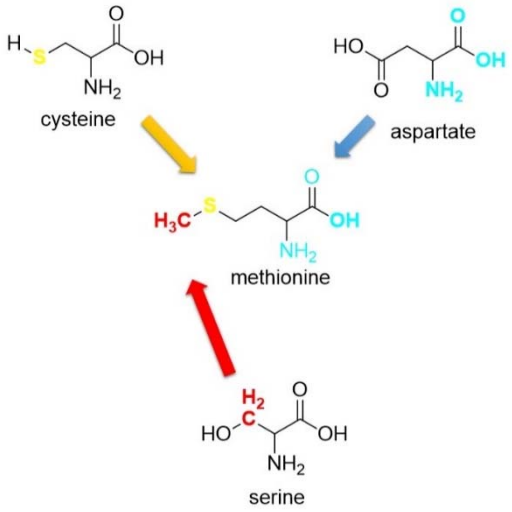

Figure 29. Origin of the methionine molecule. Yellow colour represents sulphur atom, red stands for methyl group and black/cyan for the backbone carbons

Methionine synthesis in higher plants[115] consist on the three consecutive reactions starting from *O*-phosphohomoserine (OPH). They are catalysed by cystathionine ɣ-synthase, cystathionine β-lyase and methionine synthase. The first two are catalysed by pyridoxal 5'-phosphate (PLP)-dependent enzymes and constitute the transsulphuration that constitutes in the transfer of the sulphur atom of cysteine (C_3 skeleton) to Hcy (C_4 skeleton) with the thioether cystathionine as intermediate. In the final step, catalysed by methionine synthase, a methyl group is transferred to Hcy from 5-methyltetrahydrofolate (see below).

4.2 Role of methionine in metabolism

Methionine occupies a central position in cellular metabolism, being involved in the processes of protein synthesis, methyl-group transfer through AdoMet, polyamines and ethylene syntheses.[116,117] The synthesis of proteins, among these pathways, is the only one that consumes the entire methionine molecule. However, the major metabolism of methionine is the synthesis of AdoMet: approximately 80% is engaged into this reaction.[118] There are two pathways already described in plants, which are using the methyl pyruvate 4-carbon moieties of methionine and additionally are involving AdoMet as a first intermediate. The sulphur atom of methionine is recycled in both routes. More than 90% of AdoMet is used for methyl groups transfer reactions in which the $–CH_3$ group is delivered to various acceptors. As important end products choline and its derivatives (as well as phosphatidylcholine – the major polar lipid) should be mentioned. Along with these reactions the recycling of the homocysteinyl moiety takes place and regener-

[115] B. J. Miflin, *Amino Acids and Derivatives: The Biochemistry of Plants* (Elsevier, 2014).
[116] R. Walden *et al.*, *'Polyamines: Small Molecules Triggering Pathways in Plant Growth and Development.'*, Plant Physiology, 113.4 (1997), 1009–13; E. A. Cossins, L. Chen, *'Folates and One-Carbon Metabolism in Plants and Fungi'*, Phytochemistry, 45.3 (1997), 437–52; T I. Zarembinski and A. Theologis, *'Ethylene Biosynthesis and Action: A Case of Conservation'*, Plant Molecular Biology, 26.5 (1994),.
[117] E. A. Cossins and L. Chen, *'Folates and One-Carbon Metabolism in Plants and Fungi'*, Phytochemistry, 45.3 (1997), 437–52.
[118] J. Giovanelli *et al., 'Quantitative Analysis of Pathways of Methionine Metabolism and Their Regulation in Lemna',* Plant Physiology, 78.3 (1985), 555–60.

ates methionine. Briefly, S-adenosyl-L-Hcy (AdoHcy) produced during the methyl transfer reaction is converted into Hcy via a reaction catalysed by AdoHcy hydrolase (EC 3.3.1.1.), then methionine is regenerated through methylation of Hcy. Thus, methionine synthase serves not only to catalyse the last reaction in *de novo* synthesis, but also regenerates the methyl group of AdoMet. In some plant tissues, the use of the 4-carbon moiety of AdoMet for the synthesis of polyamines and ethylene is also served by recycling of the methylthio residue of methionine.[119]

4.3 Enzymology of methyl group transfer between C1 unit and *O*-Me or *N*-Me group

4.3.1 Methionine synthase

Methylation of homocysteine to form methionine by using 5-*N*-methylthetrahydrofolate as a methyl group donor, is the last step of methionine synthesis that is localized in the cytosol[120] and is catalysed in plants by cobalamin-independent methionine synthase (EC 2.1.1.1). This enzyme has two functions, one of them is synthesis *de novo* of methionine and the second the regeneration of the methyl group of *S*-adenosylmethionine. The latter is of especial importance in mammals, that cannot synthesise Met *de novo*, but in these organisms it is catalysed by a cobalamin-dependent enzyme (EC 2.1.1.13). The characterization of methionine synthase from plants, both molecular and biochemical, is still limited. The low amount of protein present in plants is one of the issues and another is the substrate specificity of the enzyme. Normally the bacteria are able to use the monoglutameric methyltetrahydrofolate, while *Catharanthus roseus*[121] accepts only the triglutameric isoform that is not freely accessible. Activity of the cobalamin-independent methionine synthase doesn't require AdoMet or cobalamin.[122]

4.3.2 AdoMet synthetase

Methyl groups in a biological systems are transferred during countless reactions, from a few types of methyl donors to a huge variety of methyl acceptors. AdoMet is most extensively used as a biological methyl group donor.

AdoMet synthetase (EC 2.5.1.6) is the only enzyme that catalyzes the formation of Ado Met, during two-step reaction. The creation of AdoMet occurs by removing the complete triphosphate chain from ATP to form, which is further hydrolysed to PP_i and P_i and replaces with Met, before AdoMet is released.[123]

---

[119] S. Ravanel *et al.*, *'The Specific Features of Methionine Biosynthesis and Metabolism in Plants'*, Proceedings of the National Academy of Sciences, 95.13 (1998), 7805–12.

[120] R. M. Wallsgrove *et al.* , *'Intracellular Localization of Aspartate Kinase and the Enzymes of Threonine and Methionine Biosynthesis in Green Leaves'*, Plant Physiology, 71.4 (1983), 780–84.

[121] J. Eichel *et al.*, *'Vitamin-B_{12}-Independent Methionine Synthase from a Higher Plant (Catharanthus Roseus). Molecular Characterization, Regulation, Heterologous Expression, and Enzyme Properties'*, European Journal of Biochemistry / FEBS, 230.3 (1995), 1053–58.

[122] H. Hesse *et al.*, *'Current Understanding of the Regulation of Methionine Biosynthesis in Plants'*, Journal of Experimental Botany, 55.404 (2004), 1799–1808.

[123] F. Takusagawa *et al.*, *'Structure and Function of S-Adenosylmethionine Synthetase: Crystal Structures of S-Adenosylmethionine Synthetase with ADP, BrADP, and PPi at 28 Angstroms Resolution'*, Biochemistry, 35.8 (1996), 2586–96.

4.3.3 Methyl transferases

Methyl group transfer from AdoMet to a large variety of acceptor substrates, generating *S*-adenosyl homocysteine as the by-product, is catalysed by *S*-adenosyl-methionine (AdoMet)-dependent methyltrasferases (MTases). Due to the variety of roles they playing in human biology, MTases have been the subject of much biomedical research. The major target for the development of drugs used in the treatment for e.g. Parkinson's disease was catechol-*O*-methyltransferase, which serves as a donor of *O*-methyl group during the catabolism of neurotransmitters (such as dopamine) of catecholamines. In specialized metabolism in microorganisms and plants, many specific MTases have evolved. They can methylate precursors and intermediates involved in biosynthesis of natural products and often show both regio- and stereoselectively. MTases are most commonly found in the biosynthetic pathways of the major classes of natural products such as polyketides, non-ribosomal peptides, terpenoids, alkaloids and flavonoids. Their properties can be strongly affected by the presence/absence of specific methyl groups within natural product scaffold. The main focus has been put on characterizing MTases taking part in biosynthetic pathways of natural products. Methods that has been developed to alter the methylation patterns of target compounds with the aim of their purpose the improvement of their properties for therapeutic and other applications.[124]

4.4 Isotopic fractionation associated with methyl group transfer

4.4.1 Prior studies of isotope fractionation in *O*-methyl groups

In 1976, Galimov *et al*. noted that the *O*-methyl group in several natural aromatic aldehydes was depleted relative to the rest of the molecule. [125] Since then, it has become apparent that the methyl groups of many compounds are relatively depleted in ^{13}C. For example, methoxyl groups of both pectin and lignin are~33‰ depleted in ^{13}C relative to the bulk biomass,[126] while many specialized plan products also show significant depletion in the *O*-methyl and/or *N*-methyl groups. These include ferulic acid, ~20‰ depleted,[127] caffeine and theobromine, respectively ~36 and 23‰ depleted,[128] tropine and nicotine, respectively ~25 and 12‰ depleted[129] and

[124] A-W. Struck *et al.*, *'S-Adenosyl-Methionine-Dependent Methyltransferases: Highly Versatile Enzymes in Biocatalysis, Biosynthesis and Other Biotechnological Applications'*, Chembiochem: A European Journal of Chemical Biology, 13.18 (2012), 2642–55.

[125] E. M. Galimov *et al.*, *'Experimental Investigation of Intra- and Intermolecular Isotopic Effects in Biogenic Aromatic Compounds'*, Geochemistry International, 1976.

[126] F. Keppler *et al.*, *'Carbon Isotope Anomaly in the Major Plant C_1 Pool and Its Global Biogeochemical Implications'*, Biogeosciences, 1.2 (2004), 123–31.

[127] E. P. Botosoa *et al.*, *'Quantitative Isotopic ^{13}C Nuclear Magnetic Resonance at Natural Abundance to Probe Enzyme Reaction Mechanisms via Site-Specific Isotope Fractionation: The Case of the Chain-Shortening Reaction for the Bioconversion of Ferulic Acid to Vanillin*', Analytical Biochemistry, 393.2 (2009), 182–88.

[128] D. G. Diomande *et al.*, *'Position-Specific Isotope Analysis of Xanthines: A ^{13}C Nuclear Magnetic Resonance Method to Determine the ^{13}C Intramolecular Composition at Natural Abundance'*, Analytical Chemistry, 87.13 (2015), 6600–6606.

[129] K. M. Romek *et al.*, *'Non-Statistical ^{13}C Fractionation Distinguishes Co-Incident and Divergent Steps in the Biosynthesis of the Alkaloids Nicotine and Tropine'*, Journal of Biological Chemistry, 2016, jbc.M116.734087.

tramadol,~20 and 22‰ depleted respectively in the *N*-methyl and *O*-methyl groups.[130] A curious anomaly is natural vanillin, which does not show the same phenomenon.[131,132]

4.4.2 Hypothesis for the origin of low ^{13}C in O-methyl groups

The working hypothesis, then, is that the observed depletion relates to the Met metabolism, specifically the last steps of Met synthesis in which the *S*-methyl group is formed and the methyl is transferred to other compounds. It is evident that, if depletion in ^{13}C occurs during Met biosynthesis, AdoMet synthesis or methyl group transfer, then the ^{13}C distribution will be retained in the final product. The key reactions are those catalysed by serine hydroxymethyltransferase (EC 2.1.2.1), considered as the principal reaction by which the C1 unit is transferred to THF (Fig. 1).[133] Cobalamine-independent L-methionine synthase, which transfers the C1 unit from 5Me-THF to L-homocysteine (Hcy) to form Met; AdoMet synthetase, by which Met is 'activated' in a reaction in which ATP provides the adenosyl receptor and a sulphonium ion is formed, and, finally a range of *O*- and *N*-methyl transferases that transfer the methyl group from AdoMet to a suitable receptor, with the concomitant regeneration of L-homocysteine, which can effectively re-enter the cycle.

Kinetic isotope effect on the serine aldolase (serine hydroxymethyltransferase EC 2.1.2.1) reaction can be the cause of observed ^{13}C depletion of *N*- and *O*-methyl groups of natural compounds. Transfer of a formyl residue from serine to tetrahydrofolate and/or catechol-*O*-methyltransferase (COMT) will induce a significant isotopic effect.[134]

The catechol *O*-methyltransferase catalyses the transfer of a methyl group from *S*-adenosylmethionine to catechols to generate the *O*-methylated catechol and *S*-adenosylhomocysteine. This reaction of *S*-adenosylmethionine with 3,4-dihydroxyacetophenone has been studied using a α-secondary deuterium (label in the transferred methyl) and primary ^{13}C isotope effects.[135] Isotope effects were measured using direct comparison of initial velocities with 95 atom% deuterium and 85 atom% ^{13}C labelled compounds. The measured α-deuterium

---

[130] K. M. Romek *et al.*, *'A Retro-Biosynthetic Approach to the Prediction of Biosynthetic Pathways from Position-Specific Isotope Analysis as Shown for Tramadol'*, Proceedings of the National Academy of Sciences of the United States of America, 112.27 (2015), 8296–8301.

[131] N. J. Walton *et al.*, 'Vanillin', *Phytochemistry*, 63.5 (2003), 505–15.

[132] E. J. Tenailleau *et al.*, *'Authentication of the Origin of Vanillin Using Quantitative Natural Abundance ^{13}C NMR'*, Journal of Agricultural and Food Chemistry, 52.26 (2004), 7782–87; M. Greule *et al.*, *'Improved Rapid Authentication of Vanillin Using $\delta^{13}C$ and $\delta^{2}H$ Values'*, European Food Research and Technology, 231.6 (2010), 933–41; A. Chaintreau *et al.*, *'Site-Specific ^{13}C Content by Quantitative Isotopic ^{13}C Nuclear Magnetic Resonance Spectrometry: A Pilot Inter-Laboratory Study'*, Analytica Chimica Acta, 788 (2013), 108–13.

[133] R. G. Matthews and J. T. Drummond, *'Providing One-Carbon Units for Biological Methylations: Mechanistic Studies on Serine Hydroxymethyltransferase, Methylenetetrahydrofolate Reductase, and Methyltetrahydrofolate-Homocysteine Methyltransferase'*, Chemical Reviews, 90.7 (1990), 1275–90; V. Schirch and D. M. E. Szebenyi, *'Serine Hydroxymethyltransferase Revisited'*, Current Opinion in Chemical Biology, 9.5 (2005), 482–87.

[134] H-L. Schmidt *et al.*, *'Multi-Factorial in Vivo Stable Isotope Fractionation: Causes, Correlations, Consequences and Applications'*, Isotopes in Environmental and Health Studies, 51 (1), (2015), 155–99.

[135] M. F. Hegazi *et al.*, *'Alpha.-Deuterium and Carbon-13 Isotope Effects for Methyl Transfer Catalyzed by Catechol O-Methyltransferase. S_N^2-like Transition State'*, Journal of the American Chemical Society, 101.15 (1979), 4359–4365.

and ^{13}C effects are 0.83 ± 0.05 and 1.09 ± 0.05 on V for the reaction. Measurement of the initial velocities as a function of *S*-adenosylmethionine concentration with labelled and unlabelled compounds gave similar V effects and further suggested that the V and V/K effects are equal.

4.5 Experimental data

The analysis of the position specific distribution of ^{13}C in natural L-methionine. Suitable conditions were established (see METHODS) for the acquisition of ^{13}C NMR spectra from which it is possible to calculate the position specific $\delta^{13}C_i$ [‰] values for L-Met. A representative spectrum is illustrated in Figure 30.

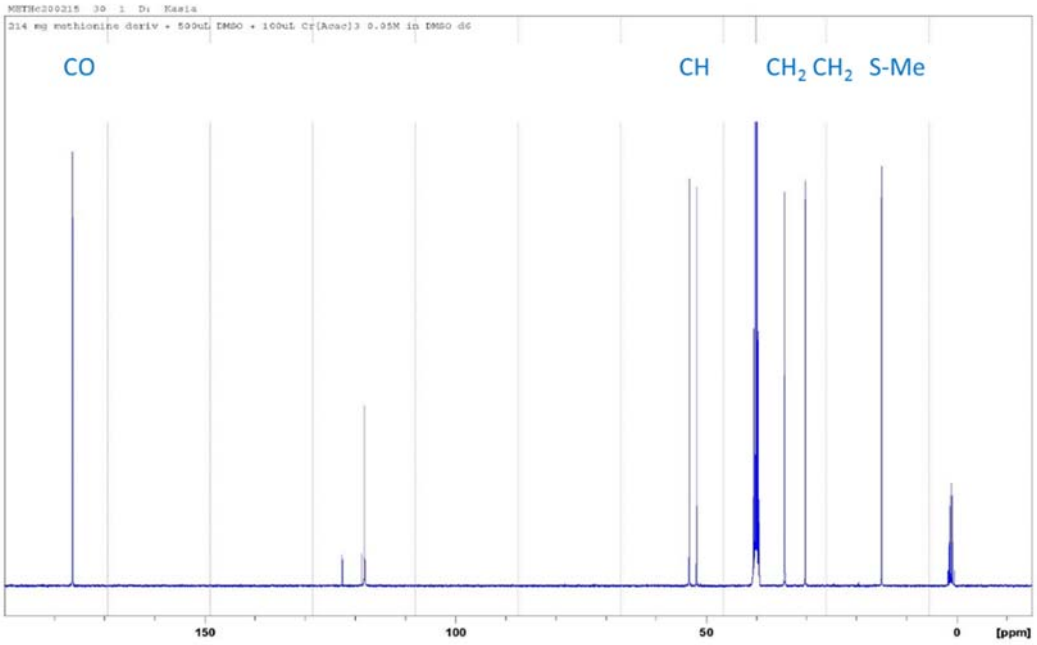

Figure 30. irm^{13}C-NMR spectrum for L-methionine

From total-line-shape curve fitting, the areas under the peak for each carbon atom *i* is obtained and the positional isotopic distribution calculated. The range of values obtained for the two samples is -12.6 to -48.2‰, with standard deviations acceptable for irm-^{13}C NMR spectrometry (~1‰; range 0.7 to 2.7‰). These $\delta^{13}C_i$ [‰] values are within the typical range for natural products. The variation in the position-specific distributions relative to the mean are illustrated in Figure 30.

What does the position specific distribution of ^{13}C in natural L-methionine tell us about the origin of the ^{13}C depletion?

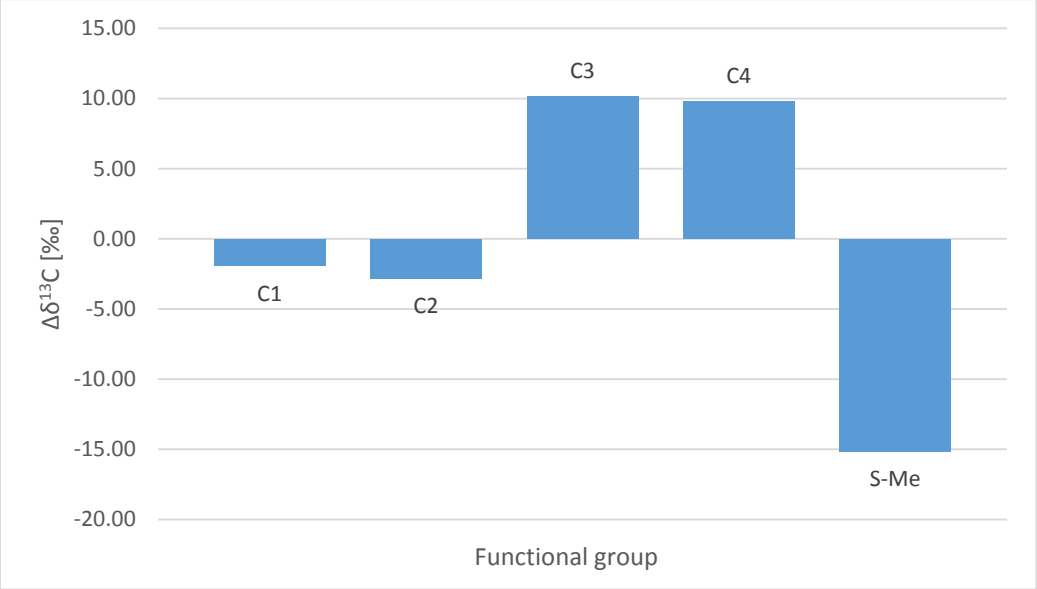

Figure 31. Position-specific $^{13}C/^{12}C$ ratio expressed as $\Delta\delta^{13}C$ [‰] for natural L-methionine

The most striking feature of Figure 31 is the extent to which the *S*-methyl group is depleted relative to the other carbon atoms in the molecule. The carbon atoms derived from L-Hcy have a mean $\delta^{13}C$ of -22‰, whereas the methyl group at -41‰ is depleted 19‰ relative to these other positions. Hence, it is apparent that the *S*-methyl carbon is strongly depleted in L-Met. The implication of this is that the general phenomenon of depletion in carbon atoms derived from this *S*-methyl can substantially be explained by the selection against ^{13}C at the level of L-Met biosynthesis. The codicil that must be added is that of the unlikely situation in which both a strong inverse and a strong normal isotope effects are manifest in subsequent reactions.

In the first of these, SAM synthetase (ATP:L-methionine S-adenosyltransferase, EC 2.5.1.6), the entire polyphosphate chain from MgATP is replaced by L-methionine, with the concomitant formation of a sulphonium. While this reaction shows a strong normal ^{14}C KIE of 1.128±0.003 (equivalent to an effect of 1.08 for ^{13}C) at the 5' carbon of the ribosyl unit of ATP, no ^{35}S KIE was seen. Furthermore, no significant ^{3}H secondary KIE on the *S*-methyl was found (1.009±0.008), indicating that the S-methyl group does not undergo any isotopic fractionation associated with this reaction.[136]

The subsequent step, the transfer of the methyl group from the sulphinium ion has not been widely studied from the isotopic point of view. Hegazi *et al*.[137] examined the ^{13}C KIE in the methylation of the unnatural substrate 3,4-dihydroxyacetophenone from AdoMet catalyzed by rat-liver catechol *O*-methyltransferase. When ^{13}C was present in the *S*-methyl group, they found a normal ^{13}C KIE of 1.09±0.05. This indicates that further depletion is probably occurring at this second methyl transfer and that methyl transfer is the kinetically limiting step of the reaction pathway. Furthermore, these authors conclude that the transition state has a tight structure,

[136] G. D. Markham *et al.*, *'A Kinetic Isotope Effect Study and Transition State Analysis of the S-Adenosylmethionine Synthetase Reaction',* The Journal of Biological Chemistry, 262.12 (1987), 5609–15.
[137] M. F. Hegazi *et al.*, *'α-deuterium and carbon-13 isotope effects for methyl transfer catalyzed by catechol O-methyltransferase. S_N^2 like transition state',* Journal of the American Chemical Society, 101 (15), (1979), 4359-4365 .

with the methyl group symmetrically located between the sulphur atom donor and the oxygen atom receptor, compatible with the high (near-maximal) value of ^{13}C KIE determined.

4.6 Theoretical calculations

While it is desirable to model the reactions for all three enzymes involved in methyl group transfer, it has only proved feasible in the time available to model the reaction mechanism for methionine synthase.

4.6.1 Reaction pathway for cobalamin-independent methionine synthase

Methyl transferases form an important class of enzymes, as they are involved in diverse pathways in primary as well as secondary metabolism. The role of this class of enzymes is to transfer methyl groups to a variety of target substrates. A key enzyme in this class is methionine synthase, which makes methionine from homocysteine in a single turnover during the AdoMet cycle. This enzyme is particularly important as methionine acts as a methyl group donor for many other methyltransferase enzymes. The enzyme exists in two isoforms: a cobalamin-independent, which exist in mammals as part of the 'methionine recovery cycle'. Despite having minimal structural homogeneity at the primary level, both enzymes require Zn^{2+}, which is involved in the binding of L-homocysteine (Hcy), a strategy exploited by a number of enzymes involved in the alkylation of thiol groups.[138] The reaction involves the transfer of a poor leaving group (the CH_3 bound to the 5-N of 5-Me-THF), this reaction is complex and as yet only described in relation to probable binding complexes.

In order to build a model of the reaction, the structure of methionine synthase was taken from the Protein Data Bank with PDB ID 4QQU[139] (Figure 32). The 4QQU crystal structure is for the cobalamin-independent methionine synthase of the yeast *Candida albicans* at 2.98Å resolution captured in a substrate-induced closed conformation. On the basis of the three-dimensional structure of the active site, three different models of possible reaction mechanism were proposed and explored using theoretical methods (Figure 33).

[138] R. Pejchal and M. L. Ludwig, *'Cobalamin-Independent Methionine Synthase (MetE): A Face-to-Face Double Barrel That Evolved by Gene Duplication'*, PLOS Biol, 3.2 (2004), e31 (p.).
[139] D. K. Ubhi and J. D. Robertus, *'The Cobalamin-Independent Methionine Synthase Enzyme Captured in a Substrate-Induced Closed Conformation'*, Journal of Molecular Biology, 427.4 (2015), 901–9.

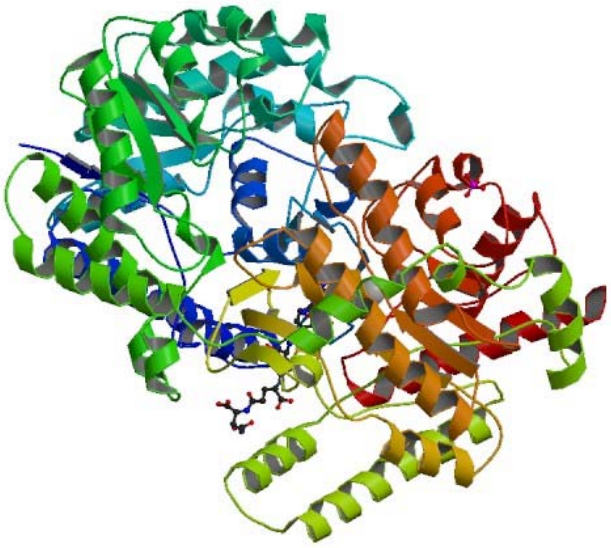

Figure 32. Cobalamine-independent methionine synthase showing the location of the 5-*N*-methyltetrahydrofolate and homocysteine with zinc as a coordination centre

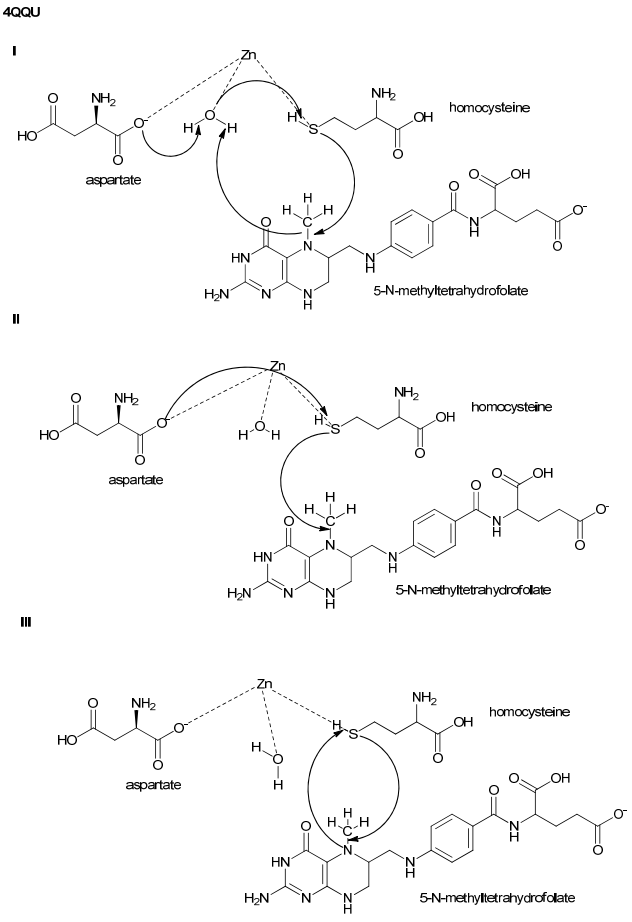

Figure 33. 3 Proposed reaction mechanisms

Model of mechanism I considers the methyl group transfer to take place by three consecutive steps. Firstly, nucleophile water molecule is activated by the ASP503 residue and takes a proton from the sulphur atom of homocysteine. Second, after homocysteine deprotonation the methyl group from 5-*N*-methyltetrahydrofolate is transferred from the nitrogen atom, to create methionine. In the last step there is proton transfer from the water molecule to the nitrogen atom on tetrahydrofolate and recycling of the water molecule by bringing back the hydrogen atom previously placed on the ASP503 residue.

Model II also involves the ASP503 residue for proton transfer from homocysteine but omits the role of a water molecule and considers a direct formation of methionine by methyl group transfer.

Model III is the simplest, in suggesting that the reaction proceeds in one step with the simultaneous transfer of proton and methyl group directly between homocysteine and 5-*N*-methyltetrahydrofolate.

The theoretical calculations conducted made it possible to select the more probable model of mechanism between these three options. For all proposed models the two-dimensional potential energy surface scans were performed for each supposed step of the reaction. Only for model I, after several modifications, was it possible to obtain the proper transfer of the established groups, and only for this model was a minimum reached. For the models II and III this initial studies did not converged to a minimum. Therefore we focused on model I for further treatment.

4.6.1.1 Methodology

The crystal structure of the cobalamin-independent methionine synthase of *Candida albicans* expressed in *Escherichia coli* BL21(DE3) was used as a starting structure for the simulation (PDB ID: 4QQU, resolution of 2.98Å). In its active site an enzyme has a zinc ion (see 8.4. Additional materials section) that acts as the coordinating molecule, homocysteine – the receiver of methyl group and 5-*N*-methyltetrahydrofolate, the donor. The overall reaction is shown on the scheme below (Figure 34).

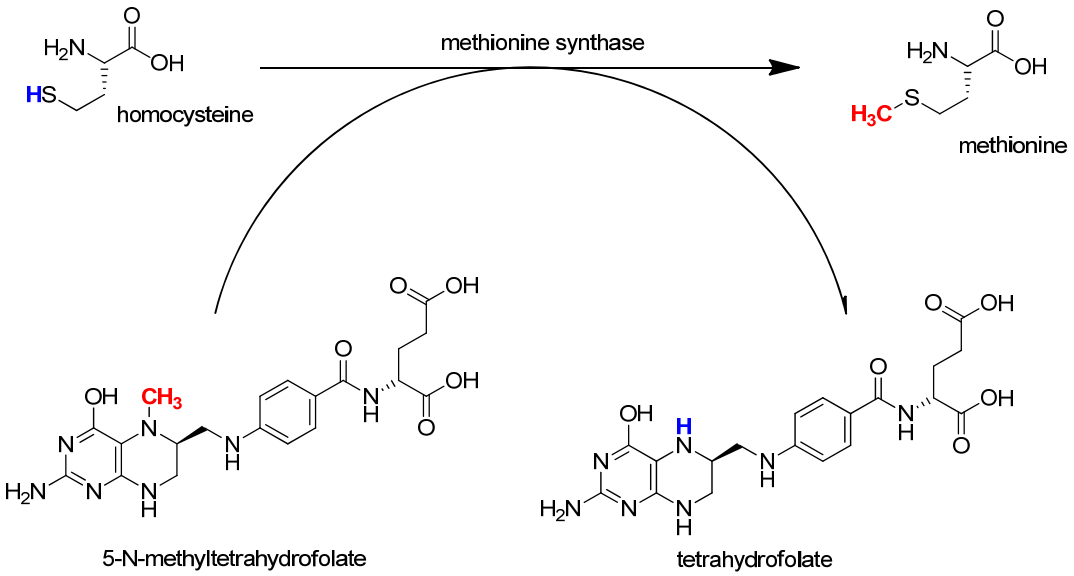

Figure 34. General scheme of the reaction for cobalamin-independent methionine synthase

The protein side chain conformation and positioning of side chain residues was confirmed with SCit tool.[140] The pK_a for titratable amino acids was calculated using PROPKA 3.0,[141] with the assumption that the pH was physiological, and missing hydrogen atoms were added using the tLEAP module of the AMBER program. Parameters for ligands (Zn, HCS, THF – see section 8.4.2. Table 7) were obtained using GAFF[142] (as implemented in AMBER tools). Optimization and dynamics simulations were performed using AMBER ff99SB[143] implemented in NAMD[144] program with time step of 1 fs. Periodic boundary conditions were applied with the particle mesh Ewald method[145] and *cut-off* for nonbonding interactions with a range radius from 14.5 to 16Å. We started with energy optimizations carried out by means of a conjugated gradient algorithm. Then, the systems were heated from 0 to 300K with a 0.001K increment and equilibrated during 200 ps of Langevin-Verlet dynamics at 300K. Our complexes were stabilized by performing 1 ns of NVT MM MD with AMBER FF (force field). Afterwards, the population of different conformations was collected during 200 ps of quantum mechanical/molecular mechanical molecular dynamics (QM/MM MD) simulations at PM3[146]/AMBER:TIP3P level of theory as imple-

[140] R. Gautier *et al.*, *'SCit: Web Tools for Protein Side Chain Conformation Analysis'*, Nucleic Acids Research, 32.suppl 2 (2004), W508–11.
[141] H. Li *et al.*, *'Very Fast Empirical Prediction and Rationalization of Protein pKa Values',* Proteins: Structure, Function, and Bioinformatics, 61.4 (2005), 704–21.
[142] J. Wang *et al.*, *'Development and Testing of a General Amber Force Field'*, Journal of Computational Chemistry, 25.9 (2004), 1157–74.
[143] L. Wickstrom *et al.*, *'Evaluating the Performance of the ff99SB Force Field Based on NMR Scalar Coupling Data',* Biophysical Journal, 97.3 (2009), 853–56.
[144] J. C. Phillips *et al.*, *'Scalable Molecular Dynamics with NAMD'*, Journal of Computational Chemistry, 26.16 (2005), 1781–1802.
[145] T. Darden *et al.*, *'Particle Mesh Ewald: An N⍰log(N) Method for Ewald Sums in Large Systems'*, The Journal of Chemical Physics, 98.12 (1993), 10089–92.
[146] P. Hobza *et al.*, *'Performance of Empirical Potentials (AMBER, CFF95, CVFF, CHARMM, OPLS, POLTEV), Semiempirical Quantum Chemical Methods (AM1, MNDO/M, PM3), and Ab Initio Hartree–Fock Method for Interaction of DNA Bases: Comparison with Nonempirical beyond Hartree–Fock Results'*, Journal of Computational Chemistry, 18.9 (1997), 1136–50.

mented in fDynamo.[147] The QM part consisted of a 10Å sphere (Zn, Hcy, Tat, His657, Cys658, Cys739, Asn498, Asp503, water; QM = 160 atoms), based on the position of the zinc ion in the active site of the enzyme. Due to the large amount of degrees of freedom, all atoms beyond 20Å from ligand-protein contacts were kept frozen.

Stability of the structure was confirmed during the MD simulation based on RMSD plot (see section 8.4. Additional materials) to verify the reliability of the implemented parameters for the zinc ion. MD simulations were performed with a time step of 1 fs and periodic boundary conditions with full electrostatics computed using the particle mesh Ewald method.

4.7 Dynamics – discussion of results

4.7.1 Results and discussion

Figure 35 shows the interactions between 5-*N*-methyltetrahydrofolate and the adjacent residues within the active site as defined by the crystal structure. Figure 36 shows the interactions between L-Hcy and the adjacent residues within the active site as defined by the crystal structure. These spatial orientations in the active site for the substrates, which put them in the most plausible positions, form the basis for the molecular modelling.

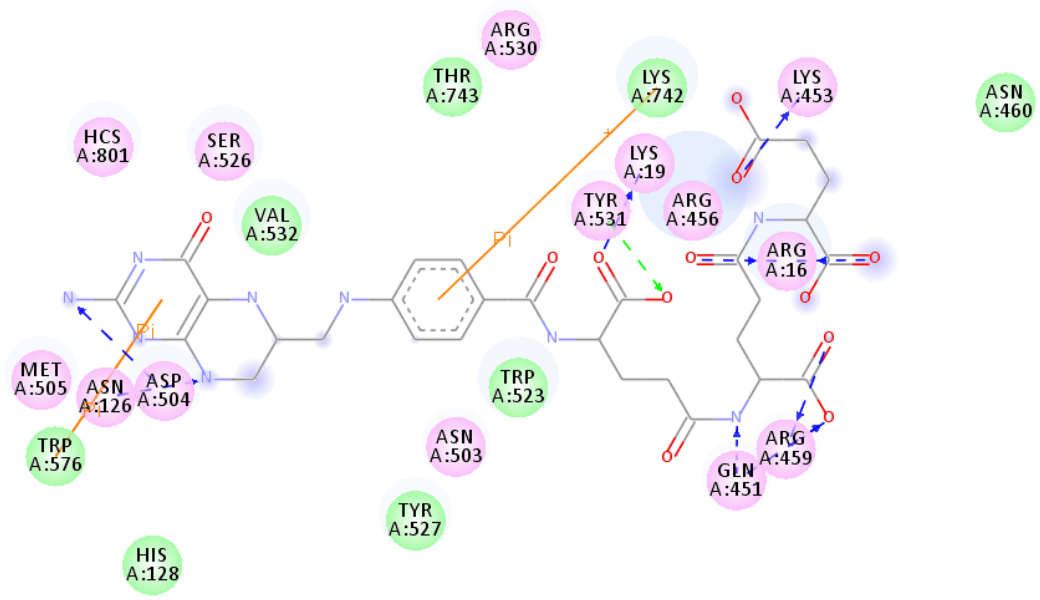

Figure 35. 5-*N*-methyltetrahydrofolate interactions with nearby residues before dynamic simulations

[147] M. J. Field *et al.*, *'The Dynamo Library for Molecular Simulations Using Hybrid Quantum Mechanical and Molecular Mechanical Potentials'*, Journal of Computational Chemistry, 21.12 (2000), 1088–1100.

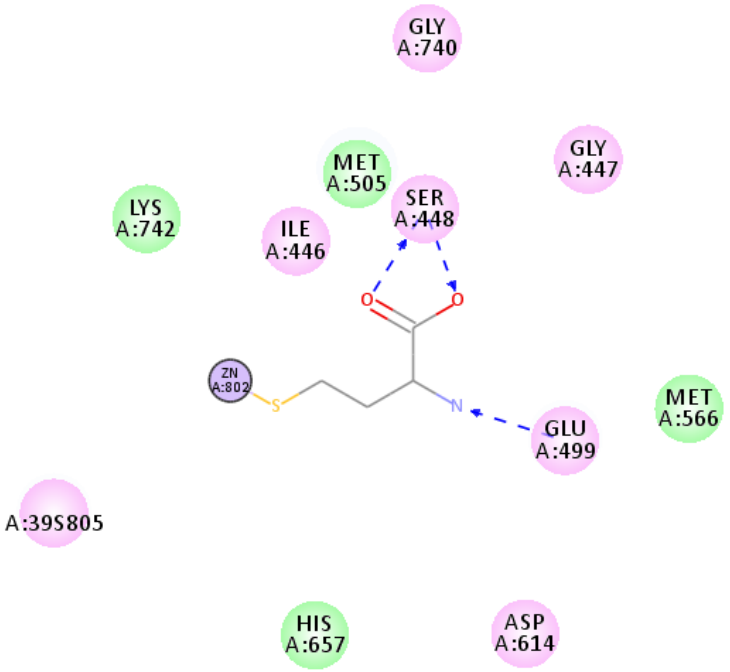

Figure 36. Homocysteine interactions with nearby residues before dynamic simulations

The local energy minimization in molecular mechanics was performed in 2000 steps to achieve the minimal total energy value for the system. Around the 1000th step it was visible that the slope reached a plateau, which indicated that the minimum had been successfully reached. In order to verify that the minimum obtained from the crystal structure was close to that expected in solution, heating from 0 to 300K was performed over 3000 steps to thaw the protein and demonstrate linearity during thawing of the protein (see section 8.4. Additional materials).

When the thermostat was set to 300K the process of energy equilibration was conducted to show that the energy level is stable. The energy of the process is exchanged with the thermostat. The temperature and energy are stabilized. The root-mean-square deviation (RMSD) for the backbone atoms was measured to confirm the enzyme stability along the dynamic simulations. The final result of the dynamic simulations made it possible to prepare the one-dimensional scan from which the optimal structure for further modelling of the mechanism could be carried out (see section 8.4. Additional materials).

Proton transfer between homocysteine and 5-*N*-methyltetrahydofolate required one water molecule and ASP503 residue participation. This creates a negative charge on sulphur and prepares the homocysteine to act as an acceptor of the methyl group (Figure 37).

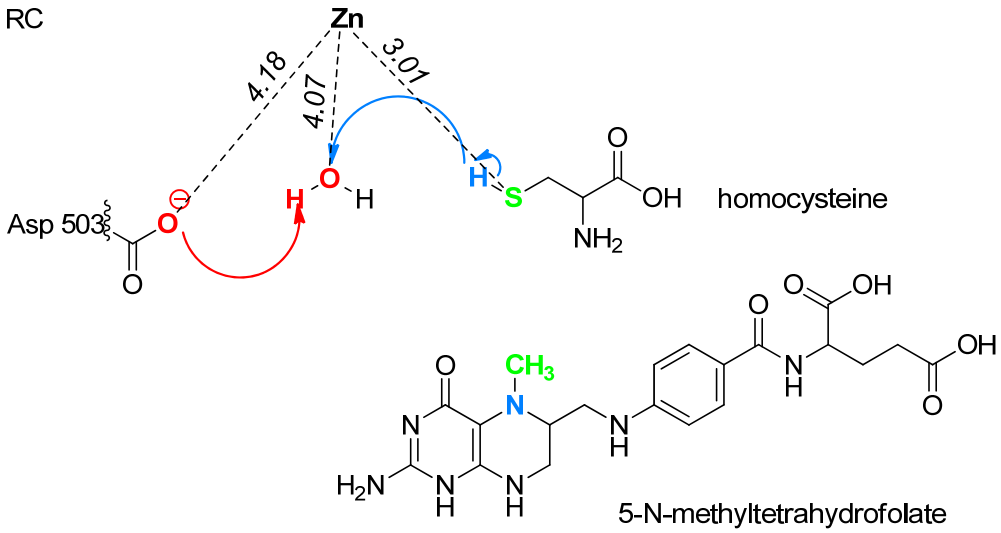

Figure 37. First stage of the reaction model. All the substrates are visible with the zinc which is coordinating the reaction. Hydrogen from homocysteine is transferred to the water molecule that gives away one of its hydrogens to the amino acid residue that possess a negative charge (ASP503). Distances between atoms are expressed in Å

The two-dimensional potential energy surface for proton transfer is shown in Figure 38. The x axis shows the progress of the hydrogen atom from water to the ASP503 residue, while the y axis shows the transfer of the hydrogen atom from the homocysteine to water. Blue areas correspond to the energetic minima and red ones to the maxima. A transition state was located from the structure marked on the figure as TS 1 in the greenish area.

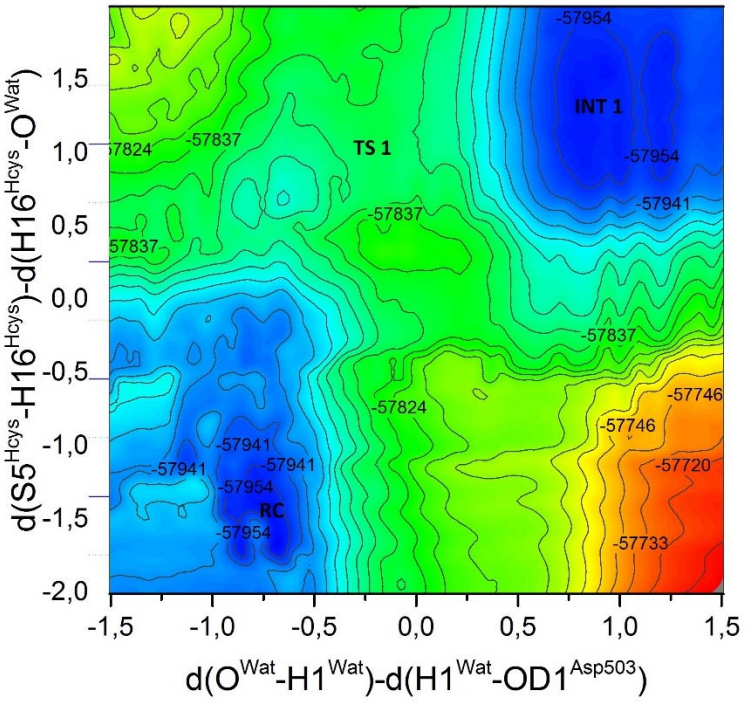

Figure 38. Two-dimensional potential energy surface scan for proton transfer from homocysteine involving the water molecule and Asparagine 503 residue. Superscripts description: Hcy – homocysteine, Wat – water molecule, ASP503 – residue asparagine 503

The atomic distances of transition state 1 for proton transfer are presented in Figure 39. One O-H bond of the water molecule has been stretched as the hydrogen is transferred to the charged to ASP503 residue. Simultaneously the S-H bond of homocysteine is stretched as the hydrogen is transferred to the water molecule.

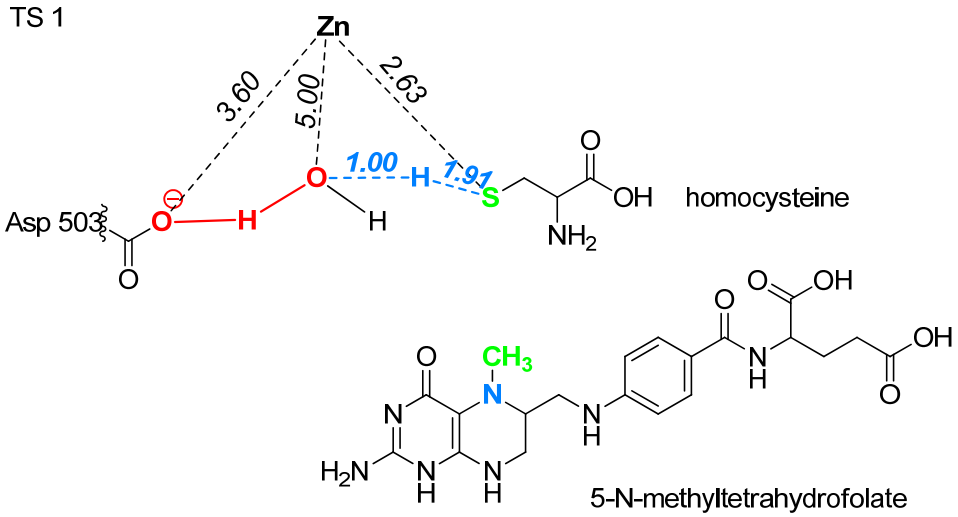

Figure 39. First transition state (TS 1) with the atomic distances expressed in Å

After the reaction mechanism has been initiated by this transfer of the protons, an intermediate can be identified (Figure 40) in which the sulphur is charged. The next step involves the methyl transfer from the 5-*N*-methyltetrahydrofolate nitrogen atom to the sulphur atom of homocysteine. Based on the two-dimensional potential energy surface the coordinates for transition state localization were chosen (Figure 41). IRC calculations confirmed that from this transition state we can go back to the reactant complex and go forward to the intermediate one. The profile on the x axis indicates the progress of the transfer of the methyl group between the atoms of nitrogen (from 5-*N*-methyltetrahydrofolate) and sulphur (from homocysteine), while the y axis shows the proton transfer between ASP503 and water molecule.

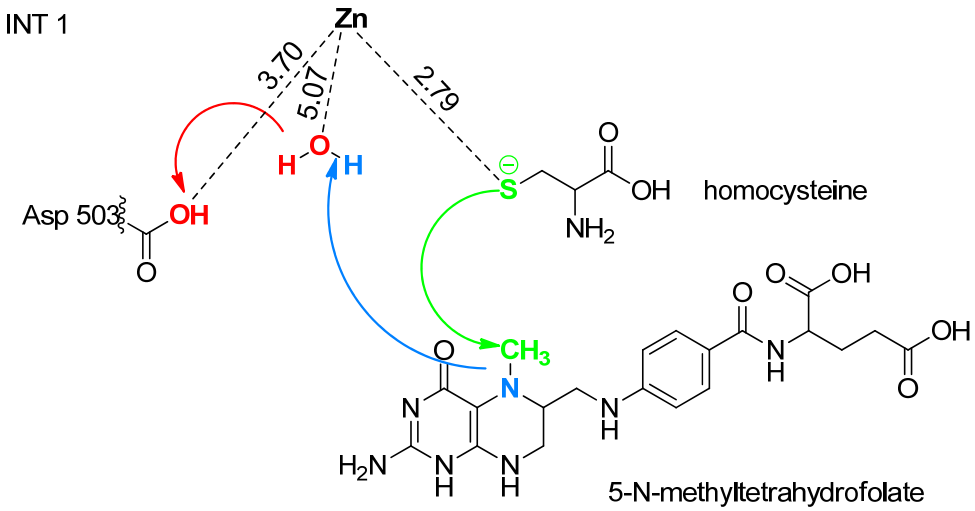

Figure 40. First intermediate (INT 1) - structure created after first transition state (TS 1) with the atomic distances expressed in Å

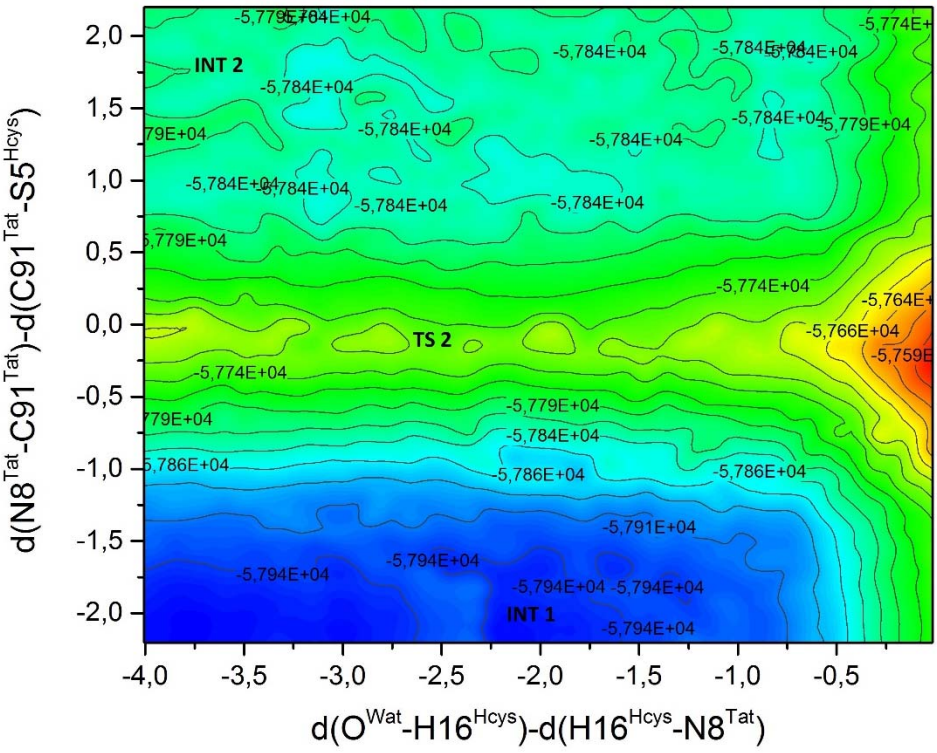

Figure 41. Two-dimensional potential energy surface chart for methyl group transfer between 5-*N*-methyltetrahydrofolate and homocysteine with simultaneous transfer of the proton. Superscripts description: Tat – 5-*N*-methyltetrahydrofolate, Hcy – homocysteine, Wat – water molecule

Reaction of methyl group transfer between 5-*N*-methyltetrahydrofolate and homocysteine is independent from the simultaneous reaction of proton transfer between water and homocysteine molecule.

The atomic distances of transition state 2 for proton transfer are presented in Figure 42. The crucial features are the symmetrical position of the methyl group between the N and S atoms and the transfer of the hydrogen atom from water to the N.

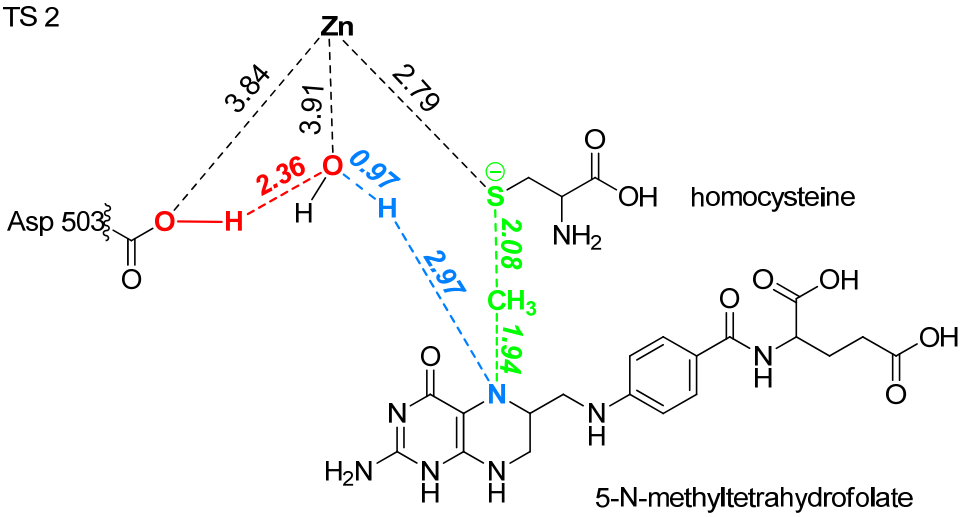

Figure 42. Second transition state (TS 2) with the atomic distances expressed in Å

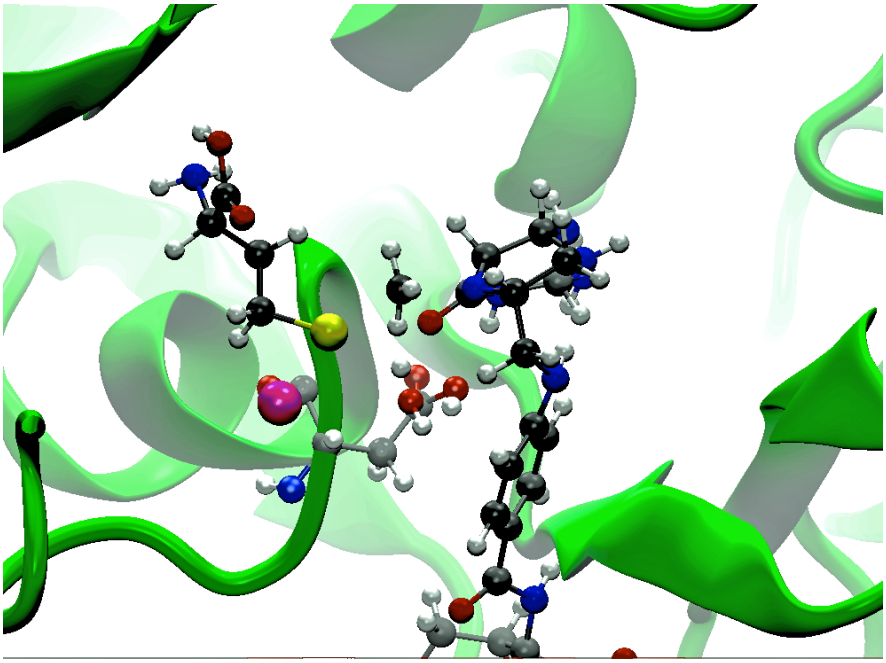

Figure 43. Second transition-state (TS 2) in active site. Methyl group is clearly visible in the middle of the picture, hanging between Hcy and 5-*N*-methyltetrahydrofolate. Zinc ion is marked in magenta

The active site of the enzyme during the second transition state is illustrated in three-dimensions in Figure 43 to highlight its structure. The methyl group is clearly seen to be located equidistant between the N and S atoms. This leads to the second intermediate (INT 2) shown in Figure 44. Where the atomic distances between nitrogen atom of 5-tetrahydrofolate and carbon atom of transferred methyl group is 2.86Å, between nitrogen atom and sulphur atom of homocysteine is 4.16Å and between sulphur atom and carbon atom of transferred methyl group is 1.81Å.

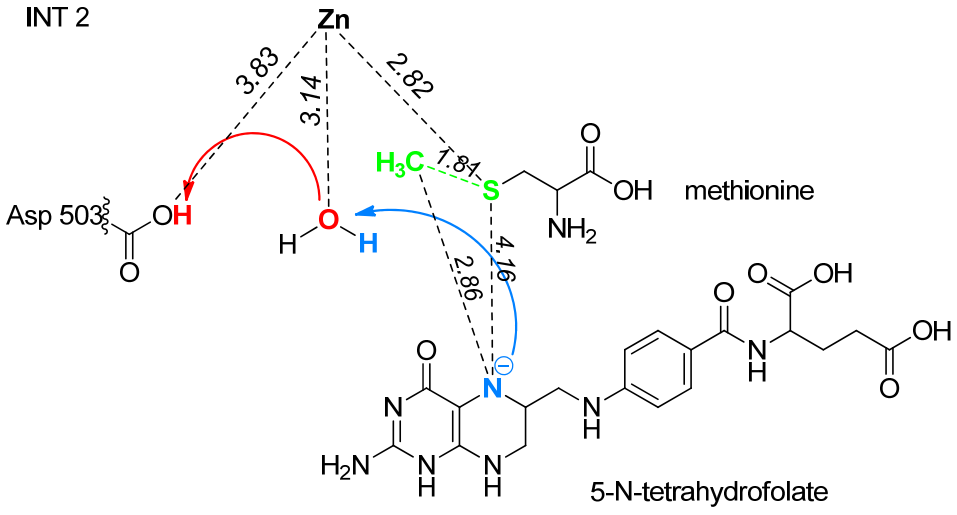

Figure 44. Second intermediate (INT 2) of the reaction after second transition state (TS 2) with the atomic distances expressed in Å

The last step of the reaction is the transfer of the hydrogen atom from water molecule to the nitrogen atom on the 5-*N*-tetrahydrofolate and hydrogen atom from ASP503 back to water (Figure 45). The two-dimensional potential energy surface of this partial reaction is illustrated

in Figure 46. The x axis shows the transfer of the water to N of tetrahydrofolate and the y axis shows the transfer of the hydrogen to water. The interatomic distances are shown in Figure 45.

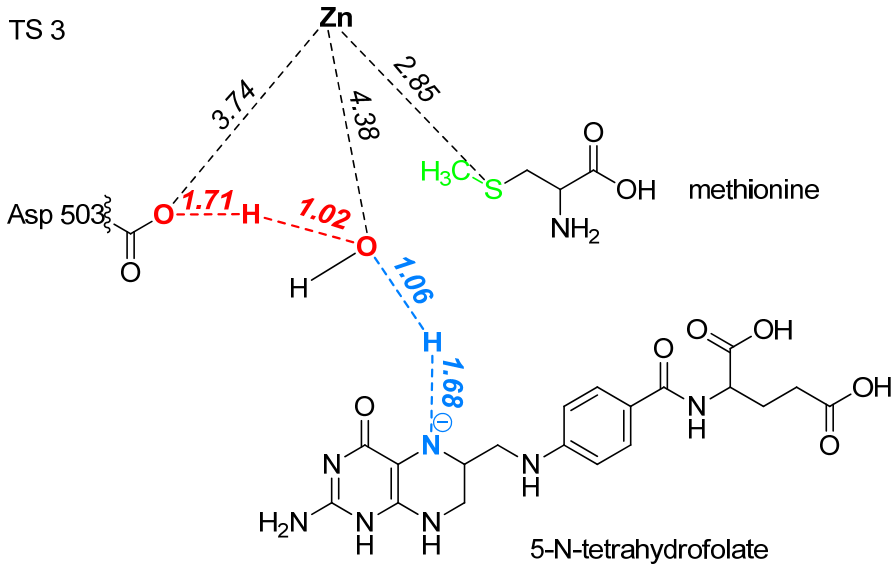

Figure 45. Third transition state (TS 3) with the atomic distances expressed in Å

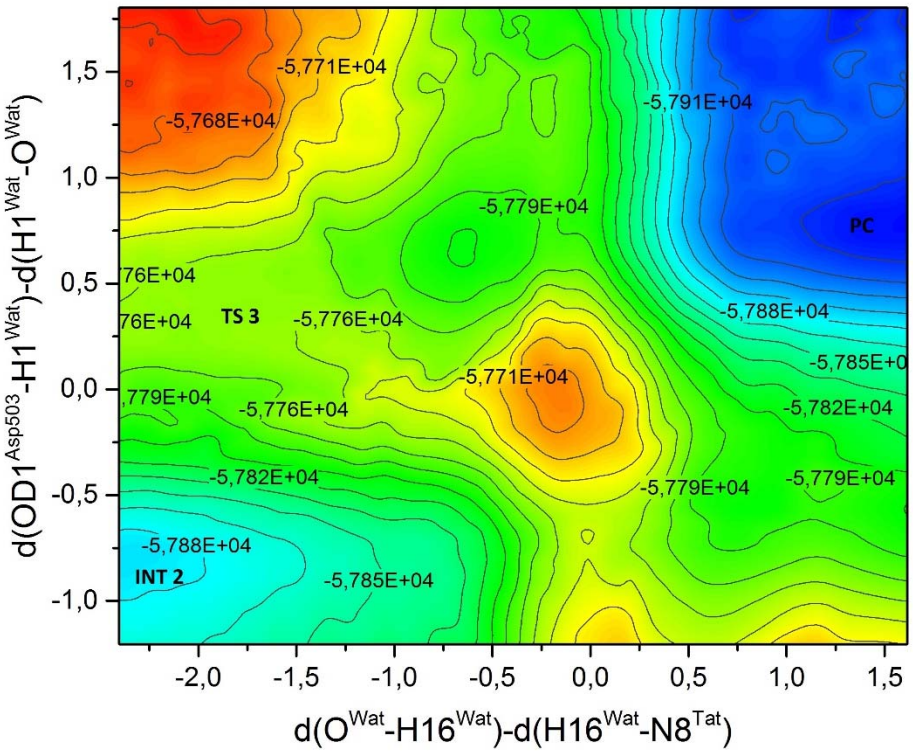

Figure 46. Two-dimensional potential energy surface scan for the final transfer of the proton on the nitrogen atom. Superscripts description: Wat – water molecule, ASP503 – residue aspartate 503, Tat – 5-*N*-methyltetrahydrofolate, Hcy – homocysteine

After localization of TS 3 (Figure 46), the reaction mechanism is completed and the products are shown on Figure 47.

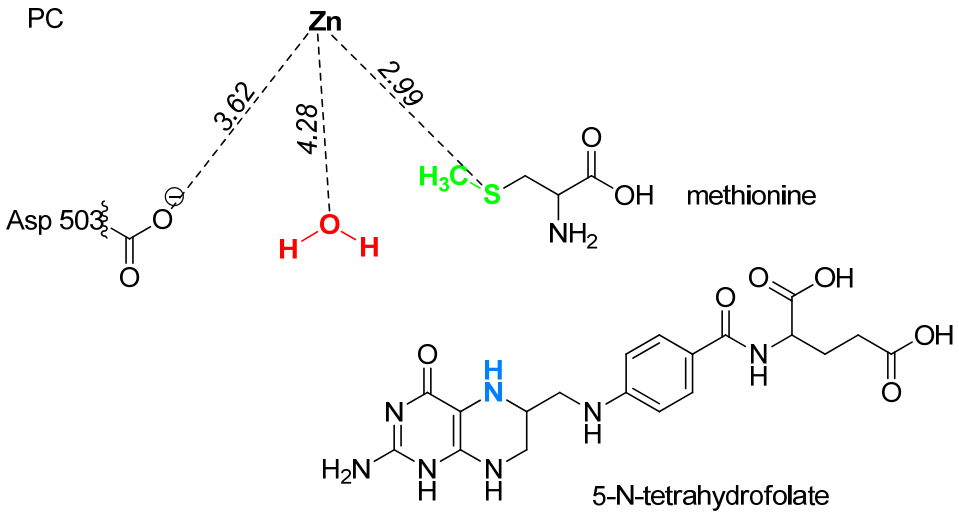

Figure 47. Products of the methyl group reaction – methionine and 5-*N*-tetrahydrofolate with the atomic distances expressed in Å

4.7.2 Kinetic isotope effects

As it is defined,[148] the rate limiting-step for the reaction is the partial reaction, which has the highest energy barrier. Previously localized transition states were then taken for intrinsic reaction coordinates (IRC) calculations, through which it was possible to localize minima and calculate potential energy for every stage of the reaction. Values obtained for the potential energy on each stage of the reaction were calculated using the semi-empirical PM3 method. This procedure using semi-empirical approach though, was conducted to obtain the plausible values which would serve more as a guidance to determine the rate limiting step. Figure 48 shows the calculation of the energetics of the reaction pathway. As can be seen, the transition from INT 1 to TS 2 shows the highest energy barrier and can be considered as the rate-limiting step for methyl transfer between 5-*N*-methyltetrahydrofolate and homocysteine.

[148] 'rate-limiting step.' A Dictionary of Biology. 2004. Encyclopedia.com..

Figure 48. Potential energy profile of methyl transfer in cobalamin-independent methionine synthase

The kinetic isotope effects (KIE) were calculated (Figure 49) using the fDynamo library:[149]

$$KIE = \frac{(\frac{Q_a}{Q_b})_L}{(\frac{Q_a}{Q_b})_H} e^{-1/RT(\Delta ZPE_L - \Delta ZPE_H)} \qquad \textit{Equation 21}$$

where Q – partition function, a – transition state structure coordinates, b – reactant complex structure coordinates, ZPE – the zero point energy factor, R – gas constant, T- temperature, L – light isotope, H – heavy isotope.

The key objective was to prove that there is a KIE for this reaction: a refined value for the KIE would be desirable but is not an absolute requirement.

[149] M. J. Field *et al.*, '*The dynamo library for molecular simulations using hybrid quantum mechanical and molecular mechanical potentials',* Journal of Computational Chemistry, 21 (12), (2000), 1088-1100.

Figure 49. KIE's calculated for homocysteine and 5-*N*-methyltetrahydrofolate; methyl group transfer reaction. Values in red shows the normal kinetic isotope effects

Two interesting points are seen. Firstly, negligible S^{34} KIE is seen for the sulphur atom of homocysteine (0.998), indicating that neither the fission of the S-H bond nor the formation of the S-CH_3 bond influences the rate of the reaction. Secondly, strong normal isotope effects are calculated for the carbon of the methyl group (1.087) and the nitrogen (1.028) of the 5-*N*-methyltetrahydrofolate, indicating that the rupture of this bond is the key event in reaction mechanism.

4.8 Conclusions

Good agreement is found between the experimental values for KIE for methyl group transfer in the formation of methionine and the KIE predicted based on a theoretical treatment of the enzyme. Firstly, then it can be concluded that theoretical calculations are serving as a complimentary results to the experimental data obtained by irm-^{13}C NMR and irm-EA/MS for methionine. Together, these data and calculations support strongly the hypothesis that the observed depletion in methyl groups in natural products can be traced back to the formation of Met by the enzyme methionine synthase. However, it still needs to be shown the extent to which further selection against ^{13}C takes place in the individual *O*- and *N*-methyltransferases.

A particularly intriguing case is that of vanillin. In this phenolic compounds derived from ferulic acid, the *O*-methyl group does not show significant depletion relative to the remainder of the molecule.[150] An explanation of this needs to be sought.

[150] E. J. Tenailleau *et al.*, *'Authentication of the origin of vanillin using quantitative natural abundance ^{13}C NMR',* Journal of Agricultural and Food Chemistry, 52 (26), (2004), 7782-7787;M. Greule *et al.*, '*Improved rapid authentication of vanillin using $\delta^{13}C$ and $\delta^{2}H$ values',* European Food Research and Technology, 231 (6), (2010), 933-941; A. Chaintreau *et al.*, '*Site-specific ^{13}C content content by quantitative isotopic ^{13}C Nuclear Magnetic Resonance Spectrometry: A pilot inter-laboratory study',* Analytica Chimica Acta, 788, (2013), 108-113.

5 Chapter V – Isotope fractionation in natural alkaloids

5.1 Introduction

There are thousands of different plant products that have nitrogen in their structures. Different groups of plants contain compounds which possess in their structure a nitrogen atom, usually heterocyclic, and which are called 'alkaloids'. The word 'alkaloid' comes from the Arabic – *al-qali* (meaning: early form of soda ash). All alkaloids are basic compounds that contain one or more heterocyclic nitrogen atoms which, in most cases, originates from an amino acid.[151] In terms of their biosynthetic origin they may be derived from many groups of compounds such as amino acids, terpenes, or aromatics, depending on the specific details of the alkaloid structure. Although most of the known nitrogen-containing specialised metabolites are described as alkaloids, some are classified otherwise, as amines or glucosinolates. The majority of alkaloids are obtained from plants, but alkaloids also occur in some marine organisms and insects.

Normally, alkaloids are grouped on the basis of their ring system. We can distinguish several common ring systems including indolizidine- and quinolizidine-based ones,[152] as well as the recently reviewed (including their biosynthesis) acridone-based group.[153] A large number of alkaloids are directly obtained from the aromatic amino acids, tyrosine, tryptophan or phenylalanine. In others, such as tobacco alkaloid, nicotine, that accumulates in plants such as tobacco (*Nicotiana tabacum*), it has been shown that part of the structure arises from aspartic acid that combines with glcerylaldehyde-3-phosphate in the production of nicotinic acid, while the other part of the molecule arises from the non-protein amino acid, ornithine (see section 5.2.).

For many years, alkaloids in plants were considered as a waste products of plant metabolism. Taking into consideration the fact that plants are energetically efficient organisms this suggestion is clearly invalid and it reflects the lack of understanding in the past of plant metabolism. It is now recognized that they have many important roles, notably as chemoprotective and antiherbivory agents in plants.[154] Simplifying, there is always a reason for the production of the alkaloids!

The use of alkaloids by people dates back several thousands of years. They were prepared as a plant extracts for poisons, stimulants, narcotics or for medicinal purposes. About 150 years ago, interest rose around the structure of natural products and much research focused on the alkaloids - or so called 'vegetable alkalis' - was conducted. Primarily, the isolation techniques were developed by British and German chemists. The ability to isolate analytically pure samples was a crucial step for the exploitation of compounds that possessed biological effects. Many of the common drugs nowadays - both used and abused - are of alkaloid origin or based on natural

[151] Paul M. Dewick, *Medicinal Natural Products: A Biosynthetic Approach* (John Wiley & Sons, 2002).
[152] J. P. Michael, *'Quinoline, Quinazoline and Acridone Alkaloids'*, Natural Product Reports, 21.5 (2004), 650–68; J. P. Michael, *'Indolizidine and Quinolizidine Alkaloids'*, Natural Product Reports, 20.5 (2003), 458–75.
[153] R. B. Herbert, *'The Biosynthesis of Plant Alkaloids and Nitrogenous Microbial Metabolites'*, Natural Product Reports, 10.6 (1993), 575.
[154] B. B. Buchanan *et al.*, *'Biochemistry and Molecular Biology of Plants'*, American Society of Plant Biologists, Wiley Blackwell, ISBN: 978-0-470-71421-8, (2015).

alkaloids. Best known examples include caffeine, nicotine and quinine. More health-hazardous examples are cocaine, morphine and strychnine. In general, many of the better-known alkaloids are pharmacologically active and have some very important medicinal properties for humans.

5.2 Alkaloids of the Solanaceae: nicotine and tropine[155]

Despite superficial structural dissimilarities, the pyrrolidine moiety of nicotine and tropine (of which atropine, hyoscyamine and scopolamine are the tropoyl ester) have a common precursor in L-ornithine, and share four enzymatic steps to the intermediate *N*-methyl-Δ^1-pyrrolinium salt (Figure 50). Thereafter, a series of diverse enzymes intervene to condense this intermediate with different groups to render more elaborated structures. A number of the enzymes involved in this pathway are well described: others remain poorly understood.

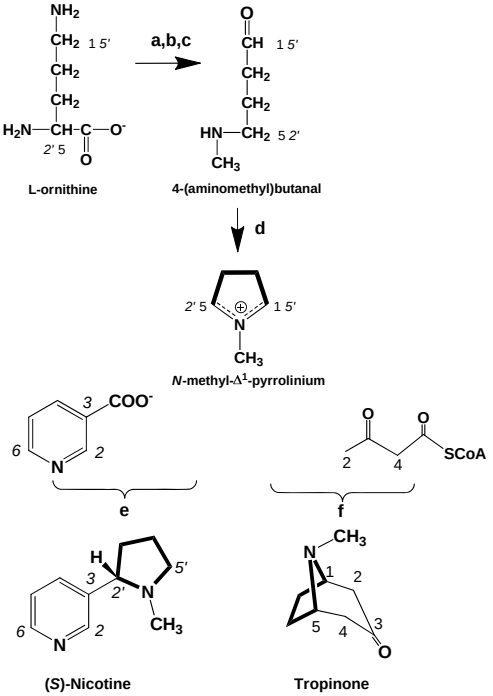

Figure 50. Schematic representation of the biosynthetic pathway to nicotine and tropine indicating the common and unique steps. Carbon atoms on the final compounds are numbered according to the IUPAC nomenclature and this numbering is used to indicate the carbon positions from which they are derived in the precursor molecules. Numbers in normal bold font refer to tropine; numbers in italic bold font refer to nicotine. The enzymes indicated are: a, ornithine decarboxylase (EC 4.1.1.17); b, putrescine *N*-methyltransferase (EC 2.1.1.53); c, *N*-methylputrescine oxidase (EC 1.4.3.6); d, undescribed activity, probably spontaneous[156]; e, nicotine synthase (undescribed activity[157]); f, undescribed activity

In both these alkaloids, the reactions by which *N*-methyl-Δ^1-pyrrolinium salt is further elaborated have resisted a number of attempts at characterization, despite their central role in

[155] This section is the publication by K. M. Romek *et al.* '*Non-statistical ^{13}C fractionation distinguishes coincident and divergent steps in the biosynthesis of the alkaloids nicotine and tropine*'.

[156] M. Naconsie *et al.*, *'Molecular Evolution of N-Methylputrescine Oxidase in Tobacco'*, Plant & Cell Physiology, 55.2 (2014), 436–44.

[157] J. B. Friesen and E. Leete, *'Nicotine Synthase - an Enzyme from Nicotiana Species Which Catalyzes the Formation of (S)-Nicotine from Nicotinic Acid and 1-Methyl-Δ'pyrrolinium Chloride'*, Tetrahedron Letters, 31.44 (1990), 6295–98.

the pathways. In the case of *S*-(-)-nicotine, a stereospecific decarboxylative condensation with a derivative of nicotinate leads to *S*-(-)-nicotine. An extremely weak 'nicotine synthase' has been reported,[158] but other authors could not repeat this finding.[159] While it has been suggested that this is possibly catalysed by an enzyme of the berberine-bridge type,[160] no details of the nature of this key enzyme nor of its mechanism are available.

In parallel fashion, condensation with the C2 position of acetoacetate (probably activated as the CoA thioester) followed by decarboxylation (probably spontaneous) leads to tropinone.[161] Despite many efforts, the enzymology of the conversion of *N*-methyl-Δ^1-pyrrolinium to tropinone remains elusive. Tropine is produced therefrom by a stereospecific oxidoreductase[162] and is esterified with phenyllactoyl-CoA thioester to form the alkaloid littorine, precursor to hyoscyamine and scopolamine.[163]

In such cases, where enzymological approaches have proved inadequate, alternative means to probe the biochemistry are required. The development of molecular biological approaches has been fruitful[164] but is challenging where the enzymology is completely unknown. In this perspective, we have therefore adopted an alternative 'retro-biosynthetic' approach involving the measurement and interpretation of the natural fractionation in ^{2}H or ^{13}C isotopes during the course of biosynthetic reactions. During the metabolic processes by which natural products are biosynthesized, isotopic fractionation[165] occurs, due to the sensitivity/insensitivity of the enzymes involved to the presence/absence of one or more heavy atoms in the reaction centre. This is the kinetic isotope effect (KIE). The position-specific isotope ratio in natural products is non-statistically distributed amongst the different positions. Of especial interest in the context of biosynthesis are the position-specific ^{13}C/^{12}C ratios, as these reflect the carbon skeleton(s) already present in the precursor molecule(s) and the biochemical processing each position has undergone at different steps in the pathway. Hence, a study of the position-specific ^{13}C/^{12}C rati-

---

[158] J. B. Friesen and E. Leete, *'Nicotine Synthase - an Enzyme from Nicotiana Species Which Catalyzes the Formation of (S)-Nicotine from Nicotinic Acid and 1-Methyl-Δ'pyrrolinium Chloride'*, Tetrahedron Letters, 31.44 (1990), 6295–98.

[159] R. E. Dewey and J. Xie, *'Molecular Genetics of Alkaloid Biosynthesis in Nicotiana Tabacum'*, Phytochemistry, 94 (2013), 10–27.

[160] R. S. Lewis *et al.*, *'Transgenic and Mutation-Based Suppression of a Berberine Bridge Enzyme-Like (BBL) Gene Family Reduces Alkaloid Content in Field-Grown Tobacco',* PLOS ONE, 10.2 (2015).

[161] R. J. Robins and N. J. Walton, *The Alkaloids: Chemistry and Pharmacology* (Academic Press, 1994).

[162] B. Dräger, *'Tropinone Reductases, Enzymes at the Branch Point of Tropane Alkaloid Metabolism'*, Phytochemistry, 67.4 (2006), 327–37.

[163] R. J. Robins *et al.*, *'Biosynthesis of Hyoscyamine Involves an Intramolecular Rearrangement of Littorine',* Journal of the Chemical Society*, Perkin Transactions 1*, 1994, 615–19; D. O'Hagan, R. J. Robins, *'Tropic Acid Ester Biosynthesis in Datura Stramonium and Related Species'*, Chemical Society Reviews, 27.3 (1998), 207–12; N. C. J. E. Chesters *et al.*, *'The Biosynthesis of Tropic Acid in Plants: Evidence for the Direct Rearrangement of 3-Phenyllactate to Tropate'*, Journal of the Chemical Society, Perkin Transactions 1, 1994, 1159–62; R. Li and others, *'Functional Genomic Analysis of Alkaloid Biosynthesis in Hyoscyamus Niger Reveals a Cytochrome P450 Involved in Littorine Rearrangement*', Chemistry & Biology, 13.5 (2006), 513–20.

[164] H. L. Dalton *et al.*, *'Effects of down-Regulating Ornithine Decarboxylase upon Putrescine-Associated Metabolism and Growth in Nicotiana Tabacum L*', Journal of Experimental Botany, 67.11 (2016), 3367–81.

[165] I. T. Baldwin, *'The Alkaloidal Responses of Wild Tobacco to Real and Simulated Herbivory*', Oecologia, 77.3 (1988), 378–81.

os should enable the interpretation of the values observed in terms of the known biochemistry[166].

This approach has proved remarkably accurate for primary metabolites and for a small number of specialized products[167]. However, accurate measurement of position-specific $^{13}C/^{12}C$ ratios has until recently been hampered by technical difficulties, when suitable conditions for isotope ratio monitoring by ^{13}C NMR (irm-^{13}C NMR) spectrometry applied to medium-sized molecules have been established.

5.2.1 Methodology

5.2.1.1 Materials

Tropine ((3-*endo*)-8-methyl-8-azabicyclo[3.2.1]octan-3-ol) (TRI-1, hydrate 98+%, batch N° S21312-474 and *S*-(-)-nicotine ((*S*)-3-[1-methylpyrrolidin-2-yl]pyridine) (NIC-1, free base >99%, batch N° 1449164V) were obtained from Sigma-Aldrich (www.sigmaaldrich.com); tropine free base (TRI-3, >97%, batch N° 1212025) was obtained from Fluka (www.sigmaaldrich.com); *S*-(-)-nicotine (NIC-3, free base >99.9%) was obtained from CHEMNOVATIC Ławecki Gęca Sp.j., Lublin, Poland. All these samples are of authenticated natural origin as indicated by their Certificate of Origin (note that the plant species used is not indicated) except for TRI-1, for which no certificate was available. Tris(2,4-pentadionato)chromium-(III) ($Cr(Acac)_3$) was from Merck (www.merck.com). Benzene-d_6 and acetonitrile-d_3 were obtained from Euriso-top (www.eurisotop.com).

5.2.1.2 Isotope ratio monitoring by mass spectrometry

The global value for the whole molecule, $\delta^{13}C_g$ [‰], is the deviation of the carbon isotopic ratio R_s relative to that of the international standard Vienna Pee Dee Belemnite, (V-PDB), $R_{V\text{-}PDB}$. It is determined by isotope ratio monitoring by mass spectrometry and calculated from:

$$\delta^{13}C_g\ [‰] = \left(\frac{R_S}{R_{V-PDB}} - 1 \right) \qquad \textit{Equation 22}$$

where the value of $R_{V\text{-}PDB}$ is 0.0111802.[168]

[166] H-L. Schmidt *et al. 'Multi-Factorial in Vivo Stable Isotope Fractionation: Causes, Correlations, Consequences and Applications'*, Isotopes in Environmental and Health Studies, 51.1 (2015), 155–99.
[167] H-L. Schmidt and G. Gleixner, *'Carbon Isotope Effects on Key Reactions in Plant Metabolism and ^{13}C-Patterns in Natural Compounds',* Stable Isotopes, ed. by H. Griffiths (Oxford: BIOS Scientific Publisher, 1998), pp. 13–25; S. M. N. Efange, *'Synthesis and Applications of Isotopically Labelled Compounds',* Radiology, 176.2 (1990), 438–438.
[168] R. A. Werner and W. A. Brand, *'Referencing strategies and techniques in stable isotope ratio analysis',* Rapid Communications in Mass Spectrometry, 15, (2001), 501-519.

5.2.1.3 Isotope ratio monitoring by ^{13}C NMR acquisition conditions

Prior to preparation of samples for irm-^{13}C NMR, purity was confirmed to be superior to 98% by recording a ^{1}H NMR spectrum. Tropine free base from Fluka (TRI-3) was re-crystallized from diethyl ether before use.

For the analysis of nicotine, 250 µL of *S*-(-)-nicotine was homogenized in 500 µL of acetonitrile-d_3. To this was added 100 µL of a solution of relaxation agent $Cr(Acac)_3$ (0.1 M) prepared by dissolving 10.5 mg $Cr(Acac)_3$ in 300 µL of acetonitrile-d_3. Under these conditions, T_1^{max}=3.74 s. Spectral acquisition was with AQ=1.0 s for 152 scans, giving a signal-to-noise ratio of ~700.

For the analysis of tropine, 150 mg of tropine was dissolved in 600 µL of benzene-d_6. As T_1^{max}=1.53 s is relatively short in these conditions, relaxation agent was not required. Spectra acquisition was with AQ=0.95 s for 400 scans, giving a signal-to-noise ratio ~550.

Quantitative ^{13}C NMR spectra were recorded at 100.6 MHz using a Bruker 400 Avance I NMR spectrometer fitted with a 5 mm $^{1}H/^{13}C$ dual^{+} probe. For *S*-(-)-nicotine, spectra were also measured on a Bruker 400 Avance III NMR spectrometer fitted with a 5 mm a BBFO probe. The temperature of the probe was set at 303 K for nicotine and 313.2 K for tropine (to decrease the viscosity of the sample). The offsets for both ^{13}C and ^{1}H were set at the middle of the frequency range for each analyte. Inverse-gated decoupling was applied and the repetition delay between each 90° pulse was set at $10\times T_1^{max}$ of the analyte to avoid the nuclear Overhauser effect and to achieve full relaxation of the magnetization. The decoupling sequence used adiabatic full-passage pulses with cosine square amplitude modulation (ν_2^{max} = 17.6 kHz) and offset independent adiabaticity with optimized frequency sweep.[169] Each measurement consisted of the average of five independently recorded NMR spectra.

Suitable conditions were established for the acquisition of ^{13}C NMR spectra amenable to the calculation of position-specific $^{13}C/^{12}C$ ratios. Representative spectra are illustrated in Figures 51-52.

[169] E. Tenailleau and S. Akoka, '*Adiabatic ^{1}H decoupling scheme for very accurate intensity measurements in ^{13}C NMR*' Journal of Magnetic Resonance, 185 (1), (2007), 50-58.

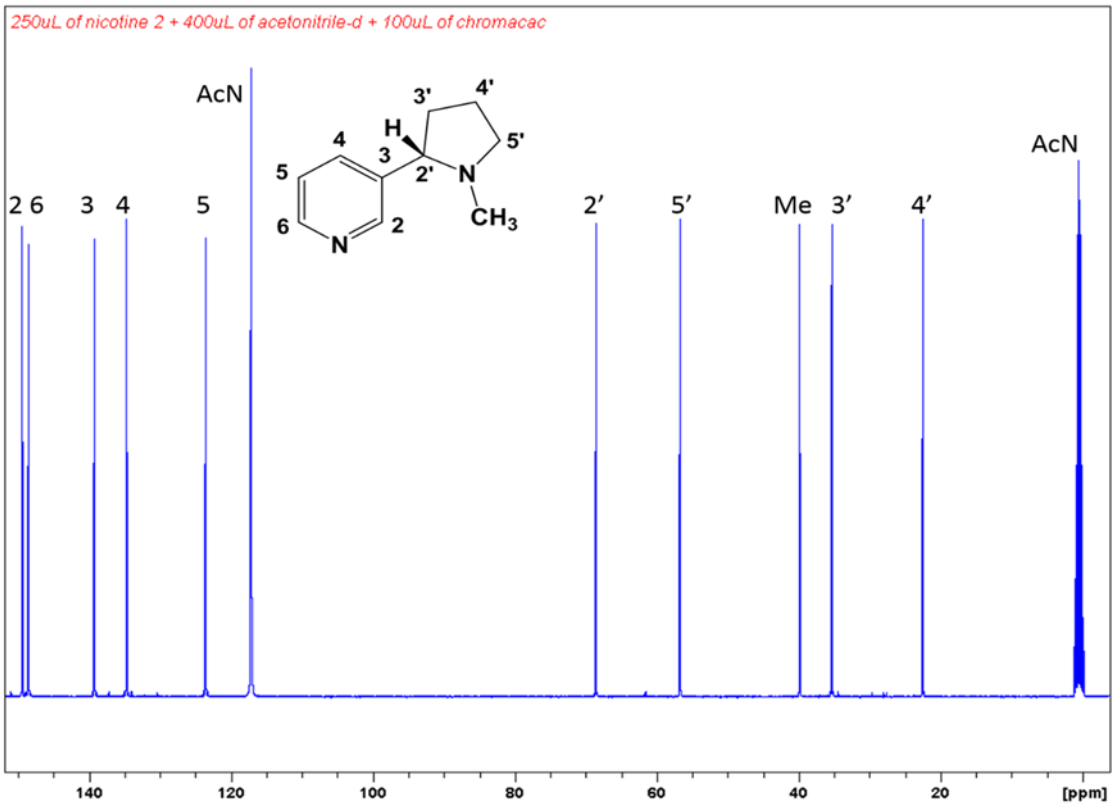

Figure 51. ^{13}C NMR spectra acquired under quantitative conditions of *S*-(-)-nicotine. Carbon atom displacements are indicated. AcN=acetonitrile

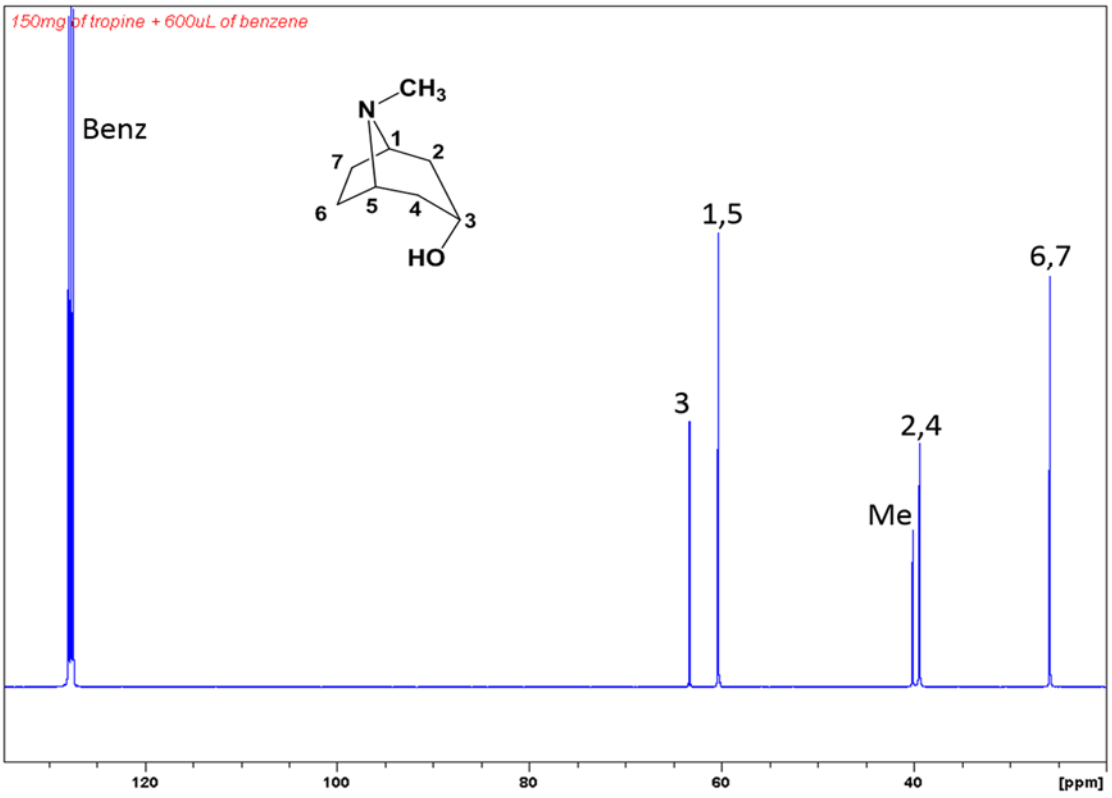

Figure 52. ^{13}C NMR spectra acquired under quantitative conditions of tropine. Carbon atom displacements are indicated. Benz=benzene

5.2.1.3.1 Spectral data processing

To obtain S_i, the area under the ^{13}C-signal in the irm-^{13}C NMR spectrum for C-atom in position *i*, curve fitting based on a total-line-shape analyses (deconvolution) was carried out with a Lorentzian mathematical model using Perch Software (Perch™ NMR Software, http://www.perchsolutions.com). In this procedure, line-shape parameters are optimized in terms of intensities, frequencies, line-width, line-shape (Gaussian/Lorentzian, phase, asymmetry) by iterative fitted to a minimal residue. For each target compound, spectral phasing and line-fitting was performed using the same parameters. The positional isotopic distribution, f_i/F_i, was then calculated from the values of S_i, hence the $\delta^{13}C_i$ [‰] value, as described previously[170]. For *S*-(-)-nicotine, due to the large range of its spectral shifts, a correction was made to data obtained on the Avance I NMR spectrometer using the data from the Avance III NMR spectrometer (see[171] for a detailed explanation). It should be noted that, since the coupling constants J (^{13}C-^{15}N) are of the order of 10 Hz, no correction for these is required as they are included within the curve fitting applied to the peak.

5.2.2 Interpretation in relation to known biosynthetic pathway

Following the successful development of the required protocols, it proved feasible to obtain position-specific ^{13}C/^{12}C ratios for all carbon atoms of the two target alkaloids. Thus, it is possible to exploit these to probe a number of aspects of the biosynthesis of these natural products.

5.2.2.1 To what extent are isotope ratios determined by the primary precursor molecules giving rise to the N-methyl-Δ^1- pyrrolinium salt?

In *S*-(-)-nicotine the carbon atoms that compose the pyrrolidine ring, C2'$_N$,[3] C3'$_N$, C4'$_N$ and C5'$_N$ are derived from L-ornithine. This involves four known enzymatic steps (Figure 53).[172]Looking further back into the metabolic precursors, these carbons can be traced to citric acid, a component of the Krebs cycle, thence to oxaloacetate and acetyl-CoA. Therefore, it can be deduced that the C2$_{OX}$ and C3$_{OX}$ of oxaloacetate become the C3'$_N$ and C2'$_N$, respectively, in nicotine. Similarly, the C1$_A$ and C2$_A$ of acetate are incorporated via citrate into the C5'$_N$ and C4'$_N$, respectively.

---

[170] K. Bayle *et al.*, *'Isotopic ^{13}C NMR Spectrometry to Assess Counterfeiting of Active Pharmaceutical Ingredients: Site-Specific ^{13}C Content of Aspirin and Paracetamol'*, Journal of Pharmaceutical and Biomedical Analysis, 50.3 (2009), 336–41; A. Chaintreau *et al.*, *'Site-Specific ^{13}C Content by Quantitative Isotopic ^{13}C Nuclear Magnetic Resonance Spectrometry: A Pilot Inter-Laboratory Study'*, Analytica Chimica Acta, 788 (2013), 108–13.

[171] K. Bayle *et al.*, *'Conditions to obtain precise and true measurements of the intramolecular ^{13}C distribution in organic molecules by isotopic ^{13}C Nuclear Magnetic Resonance spectrometry'* Analytica Chimica Acta, 846, (2014), 1-7.

[172] R. E. Dewey and J. Xie, *'Molecular genetics of alkaloid biosynthesis in Nicotiana tabacum'* Phytochemistry, 94, (2013), 10-27.

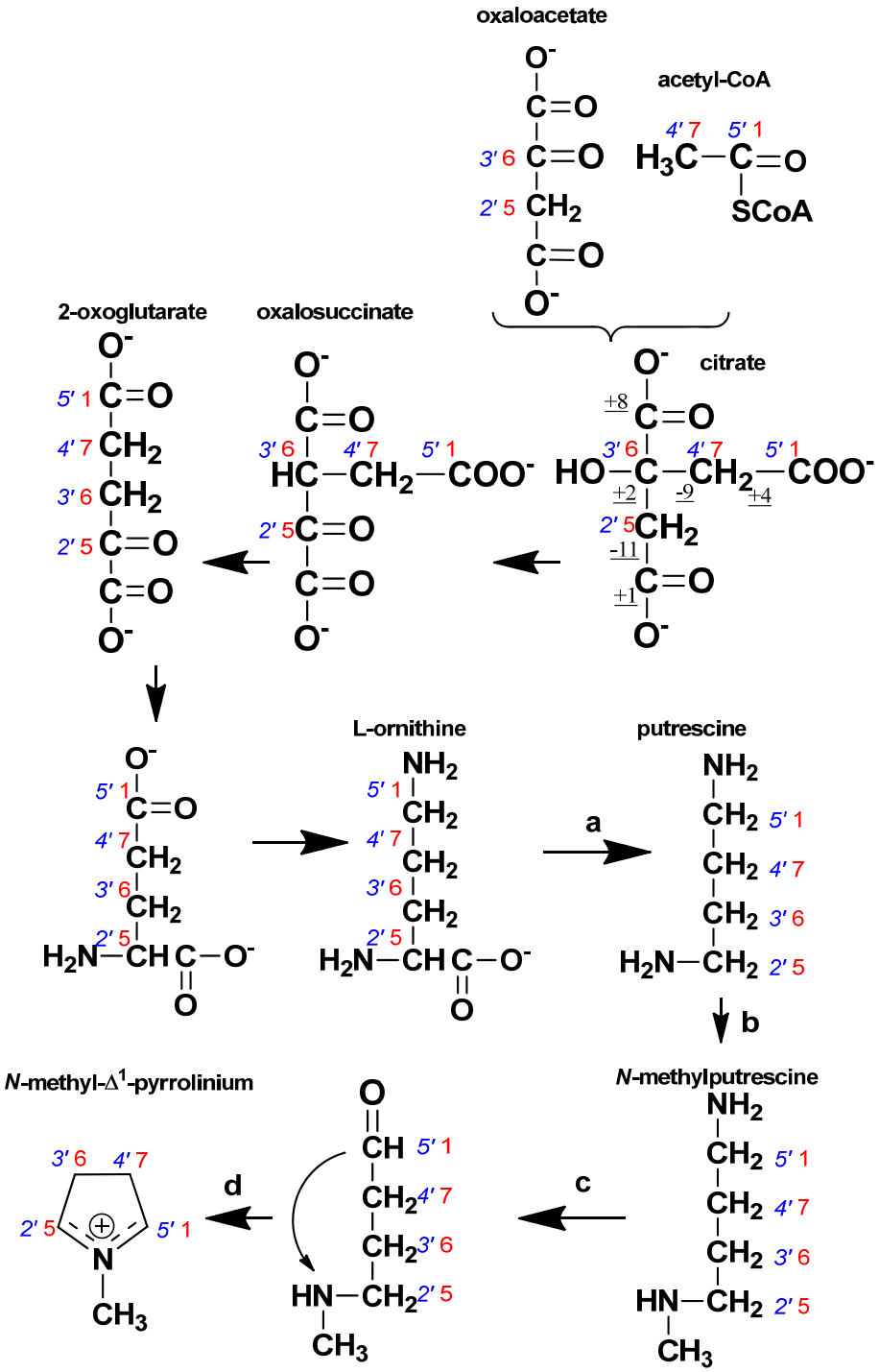

Figure 53. Schematic representation of the biosynthetic pathway to *N*-methyl-Δ^1-pyrrolinium salt from primary precursors. Carbon atoms on the final compounds are numbered according to the IUPAC nomenclature and this numbering is used to indicate the carbon positions from which they are derived in the precursor molecules. Numbers in red font refer to tropine; numbers in blue font refer to nicotine. Values for $\delta^{13}C_i$ [‰] of citrate acting as a metabolic intermediate taken from[173] are indicated underlined

[173] H-L. Schmidt and G. Gleixner, *'Carbon isotope effects on key reactions in plant metabolism and ^{13}C-patterns in natural compounds'*, Stable Isotopes, Integration of Biological, Ecological and Geochemical Processes, Oxford, (1998), pp.13-25.

For tropine, by a similar argument, it can be deduced that the $C2_{OX}$ and $C3_{OX}$ of oxaloacetate become the $C6_T$ and $C5_T$, respectively, while the $C1_A$ and $C2_A$ of acetate are incorporated into the $C1_T$ and $C7_T$, respectively (Figure 53).

This ancestry will play a significant role in determining the position-specific $^{13}C/^{12}C$ ratios observed, as they will either essentially be retained, or will be modified due to KIEs in the enzymes involved in the pathway.

Since tropine is spectrally the simpler of the two target molecules, its isotope pattern will be analyzed first. As can be seen from Figure 52, the pairs of carbons showing the same degree of deshielding, $C2_T$+$C4_T$, $C1_T$+$C5_T$ and $C6_T$+$C7_T$ result in coincident peaks in the ^{13}C NMR spectrum. The impact of this on interpreting the $^{13}C/^{12}C$ ratios measured is, however, minimal, as the $C1_T$+$C5_T$ and $C6_T$+C7T pairs of positions are biosynthetically equivalent. Not only is *N*-methyl-Δ^1-pyrrolinium a symmetrical molecule, but it is derived from the symmetrical molecule, putrescine. As there is no evidence of metabolic tunneling between L-ornithine and *N*-methylputrescine[174], it can be presumed that methylation of putrescine can occur on either the 1- or the 4-amino group with equal probability. Hence, the ($C2_O$;$C5_O$) and ($C3_O$;$C4_O$) positions in L-ornithine become indistinguishable in putrescine, hence in *N*-methylputrescine. Furthermore, tautomerism occurs around the quaternary nitrogen in *N*-methyl-Δ^1-pyrrolinium[175], so no distinction is made as to at which carbon the substitution that leads to the elaborated molecules takes place.

Considering the history of the four carbon atoms derived from *N*-methyl-Δ^1-pyrrolinium, the $C6_T$ and $C7_T$ have undergone no bond-forming reaction since the formation of citrate (Figure 53). As isotopic fractionation is associated with bond forming and breaking, so the opposite is true: carbon atoms not undergoing reactions are likely not to be significantly fractionated. Hence, at these positions the chances for isotopic fractionation are minimal, and this is reflected in these positions having a relatively high $\delta^{13}C_i$ [‰] value: -11.9‰ (Figures 54 and 55, Table 4). The $C(1+5)_T$ is however, relatively depleted, having a $\Delta\delta^{13}C_i$ [‰] value 10.4‰ lower than the $C(6+7)_T$. This can be explained by two contributing factors. The $C(1+5)_T$ is derived from the carboxyl group ($C1_A$) of acetyl-CoA, which in eukaryotes is enriched relative to the methyl group in conditions in which commitment of acetyl-CoA to synthesis is significant.[176] The degree of this varies. In lipids of eukaryotic origin (*Saccharomyces cerevisiae*) carbon positions derived from

[174] R. J. Robins *et al., 'Progress in the Genetic Engineering of the Pyridine and Tropane Alkaloid Biosynthetic Pathways of Solanaceous Plants'*, Genetic Engineering of Plant Secondary Metabolism, Recent Advances in Phytochemistry, 28 (Springer US, 1994), pp. 1–33.

[175] E. Leete, *'Biosynthesis of the Nicotiana Alkaloids. XI. Investigation of Tautomerism in N-Methyl-Δ^1-Pyrrolinium Chloride and Its Incorporation into Nicotine'*, Journal of the American Chemical Society, 89.26 (1967), 7081–84.

[176] H-L. Schmidt and G. Gleixner, *'Carbon isotope effects on key reactions in plant metabolism and ^{13}C-patterns in natural compounds'* Stable Isotope, Integration of Biological, Ecological and Geochemical Processes, BIOS Scientific, Oxford, (1998), pp. 13-25; H-L. Schmidt, *'Isotopic patterns in natural products: labels without labelling'*, Synthesis and applications of isotopically labelled compounds, (1994), pp. 869-874; K. D. Monson and J. Hayes, *'Biosynthetic control of the natural abundance of carbon-13 at specific positions within fatty acids in Saccharomyces cerevisiae. Isotopic fractionation in lipid synthesis as evidence for peroxisomal regulation',* Journal of Biological Chemistry, 257, (1982), 5568-5575.

the $C1_A$ are enriched relative to those from the $C2_A$ by ~5‰[177]. Similarly in ethanol from C_3 plants, although here the difference is closer to 2‰.[178] In tropine, the impact of this is, however, compensated by the relative depletion at the C2 of citrate ($C2_C$), and, based on estimated values for citrate where it is acting as a metabolic intermediate,[179] a $\Delta\delta^{13}C_i=[C(1+5)_T-C(6+7)_T]$ value of ~9‰ can be deduced. This is close to the observed differences in tropine.

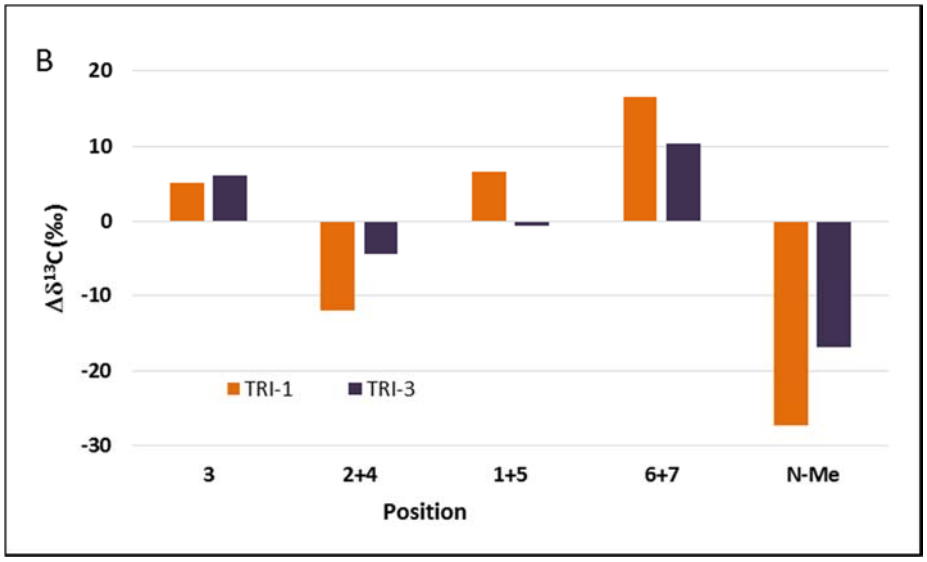

Figure 54. Position-specific $^{13}C/^{12}C$ ratios expressed as $\Delta\delta^{13}C_i$ [‰] for two samples of tropine; TRI-1 – natural sample of tropine, TRI-3 – commercial sample of tropine

[177] K. D. Monson and J. Hayes, *'Biosynthetic control of the natural abundance of carbon-13 at specific positions within fatty acids in Saccharomyces cerevisiae. Isotopic fractionation in lipid synthesis as evidence for peroxisomal regulation',* Journal of Biological Chemistry, 257, (1982), 5568-5575

[178] A. Gilbert *et al.*, *'The Intramolecular ^{13}C-Distribution in Ethanol Reveals the Influence of the CO_2-Fixation Pathway and Environmental Conditions on the Site-Specific ^{13}C Variation in Glucose'*, Plant, Cell & Environment, 34.7 (2011), 1104–12.

[179] H-L. Schmidt and G. Gleixner, *'Carbon isotope effects on key reactions in plant metabolism and ^{13}C-patterns in natural compounds'* Stable Isotope, Integration of Biological, Ecological and Geochemical Processes, BIOS Scientific, Oxford, (1998), pp. 13-25

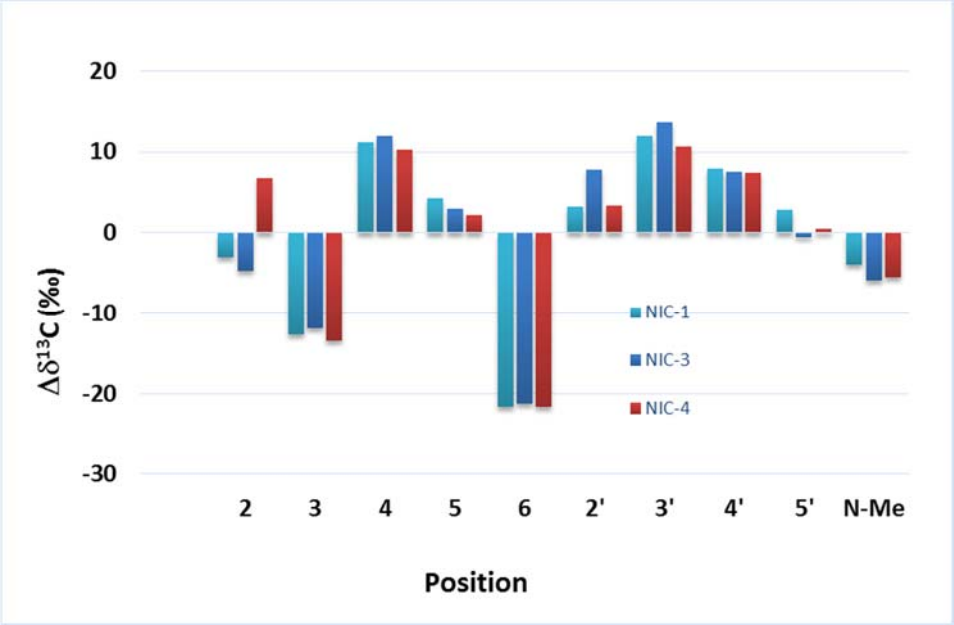

Figure 55. Position-specific $^{13}C/^{12}C$ ratios expressed as $\Delta\delta^{13}C_i$ [‰] for three samples of nicotine; NIC-1 and NIC-4 – natural sample of nicotine, NIC-3 – commercial sample of nicotine labelled 'synthetic'

Additionally, potential source of fractionation at the $C(1+5)_T$ value (but not the $C(6+7)_T$ value) is the two reactions involved in the final steps of the common pathway forming *N*-methyl-Δ^1-pyrrolinium, in both of which bond breaking/creation occurs. The ring closure reaction (Fig. 53, step d), in which a C–N bond is formed, is considered spontaneous,[180] the two compounds being in equilibrium. This step is unlikely to contribute a significant isotope fractionation as, even if there is an equilibrium isotope effect, the compound in either open or ring-closed structure is fully committed to the pathway. The previous step, in which a C–N bond is broken and a C=O bond is formed is catalyzed by the enzyme *N*-methylputrescine oxidase (EC 1.4.3.6) (Figure 53, step c). An intramolecular normal KIE associated with amine oxidase have been reported,[181] so a fractionation during the deamination of *N*-methylputrescine would select in favor of isotopomers containing ^{12}C at the $C1_T$ position, since it involves an $sp^3 \rightarrow sp^2$ conversion[182]. This would lead to a ^{13}C depletion of the C-atom. However, as the commitment of *N*-methylputrescine to tropine biosynthesis is very high, this intermediate being a dedicated component of the pathway, isotope fractionation due to this enzyme is unlikely to be significant (see [183] for a detailed discussion of this phenomenon).

These arguments apply equally to the equivalent four carbon atoms of the pyrrolidine ring in *S*-(-)-nicotine biosynthesis ($C2'_N$, $C3'_N$, $C4'_N$, $C5'_N$). In this analyte, however, these four carbons are resolved in the ^{13}C NMR spectrum (Figure 51), which enables a more detailed inter-

[180] M. Naconsie *et al.*, *'Molecular evolution of N-methylputrescine oxidase in tobacco'*, Plant and Cell Physiology, 55, (2014), 436-444.
[181] J. M. Kim *et al.*, *'Mechanistic Analysis of the 3-Methyllumiflavin-Promoted Oxidative Deamination of Benzylamine. A Potential Model for Monoamine Oxidase Catalysis'*, Journal of the American Chemical Society, 115.23 (1993), 10591–95.
[182] F. J. Winkler, *'Reaction Rates of Isotopic Molecules'*, Angewandte Chemie, 93.2 (1981), 220–220.
[183] H-L. Schmidt, *'Fundamentals and Systematics of the Non-Statistical Distributions of Isotopes in Natural Compounds'*, Naturwissenschaften, 90, (2003), 537-52 .

pretation (see below). Once again, the $C3'_N$ and $C4'_N$, derived from citrate essentially without undergoing further reaction, are enriched relative to the $C5'_N$ and $C2'_N$, which have undergone deaminative oxidation and C–N bond formation, respectively (Figure 53). Furthermore, the relative depletion at the $C(2'+5')_N$ relative to the $C(3'+4')_N$ of ~7‰ is in the same sense and of a similar size to this comparison in tropine (~10‰).

Hence, it can be concluded (i), that the values obtained in the common compound *N*-methyl-Δ^1-pyrrolinium can be explained on the basis of the values in their distal precursors and (ii), that this relationship is dictated primarily by the metabolic pathway, and is relatively independent of the plant species involved.

5.2.2.2 To what extent are isotope ratios determined by the primary precursor molecules giving rise to the nicotinic acid-derived moiety of S-(-)-nicotine?

Nicotinic acid in plants is considered to be synthesized primarily from aspartate plus dihydroxyacetone phosphate/glyceraldehyde-3-phosphate (DHAP/G3P).[184] The incorporation of [3-^{14}C]aspartate into both the $C2_N$ and $C3_N$ of *S*-(-)-nicotine effectively demonstrated this origin for the pyridine ring.[185] Considering that nicotinate is a predominant source of precursor for *S*-(-)-nicotine, which is a major sink for carbon, then some characteristics can potentially be traced back to the precursor pools. $C2_N$ and $C3_N$ are derived from the $C1_{ASP}$ and $C2_{ASP}$, respectively, while the $C4_N$, $C5_N$ and $C6_N$ are from DHAP/G3P (Figure 56). (Note that the interconversion of DHAP and G3P in primary metabolism means that the $C4_N$ and $C6_N$ are of equivalent origin.) During the synthesis of nicotinic acid, all these positions are involved in reactions, although only the $C3_N$, $C4_N$ and $C6_N$ positions are involved in bond-formation. Again, therefore, it is these three positions that might be expected to show isotopic fractionation.

[184] A. Katoh *et al.*, *'Early Steps in the Biosynthesis of NAD in Arabidopsis Start with Aspartate and Occur in the Plastid',* Plant Physiology, 141.3 (2006), 851–57.
[185] T. M. Jackanicz and R. U. Byerrum, *'Incorporation of Aspartate and Malate into the Pyridine Ring of Nicotine'*, The Journal of Biological Chemistry, 241.6 (1966), 1296–99.

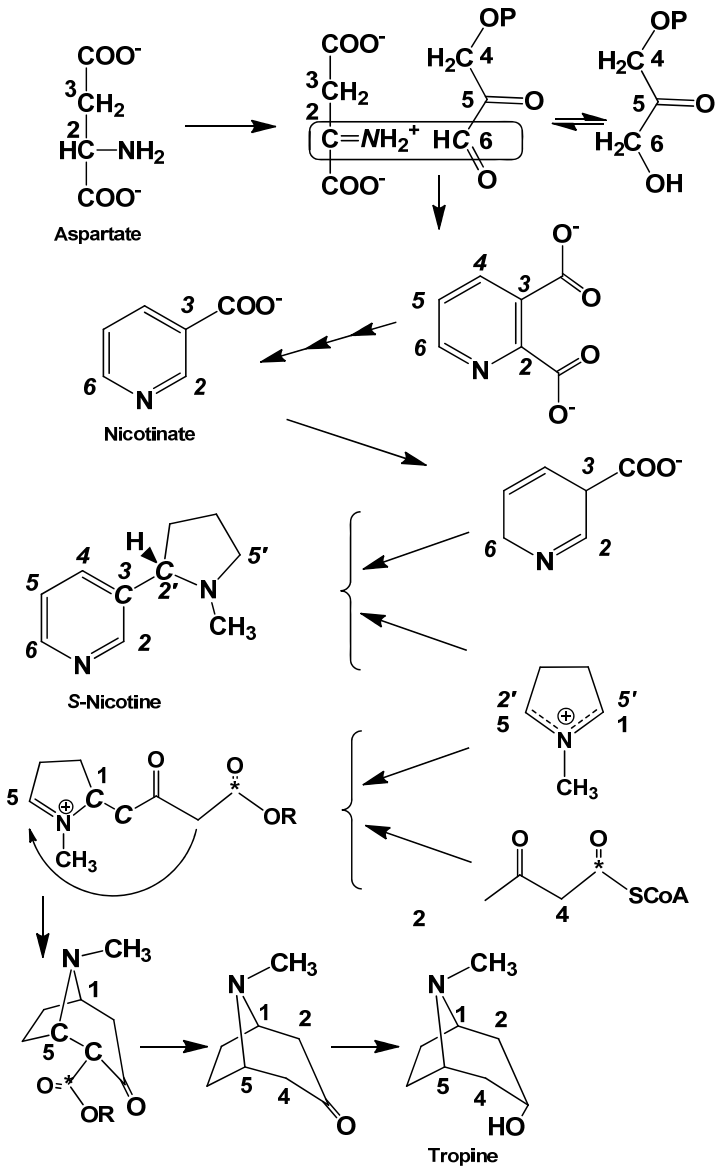

Figure 56. Schematic representation of the biosynthetic pathway to *S*-(-)-nicotine and tropine indicating the origins of the carbon atoms. Those carbon and nitrogen atoms involved in the formation of bonds, and therefore the more likely undergo isotope fractionation are indicated in italics. Carbon atoms on the final compounds are numbered according to the IUPAC nomenclature. For all other compounds, the numbering indicates the position in the analyte in which the give carbon will be found. Numbers in normal bold font refer to tropine; numbers in italic bold font refer to nicotine

First, let us consider the three carbon positions showing the least relative depletion in the pyridine ring, $C2_N$, $C4_N$ and $C5_N$. The $C5_N$ ($\delta^{13}C_i$ = -26.7‰) is from the keto group of DHAP and undergoes an $sp^2 \rightarrow \pi$ transition in the formation of quinolinic acid. The $C4_N$ is the most enriched position ($\delta^{13}C_i$ = -18.9‰) and, although this carbon is involved in the formation of a C–C bond with the $C3_N$ in the formation of quinolinic acid and an $sp^3 \rightarrow \pi$ transition, its bonding thereafter is unchanged. In both of these positions, it is apparent that negligible fractionation has occurred, at least relative to the other three positions in the pyridine ring. The $C2_N$ is involved in the de-carboxylation of quinolinic acid and has a $\delta^{13}C_i$ ~15‰ and ~7‰ depleted relative to the $C4_N$ and $C5_N$, respectively. Although decarboxylation can take place with negligible ^{13}C KIE on the α-

carbon,[186] it would appear that fractionation is occurring here and that decarboxylation is probably a kinetically regulating step.

The $C3_N$ at $\delta^{13}C_i \approx -42.8‰$ is ~8‰ depleted relative to the mean for the pyridine ring. This may be due to two additive effects. The first is the origin of this carbon: the $C3_{OX}$ of oxaloacetate. This carbon is estimated to be markedly depleted,[187] by ~11‰ relative to the other carbons of oxaloacetate (the immediate precursor of L-aspartate). Furthermore, $C3_N$ is involved in two bond-forming and one bond-breaking reactions, each of which may lead to selection against ^{13}C in this position (see below), hence relative depletion.

However, the most depleted position is the $C6_N$, which at $\delta^{13}C_i = -52‰$ is ~17‰ depleted relative to the mean for the pyridine ring. This position is involved in the formation of the C=N bond created when it is joined to the imino group of iminoaspartate by quinolinate synthase (EC 2.5.1.72) (Fig. 56, boxed positions in the first row). Two mechanisms have been proposed for this enzyme, which differ essentially in the order in which the two bonds are formed: there is no experimental evidence to favor one over the other.[188] However, in both cases the formation of the new C–C bond involves the nucleophilic attack of either $–NH_2$ or $=NH_2^+$ on a >C=O group. The degree of electrophilicity of the >C=O is considered likely to have a major influence on the $^{13}C/^{12}C$ ratio at this atom. Based on our data, a strong normal KIE is indicated.

5.2.2.3 To what extent do the reactions involving the conversion of *N*-methyl-Δ^1-pyrrolinium to tropinone influence the observed isotope ratios in tropine?

The elaboration of *N*-methyl-Δ^1-pyrrolinium to tropinone involves the introduction of the three carbons $C2_T$, $C3_T$ and $C4_T$ and the creation of two new C–C bonds at the $C1_T$ and $C5_T$ positions (Figure 49). These three carbons are derived from acetate, via acetoacetyl-CoA and 4-(1-methyl-2-pyrrolidinyl)-3-oxobutyrate (probably as the CoA thioester).[189] On the basis of the above discussion of the relative enrichments in acetyl-CoA, the $C3_T$, derived from the carboxyl in acetoacetyl-CoA, might be expected to be slightly enriched relative to the $C(2+4)_T$ if no other factors come into play. In fact, the $\Delta\delta^{13}C_i=[(C3_T)–(C(2+4)_T)]$ of ~13‰ implies a significant KIE associated with the formation of this moiety. This greater relative enrichment is, however, consistent with the characteristic strong ^{13}C KIE associated with aldol reactions of acetyl-CoA in the biosynthesis of natural products when there is a high commitment of acetyl-CoA. In these cases, a large depletion in the carbons derived from the methylene group is observed. Similarly, in citrate extracted from fruit juice, in which there is again a high commitment of acetyl-CoA to this

[186] E. Melzer and H-L. Schmidt, *'Carbon Isotope Effects on the Decarboxylation of Carboxylic Acids. Comparison of the Lactate Oxidase Reaction and the Degradation of Pyruvate by H_2O_2'*, Journal of Biochemistry, 252, (1988), 913-915.

[187] H-L. Schmidt and G. Gleixner, *'Carbon isotope effects on key reactions in plant metabolism and ^{13}C-patterns in natural compounds'*, Stable Isotopes. Integration of Biological, Ecological and Geochemical Processes, BIOS Scientific, Oxford, (1998), pp. 13-25.

[188] M. V. Cherrier *et al.*, *'The Crystal Structure of Fe_4S_4 Quinolinate Synthase Unravels an Enzymatic Dehydration Mechanism That Uses Tyrosine and a Hydrolase-Type Triad'*, Journal of the American Chemical Society, 136.14 (2014), 5253–56.

[189] R. J. Robins *et al.*, *'The Biosynthesis of Tropane Alkaloids in Datura Stramonium: The Identity of the Intermediates between N-Methylpyrrolinium Salt and Tropinone'*, Journal of the American Chemical Society, 119.45 (1997), 10929–34.

end-product, the $C2_{CIT}$ is relatively depleted, by ~11‰. Hence, it is probable that these positions in acetoacetyl-CoA are more depleted relative to the carboxyl positions than in acetyl-CoA.

In addition, the condensation of *N*-methyl-Δ^1-pyrrolinium with acetoacetyl-CoA is likely to have normal ^{13}C KIEs for both the formation of the $C1_T$–$C2_T$ bond in the synthesis of 4-(1-methyl-2-pyrrolidinyl)-3-oxobutyrate, and for the formation of the $C4_T$–$C5_T$ bond created during the synthesis of the 8-azabicyclo[3.2.1]octan-3-ol ring. This should lead to a further relative depletion in the $C(2+4)_T$ position, compatible with the observed values. Unfortunately, due to the coincidence of the $C2_T$ and $C4_T$ in the ^{13}C NMR spectrum (Figure 52), it is not possible to assess whether the first or second bond formation has a major influence on the $^{13}C/^{12}C$ ratios observed.

5.2.2.4 To what extent do the reactions involving the conversion of *N*-methyl-Δ^1- pyrrolinium to *S*-(-)-nicotine influence the observed isotope ratios?

The elaboration of *N*-methyl-Δ^1-pyrrolinium to *S*-(-)-nicotine involves the creation of a new C–C bond linking the $C3_N$ and $C2'_N$ positions, thus joining the nicotinate-derived moiety to the *N*-methyl-Δ^1-pyrrolinium-derived moiety (Fig. 50). Once again, the symmetry of the *N*-methyl- Δ^1-pyrrolinium salt means that in this precursor the $C2'_N = C5'_N$ and $C3'_N = C4'_N$. However, the values observed at the $C2'_N$ and $C5'_N$ are not equivalent (Figure 58, Table 4): the $C2'_N$, the carbon at which the C–C bond with the nicotinate moiety is made, is found to be ~4‰ enriched relative to the $C5'_N$. The observed difference needs therefore to be accounted for by another cause. It is proposed that this is due to an inverse ^{13}C KIE associated with the mechanism of the 'nicotine synthase' reaction condensing the *N*-methyl-Δ^1-pyrrolinium- and nicotinate-derived moieties (Fig. 50). While the mechanism of this reaction is not known, some suggestions can be made on the basis of the isotope fractionation, hence the intrinsic KIE of the reaction. The $C2'_N$ undergoes a change of state from a semi-aromatic nature with delocalized electrons to a tertiary aliphatic carbon (Figure 57). Our data indicate that this reaction favors the $^{13}C{=}N^+$ over the $^{12}C{=}N^+$, as known for $sp^2 \rightarrow sp^3$ conversions.[190] Such a KIE will lead to relative enrichment in the position becoming the $C2'_N$ and an equivalent relative depletion in the $C5'_N$ must occur. This is clearly seen in Figure 55. Furthermore, the $C3_N$ position is strongly depleted, which would indicate a selection against ^{13}C at this position, compatible with a mechanism in which the $C3_N$ undergoes an $sp^3 \rightarrow sp^2$ conversion with kinetic limitation (Figure 57). Further support for this proposal needs to be sought using specifically-labelled substrates.

[190] F. J. Winkler *et al.*, '*Reaction rates of Isotopic Molecules*', Angewandte Chimie, 2 (93), (1981), 220-220.

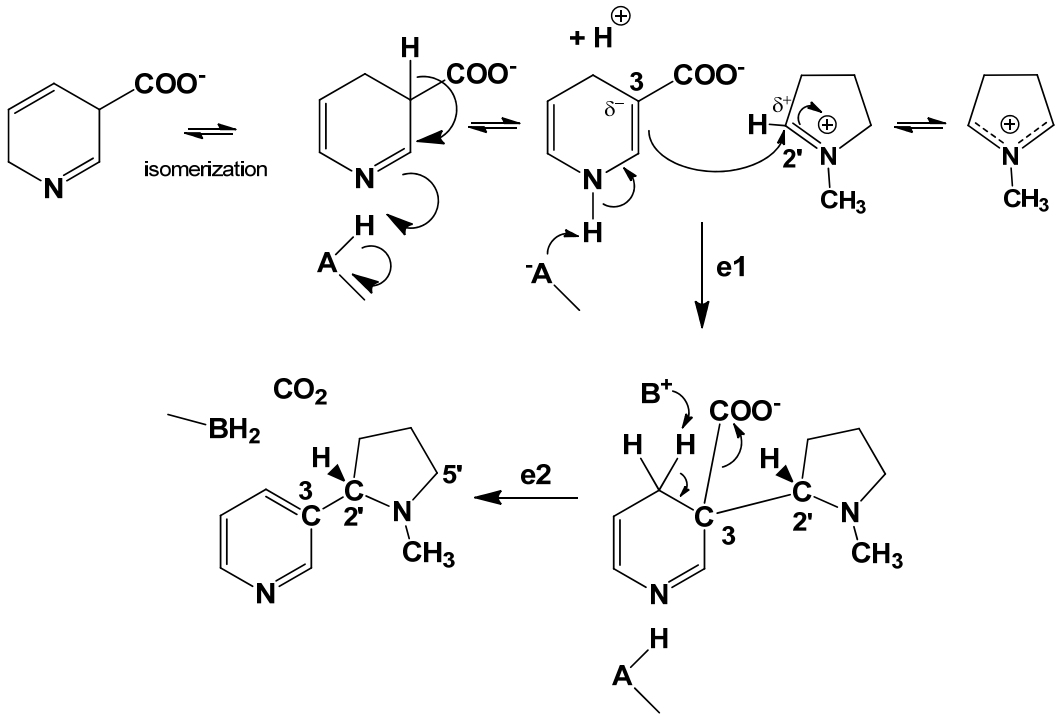

Figure 57. Schematic representation of the proposed mechanism for 'nicotine synthase', the last step on the biosynthetic pathway to S-(-)-nicotine, based on the observed site-specific $^{13}C/^{12}C$ isotopic fractionation. Partial enzymatic steps are given as: e1, the formation of the bond between $C2'_N$ and $C3_N$ in which the $C2'_N$ undergoes an sp^2sp^3 with kinetic limitation leading to selection for ^{13}C at the $C3_N$ position; e2, the decarboxylation at the $C3_N$ position, in which the $C3_N$ undergoes an sp^3sp^2 with selection for ^{12}C at the $C3_N$ position. Carbon atoms on the final compounds are numbered according to the IUPAC nomenclature.

5.2.2.5 What can be deduced about the introduction of the *N*-methyl group based on the observed isotope ratios?

In addition to having the Δ^1-pyrrolinium moiety in common, the *N*-methyl group in both tropine and *S*-(-)-nicotine is derived from the common source, *S*-adenosylmethionine (AdoMet) and is introduced by the enzyme putrescine *N*-methyltransferase EC 2.1.1.53).[191] In both compounds, this carbon is found to be depleted relative to the other putrescine-derived positions, with which it should directly be compared (rather than with the whole molecule). In tropine, the extent of depletion is the major difference between the two samples: relative to the putrescine-derive part: ~38‰ and ~22‰ in TRI-1 and TRI-3, respectively. In nicotine, similarly, when the comparison is made only with the putrescine-derived atoms, then the relative depletion is ~12‰, rather less than in tropine but still well below the average of the other carbon atoms in this moiety.

This relative depletion in the $^{13}C/^{12}C$ isotope ratio of the *N*-methyl group appears to be characteristic for AdoMet-derived methylation in natural products, previously recognized for *O*-

[191] S. Biastoff *et al.*, *'Putrescine N-Methyltransferase--the Start for Alkaloids'*, Phytochemistry, 70.15–16 (2009), 1708–18.

methyl groups.[192] The position-specific analysis of $^{13}C/^{12}C$ isotope ratios of *N*-methyl group has only recently been investigated by using irm-^{13}C NMR and so far only for a very few alkaloids. Nonetheless, comparison can be made with the purine alkaloids, caffeine and theobromine,[193] in which the *N*-methyl group is AdoMet-derived.[194] In caffeine extracted from coffee the mean of the three *N*-methyl groups is on average ~36‰ depleted relative to the other carbon atoms, while in theobromine extracted from cocoa, the mean of the two *N*-methyl groups is on average ~23‰ below that of the other carbon atoms. These values suggest that relative depletion in the *N*-methyl group is a general phenomenon reflecting the biochemistry of methyl group insertion. The degree of depletion varies, but in all four alkaloids so far analyzed, including tropine and *S*-(-)-nicotine (Figure 54-55), it is marked. This also parallels the relative depletion in a number of *O*-methyl groups, for example, ferulic acid. In tramadol, the *N*-Me_2 is also depleted relative to the part of the molecule considered to be derived from L-lysine by ~12‰[195], which encouraged us to consider SAM as its probable origin. The *O*-methyl group of tramadol was also relatively depleted, although only by ~7‰. Overall, then, the depletion found in tropine and *S*-(-)-nicotine, compares favorably with that in other *N*- and *O*-methyl groups, supporting the suggestion that this is a general phenomenon related to AdoMet metabolism.[196] As presented above (section IV), there is now good evidence that this is associated with the enzyme methionine synthase.

The application of irm-^{13}C NMR to the study of compounds of known biosynthetic pathways has made possible the interpretation of the origin of the $\delta^{13}C_i$ (‰) values obtained for two alkaloids, *S*-(-)-nicotine and tropine. Generally, we can conclude that the majority of the carbon positions show an isotope fractionation that is dominated by the position-specific $^{13}C/^{12}C$ isotope ratios in the primary precursors that are exploited by the pathway. Thus, where moieties are incorporated that have other functions in the cell, for example acetate via acetyl-CoA or acetoacetyl-CoA, then isotopic fractionation against the cellular pool can occur, as these precursors fulfill many other metabolic roles. The strength of this link will reflect the extent to which the primary precursors are committed to the synthesis of the specialized compounds, offering access to improved understanding of the primary/specialized metabolite interface in plant metabolism.

Once a major commitment of the substrate/product cascade to the final product is made, overall fractionation must be expected to have a more limited impact, as there is no

---

[192] E. P. Botosoa *et al.*, *'Quantitative Isotopic ^{13}C Nuclear Magnetic Resonance at Natural Abundance to Probe Enzyme Reaction Mechanisms via Site-Specific Isotope Fractionation: The Case of the Chain-Shortening Reaction for the Bioconversion of Ferulic Acid to Vanillin'*, Analytical Biochemistry, 393.2 (2009), 182–88; M. Greule and F. Keppler, *'Stable Isotope Determination of Ester and Ether Methyl Moieties in Plant Methoxyl Groups'*, Isotopes in Environmental and Health Studies, 47.4 (2011), 470–82.

[193] D. G. Diomande *et al.*, *'Position-Specific Isotope Analysis of Xanthines: A ^{13}C Nuclear Magnetic Resonance Method to Determine the ^{13}C Intramolecular Composition at Natural Abundance'*, Analytical Chemistry, 87.13 (2015), 6600–6606.

[194] K. A. E. Larsson *et al.*, *'N-Methyltransferase Involved in Gramine Biosynthesis in Barley: Cloning and Characterization'*, Phytochemistry, 67.18 (2006), 2002–8.

[195] K. M. Romek *et al.*, *'A Retro-Biosynthetic Approach to the Prediction of Biosynthetic Pathways from Position-Specific Isotope Analysis as Shown for Tramadol'*, Proceedings of the National Academy of Sciences of the United States of America, 112.27 (2015), 8296–8301.

[196] T. Weilacher *et al.*, *'Carbon Isotope Pattern in Purine Alkaloids a Key to Isotope Discriminations in C_1 Compounds'*, *Phytochemistry*, 41.4 (1996), 1073–77.

branching taking place. Nevertheless, some intra-molecular fractionation can be observed when C–C bond formation/breaking takes place. In contrast, isotopic fractionation is minimal for those carbon atoms that undergo no bond-forming reactions. These position-specific observations make possible deductions as to the putative reaction mechanism involved, as in the present case of the 'nicotine synthase' condensation.

Table 5. Data obtained by irm-^{13}C NMR for the ^{13}C distribution in natural tropine or natural *S*-(-)-nicotine

Tropine					
Sample	TRI-1		TRI-3		
Origin	Natural		Natural		
N° spectra	10		10		
δ_g (‰)	-25.56		-25.11		
	Mean [a]	SEM	Mean [a]	SEM	Average [b]
f_i/F_i [c] C3	1.00508879	0.00263500	1.00633672	0.00231333	
f_i/F_i C(2+4)	1.00641651	0.00640000	0.99957955	0.00334667	
f_i/F_i C(1+5)	0.97287264	0.00381500	0.98261329	0.00224000	
f_i/F_i C(6+7)	0.98809680	0.00484000	0.99539280	0.00270000	
f_i/F_i CH_3	1.01650598	0.00179150	1.01055264	0.00139333	
	Mean	SEM	Mean	SEM	
δ_i C3 (‰)	-20.50	1.23	-19.04	1.25	-19.77
δ_i C(2+4) (‰)	-37.53	2.65	-29.51	0.86	-33.52
δ_i C(1+5) (‰)	-19.01	1.26	-25.61	0.66	-22.31
δ_i C(6+7) (‰)	-9.09	0.98	-14.70	0.68	-11.90
δ_i CH_3 (‰)	-52.69	1.33	-42.18	1.01	-47.44
S-(-)-Nicotine					
Sample	NIC-1		NIC-3		
N° spectra	5		5		
δ_g (‰)	-29.99		-30.93		
	Mean [d]	SEM	Mean [d]	SEM	
f_i/F_i C2	1.0000610	0.0109500	0.9986821	0.0110000	
f_i/F_i C3	0.9897313	0.0126100	0.9907477	0.0146000	
f_i/F_i C4	1.0136892	0.0045000	1.0148068	0.0107200	

f_i/F_i C5	1.0074270	0.0069000	1.0049678	0.0158000	
f_i/F_i C6	0.9806073	0.0135700	0.9817312	0.0110000	
f_i/F_i C2’	1.0039115	0.0011500	1.0065792	0.0072000	
f_i/F_i C3’	1.0085256	0.0086000	1.0104814	0.0124000	
f_i/F_i C4’	1.0034714	0.0110600	1.0034401	0.0059600	
f_i/F_i C5’	1.0002778	0.0077300	0.9977597	0.0000000	
f_i/F_i CH_3	0.9922977	0.0056200	0.9908040	0.0056000	
	Mean	SEM	Mean	SEM	Average [b]
δ_i C2 (‰)	-33.09	1.23	-35.71	0.86	-34.40
δ_i C3 (‰)	-42.64	0.70	-42.87	1.17	-42.76
δ_i C4 (‰)	-18.78	0.99	-19.03	1.71	-18.90
δ_i C5 (‰)	-25.76	1.47	-27.99	1.61	-26.88
δ_i C6 (‰)	-51.71	1.36	-52.26	0.77	-51.98
δ_i C2’ (‰)	-26.76	2.09	-23.09	0.80	-24.93
δ_i C3’ (‰)	-18.01	0.97	-17.26	1.79	-17.64
δ_i C4’ (‰)	-22.09	0.83	-23.39	1.63	-22.74
δ_i C5’ (‰)	-27.23	1.82	-31.02	0.84	-29.12
δ_i CH_3 (‰)	-33.98	0.72	-36.81	0.86	-35.40

Footnotes:

[a]Mean of ten spectral acquisitions obtained as two separate preparations from the same sample (5 spectra per preparation).

[b]As these are independent samples, it is not appropriate to use the mean value. Rather, so as to given an indicative value for text discussion, an average of the two samples each for nicotine and of tropine is given.

[c]f_i/F_i is the positional isotopic distribution, i.e. the variation of the δ_i from the statistical distribution.

[d]Mean of five spectral acquisitions. A field-homogenizing correction factor is applied for the data for *S*-(-)-nicotine.[197]

[197] K. Bayle *et al.*, *'Non-statistical ^{13}C distribution during carbon transfer from glucose to ethanol during fermentation is determined by the pathway exploited*', Journal of Biological Chemistry, 290, (2015), 4118-4128.

5.2.3 Natural versus synthetic

Data for 4 samples of nicotine from different origins were collected with irm-^{13}C NMR spectroscopy under quantitative conditions. The profiles obtained are presented in Figure 58.

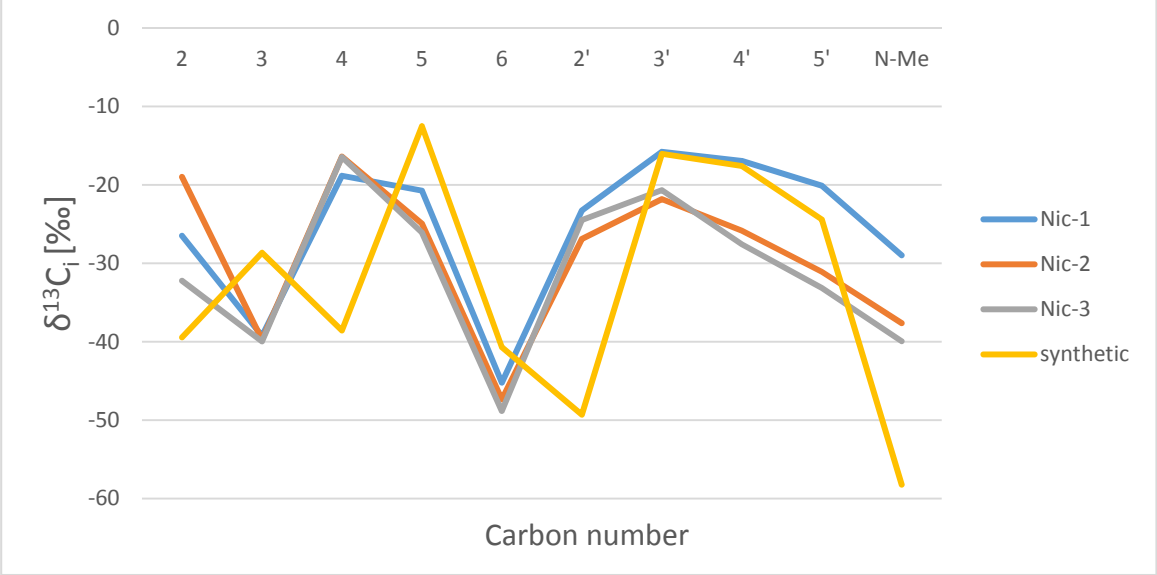

Figure 58. $\delta^{13}C_i$ [‰] values for 4 samples of nicotine; Nic-1 – *S*-nicotine from Sigma-Aldrich (product N3876-5ML, batch 1449194V, designated 'natural' on the CoO), Nic-2 – *S*-nicotine from Fluka (product 36733-1G, batch SZBE245XV, designated 'synthetic' on the CoO), Nic-3 – *S*-nicotine from Chemnovatic (natural), synthetic – *R,S*-nicotine synthesized in the laboratory

Nic-1 and Nic-3 are samples of *S*-nicotine designated as of natural origin and are seen to fit to the natural isotopic pattern described above with high repeatability. It is also visible that *R,S*-nicotine synthesized (by Dr Pierrick Nun) using the method of Felpin *et al*.[198] (marked in yellow), presents significant deviations and a pattern that does not fit that of the natural samples Nic-1 and Nic-3. It is facile to distinguish the origins: especially for the C-4 and C-2' carbon positions, for which the variation of $\delta^{13}C_i$ values is about 25‰ and the values are completely different compared with the adjacent positions.

Examining next the data obtained for the *S*-nicotine obtained from Fluka and labelled as a synthetic sample (Nic-2), it is apparent that this sample has a profile closely resembling that of the two natural samples, in particular that of Nic-3. Certainly, it does not follow the isotopic profile of our synthetic *R,S*-nicotine. Why therefore is it labelled as 'synthetic'? It would appear that this may be an example of those cases where the supplier is obliged to so-label a compounds because the process used to manufacture them involved one or more chemical treatments which require that the labelling is not 'natural'. In this case it can be reasonably proposed that the compound is, to all intense and purposes, extracted from a plant. In addition, it should be noted that it is commercially impractical to produce *S*-nicotine by laboratory synthesis. The time and cost of such an operation is approximately 10 times greater than obtaining nicotine through extraction from the plant material that is widely available.

[198] F-X. Felpin *et al.*, *'Efficient Enantiomeric Synthesis of Pyrrolidine and Piperidine Alkaloids from Tobacco'*, The Journal of Organic Chemistry, 66.19 (2001), 6305–12.

5.3 Tramadol

5.3.1 Brief history of Tramal/Ultram/Tramadol/Ryzolt

2-[(Dimethylamino)methyl]-1-(3-methoxyphenyl)cyclohexanol, marketed as Tramal, Ultram, Ryzolt, Tramadol, was synthesized for the first time in 1967 by Grunenthal G.m.b.H. in Germany.[199] They patented the synthesis of 1-(*m*-substituted phenyl)-2-aminomethyl cyclohexanols, that are useful as analgesic drugs. It caused a great interest, because most of the commonly known opioid pharmaceuticals (such as morphine) carry a high risk of potentially dangerous side-effects, including addiction to these substances. Even though tramadol is free from neither a high degree of tolerance nor drug dependence, it still is considered as safer than other morphine alkaloids.

The overall scheme of the synthesis is presented below (Figure 59).

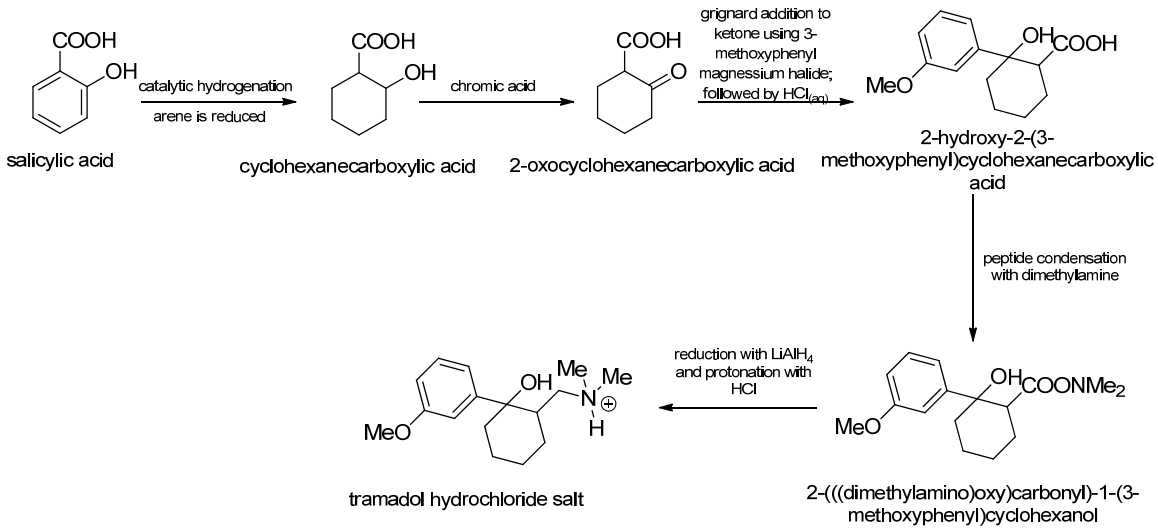

Figure 59. Tramadol synthesis pathway[200]

The extraction of tramadol from the roots of *Nauclea latifolia* excited great interest worldwide. This was the first time that a widely marketed synthetic drug was found as an apparently natural product at high abundance. As a conventional approach to study its probable biosynthetic precursors, enzymatic steps, and intermediate metabolites is not currently feasible, the proposition of the concept of a retro-biosynthesis by examining the position-specific isotope distribution within the molecule was put forward along with the rationally interpreting the data in terms of known plant biochemical processes that may be involved in a biosynthesis of tramadol.

5.3.2 Obtained results, natural contra synthetic[201]

[200] P. Dayer *et al.*, *'Pharmacology of Tramadol',* Drugs, 53, (2), (1997), 18-24.
[201] This section is the publication by K. M. Romek *et al., 'A retro-biosynthetic approach to the prediction of biosynthetic pathways from position-specific isotope analysis as shown for tramadol*'.

The objective of this work was first to obtain by irm-^{13}C NMR the position-specific $^{13}C/^{12}C$ ratios in isotopomers of tramadol extracted from the root bark of *N. latifolia* and, secondly to probe the potential biosynthetic cause of the extensive non-statistical distribution observed.

5.3.3 Discussion of results/possible origin

First, it should be noted that all of the structural features seen in tramadol (Figure 60 **B**) have been characterized in various natural products. The *N,N*-dimethyl group occurs in many alkaloids, such as hordenine [4-(2-dimethylaminoethyl)phenol],[202] and products possessing a *N,N*-dimethyl-2-aminomethyl-cyclohexaxne moiety are known.[203] Many phenolic natural products derived from a number of biosynthetic routes contain a *meta*-methoxyl group, such as gallic acid, ferulic acid, vanillin, stilbenes, and aurones.[204] 3-Methoxyacetophenone moiety, probably derived from 3-methoxyacetophenone, has been isolated from *Lobelia siphilitica*.[205]

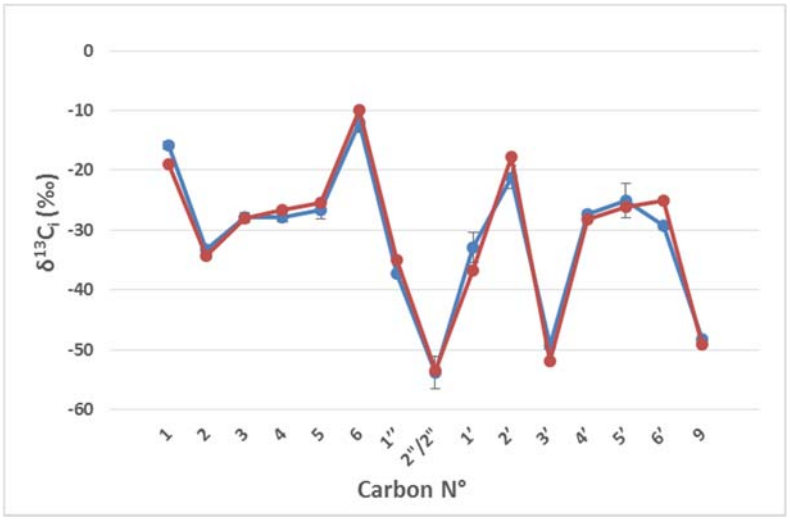

A **B**

Figure 60. The $\delta^{13}C_i$ [‰] values for tramadol obtained by irm-^{13}C NMR from two independent extractions of the root bark of *N. latifolia*. (A) The $\delta^{13}C_i$ [‰] values of the 15 carbon positions. (B) The structure of tramadol

Second, drawing on these known natural structures and on a sound knowledge of parallel biochemistry, several hypothetical pathways can be proposed: the more plausible are given in Figure 61 **A** and **B**.

[202] J. Lundstrom, *The Alkaloids: Chemistry and Pharmacology* (Academic Press, 1989).
[203] D. A. Wright *et al.*, *'A Great Barrier Reef Sinularia Sp. Yields Two New Cytotoxic Diterpenes'*, Marine Drugs, 10.8 (2012), 1619–30.
[204] T. Vogt, *'Phenylpropanoid Biosynthesis'*, Molecular Plant, 3.1 (2010), 2–20.
[205] J. R. Kesting *et al.*, *'Piperidine and Tetrahydropyridine Alkaloids from Lobelia Siphilitica and Hippobroma Longiflora'*, Journal of Natural Products, 72.2 (2009), 312–15.

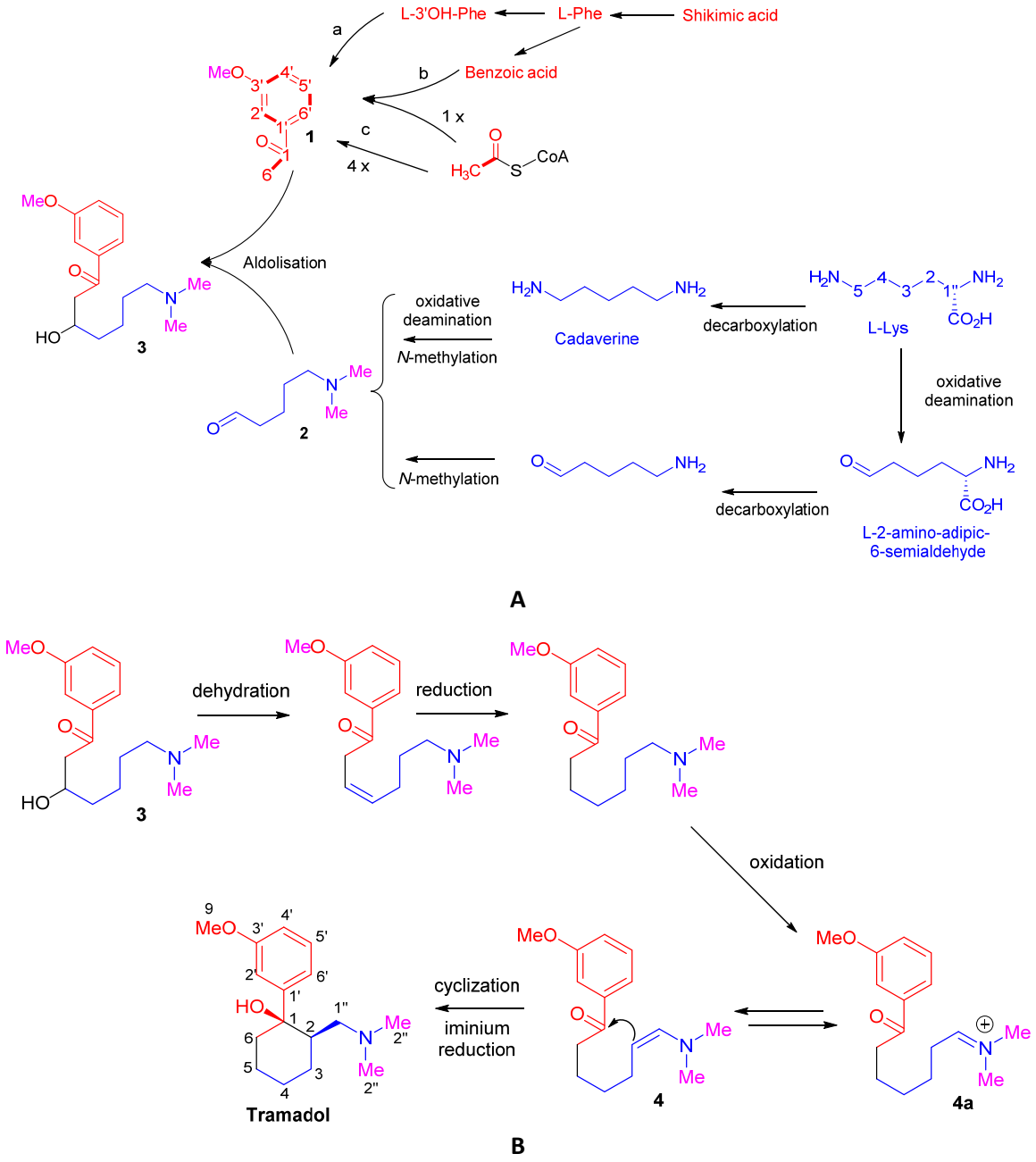

Figure 61. Proposed origins of the carbon atoms in biosynthetic tramadol. (A) Condensation of the carbon skeleton. (B) Reaction leading to ring closure and tramadol. Racemic (1R, 2R)-tramadol is likely to be due to the final cyclization/reduction step. Origins from L-Phe in red, L-Lys in blue, and SAM in violet. All carbons are numbered by their respective positions in the tramadol molecule. The bold bonds in 1 show those that would be retained intact in a polyketide-derived structure

Two potential biosynthetic origins can be put forward as the origin of the aromatic ring: an acetyl-CoA-derived polyketide or a shikimate-derived amino acid. Feeding studies in *Camellia sinensis* flowers[206] and in the fungus *Bjerkandera adusta*[207] have shown that the acetophenone

[206] F. Dong *et al.*, *'Characterization of L-Phenylalanine Metabolism to Acetophenone and 1-Phenylethanol in the Flowers of Camellia Sinensis Using Stable Isotope Labeling'*, Journal of Plant Physiology, 169.3 (2012), 217–25.

skeleton can be biosynthesized from L-Phe, probably via a β-oxidation pathway from cinnamic acid. Plant enzymes that lead to acetophenone derivatives from ferulouyl-CoA[208] are known and the production of L-3'-hydroxyphenylalanine (3'-OH-Phe), an important nonprotein amino acid described in the grass *Festuca rubra*[209] implicates a role for phenylalanine 3-hydroxylase, an enzyme that has so far only been characterized in a streptomycete.[210] Thus, 3'-oxidation followed by methylation through S-adenosylmethionine (AdoMet) methyltransferase would introduce the 3'-methoxyl group and β-oxidation[211] would lead to **1**. However, an alternative pathway from acetyl-CoA was demonstrated in *Kniphofia pumila.*[212] Discriminating between these alternative pathways is discussed in relation to the experimental results.

The biosynthesis of **2** could follow one of two pathways from L-Lys. The first is the route common to the biosynthesis of alkaloids in which decarboxylation of L-Lys leads to the symmetrical diamine, cadaverine (1,5-diaminopentane), which undergoes oxidative deamination to 5-aminopentanal (Fig.60 **A**).[213,214] However, the 5-carbon unit could equally well be incorporated from L-Lys, via another degradation product, L-2-amino-adipic-6-semialdehyde, a pathway in which oxidative deamination precedes decarboxylation. In either case, *N,N*-dimethylation of the amine group leads to **2.**[215] Again, a distinction between these alternative pathways can be deduced from the experimental results.

Subsequently, two key steps are invoked. The first is the condensation of **1** with **2** involving aldolization to form **3**: the second is a cyclization converting **4**/**4a** to tramadol.

5.3.3.1 Support from the experimental data for proposed biosynthetic pathway

Considering those atoms proposed to be derived from L-Lys, these give mean $\delta^{13}C_g$ value of -30.2‰ (Table 5), compatible with literature values for amino acids from C_3 plants.[216]

---

[207] C. Lapadatescu *et al.*, *'Novel Scheme for Biosynthesis of Aryl Metabolites from L-Phenylalanine in the Fungus Bjerkandera Adusta'*, Applied and Environmental Microbiology, 66.4 (2000), 1517–22.
[208] J. Negrel and F. Javelle, *'The Biosynthesis of Acetovanillone in Tobacco Cell-Suspension Cultures'*, Phytochemistry, 71.7 (2010), 751–59.
[209] C. Bertin *et al.*, *'Grass Roots Chemistry: Meta-Tyrosine, an Herbicidal Nonprotein Amino Acid'*, Proceedings of the National Academy of Sciences, 104.43 (2007), 16964–69.
[210] W. Zhang *et al.*, *'Identification of Phenylalanine-3-Hydroxylase for Meta-Tyrosine Biosynthesis',* Biochemistry, 50.24 (2011), 5401–3.
[211] J. Negrel and F. Javelle, *'The biosynthesis of acetovanillinone in tobacco cell-suspension cultures'*, Phytochemistry, 71 (7), (2010), 751-759.
[212] G. Bringmann *et al.*, *'Polyketide Folding in Higher Plants: Biosynthesis of the Phenylanthraquinone Knipholone',* The Journal of Organic Chemistry, 72.9 (2007), 3247–52.
[213] S. Bunsupa *et al.*, *'Quinolizidine Alkaloid Biosynthesis: Recent Advances and Future Prospects',* Frontiers in Plant Science, 3 (2012).
[214] R. J. Robins and N. J. Walton, *'The Alkaloids: Chemistry and Pharmacology'*, Academic Press, ISBN: 978-0-08-086568-3, (1994).
[215] K. A. E. Larsson *et al.*, *'N-methyltransferase involved in gramine biosynthesis n barley: Cloning and characterization',* Phytochemistry, 18, (67), (2006), 2002-2008.
[216] T. Larsen *et al.*, *'Stable Isotope Fingerprinting: A Novel Method for Identifying Plant, Fungal, or Bacterial Origins of Amino Acids'*, Ecology, 90.12 (2009), 3526–35.

Table 6. Values for $\delta^{13}C_g$ [‰] for different parts of the tramadol molecule obtained by irm-^{13}C NMR spectrometry

	$\Delta^{18}C_l$ [‰]	
Sample	*Sigma*	*N. latifolia*
N	*4*	*2*
$^{13}C\ \delta_{g(all)}$	*-29.08*	*-31.15*
$^{13}C\ \delta_{g(phe)}$	*-25.38*	*-26.72*
$^{13}C\ \delta_{g(lys)}$	*-31.26*	*-30.23*
$^{13}C\ \delta_{g(Me)}$	*-38.42*	*-51.12*

The key difference between the two postulates alternative routes-via cadaverine or via L-2-amino-adipic-6-semialdehyde – is that the former involves a symmetrical intermediate, whereas the latter does not. Biosynthesis via a symmetrical compound would lead to scrambling of the original $C2_L$ and $C6_L$ of L-Lys (yielding $C1'_T$ and $C5_T$ in Fig.61 **A**) and of the $C3_L$ and $C5_L$ positions (yielding atoms $C2_T$ and $C4_T$ in Figure 61 **B**). [The notation CX_L, CX_P, CX_F, ad CX_T indicates the relevant carbon atom in L-Lysine (L), L-phenylalanine (P), ferulic acid (F), or tramadol (T), respectively.] Therefore, the $\delta^{13}C$ values of the $C2_T$ and $C4_T$ should be identical, which is clearly not the case ($\Delta C4_T$ - $C2_T$ = 6.6‰). [Δ is the difference in $\delta^{13}C_i$ [‰] values between two carbon positions. Thus $\Delta C4_T - C2_T$ means the difference between the $\delta^{13}C_i$ of the C4 position of tramadol and the $\delta^{13}C_i$ of the C2 position of tramadol. For convenience, Δ is always attributed a positive sign.] In addition, the oxidative deamination of cadaverine should imply an intramolecular kinetic carbon isotope effect.[217] As a result, competition between equivalent positions of the symmetrical precursors should select in favour of isotopomers containing ^{12}C at this position, leading to a ^{13}C depletion of the C atom bearing the oxygen function ($C5_T$) relative to that bound to N ($C1''_T$). Both these predictions are not met: on the contrary, $C1''_T$ is depleted relative to $C5_T$ ($\Delta C5_T - C1''_T$ = 10.2‰). Hence, the ^{13}C isotope data argue strongly in favour of the precursor being a non-symmetrical molecule. Incorporation of L-Lys via L-2-amino-adipic-6-semialdehyde, in contrast, would not invoke scrambling of the original $C2_L$ and $C6_L$ positions of L-Lys and is fully compatible with the observed isotope distribution pattern. Furthermore, the relative depletion of the $C1''_T$ is in accord with a general ^{13}C depletion at the α-atom of amino acids from auxotrophs.[218]

These arguments are further supported by the ^{13}C isotope data in those positions involved in the aldolization reaction condensing the two moieties **1** and **2** (Figure 61). A kinetic isotope effect (KIE) on the reaction will predict relative ^{13}C depletion for $C5_T$ and a relative enrichment for $C6_T$. The determined values are fully in agreement with this postulate.[219]

Turning to the origin of moiety **1**, the acetophenone skeleton, two alternatives have been indicated: an acetyl-CoA-derived polyketide or a phenylpropanoid from the shikimic acid

[217] S. Dragulska *et al.*, *'Isotope Effects in the Enzymatic Oxidation of Tryptamine to 3-Indolyl-Acetaldehyde'*, Isotopes in Environmental and Health Studies, 50.2 (2014), 269–76.
[218] P. H. Abelson, and T. C. Hoering, *'Carbon isotope fractionation in formation of amino acids by photosynthetic organisms',* Proceedings of National Academy of Sciences of the United States, 5, (47), (1961), 623-632.
[219] G. Tcherkez and G.D. Farquhar, *'Carbon Isotope Effect Predictions for Enzymes Involved in the Primary Carbon Metabolism of Plant Leaves'*, Functional Plant Biology, 32.4 (2005), 277–91.

pathway. In general, a *meta*-substituent oxygen function in an aromatic ring of a natural product can suggest its origin from a polyketide.[220] However, the *meta* positioning of this oxygen function to that in the side chain is not in agreement with the expected alternating sequence for a polyketide, which would be predicted to carry oxygen substitutions on even positions, those derived from the carbonyl of the acetyl-CoA.[221] Hence, this origin can be argues as incompatible with the presence of a C3'$_T$ methoxyl substituent. The analysis of the ^{13}C isotope distribution data supports this conclusion in several ways (Fig. 62).

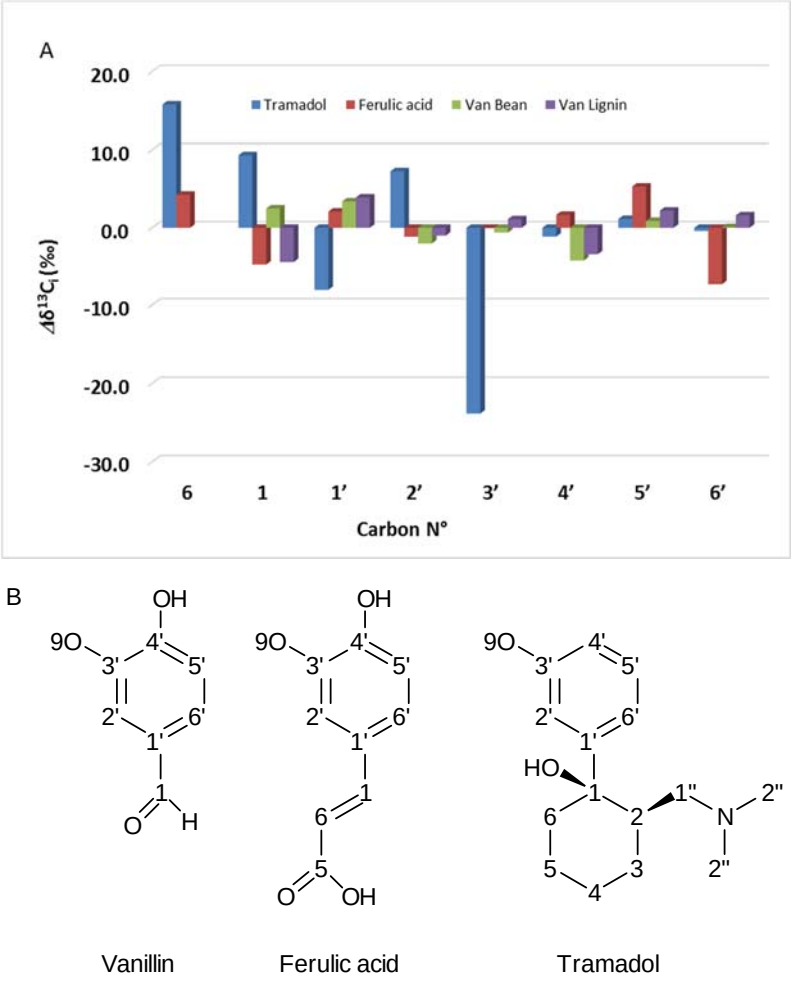

Figure 62. Variation in $\Delta\delta^{13}C_i$ [‰] of the aromatic ring of tramadol from *N. latifolia*, ferulic acid from *Oryza sativa*, vanillin from *Vanilla planifolia* (Van Bean), and vanillin synthesized from natural lignin from *Picea* sp. (Van Lignin). (A) Values illustrated as the $\Delta\delta^{13}C_i$ relative to the mean for the positioning being considered, because $\Delta\delta^{13}C_i$ expresses the deviation for a given position *I* independently of the value $\Delta\delta^{13}C_g$ [‰] for each molecule. Numbering as for tramadol. (B) Structures of tramadol, ferulic acid, and vanillin with carbon positions numbered as for tramadol

[220] H-L. Schmidt and G. Gleixner, *'Carbon isotope effects on key reactions in plant metabolism and ^{13}C-patterns in natural compounds'*, Stable Isotopes. Integration of Biological, Ecological and Geochemical Processes, BIOS Scientific, Oxford, (1998), pp. 13-25..

[221] G. Bringmann *et al.*, *'Polyketide folding in higher plants: biosynthesis of the phenylanthraquinone knipholone',* The Journal of Organic Chemistry, 9, (72), (2007), 3247-3252.

First, the mean $\delta^{13}C_g$ values for the aromatic ring is -26.7‰ (Table 5), compatible with literature values for aromatic amino acids from C_3 plants[222] but richer than those for acetyl-CoA-derived compounds.[223] Second, the condensation of four units of acetate via acetyl-CoA generates a sequential pattern of two-carbon units (a pattern indicated as bold bonds Figure 60 **A**) with the CH_3-derived $\delta^{13}C_i$ value higher than the (impoverished) C=O-derived value[224], due to the kinetic isotope effects associated with the pyruvate decarboxylase reaction.[225] The resulting pattern in tramadol should be C1'>C2', C3'>C4', and C5'>C6'. This is clearly not the case (Figure 60).

What evidence can be put forward to support an origin from the shikimic acid pathway? Focusing first on the $\delta^{13}C_i$ pattern of the aromatic ring of tramadol, it is apparent that the $C4'_T$, $C5'_T$ and $C6'_T$ have values closely related to those obtained from vanillin and ferulic acid,[226,227,228] derived from L-Phe, despite the different compounds having been obtained from different plants and from different geographical areas. However, at the $C1'_T$, and $C2'_T$ positions, the match is less evident, whereas the $C3'_T$ is distinguished by being very impoverished relative to the equivalent position of the other 3-hydroxylated compounds. As, currently, neither isotopic nor enzyme mechanistic evidence is available for the *m*-hydroxylation, interpreting this observation requires further investigation. In particular, data from other *m*-hydroxylated compounds, notably the 3'-OH-Phe found in *F. rubra,*[229] would be valuable. It might indicate a mechanism for 3-hydroxylation in tramadol biosynthesis different from the well-described 3-coumaroyl-CoA hydroxylase of phenylpropanoid metabolism,[230] which require 4-hydroxylation before 3-hydroxylation. It should be noted that the 3-positioned O atom in vanillin and ferulic acid is in effect introduced by an *ortho*-hydroxylation relative to the first oxygen function in the 4-

[222] T. Larsen *et al.*, *'Stable isotope fingerprinting: a novel method for identifying plant, fungal, or bacterial origins of amino acids',* Ecology, 12, (90), (2009), 3526-3535.
[223] H-L. Schmidt and G. Gleixner, *'Carbon isotope effects on key reactions in plant metabolism and ^{13}C-patterns in natural compounds'*, Stable Isotopes. Integration of Biological, Ecological and Geochemical Processes, BIOS Scientific, Oxford, (1998), pp. 13-25.
[224] K. D. Monson and J. M. Hayes, *'Biosynthetic control of the natural abundance of carbon-13 at specific positions within fatty acids in Escherichia coli. Evidence regarding the coupling of fatty acids and phospholipid synthesis',* Journal of Biological Chemistry, 23, (255), 11435-11441.
[225] E. Melzer and H-L. Schmidt, *'Carbon Isotope Effects on the Pyruvate Dehydrogenase Reaction and Their Importance for Relative Carbon-13 Depletion in Lipids.'*, Journal of Biological Chemistry, 262.17 (1987), 8159–64.
[226] E. P. Botosoa *et al.* , *'Quantitative isotopic ^{13}C nuclear magnetic resonance at natural abundance to probe enzyme reaction mechanisms via site-specific isotope fractionation: the case of the chain-shortening reactionfor the bioconversion of ferulic acid to vanillin',* Analytical Biochemistry, 2, (393), (2009), 182-188.
[227] E. P. Botosoa *et al.*, *'Unexpected fractionation in site-specific ^{13}C isotopic distribution detected by quantitative ^{13}C NMR at natural abundance',* Journal of the American Chemical Society, 130, (2), (2008), 414-415.
[228] A. Chaintreau *et al.*, *'Site-specific ^{13}C content by quantitative isotopic ^{13}C Nuclear Magnetic Resonance spectrometry: A pilot inter-laboratory study',* Analytica Chimica Acta, 788, (2013), 108-113.
[229] C. Bertin *et al.*, '*Grass root chemistry: meta-Tyrosine, an herbicidal nonprotein amino acid',* Proceedings of the National Academy of Sciences, 104, (43), (2007), 16964-16969.
[230] T. Vogt, *'Phenylpropanoid biosynthesis',* Molecular Plant, 3, (1), (2010), 2-20.

position. It has been shown from ^{2}H analysis that this can have fundamental effects on isotope patterns.[231]

For the positions that are assumed to be derived from the nonaromatic part of the C_6-C_3 molecule, the enrichment of the $C6_T$ position relative to the $C1_T$ ($\Delta C6_T - C1_T$ = 6.5‰) is consistent with the known enrichment in the carbon derived from the α-C (C2) of aromatic amino acids.[232] An enrichment relative to the β-C (C3) of the same order is observed (Fig. 60) in natural ferulic acid ($\Delta C6_F - C1_F$ = 9.0‰)[233] derived from L-Phe. Similarly, the $C1_T$ of both tramadol and natural vanillin show enrichment, whereas that in ferulic acid and lignin-derived vanillin does not. This is compatible with the involvement of a >C=O at the equivalent position to the $C1_T$ in the two former but not in the two latter compounds. However, an alternative option must be considered is that the aromatic ring and $C1_T$ are derived from L-Phe via benzoic acid (Fig. 61 **A**, option **b**) or even from an earlier intermediate of the shikimic acid pathway, as shown for gallic acid.[234]

5.3.3.2 Support from the $^{18}O/^{16}O$ isotope ratio in tramadol for the proposed biosynthetic pathway

The values of $\delta^{18}O$ have been obtained for three samples of pure tramadol, for the whole-root tissue of the same trees (Table 6).

Table 7. Values for $\delta^{18}O$ [‰] measured by irm-EA/pyrolysis/MS for tramadol purified from three different root samples (L, 6, B) and for the dry matter obtained from various tissues of *N. latifolia*

	$\Delta^{18}O$ [‰]	
Sample	*Mean*	*SD*
Fruit pericarp	*23.47*	*0.31*
Root total dry matter	*26.51*	*0.07*
Leaf dry matter	*28.33*	*0.05*
Leaf dry matter (deproteinated)	*25.03*	*0.39*
Root-derived tramadol (L)	*10.68*	*0.46*
Root-derived tramadol (6)	*11.10*	*0.49*
Root-derived tramadol (B)	*11.21*	*0.30*
Commercial tramadol (Sigma)	*7.01*	*0.62*

[231] H-L. Schmidt *et al.*, *'The prediction of isotopic patterns in phenylpropanoids from their precursors and the mechanism of the NIH-shift; Basis of the isotopic characteristics of natural aromatic compounds',* Phytochemistry, 67, (11), (2006), 1094-1003.
[232] M. Butzenlechner *et al. ,'Inter- and Intramolecular Isotopic Correlations in Some Cyanogenic Glycosides and Glucosinolates and Their Practical Importance'*, Phytochemistry, 43.3 (1996), 585–92.
[233] E. P. Botosoa *et al.*, *'Quantitative isotopic ^{13}C nuclear magnetic resonance at natural abundance to probe enzyme reaction mechanisms via site-specific isotope fractionation: the case of the chain-shortening reactionfor the bioconversion of ferulic acid to vanillin',* Analytical Biochemistry, 2, (393), (2009), 182-188.
[234] I. Werner *et al.*, *'Retrobiosynthetic NMR Studies with 13C-Labeled Glucose formation of gallic acid in plants and fungi'*, Journal of Biological Chemistry, 272.41 (1997), 25474–82.

The values, in the range of 23.5 - 28.3‰, are typical for above-ground dry matter of C3 plants, from a moderate to semiarid climate of 27 ± 4‰ above leaf water.[235] The slightly lower value for root and fruit may be due to either higher concentration of other material [e.g., lignin that has $\delta^{18}O$ ~ 12‰][236] or to more impoverished source water, respectively. Although the isotopic discrimination Δ of 27 ± 4‰ is also generally taken for carbonyl groups fully equilibrated with source water, for many carboxyl groups isotopic discrimination Δ values of 19 ± 2‰ are found.[237]

In contrast, the oxygen atom of hydroxyl groups of aromatic compounds originate from atmospheric O_2 ($\delta^{18}O$ = 23.8‰) and is introduced by monooxygenase reactions, accompanied by a KIE of ~1.018, leading to $\delta^{18}O$ values of 6 ± 1‰. Water addition to >C=C< is catalysed by lyases, implying large ^{18}O KIEs (>1.01), leading to $\delta^{18}O$ values of hydroxyl groups of more than -10‰ below water.[238] Turning to the tramadol extracted from the root tissue, it is found that the values for the three samples are closely similar, giving a mean of 11.0 ± 0.3‰. According to the proposed biosynthetic biosynthesis of tramadol (Figure 61), both oxygen atoms originate from precursor **1**: the methoxyl group on position $C3'_T$ by aromatic hydroxylation ($\delta^{18}O$ = 6‰) and that in position $C1_T$ from water, either via the carboxyl group of a benzoic acid intermediate (Δ = 19‰)[239] or from the carbonyl group of precursor **1** itself (Δ = 27‰).

Data from northern Cameroon give shallow groundwater values of -2.42 ± 1.56‰ (*n* = 19) and deep groundwater values of -4.86 ± 0.55‰ (*n* = 24), giving $\delta^{18}O$ values for dry matter closely compatible with those determined (Table 6). The $\delta^{18}O$ value of the source water in the roots of *N. latifolia* should be near to those of the groundwater, and from here, the $\delta^{18}O$ of the oxygen atom on position $C1_T$ of tramadol as a product of the plant roots should be correlated to that of the groundwater, by one or the other correlations given above. A calculation of the bulk $\delta^{18}O$ value of tramadol has to take into account the range limits of the source water and the alternative equilibrations with either carboxyl or a carbonyl group, respectively. This yields in‰, with the source of the oxygen atom on C-1 being as follows:

A carboxyl group: 0.5X (-2.4 + 19 + 6) = 11.3 or 0.5X (-4.9 + 19 + 6) = 10.1;

A carbonyl group: 0.5X (-2.4 + 27 +6) = 15.3 or 0.5X (-4.9 + 27 + 6) = 14.1

The mean bulk experimental value for tramadol of 11.0 + 0.3‰ (Table 5) agrees excellently with the reaction sequence **b** in Fig. 61, the synthesis of **1** via degradation of the side chain of L-Phe to benzoic acid and its methoxylation. However, the first alternative reaction sequence (**a** in Fig. 61) cannot be excluded, as the cyclization reaction of intermediate **4** (Figure 61 **B**) could imply an ^{18}O KIE contributing to an additional ^{18}O depletion in the case of incomplete conversion.

---

[235] L. da Silveira Lobo Sternberg, *'Oxygen and Hydrogen Isotope Ratios in Plant Cellulose: Mechanisms and Applications'*, Stable Isotopes in Ecological Research, 68 (Springer New York, 1989), pp. 124–41.

[236] J. Gray and P. Thompson, *'Climatic Information from $^{18}O/^{16}O$ Analysis of Cellulose, Lignin and Whole Wood from Tree Rings'*, Nature, 270.5639 (1977), 708–9.

[237] H-L. Schmidt *et al.*, *'^{18}O Pattern and Biosynthesis of Natural Plant Products'*, Phytochemistry, 58.1 (2001), 9–32.

[238] P. F. Cook, *'Enzyme mechanisms from isotope effect',* CRC Press, ISBN: 978-0-8493-5312-3, (1991).

[239] H-L. Schmidt *et al.*, *'^{18}O Pattern and Biosynthesis of Natural Plant Products'*, Phytochemistry, 58.1 (2001), 9–32.

In contrast, an origin via malonyl-CoA would lead to a value closer to that of both oxygens being from water, giving $\delta^{18}O$ ~18‰. Hence, from the bulk $\delta^{18}O$ analysis it can be clearly deduced that the oxygen atoms in tramadol have as origin one from water and one from O_2, in line with the proposed biosynthetic pathway. Positional $\delta^{18}O$ analysis should provide further evidence to support this deduction.

5.3.4 Methodology of measurements

5.3.4.1 Extraction and purification of Tramadol.

Tramadol was extracted from freshly collected root bark and wood.[240] This extract was further purified by column chromatography on Si gel (63 mesh) eluted with AcOEt/MeOH (9:1) and crystallization of the pooled fractions from aqueous acetone.

Reference Tramadol was obtained as a free base from commercial samples by extraction of a basic solution (5g of tramadol•HCl in 50mL of water with 1g of $NaHCO_3$) with $CHCl_3$ (3x1 vol). After drying the combined organic phases over anhydrous $MgSO_4$, the solvent was removed by exhaustive drying in vacuum.

Purified tramadol was rinsed in a small volume of water, and then the damp powder was taken into minimal volume of ice-cold acetone and left for 30 min on ice until the appearance of white crystals, after which it was left for 48-96h in the refrigerator (4°C). The white crystals were collected and dried in vacuum. Purity of the final compound used for ^{13}CNMR was >99.5% as assessed by ^{1}H NMR.

5.3.4.2 Establishing the methodology for tramadol analysis.

The methodology of irm-^{13}C NMR spectrometry needs fine-tuning for each target compound in relation to the relaxation properties, solubility, stability, and purification of the target molecule. Suitable conditions for irm-^{13}C NMR spectrometry on tramadol were established and validated on free tramadol base obtained by basification of a synthetic commercial sample of tramadol•HCl. Tramadol of purity >99.5% (wt/wt) was obtained by crystallization from aqueous acetone, a technique that has the advantage that it does not introduce isotopic fractionation. Irm-^{13}C NMR spectra were acquired using 200 mg of purified synthetic tramadol in slightly aqueous acetone. Spectra were obtained with a signal-to-noise ratio of ~650, from which the distribution of ^{13}C at each carbon position, the reduced molar fraction f_i/F_i, was calculated from the areas under the peaks. This was then converted to $\delta^{13}C_i$ [‰] values using the $\delta^{13}C_g$ [‰] obtained by irm-MS.

Five separate acquisitions, each of five spectra, showed good repeatability with the worst S.D. of 2.4‰ for the C4' position. Hence, it was verified that the protocol gives position-specific values of the distribution of ^{13}C with sufficient accuracy.

A representative spectrum is shown in Figure 63.

[240] A. Boumendjel *et al.*, *'Occurrence of the Synthetic Analgesic Tramadol in an African Medicinal Plant'*, Angewandte Chemie, 125.45 (2013), 11996–0.

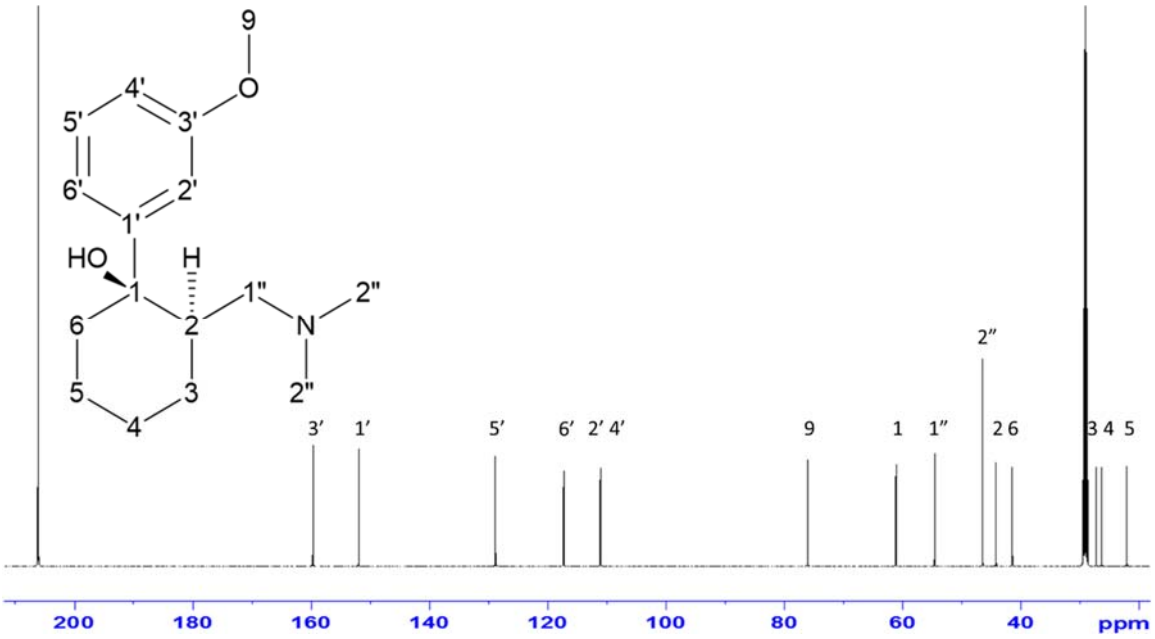

Figure 63. ^{13}C NMR spectrum of tramadol acquired under quantitative conditions

5.3.4.3 Isotope ratio monitoring by ^{13}C NMR spectral conditions.

Samples were prepared by dissolving 200 mg of purified tramadol in 600 µL of acetone-d_6 and adding 10 mg of water. The resulting solution was thoroughly mixed and transferred to a 5-mm NMR tube via a filter (Pasteur pipette with cotton wool).

Quantitative ^{13}C NMR spectra were recorded on a Bruker 500 Avance III spectrometer fitted with a 5-mm-i.d. ^{13}C/^{1}H dual cryoprobe carefully tuned to the recording frequency of 125.76 MHz. The temperature of the probe was set as 303K. The experimental parameters for spectral acquisition were the following:[241] pulse width, 11.3 µs (90°); sampling period, 1 s. The offsets for both ^{13}C and ^{1}H were set at the middle of the frequency range for tramadol. Twenty-four scans were acquired using a repetition delay of 120 s leading to a signal-to-noise ratio of ~650. Inverse-gated decoupling was applied to avoid nuclear Overhauser effect. The decoupling sequence used a cosine adiabatic pulse with appropriate phase cycles.[242] Each measurement consisted of the average of five independently recorded NMR spectra. In addition, a quantitative ^{13}C NMR reference spectrum was recorded on a Bruker 400 Avance III spectrometer fitted with a BBFO+ probe carefully tuned to the recording frequency of 100.62 MHz, which was used to calibrate the 500-MHz spectrometer.[243]

[241] V. Silvestre *et al.*, *'Isotopic ^{13}C NMR spectrometry to assess counterfeiting of active pharmaceutical ingredients: Site-specific ^{13}C content of aspirin and paracetamol',* Journal of Pharmaceutical and Biomedical Analysis, 50, (3), (2009), 336-341.
[242] E. Tenailleau and S. Akoka, *'Adiabatic ^{1}H decoupling scheme for very accurate intensity measurements in ^{13}C NMR',* Journal of Magnetic Resonance, 1, (185), (2007), 50-58.
[243] A. Chaintreau *et al.*, *'Site-specific ^{13}C content by quantitative isotopic ^{13}C Nuclear Magnetic Resonance spectrometry: A pilot inter-laboratory study',* Analytica Chimica Acta, 788, (2013,), 108-113; K. Bayle *et al.*,

Chemical shifts were reported in parts per million (δ), with the residual acetone signal (δ_c 29.84) used as internal reference. Acetone-d_6 was used as deuterium lock. Free induction decay was submitted to an exponential multiplication inducing a line broadening of 1.4 Hz. The curve fitting was carried out with a Lorentzian mathematical model using Perch Software (Perch NMR Software; University of Kuopio, Kuopio, Finland).

Data were processed as described previously, and the $\delta^{13}C_i$ [‰] values were calculated from the reduced molar fraction f_i/F_i and the $\delta^{13}C_g$ [‰] obtained by isotope ratio measurement by mass spectrometry.[244]

5.3.4.4 Isotope ratio monitoring by mass spectrometry.

The $\delta^{13}C_g$ [‰] values were measured using irm-elemental analyser (EA)/MS. Approximately 1.0mg of tramadol was weighted into each of two tin capsules (solids "light" 5x9 mm; Thermo Fisher Scientific) and the $^{13}C/^{12}C$ ratios measured using a Sigma2 mass spectrometer (Sercon Instruments) linked to a Sercon elemental analyser. Isotope ratios ($\delta^{13}C_g$ [‰]) were expressed relative to $\delta^{13}C_{VPDB}$ [‰]. The instrument was calibrated for $\delta^{13}C$ using the international reference materials NBS-22 ($\delta^{13}C_{PDB}$ = -30.03‰), SUCROSE-C6 ($\delta^{13}C_{PDB}$ = -10.8‰), and IAEA-CH-7 PEF-1 ($\delta^{13}C_{PDB}$ = -32.15‰) (International Atomic Energy Agence, Vienna, Austria), and instrumental deviation followed via a laboratory standard of glutamic acid.

The $\delta^{18}O$ [‰] values were obtained by irm-EA/pyrolysis/MS in continuous flow. Approximately 1.0mg of tramadol was weighted into each of three capsules, and the $^{18}O/^{16}O$ ratios were determined using a EuroVector EuroEA3028-HT system (EuroVector SpA) interfaced to an IsoPrime mass spectrometer working in continuous-flow mode. For each sample, the first value was discarded to avoid memory effects. Calibration was by the working standard NBS120c, calibrated against the international standard $\delta^{18}O_{V\text{-}SMOW}$ (21.7‰).

Conditions to obtain precise and true measurements of the intramolecular ^{13}C distribution in organic molecules by isotopic ^{13}C nuclear magnetic resonance spectrometry', Analytica Chimica Acta, 846, (2014), 1-7.

[244] K. Bayle *et al.*, *'Nonstatistical ^{13}C distribution during carbon transfer from glucose to ethanol during fermentation is determined by the catabolic pathway exploited',* Journal of Biological Chemistry, 7, (290), (2015), 4118-4128; V. Silvestre *et al.*, *'Isotopic ^{13}C NMR spectrometry to assess counterfeiting of active pharmaceutical ingredients: Site-specific ^{13}C content of aspirin and paracetamol',* Journal of Pharmaceutical and Biomedical Analysis, 50, (3), (2009), 336-341.

6 Chapter VI – Conclusions and perspectives

6.1 Conclusions

Throughout the thesis, I have interpreted the data within each chapter and drawn appropriate conclusions. This section, therefore, only presents a brief summary of the general conclusions that can be made from the previously-presented work and some suggestions as to what is now needed to consolidate and advance the approach used.

6.1.1 Is it possible to obtain an overview of biosynthetic pathways by irm-^{13}C NMR?

The technique of irm-^{13}C NMR spectrometry has been shown to be amenable for getting basic general information on how ^{13}C is fractionated during biosynthetic pathways for a range of natural and synthetic compounds. It is now clear that position-specific intramolecular isotope fractionation can give insight into metabolic pathways and common features of metabolism can be identified and described.

A good example of this is the data obtained for the amino acid, L-tyrosine. Here, a good agreement of the pattern of ^{13}C position-specific distribution is seen with the phenylpropanoid ferulic acid (Figure 26). These two compounds have the same origin, the shikimate pathway, and clearly the fundamental pattern established during the formation of chorismate is retained within these different compounds derived from this common origin.

The other feature of the data obtained during this project and presented in this thesis is that it is shown possible to obtain hints as to probable biochemistry by interpreting observed intramolecular isotope fractionation in relation to known isotope effects, even when the biochemistry of the pathway is unknown. This technique of "retro-biosynthesis" has proved able to indicate a probable pathway for the alkaloid tramadol and to give indications as to possible reaction mechanism for undefined steps of nicotine biosynthesis.

6.1.2 How to distinguish between the natural and synthetic origin of naturally occurring compounds?

The technique of irm-NMR is well established as a powerful method to distinguish between chemicals of different origins. In this thesis, I have not been focussed on this aspect of the application of this technique, since the main objective was to apply the method to study causes of isotope fractionation. However, a small study has been made on nicotine, as presented in Section 5.2.3. This example shows the inherent difficulties in the labelling of compounds as 'synthetic' or 'natural' and causes us to question the labelling of some of these. This is evidently the case with *S*-nicotine, for which the Fluka sample (SZBE245XV) shows a close match to authenticated natural samples but is widely divergent from the sample of *R,S*-nicotine made in the lab. Add to this that the preparation of S-nicotine by synthesis is laborious and time-consuming, whereas the purification of S-nicotine from *N. tabacum* is relative cheap and straightforward, it seems improbable that this sample is made by synthesis. Why therefore is it labelled as 'synthetic'? It would appear that this is an example of those cases where the supplier is obliged to so-label a

compounds because the process used to manufacture them involved one or more chemical treatments which require that the labelling is not 'natural'. Nevertheless, in this case it can be reasonably proposed that the compound is, to all intense and purposes, extracted from a plant.

A similar situation may also exist with the amino acids of different origins examined by irm^{13}C-NMR spectrometry, although the number of analyses so far conducted is insufficient to draw any specific conclusions. For example, the L-alanine studied (see section 3.4.1) shows a profile compatible with it being of natural origin, although it is labelled as 'synthetic'.

In this context, combining irm-EA/MS and irm^{13}C-NMR spectrometry allows us to have an insight into the position specific isotope ratios for each carbon position of the studied molecule which can more easily help to distinguish their origin.

6.1.3 Do the theoretical calculations confirm the experimental data?

Within the context of the biosynthesis of L-methionine, we have carried out a study involving a combined approach with both experimental and theoretical analyses. The experimental data show that the *S*-methyl group is impoverished in methionine. In the light of the theoretical modelling conducted for the proposed reaction scheme of methyl group transfer from 5-*N*-Me-tetrahydrofalate to homocysteine, forming methionine, it was possible to establish that the reaction is going to favour ^{13}C depletion in transferred group. This is indicated by the strong normal kinetic isotope effect calculated for the carbon atom of the methyl group of 5-*N*-Me-tetrahydrofalate and also for the 5-nitrogen atom that is also involved in bond breaking. This shows that breaking the carbon–nitrogen bond is the key event in the occurring reaction and strongly supports the hypothesis that the general depletion seen in methyl groups is due to the *S*-methyl group being impoverished in methionine.

Such an approach shows how general aspects of isotope fractionation can be related to biochemical events that the compounds have in common, as also seen for tyrosine and ferulic acid.

6.2 Perspectives

6.2.1 The analysis of isotope fractionation in amino acids

In the 45 years since the pioneering work of Abelson and Hoering[245] was published, little further understanding has been established relating the position-specific distribution of ^{13}C in amino acids to their biosynthetic origin. The work presented in this thesis must only be taken as a 'proof of concept' and it is now necessary to collect further data to provide a whole range of the information required to create an amino acid isotopic-variation 'data base'. This topic requires further attention and isotopic measurements. In the first place, it would be desirable to look at the range in amino acids coming from the same protein source. Then, it would be desirable to work through the amino acids from the metabolic pathways of C_3 and C_4 plants, as well as from different organisms growing under distinct conditions.

[245] P.H. Abelson and T.C.Hoering, '*Carbon isotope fractionation in formation of amino acids by photosynthetic organisms*', Proceedings of National Academy of Sciences of the US, (1961), 47 (5), 623-632.

6.2.2 Natural products – nicotine, tropine, tramadol

The principle has been shown that biosynthetic information can be inferred from isotopic distributions using these three alkaloids. For the purpose of obtaining greater amounts of data, in the way of elucidation of biosynthetic pathways and dependencies between certain steps, it is now required to look at the wider range of natural products, in particular focussing on those that have certain aspects in common and others that are specific. In this way, an isotopic grid can be established that show how similar reactions even in very different compounds, can lead to a similar isotopic affiliation. A further aspect of importance is to establish the affiliations with primary precursors: for example, the relationships between methionine and glucose in microbial fermentation systems. This would provide a wider explanation of the origin of *O*-methyl and *N*-methyl groups and the large depletion observed.

6.2.3 Theoretical calculations

Isotopic fractionation in methionine synthase has been studied at a low level of theory to obtain the energy profile for the methyl group transfer reaction. The energy barrier is, however probably overestimated and, although the presented data is sufficient to show the agreement between calculated and measured fractionation, the study needs to be extended to a more rigorous theoretical treatment to obtain significant information about the reaction scheme and kinetic isotope effects of the reaction of the methyl group transfer. It is now desirable therefore to carry on with theoretical calculations expanded to the higher level of the theory. In addition, it is desirable to study the other enzymes of the cycle, notably AdoMet synthetase that catalyses the 'activation' of the methyl group in a form available for transfer. Finally, studies of the methyl transferases that form the *O*-methyl and *N*-methyl groups need to be expanded. In this context, a very recent paper from the Klinman[246] group indicates that the barrier for the transfer of methyl by catechol O-methyl transferase is quite low.

[246] H. J. Kulik *et al.*, *'How Large Should the QM Region Be in QM/MM Calculations? The Case of Catechol O-Methyltransferase'*, The Journal of Physical Chemistry B, (2016).

7 References

Abelson P. H. and T. C. Hoering, 'Carbon isotope fractionation in formation of amino acids by photosynthetic organisms*', *Proceedings of the National Academy of Sciences of the United States of America*, 47 (1961), 623–32

Ahn N. and J. P. Klinman, 'Mechanism of Modulation of Dopamine Beta-Monooxygenase by pH and Fumarate as Deduced from Initial Rate and Primary Deuterium Isotope Effect Studies', *Biochemistry*, 22 (1983), 3096–3106

Armstrong E. F., 'Enzymes. By J.B.S. Haldane, M.A. Monographs on Biochemistry. Edited by R.H.A. Plimmer, D.Sc., and Sir F. G. Hopkins, M.A., M.B., D.Sc., F.R.S. Pp. vii+235. London: Longmans, Green & Co., 1930. Price 14s', *Journal of the Society of Chemical Industry*, 49 (1930), 919–20

Azevedo R. A., P. Arruda, W. L. Turner and P. J. Lea, 'The Biosynthesis and Metabolism of the Aspartate Derived Amino Acids in Higher Plants', *Phytochemistry*, 46 (1997), 395–419

Baldwin I. T., 'The Alkaloidal Responses of Wild Tobacco to Real and Simulated Herbivory', *Oecologia*, 77 (1988), 378–81

Barbour M. M., 'Stable Oxygen Isotope Composition of Plant Tissue: A Review', *Functional Plant Biology*, 34 (2007), 83

Bayle K., S. Akoka, G. S. Remaud and . J. Robins, 'Nonstatistical ^{13}C Distribution during Carbon Transfer from Glucose to Ethanol during Fermentation Is Determined by the Catabolic Pathway Exploited', *The Journal of Biological Chemistry*, 290 (2015), 4118–28

Bayle K., A. Gilbert, M. Julien, K. Yamada, V. Silvestre, R. J. Robins and others, 'Conditions to Obtain Precise and True Measurements of the Intramolecular ^{13}C Distribution in Organic Molecules by Isotopic ^{13}C Nuclear Magnetic Resonance Spectrometry', *Analytica Chimica Acta*, 846 (2014), 1–7

Bendall M. R. and T. E. Skinner, 'Calibration of STUD+ Parameters to Achieve Optimally Efficient Broadband Adiabatic Decoupling in a Single Transient', *Journal of Magnetic Resonance (San Diego, Calif.: 1997)*, 134 (1998), 331–49

Bertin C., L. A. Weston, T. Huang, G. Jander, T. Owens, J. Meinwald and others, 'Grass Roots Chemistry: Meta-Tyrosine, an Herbicidal Nonprotein Amino Acid', *Proceedings of the National Academy of Sciences*, 104 (2007), 16964–69

Biastoff S., W. Brandt and B. Dräger, 'Putrescine N-Methyltransferase--the Start for Alkaloids', *Phytochemistry*, 70 (2009), 1708–18

Billault I., S. Guiet, F. Mabon and R. Robins, 'Natural Deuterium Distribution in Long-Chain Fatty Acids Is Nonstatistical: A Site-Specific Study by Quantitative ^{2}H NMR Spectroscopy', *ChemBioChem*, 2 (2001), 425–31

'Biochemistry and Molecular Biology of Plants - Google Książki'

Botosoa E. P., C. Blumenstein, D. A. MacKenzie, V. Silvestre, G. S. Remaud, R. A. Kwiecień and others, 'Quantitative Isotopic ^{13}C Nuclear Magnetic Resonance at Natural Abundance to Probe Enzyme Reaction Mechanisms via Site-Specific Isotope Fractionation: The Case of the Chain-Shortening Reaction for the Bioconversion of Ferulic Acid to Vanillin', *Analytical Biochemistry*, 393 (2009), 182–88

Botosoa E. P., E. Caytan, V. Silvestre, R. J. Robins, S. Akoka and G. S. Remaud, 'Unexpected Fractionation in Site-Specific ^{13}C Isotopic Distribution Detected by Quantitative ^{13}C NMR at Natural Abundance', *Journal of the American Chemical Society*, 130 (2008), 414–15

Boumendjel A., G. S. Taïwe, E. Ngo Bum, T. Chabrol, C. Beney, V. Sinniger and others, 'Occurrence of the Synthetic Analgesic Tramadol in an African Medicinal Plant', *Angewandte Chemie*, 125 (2013), 11996–0

Brent F. and E. Leete, 'Nicotine Synthase - an Enzyme from Nicotiana Species Which Catalyzes the Formation of (S)-Nicotine from Nicotinic Acid and 1-Methyl-Δ'pyrrolinium Chloride', *Tetrahedron Letters*, 31 (1990), 6295–98

Bringmann G., Torsten F. Noll, T. Gulder, M. Dreyer, M. Grüne and D. Moskau, 'Polyketide Folding in Higher Plants: Biosynthesis of the Phenylanthraquinone Knipholone', *The Journal of Organic Chemistry*, 72 (2007), 3247–52

Bunsupa S., M. Yamazaki and K. Saito, 'Quinolizidine Alkaloid Biosynthesis: Recent Advances and Future Prospects', *Frontiers in Plant Science*, 3 (2012)

Butzenlechner M., S. Thimet, K. Kempe, H. Kexel, and H-L. Schmidt, 'Inter- and Intramolecular Isotopic Correlations in Some Cyanogenic Glycosides and Glucosinolates and Their Practical Importance', *Phytochemistry*, 43 (1996), 585–92

Chaintreau A., W. Fieber, H. Sommer, A. Gilbert, K. Yamada, N. Yoshida and others, 'Site-Specific ^{13}C Content by Quantitative Isotopic ^{13}C Nuclear Magnetic Resonance Spectrometry: A Pilot Inter-Laboratory Study', *Analytica Chimica Acta*, 788 (2013), 108–13

Cherrier M. V., A. Chan, C. Darnault, D. Reichmann, P. Amara, S. Ollagnier de Choudens and others, 'The Crystal Structure of Fe_4S_4 Quinolinate Synthase Unravels an Enzymatic Dehydration Mechanism That Uses Tyrosine and a Hydrolase-Type Triad', *Journal of the American Chemical Society*, 136 (2014), 5253–56

Chesters N. C. J. E., D. O'Hagan and R. J. Robins, 'The Biosynthesis of Tropic Acid in Plants: Evidence for the Direct Rearrangement of 3-Phenyllactate to Tropate', *Journal of the Chemical Society, Perkin Transactions 1*, 1994, 1159–62

Cleland, W. W, 'The Kinetics of Enzyme-Catalyzed Reactions with Two or More Substrates or Products', *Biochimica et Biophysica Acta (BBA) - Specialized Section on Enzymological Subjects*, 67 (1963), 104–37 <https://doi.org/10.1016/0926-6569(63)90211-6>

Cleland W. W., 'Mechanistic Deductions from Isotope Effects in Multi Reactant Enzyme Mechanisms', *Biochemistry*, 1981

Cleland W. W., 'The Use of Isotope Effects to Determine Enzyme Mechanisms', *Archives of Biochemistry and Biophysics*, 433 (2005), 2–12

Cockburn W., I. P. Ting and L. O. Sternberg, 'Relationships between Stomatal Behavior and Internal Carbon Dioxide Concentration in Crassulacean Acid Metabolism Plants', *Plant Physiology*, 63 (1979), 1029–32

Cook P. F., 'Kinetic Studies to Determine the Mechanism of Regulation of Bovine Liver Glutamate Dehydrogenase by Nucleotide Effectors', *Biochemistry*, 21 (1982), 113–16

Cook P. F., *Enzyme Mechanism from Isotope Effects* (CRC Press, 1991)

Cossins E. A. and Liangfu Chen, 'Folates and One-Carbon Metabolism in Plants and Fungi', *Phytochemistry*, 45 (1997), 437–52

Craig H., 'Isotopic Variations in Meteoric Waters', *Science*, 133 (1961), 1702–3

Dalton H. L., C. K. Blomstedt, A. D. Neale, R. Gleadow, K. D. DeBoer and J. D. Hamill, 'Effects of down-Regulating Ornithine Decarboxylase upon Putrescine-Associated Metabolism and Growth in Nicotiana Tabacum L', *Journal of Experimental Botany*, 67 (2016), 3367–81

Darden T., D. York and L. Pedersen, 'Particle Mesh Ewald: An N·log(N) Method for Ewald Sums in Large Systems', *The Journal of Chemical Physics*, 98 (1993), 10089–92

Dayer P., Desmeules J., Collart L., 'Pharmacology of Tramadol'

Dewey R. E. and J. Xie, 'Molecular Genetics of Alkaloid Biosynthesis in Nicotiana Tabacum', *Phytochemistry*, 94 (2013), 10–27

Dewick P. M., *Medicinal Natural Products: A Biosynthetic Approach* (John Wiley & Sons, 2002)

Diomande D. G., E. Martineau, A. Gilbert, P. Nun, A. Murata, K. Yamada and others, 'Position-Specific Isotope Analysis of Xanthines: A ^{13}C Nuclear Magnetic Resonance Method to Determine the ^{13}C Intramolecular Composition at Natural Abundance', *Analytical Chemistry*, 87 (2015), 6600–6606

Dong, F., Z. Yang, S. Baldermann, Y. Kajitani, S. Ota, H. Kasuga and others, 'Characterization of L-Phenylalanine Metabolism to Acetophenone and 1-Phenylethanol in the Flowers of Camellia Sinensis Using Stable Isotope Labeling', *Journal of Plant Physiology*, 169 (2012), 217–25

Dräger B., 'Tropinone Reductases, Enzymes at the Branch Point of Tropane Alkaloid Metabolism', *Phytochemistry*, 67 (2006), 327–37

Dragulska S., E. Winnicka and M. Kańska, 'Isotope Effects in the Enzymatic Oxidation of Tryptamine to 3-Indolyl-Acetaldehyde', *Isotopes in Environmental and Health Studies*, 50 (2014), 269–76

Efange S. M. N., 'Synthesis and Applications of Isotopically Labelled Compounds', *Radiology*, 176 (1990), 438–438

Eichel J., J. C. González, M. Hotze, R. G. Matthews and J. Schröder, 'Vitamin-B12-Independent Methionine Synthase from a Higher Plant (Catharanthus Roseus). Molecular Characterization, Regulation, Heterologous Expression, and Enzyme Properties', *European Journal of Biochemistry / FEBS*, 230 (1995), 1053–58

Farquhar G. D., K. T. Hubick, A. G. Condon and R. A. Richards, 'Carbon Isotope Fractionation and Plant Water-Use Efficiency', in *Stable Isotopes in Ecological Research*, ed. by P. W. Rundel, J. R. Ehleringer, and K. A. Nagy (Springer New York, 1989), pp. 21–40

Farquhar G. D. and Jon Lloyd, 'Carbon and Oxygen Isotope Effects in the Exchange of Carbon Dioxide between Terrestrial Plants and the Atmosphere', in *Stable Isotopes and Plant Carbon-Water Relations* (Elsevier, 1993), pp. 47–70

Farquhar G. D., M.H. O'Leary and Joe A. Berry, 'On the Relationship between Carbon Isotope Discrimination and the Intercellular Carbon Dioxide Concentration in Leaves', *Functional Plant Biology*, 9 (1982), 121–137

Felpin S., G., G. Vo-Thanh, R. J. Robins, J. Villiéras and J. Lebreton, 'Efficient Enantiomeric Synthesis of Pyrrolidine and Piperidine Alkaloids from Tobacco', *The Journal of Organic Chemistry*, 66 (2001), 6305–12

Field M. J., M. Albe, C. Bret, F. Proust-De Martin and A. Thomas, 'The Dynamo Library for Molecular Simulations Using Hybrid Quantum Mechanical and Molecular Mechanical Potentials', *Journal of Computational Chemistry*, 21 (2000), 1088–1100

G D Farquhar, J. R. Ehleringer, and K. T. Hubick, 'Carbon Isotope Discrimination and Photosynthesis', *Annual Review of Plant Physiology and Plant Molecular Biology*, 40 (1989), 503–37

Galimov E., *The Biological Fractionation of Isotopes* (Elsevier, 2012)

Galimov E., Kodina L. A, and Generalova V. N, 'Experimental Investigation of Intra- and Intermolecular Isotopic Effects in Biogenic Aromatic Compounds', *Geochemistry International*, 9 (1976), 9-13

Gautier R., A.-C. Camproux and P. Tufféry, 'SCit: Web Tools for Protein Side Chain Conformation Analysis', *Nucleic Acids Research*, 32 (2004), W508–11

Gerdov S. M., Yu K. Grishin, V. A. Roznyatovsky, Yu A. Ustynyuk, A. V. Kuchin, I. N. Alekseev and others, 'Quantitative 2H NMR Spectroscopy 2. "H/D-Isotope Portraits" of Cyclic Monoterpenes and Discrimination of Their Biosynthetic Pathways', *Russian Chemical Bulletin*, 54 (2005), 1258–65

Gilbert A., R. J. Robins, G. S. Remaud and G. G. B. Tcherkez, 'Intramolecular ^{13}C Pattern in Hexoses from Autotrophic and Heterotrophic C_3 Plant Tissues', *Proceedings of the National Academy of Sciences of the United States of America*, 109 (2012), 18204–9

Gilbert A., V. Silvestre, R. J. Robins and G. S. Remaud, 'Accurate Quantitative Isotopic ^{13}C NMR Spectroscopy for the Determination of the Intramolecular Distribution of ^{13}C in Glucose at Natural Abundance', *Analytical Chemistry*, 81 (2009)

Gilbert A. and others, 'Impact of the Deuterium Isotope Effect on the Accuracy of ^{13}C NMR Measurements of Site-Specific Isotope Ratios at Natural Abundance in Glucose', *Analytical and Bioanalytical Chemistry*, 398 (2010), 1979–84

Gilbert A., V. Silvestre, R. J. Robins, G. S. Remaud and G. Tcherkez, 'Biochemical and Physiological Determinants of Intramolecular Isotope Patterns in Sucrose from C_3, C_4 and CAM Plants

Accessed by Isotopic ^{13}C NMR Spectrometry: A Viewpoint', *Natural Product Reports*, 29 (2012), 476–86

Gilbert A., V. Silvestre, N. Segebarth, G. Tcherkez, C. Guillou, R. J. Robins and others, 'The Intramolecular ^{13}C-Distribution in Ethanol Reveals the Influence of the CO_2-Fixation Pathway and Environmental Conditions on the Site-Specific ^{13}C Variation in Glucose', *Plant, Cell & Environment*, 34 (2011), 1104–12

Giovanelli J. and S. H. Mudd, 'Synthesis of Homocysteine and Cysteine by Enzyme Extracts of Spinach', *Biochemical and Biophysical Research Communications*, 27 (1967), 150–56

Giovanelli J., S. H. Mudd and A. H. Datko, 'Quantitative Analysis of Pathways of Methionine Metabolism and Their Regulation in Lemna', *Plant Physiology*, 78 (1985), 555–60

Grassineau N. V., 'High-Precision EA-IRMS Analysis of S and C Isotopes in Geological Materials', *Applied Geochemistry*, Frontiers in Analytical Geochemistry–An IGC 2004 Perspective, 21 (2006), 756–65

Gray J. and P. Thompson, 'Climatic Information from $^{18}O/^{16}O$ Analysis of Cellulose, Lignin and Whole Wood from Tree Rings', *Nature*, 270 (1977), 708–9

Greule M. and F. Keppler, 'Stable Isotope Determination of Ester and Ether Methyl Moieties in Plant Methoxyl Groups', *Isotopes in Environmental and Health Studies*, 47 (2011), 470–82

Greule M., L. D. Tumino, T. Kronewald, U. Hener, J. Schleucher, A. Mosandl and others, 'Improved Rapid Authentication of Vanillin Using $\delta^{13}C$ and $\delta^{2}H$ Values', *European Food Research and Technology*, 231 (2010), 933–41

Hayes J. M., 'Fractionation of Carbon and Hydrogen Isotopes in Biosynthetic Processes', *Reviews in Mineralogy and Geochemistry*, 43 (2001), 225–77

Hayes J. M, 'Isotopic Order, Biogeochemical Processes, and Earth History: Goldschmidt Lecture, Davos, Switzerland, August 2002', *Geochimica et Cosmochimica Acta*, 68 (2004), 1691–1700

Hegazi M. F., R. T. Borchardt and R. L. Schowen, '. Alpha.-Deuterium and Carbon-13 Isotope Effects for Methyl Transfer Catalyzed by Catechol O-Methyltransferase. SN2-like Transition State', *Journal of the American Chemical Society*, 101 (1979), 4359–4365

Herbert R. B., 'The Biosynthesis of Plant Alkaloids and Nitrogenous Microbial Metabolites', *Natural Product Reports*, 10 (1993), 575

Herries D. G., 'Enzyme Structure and Mechanism (Second Edition), by Alan Fersht. Pp 475. W H Freeman, New York. 1984. £28.95 or £14.95 (Paperback) ISBN 0–7167–1614–3 or ISBN 0–7167–1615–1 (Pbk)', *Biochemical Education*, 13 (1985), 146–146

Hesse H., O. Kreft, S. Maimann, M. Zeh and R. Hoefgen, 'Current Understanding of the Regulation of Methionine Biosynthesis in Plants', *Journal of Experimental Botany*, 55 (2004), 1799–1808

Hobbie E. and R. A. Werner, 'Intramolecular, Compound-Specific, and Bulk Carbon Isotope Patterns in C_3 and C_4 Plants: A Review and Synthesis', *New Phytologist*, 161 (2004), 371–85

Hobza P., M. Kabeláč, J. Šponer, P. Mejzlík and J. Vondrášek, 'Performance of Empirical Potentials (AMBER, CFF95, CVFF, CHARMM, OPLS, POLTEV), Semiempirical Quantum Chemical Methods (AM1, MNDO/M, PM3), and Ab Initio Hartree–Fock Method for Interaction of DNA Bases: Comparison with Nonempirical beyond Hartree–Fock Results', *Journal of Computational Chemistry*, 18 (1997), 1136–50

Jackanicz T. M. and R. U. Byerrum, 'Incorporation of Aspartate and Malate into the Pyridine Ring of Nicotine', *The Journal of Biological Chemistry*, 241 (1966), 1296–99

Jiao J. and R. Chollet, 'Posttranslational Regulation of Phosphoenolpyruvate Carboxylase in C_4 and Crassulacean Acid Metabolism Plants 1', *Plant Physiology*, 95 (1991), 981–85

Katoh A., K. Uenohara, M. Akita and T. Hashimoto, 'Early Steps in the Biosynthesis of NAD in Arabidopsis Start with Aspartate and Occur in the Plastid', *Plant Physiology*, 141 (2006), 851–57

Keppler F., R. M. Kalin, D. B. Harper, W. C. Mcroberts and J. T. G. Hamilton, 'Carbon Isotope Anomaly in the Major Plant C_1 Pool and Its Global Biogeochemical Implications', *Biogeosciences*, 1 (2004), 123–31

Kesting J. R., I-L. Tolderlund, A. F. Pedersen, M. Witt, J. W. Jaroszewski and D. Staerk, 'Piperidine and Tetrahydropyridine Alkaloids from Lobelia Siphilitica and Hippobroma Longiflora', *Journal of Natural Products*, 72 (2009), 312–15

Kigel J., *Seed Development and Germination* (CRC Press, 1995)

Kim J. M., M. A. Bogdan and P. S. Mariano, 'Mechanistic Analysis of the 3-Methyllumiflavin-Promoted Oxidative Deamination of Benzylamine. A Potential Model for Monoamine Oxidase Catalysis', *Journal of the American Chemical Society*, 115 (1993), 10591–95

Kodina L. A., 'Carbon Isotope Fractionation in Various Forms of Biogenic Organic Matter: I. Partitioning of Carbon Isotopes between the Main Polymers of Higher Plant Biomass', *Geochemistry International*, 48 (2010), 1157–65

Kohn M. J., 'Predicting Animal $\delta^{18}O$: Accounting for Diet and Physiological Adaptation', *Geochimica et Cosmochimica Acta*, 60 (1996), 4811–29

Kreuzer-Martin H. W., J. R. Ehleringer and E. L. Hegg, 'Oxygen Isotopes Indicate Most Intracellular Water in Log-Phase Escherichia Coli Is Derived from Metabolism', *Proceedings of the National Academy of Sciences of the United States of America*, 102 (2005), 17337–41

Krivachy (Tanz) N., A. Rossmann and H-L. Schmidt, 'Potentials and Caveats with Oxygen and Sulfur Stable Isotope Analyses in Authenticity and Origin Checks of Food and Food Commodities', *Food Control*, Recent Advances of Food Analysis, 48 (2015), 143–50

Kulik H. J., J. Zhang, J. P. Klinman and T. J. Martinez, 'How Large Should the QM Region Be in QM/MM Calculations? The Case of Catechol O-Methyltransferase', *The Journal of Physical Chemistry B*, 2016

Kupce Ē. and R. Freeman, 'Stretched Adiabatic Pulses for Broadband Spin Inversion', *Journal of Magnetic Resonance, Series A*, 117 (1995), 246–56

Laing W. A. and J. T. Christeller, 'A Model for the Kinetics of Activation and Catalysis of Ribulose 1, 5-Bisphosphate Carboxylase', *Biochemical Journal*, 159 (1976), 563–570

Lapadatescu C., C. Giniès, J-L. Le Quéré and P. Bonnarme, 'Novel Scheme for Biosynthesis of Aryl Metabolites from L-Phenylalanine in the Fungus Bjerkandera Adusta', *Applied and Environmental Microbiology*, 66 (2000), 1517–22

Larsen T. D., L. Taylor, M. B. Leigh and D. M. O'Brien, 'Stable Isotope Fingerprinting: A Novel Method for Identifying Plant, Fungal, or Bacterial Origins of Amino Acids', *Ecology*, 90 (2009), 3526–35

Larsson K. A. E., I. Zetterlund, G. Delp and L. M. V. Jonsson, 'N-Methyltransferase Involved in Gramine Biosynthesis in Barley: Cloning and Characterization', *Phytochemistry*, 67 (2006), 2002–8

Leete E., 'Biosynthesis of the Nicotiana Alkaloids. XI. Investigation of Tautomerism in N-Methyl-.DELTA.1-Pyrrolinium Chloride and Its Incorporation into Nicotine', *Journal of the American Chemical Society*, 89 (1967), 7081–84

Levy G. C. and J. D. Cargioli, 'Spin-Lattice Relaxation in Solutions Containing Cr(III) Paramagnetic Relaxation Agents', *Journal of Magnetic Resonance (1969)*, 10 (1973), 231–34

Lewis R. S., H. O. Lopez, S. W. Bowen, K. R. Andres, W. T. Steede and R. E. Dewey, 'Transgenic and Mutation-Based Suppression of a Berberine Bridge Enzyme-Like (BBL) Gene Family Reduces Alkaloid Content in Field-Grown Tobacco', *PLOS ONE*, 10 (2015), e0117273

Li H., A. D. Robertson and J. H. Jensen, 'Very Fast Empirical Prediction and Rationalization of Protein pKa Values', *Proteins: Structure, Function, and Bioinformatics*, 61 (2005), 704–21

Li J. and Y. Sha, 'A Convenient Synthesis of Amino Acid Methyl Esters', *Molecules*, 13 (2008), 1111–19

Li R., D. W. Reed, E. Liu, J. Nowak, L. E. Pelcher, J. E. Page and others, 'Functional Genomic Analysis of Alkaloid Biosynthesis in Hyoscyamus Niger Reveals a Cytochrome P450 Involved in Littorine Rearrangement', *Chemistry & Biology*, 13 (2006), 513–20

Luck L. A. and C. R. Landis, 'Aprotic, Viscous Solvent Mixtures for Obtaining Large, Negative NOE Enhancements in Small Inorganic and Organic Molecules: Ideal Solvent Systems for Deducing Structures by NMR Techniques', *Organometallics*, 11 (1992), 1003–5

Lumbroso A., V. Coeffard, E. Le Grognec, I. Beaudet and J-P. Quintard, 'An Efficient and Scalable Synthesis of N-(Benzyloxycarbonyl)- and N-(Methyloxycarbonyl)-(S)-Vinylglycinol', *Tetrahedron Letters*, 51 (2010), 3226–28

Lundstrom J., *The Alkaloids: Chemistry and Pharmacology* (Academic Press, 1989)

Lynch A. H., N. J. Kruger, R. E. M. Hedges and J. S. O. McCullagh, 'Variability in the Carbon Isotope Composition of Individual Amino Acids in Plant Proteins from Different Sources: 1 Leaves', *Phytochemistry*, 125 (2016), 27–34

Lynch A. H., J. S. O. McCullagh and R. E. M. Hedges, 'Liquid Chromatography/isotope Ratio Mass Spectrometry Measurement of $\delta^{13}C$ of Amino Acids in Plant Proteins', *Rapid Communications in Mass Spectrometry*, 25 (2011), 2981–88

Maeda H. and N. Dudareva, 'The Shikimate Pathway and Aromatic Amino Acid Biosynthesis in Plants', *Annual Review of Plant Biology*, 63 (2012), 73–105

Markham G. D., D. W. Parkin, F. Mentch and V. L. Schramm, 'A Kinetic Isotope Effect Study and Transition State Analysis of the S-Adenosylmethionine Synthetase Reaction', *The Journal of Biological Chemistry*, 262 (1987), 5609–15

Marshall J. D., J. R. Brooks and K. Lajtha, 'Sources of Variation in the Stable Isotopic Composition of Plants', in *Stable Isotopes in Ecology and Environmental Science*, ed. by Robert Michener and Kate Lajtha

Martin G. J., S. Lavoine-Hanneguelle, F. Mabon and M. L. Martin, 'The Fellowship of Natural Abundance ^{2}H-Isotopomers of Monoterpenes', *Phytochemistry*, 65 (2004), 2815–31

Matthews R. G. and J. T. Drummond, 'Providing One-Carbon Units for Biological Methylations: Mechanistic Studies on Serine Hydroxymethyltransferase, Methylenetetrahydrofolate Reductase, and Methyltetrahydrofolate-Homocysteine Methyltransferase', *Chemical Reviews*, 90 (1990), 1275–90

Melzer E. and H-L. Schmidt, 'Carbon Isotope Effects on the Decarboxylation of Carboxylic Acids. Comparison of the Lactate Oxidase Reaction and the Degradation of Pyruvate by H_2O_2', *The Biochemical Journal*, 252 (1988), 913–15

Melzer E., 'Carbon Isotope Effects on the Pyruvate Dehydrogenase Reaction and Their Importance for Relative Carbon-13 Depletion in Lipids.', *Journal of Biological Chemistry*, 262 (1987), 8159–64

Michael J. P., 'Indolizidine and Quinolizidine Alkaloids', *Natural Product Reports*, 20 (2003), 458–75

Michael J. P., 'Quinoline, Quinazoline and Acridone Alkaloids', *Natural Product Reports*, 21 (2004), 650–68

Miflin B. J., *Amino Acids and Derivatives: The Biochemistry of Plants* (Elsevier, 2014)

Monson K. D. and J. M. Hayes, 'Biosynthetic Control of the Natural Abundance of Carbon 13 at Specific Positions within Fatty Acids in Escherichia Coli. Evidence Regarding the Coupling of Fatty Acid and Phospholipid Synthesis.', *Journal of Biological Chemistry*, 255 (1980), 11435–41

Monson K. D. and J. M. Hayes, 'Carbon Isotopic Fractionation in the Biosynthesis of Bacterial Fatty Acids. Ozonolysis of Unsaturated Fatty Acids as a Means of Determining the Intramolecular Distribution of Carbon Isotopes', *Geochimica et Cosmochimica Acta*, 46 (1982), 139–49

Naconsie M., K. Kato, T. Shoji and T. Hashimoto, 'Molecular Evolution of N-Methylputrescine Oxidase in Tobacco', *Plant & Cell Physiology*, 55 (2014), 436–44

Natelson S., 'Canavanine to Arginine Ratio in Alfalfa (Medicago Sativa), Clover (Trifolium), and the Jack Bean (Canavalia Ensiformis)', *Journal of Agricultural and Food Chemistry*, 33 (1985), 413–19

Negrel J. and F. Javelle, 'The Biosynthesis of Acetovanillone in Tobacco Cell-Suspension Cultures', *Phytochemistry*, 71 (2010), 751–59

Neuhaus D., M. P. Williamson and others, *The Nuclear Overhauser Effect in Structural and Conformational Analysis* (VCH New York, 1989)

Noggle J., *The Nuclear Overhauser Effect* (Elsevier, 2012)

O'Hagan D. and R. J. Robins, 'Tropic Acid Ester Biosynthesis in Datura Stramonium and Related Species', *Chemical Society Reviews*, 27 (1998), 207–12

O'Leary M. H., S. Madhavan and P. Paneth, 'Physical and Chemical Basis of Carbon Isotope Fractionation in Plants', *Plant, Cell & Environment*, 15 (1992), 1099–1104

O'Leary M. H., 'Carbon Isotope Fractionation in Plants', *Phytochemistry*, 20 (1981), 553–67

O'Leary, M. H. and C. B. Osmond, 'Diffusional Contribution to Carbon Isotope Fractionation during Dark CO_2 Fixation in CAM Plants 1', *Plant Physiology*, 66 (1980), 931–34

O'Leary M. H., J. E. Rife and J. D. Slater, 'Kinetic and Isotope Effect Studies of Maize Phosphoenolpyruvate Carboxylase', *Biochemistry*, 20 (1981), 7308–7314

Owens T. G., 'Plant Physiology, Biochemistry and Molecular Biology. David T. Dennis David H. Turpin', *The Quarterly Review of Biology*, 67 (1992), 61–61

Oza V. B., C. Smith, P. Raman, E. K. Koepf, H.l A. Lashuel, H. Mike Petrassi and others, 'Synthesis, Structure, and Activity of Diclofenac Analogues as Transthyretin Amyloid Fibril Formation Inhibitors', *Journal of Medicinal Chemistry*, 45 (2002), 321–332

Park R. and S. Epstein, 'Carbon Isotope Fractionation during Photosynthesis', *Geochimica et Cosmochimica Acta*, 21 (1960), 110–26

Pataki D. E., J. R. Ehleringer, L. B. Flanagan, D. Yakir, D. R. Bowling, C. J. Still, and others, 'The Application and Interpretation of Keeling Plots in Terrestrial Carbon Cycle Research', *Global Biogeochemical Cycles*, 17 (2003), 1022

Pejchal R. and M. L. Ludwig, 'Cobalamin-Independent Methionine Synthase (MetE): A Face-to-Face Double Barrel That Evolved by Gene Duplication', *PLOS Biol*, 3 (2004), e31

Phillips J. C., R. Braun, W. Wang, J. Gumbart, E. Tajkhorshid, E. Villa and others, 'Scalable Molecular Dynamics with NAMD', *Journal of Computational Chemistry*, 26 (2005), 1781–1802

Podlesak D. W., G. J. Bowen, S. O'Grady, T. E. Cerling and J. R. Ehleringer, 'δ^2H and $\delta^{18}O$ of Human Body Water: A GIS Model to Distinguish Residents from Non-Residents in the Contiguous USA', *Isotopes in Environmental and Health Studies*, 48 (2012), 259–79

Purich D. L. and R. D. Allison, 'Isotope Exchange Methods for Elucidating Enzymic Catalysis', in *Methods in Enzymology*, ed. by Daniel L. Purich, Enzyme Kinetics and Mechanism - Part B: Isotopic Probes and Complex Enzyme Systems (Academic Press, 1980), LXIV, 3–46

"rate-Limiting step." A Dictionary of Biology. 2004. Encyclopedia.com.

Raushel F. M. and J. J. Villafranca, 'Positional Isotope Exchang', *Critical Reviews in Biochemistry*, 23 (1988), 1–26

Ravanel S., B. Gakière, D. Job and R. Douce, 'The Specific Features of Methionine Biosynthesis and Metabolism in Plants', *Proceedings of the National Academy of Sciences*, 95 (1998), 7805–12

Reuben J., 'Effects of Solvent and Hydroxyl Deuteration on the Carbon-13 NMR Spectrum of D-Idose: Spectral Assignments, Tautomeric Compositions, and Conformational Equilibria', *Journal of the American Chemical Society*, 107 (1985), 5867–70

Reuben J., 'Isotopic Multiplets in the Carbon-13 NMR Spectra of Polyols with Partially Deuterated Hydroxyls. 3. Fingerprints of Molecular Structure and Hydrogen Bonding Effects in the Carbon-13 NMR Spectra of Monosaccharides with Partially Deuterated Hydroxyls', *Journal of the American Chemical Society*, 106 (1984), 6180–86

Robins R. J., T. W. Abraham, A. J. Parr, J. Eagles and N. J. Walton, 'The Biosynthesis of Tropane Alkaloids in Datura Stramonium: The Identity of the Intermediates between N-Methylpyrrolinium Salt and Tropinone', *Journal of the American Chemical Society*, 119 (1997), 10929–34

Robins R. J., P. Bachmann and J. G. Woolley, 'Biosynthesis of Hyoscyamine Involves an Intramolecular Rearrangement of Littorine', *Journal of the Chemical Society, Perkin Transactions 1*, 1994, 615–19

Robins R. J., N. J. Walton, A. J. Parr, E. Lindsay H. Aird, Michael J. C. Rhodes and J. D. Hamill, 'Progress in the Genetic Engineering of the Pyridine and Tropane Alkaloid Biosynthetic Pathways of Solanaceous Plants', in *Genetic Engineering of Plant Secondary Metabolism*, ed. by Brian E. Ellis, Gary W. Kuroki, and Helen A. Stafford, Recent Advances in Phytochemistry, 28 (Springer US, 1994), pp. 1–33

Robins R. J., Walton N. J., *The Alkaloids: Chemistry and Pharmacology* (Academic Press, 1994)

Roeske C. A. and M. H. O'Leary, 'Carbon Isotope Effects on Enzyme-Catalyzed Carboxylation of Ribulose Bisphosphate', *Biochemistry*, 23 (1984), 6275–6284

Romek K. M., P. Nun, G. S. Remaud, V. Silvestre, G. S. Taïwe, F. Lecerf-Schmidt and others, 'A Retro-Biosynthetic Approach to the Prediction of Biosynthetic Pathways from Position-Specific Isotope Analysis as Shown for Tramadol', *Proceedings of the National Academy of Sciences of the United States of America*, 112 (2015), 8296–8301

Romek K. M., G. S. Remaud, V. Silvestre, P. Paneth and R. J. Robins, 'Non-Statistical ^{13}C Fractionation Distinguishes Co-Incident and Divergent Steps in the Biosynthesis of the Alkaloids Nicotine and Tropine', *Journal of Biological Chemistry*, 2016, jbc.M116.734087

Rose I. A., 'The Isotope Trapping Method: Desorption Rates of Productive E.S Complexes', *Methods in Enzymology*, 64 (1980), 47–59

Rossmann A., M. Butzenlechner and H-L. Schmidt, 'Evidence for a Nonstatistical Carbon Isotope Distribution in Natural Glucose', *Plant Physiology*, 96 (1991), 609–14

Savidge W. B. and N. E. Blair, 'Patterns of Intramolecular Carbon Isotopic Heterogeneity within Amino Acids of Autotrophs and Heterotrophs', *Oecologia*, 139 (2004), 178–89

Schirch V. and D. M. E. Szebenyi, 'Serine Hydroxymethyltransferase Revisited', *Current Opinion in Chemical Biology*, 9 (2005), 482–87

Schmidt H-L. and H. Kexel, 'Metabolite Pools and Metabolic Branching as Factors of in-Vivo Isotope Discriminations by Kinetic Isotope Effects', *Isotopes in Environmental and Health Studies*, 33 (1997), 19–30

Schmidt H-L., '^{13}C-Kinetic Isotope Effects in Photosynthetic Carboxylation Reactions and δ^{13}C-Values of Plant Material - Schmidt - 2013 - Israel Journal of Chemistry

Schmidt H-L., 'Fundamentals and Systematics of the Non-Statistical Distributions of Isotopes in Natural Compounds', *Naturwissenschaften*, 90 (2003), 537–52

Schmidt H-L., R. J. Robins and R. A. Werner, 'Multi-Factorial in Vivo Stable Isotope Fractionation: Causes, Correlations, Consequences and Applications', *Isotopes in Environmental and Health Studies*, 51 (2015), 155–99

Schmidt H-L., R. A. Werner and W. Eisenreich, 'Systematics of ^{2}H Patterns in Natural Compounds and Its Importance for the Elucidation of Biosynthetic Pathways', *Phytochemistry Reviews*, 2 (2003), 61–85

Schmidt H-L., R. A. Werner, W. Eisenreich, C. Fuganti, G. Fronza, G. Remaud and others, 'The Prediction of Isotopic Patterns in Phenylpropanoids from Their Precursors and the Mechanism of the NIH-Shift: Basis of the Isotopic Characteristics of Natural Aromatic Compounds', *Phytochemistry*, 67 (2006), 1094–1103

Schmidt H-L., R. A. Werner and A. Roßmann, '^{18}O Pattern and Biosynthesis of Natural Plant Products', *Phytochemistry*, 58 (2001), 9–32

Schmidt H-L. and G. Gleixner, 'Carbon Isotope Effects on Key Reactions in Plant Metabolism and ^{13}C-Patterns in Natural Compounds', in *Stable Isotopes*, ed. by H. Griffiths (Oxford: BIOS Scientific Publisher, 1998), pp. 13–25

Shoji T. and T. Hashimoto, 'Stress-Induced Expression of NICOTINE2-Locus Genes and Their Homologs Encoding Ethylene Response Factor Transcription Factors in Tobacco', *Phytochemistry*, 113 (2015), 41–49

Silvestre V., V. M. Mboula, C. Jouitteau, S. Akoka, R. J. Robins and G. S. Remaud, 'Isotopic ^{13}C NMR Spectrometry to Assess Counterfeiting of Active Pharmaceutical Ingredients: Site-Specific ^{13}C Content of Aspirin and Paracetamol', *Journal of Pharmaceutical and Biomedical Analysis*, 50 (2009), 336–41

Spalding M. H., D. K. Stumpf, M. S. B. Ku, R. H. Burris and G. E. Edwards, 'Crassulacean Acid Metabolism and Diurnal Variations of Internal CO_2 and O_2 Concentrations in Sedum Praealtum DC', *Australian Journal of Plant Physiology*, 1979

Starcuk Z., K. Bartusek and Z. Starcuk, 'Heteronuclear Broadband Spin-Flip Decoupling with Adiabatic Pulses', *Journal of Magnetic Resonance, Series A*, 107 (1994), 24–31

Sternberg L. da Silveira Lobo, 'Oxygen and Hydrogen Isotope Ratios in Plant Cellulose: Mechanisms and Applications', in *Stable Isotopes in Ecological Research*, ed. by P. W. Rundel, J. R. Ehleringer, and K. A. Nagy, Ecological Studies, 68 (Springer New York, 1989), pp. 124–41

Struck A-W., M. L. Thompson, L. S. Wong and J. Micklefield, 'S-Adenosyl-Methionine-Dependent Methyltransferases: Highly Versatile Enzymes in Biocatalysis, Biosynthesis and Other Biotechnological Applications', *Chembiochem: A European Journal of Chemical Biology*, 13 (2012), 2642–55

Suess H. E., 'Radiocarbon Concentration in Modern Wood', *Science*, 122 (1955), 415–17

Takusagawa F., S. Kamitori and G. D. Markham, 'Structure and Function of S-Adenosylmethionine Synthetase: Crystal Structures of S-Adenosylmethionine Synthetase with ADP, BrADP, and PPi at 28 Angstroms Resolution', *Biochemistry*, 35 (1996), 2586–96

Tcherkez G., and G.D. Farquhar, 'Carbon Isotope Effect Predictions for Enzymes Involved in the Primary Carbon Metabolism of Plant Leaves', *Functional Plant Biology*, 32 (2005), 277–91

Tcherkez G. G. B., G. D. Farquhar and T. J. Andrews, 'Despite Slow Catalysis and Confused Substrate Specificity, All Ribulose Bisphosphate Carboxylases May Be Nearly Perfectly Optimized', *Proceedings of the National Academy of Sciences*, 103 (2006), 7246–51

Tcherkez G. and M. Hodges, 'How Stable Isotopes May Help to Elucidate Primary Nitrogen Metabolism and Its Interaction with (Photo)respiration in C_3 Leaves', *Journal of Experimental Botany*, 59 (2008), 1685–93

Tenailleau E. and S. Akoka, 'Adiabatic ^{1}H Decoupling Scheme for Very Accurate Intensity Measurements in ^{13}C NMR', *Journal of Magnetic Resonance*, 185 (2007), 50–58

Tenailleau E. J., P. Lancelin, R. J. Robins and S. Akoka, 'Authentication of the Origin of Vanillin Using Quantitative Natural Abundance ^{13}C NMR', *Journal of Agricultural and Food Chemistry*, 52 (2004), 7782–87

Tenailleau E., P. Lancelin, R. J. Robins and S. Akoka, 'NMR Approach to the Quantification of Nonstatistical ^{13}C Distribution in Natural Products: Vanillin', *Analytical Chemistry*, 76 (2004), 3818–25

Thomazeau K., R. Dumas, F. Halgand, E. Forest, R. Douce and V. Biou, 'Structure of Spinach Acetohydroxyacid Isomeroreductase Complexed with Its Reaction Product Dihydroxymethylvalerate, Manganese and (Phospho)-ADP-Ribose', *Acta Crystallographica. Section D, Biological Crystallography*, 56 (2000), 389–97

Ubhi D. K. and J. D. Robertus, 'The Cobalamin-Independent Methionine Synthase Enzyme Captured in a Substrate-Induced Closed Conformation', *Journal of Molecular Biology*, 427 (2015), 901–9

'University College London - Short Lectures for NMR'

Urey H. C. and L. J. Greiff, 'Isotopic Exchange Equilibria', *Journal of the American Chemical Society*, 57 (1935), 321–27

Vogt T., 'Phenylpropanoid Biosynthesis', *Molecular Plant*, 3 (2010), 2–20

Walden R., A. Cordeiro and A. F. Tiburcio, 'Polyamines: Small Molecules Triggering Pathways in Plant Growth and Development.', *Plant Physiology*, 113 (1997), 1009–13

Wallsgrove R. M., P. J. Lea and B. J. Miflin, 'Intracellular Localization of Aspartate Kinase and the Enzymes of Threonine and Methionine Biosynthesis in Green Leaves', *PLANT PHYSIOLOGY*, 71 (1983), 780–84

Walton N. J., M. J. Mayer and A. Narbad, 'Vanillin', *Phytochemistry*, 63 (2003), 505–15

Wang J., R. M. Wolf, J. W. Caldwell, P. A. Kollman, and D. A. Case, 'Development and Testing of a General Amber Force Field', *Journal of Computational Chemistry*, 25 (2004), 1157–74

Weilacher T., G. Gleixner and H-L. Schmidt, 'Carbon Isotope Pattern in Purine Alkaloids a Key to Isotope Discriminations in C1 Compounds', *Phytochemistry*, 41 (1996), 1073–77

Weiss E., 'Transaminase Activity and Other Enzymatic Reactions Involving Pyruvate and Glutamate in Chlamydia (Psittacosis-Trachoma Group)', *Journal of Bacteriology*, 93 (1967), 177–84

Werner I., A. Bacher and W. Eisenreich, 'Retrobiosynthetic NMR Studies with ^{13}C-Labeled Glucose formation of gallic acid in plants and fungi', *Journal of Biological Chemistry*, 272 (1997), 25474–82

Werner R. A. and W. A. Brand, 'Referencing Strategies and Techniques in Stable Isotope Ratio Analysis', *Rapid Communications in Mass Spectrometry: RCM*, 15 (2001), 501–19

Whelan T., W. M. Sackett and C. R. Benedict, 'Enzymatic Fractionation of Carbon Isotopes by Phosphoenolpyruvate Carboxylase from C_4 Plants 1', *Plant Physiology*, 51 (1973), 1051–54

White J. W. C., 'Stable Hydrogen Isotope Ratios in Plants: A Review of Current Theory and Some Potential Applications', in *Stable Isotopes in Ecological Research*, ed. by P. W. Rundel, J. R. Ehleringer, and K. A. Nagy, Ecological Studies, 68 (Springer New York, 1989), pp. 142–62

Wickstrom L., A. Okur and C. Simmerling, 'Evaluating the Performance of the ff99SB Force Field Based on NMR Scalar Coupling Data', *Biophysical Journal*, 97 (2009), 853–56

Winkler F. J., 'Reaction Rates of Isotopic Molecules. Von L. Melander Und W. H. Saunders, Jr. Wiley, New York 1980. XIV, 391 S., Geb. £ 16.30', *Angewandte Chemie*, 93 (1981), 220–220

Wright A. D., J. L. Nielson, D. M. Tapiolas, C. H. Liptrot and C. A. Motti, 'A Great Barrier Reef Sinularia Sp. Yields Two New Cytotoxic Diterpenes', *Marine Drugs*, 10 (2012), 1619–30

Zarembinski T. I. and A. Theologis, 'Ethylene Biosynthesis and Action: A Case of Conservation', *Plant Molecular Biology*, 26 (1994), 1579–97

Zhang W., B. D. Ames and C. T. Walsh, 'Identification of Phenylalanine-3-Hydroxylase for Meta-Tyrosine Biosynthesis', *Biochemistry*, 50 (2011), 5401–3

8 Annexes

8.1 Tables

8.2 Figures

8.3 Scientific productions

8.3.1 Master

8.3.1.1 Publications

1. *Simultaneous determination of natural-abundance $\delta^{15}N$ values and quantities of individual amino acids in proteins from milk of lactating women and from infant hair using gas chromatography/isotope ratio mass spectrometry.*

   Illa Tea, Adrien Le Guennec, Marine Frasquet-Darrieux, Maxime Julien, Katarzyna Romek, Ingrid Antheaume, Régis Hankard and Richard J. Robins, *Rapid Commun. Mass Spectrom.,* **2013**, 27, 1345-1353

2. *Human baby hair amino acid natural-abundance ^{15}N-isotope values are not related to the ^{15}N-isotope values of amino acids in mother's breast milk protein.*

   Katarzyna. M. Romek, M. Julien, M. Frasquet-Darrieux, I. Tea, R. Hankard, R. J. Robins, ,*Amino acids,* **2013**, 45 (6), 1365-72

8.3.1.2 Posters

1. *Natural abundance ^{15}N-isotope values of human baby hair protein are not dictated by ^{15}N-isotope values of mother's breast-milk.*

   Katarzyna M. Romek, Maxime Julien, Marine Frasquet-Darrieux, Illa Tea, Ingrid Antheaume, Régis Hankard and Richard J. Robins, **2013**, June 16-21, Sopot, Poland, **ISOTOPES 2013**

Natural–abundance ^{15}N-isotope values of human baby hair protein are not dictated by ^{15}N-isotope values of mother's breast-milk[1]

Katarzyna M. Romek[1,2], Maxime Julien[2], Marine Frasquet-Darrieux[3], Illa Tea[2], Ingrid Antheaume[2], Régis Hankard[3] and Richard J. Robins[2]

1. Laboratory for Isotope Effects Studies, Department of Chemistry, Institute of Applied Radiation Chemistry, Technical University, Zeromskiego 116, 90-924 Łodź, Poland, romek.katarzyna@gmail.com
2. Elucidation of Biosynthesis by Isotopic Spectrometry Group, CEISAM, University of Nantes–CNRS UMR6230, France.
3. Inserm, CIC 0802, University of Poitiers and CHU Poitiers, PoiAtiers, F-86000, France.

Protein intake plays a key role in fetal and post-natal growth. A number of studies have shown the importance of balanced protein intake in infancy and intra-uterine growth. [2],[3] However, the present work shows ^{15}N-isotope values of human baby hair are not dictated by ^{15}N-isotope values of mother's breast-milk.

Is it the infant nitrogen metabolism dominating over nutrient source?

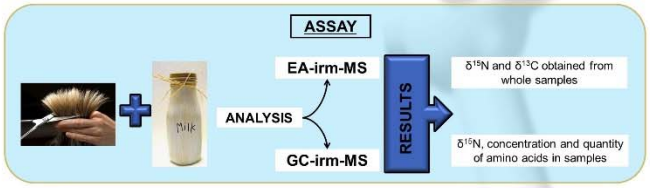

In order to relate different sets of data to a standard set of conditions, values for analytes were normalized. After first correction, further ones were applied so as to compare fully results obtained in EA-irms-MS and GC-irms-MS.

$$\delta^{15}N_{GC\text{-}Acor} = \delta^{15}N_{GC\text{-}A} + \delta^{15}N_{EA\text{-}A}$$ [1]

Comparison of $\delta^{15}N$ values obtained by EA and obtained by calculation based on the individual $\delta^{15}N$ and quantities from irm-MS; values from milk and hair the same mother-infant pairs.

This demonstrates a regular shift in the values obtained by the two different methods.

For milk, the difference (Calc $\delta^{15}N$; EA $\delta^{15}N$) = 0,95 ‰

The difference for hair (Calc $\delta^{15}N$; EA $\delta^{15}N$) = 1,29 ‰

Sample N°	MILK Calc δ15N (‰)	MILK EA δ15N (‰)	MILK D (C-E)	HAIR Calc δ15N (‰)	HAIR EA δ15N (‰)	HAIR D (C-E)	H-M DCalc δ15N (H-M) (‰)	H-M DEA δ15N (H-M) (‰)
A. Full data set for both hair and milk samples								
59	5.58	5.22	0.36	9.42	9.12	0.30	4.57	3.90
63	6.62	4.92	1.70	11.62	7.69	4.73	5.20	2.17
72	4.91	4.76	0.15	9.29	6.86	2.43	4.38	2.10
74	7.50	7.40	0.10	11.56	8.38	3.58	4.46	0.98
81	6.05	6.00	0.05	9.23	9.53	-0.30	3.18	3.54
91	7.75	4.44	3.31	9.70	9.83	-0.13	1.95	5.39
108	6.58	4.86	1.72	8.01	9.61	-1.60	1.43	4.75
N	7	7	7	7	7	7	7	7
Mean	6.43	5.37	0.95	9.92	8.63	1.29	3.50	3.26
SD	1.01	1.02	1.33	1.45	1.23	2.32	1.44	1.58
B. Partial data sets only for either hair or milk samples								
N	41	45	40	13	33	8	11	19
Mean	7.55	5.91	1.51	10.37	9.46	1.41	3.22	3.58
SD	1.25	1.09	1.16	1.39	1.05	2.18	1.36	1.15

It should also be noted that the (Hair-Milk) difference based on the Calc $\delta^{15}N$ values of 3,26 ‰ is the same...

...as that based on the EA-IRMS $\delta^{15}N$ values of 3,59 ‰.

The amino acid composition of hair and milk proteins did not account for the observed difference in isotope content.

$\delta^{15}N$ shift is consistent whether obtained by EA measurement or obtained on the basis of the individual amino acids.

2D isotope plot for $\delta^{13}C_1$ and $\delta^{15}N_t$(‰) values for total hair and milk solids. Each data point represents one mother-infant pair, analyzed by EA-irm-Ms.

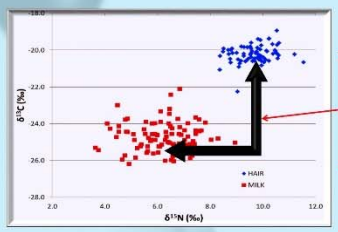

Horizontal and vertical shift between hair and milk $\delta^{15}N$ and $\delta^{13}C$ values

Isotope ratios $\delta^{15}N$ and $\delta^{13}C$ (‰) were significantly higher in infant hair than in breast milk. Likewise, $\delta^{15}N$ (‰) of amino acid fraction obtained from infant hair was also significantly higher than from maternal milk.

Low values of $\delta^{13}C$ could be explained by the high fat content in milk causing those differences. In the case of $\delta^{15}N$ values – high metabolic rate of baby and/or differences in amino acids between milk and hair could be the cause.

Number of pairs analyzed. If N < 11, then the peak area was insufficient in one or more samples

Amino acid	N [1]	R²
Ala	11	0.169
Val	10	0.301
Xle	11	0.170
Gly	11	0.009
Pro	11	0.359
Ser	7	0.266
Asx	11	0.019
Total [2]	73	0.108

Total number of mother–infant pairs analyzed for correlations of unhydrolyzed hair and milk proteins and determined by EA-irm-MS

Correlations between isotopic values of $\delta^{15}N$ (‰) for hair and milk proteins for individual amino acid in the mother-infant pairs

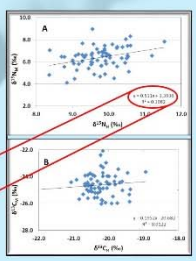

Correlation of the isotope values for the mother milk and infant hair (*A*) $\delta^{15}N$ values and (*B*) $\delta^{13}C$ values. Each data point represents one mother–infant pair, analyzed by EA-irm-MS.

Differences in global $\delta^{15}N$-isotope values tend to confirm lower level of enrichment of human milk. Existence of other nitrogenous compounds may be the major reason.

Isotope distribution in infant protein is dictated by its intrinsic nitrogen metabolism and is not determined by $\delta^{15}N$ of the amino acids provided in mother's milk. Metabolism has a much greater influence than does nurture.

References:
[1] Romek K.M., Julien M., Frasquet-Darrieux M., Tea I., Anthéaume I., Hankard R. and Robins R. J., **Natural-abundance ^{15}N-isotope values of human baby hair protein are not dictated by ^{15}N-isotope values of mother's breast-milk: infant nitrogen metabolism dominates over nutrient source. AJCN, 2013**
[2] Paolini C., Marconi A., Ronzoni S., et al. Placental transport of leucine, phenylalanine, glycine, and proline in intrauterine growth-restricted pregnancies. J Clin Endocrinol Metab. 2001;86:5427-32.
[3] Tea I, Le Gall G, Küster A, et al. ^{1}H-NMR-based metabolic profiling of maternal and umbilical cord blood indicates altered materno-foetal nutrient exchange in preterm infants. PloS One 2012;7:e29947 (12 pages)

8.3.2 PhD

8.3.2.1 Publications

1. *A retro-biosynthetic approach to the prediction of biosynthetic pathways from position-specific isotope analysis as shown for tramadol.*
   Katarzyna M. Romek, Pierrick Nun, Gérald S. Remaud, Virginie Silvestre, Germain Soitong Taïwe, Florine Lecerf-Schmidt, Ahcéne Boumendjel, Michel De Waard and Richard J. Robins, *Proceedings of the National Academy of Sciences*, **2015**, 112 (27), 8296-8301
2. *Non-statistical ^{13}C fractionation distinguishes co-incident and divergent steps in the biosynthesis of the alkaloids nicotine and tropine.*
   Katarzyna M. Romek, Gérald S. Remaud, Virginie Silvestre, Piotr Paneth and Richard J. Robins, *The Journal of Biological Chemistry*, **2016**, 291 (32), 16620-9

8.3.2.2 Oral communications

1. *Position-specific isotope analysis – a retro-biosynthetic approach to elucidate and predict biosynthetic pathways?*
   Katarzyna M. Romek, Pierrick Nun, Gérald S. Remaud, Virginie Silvestre, Germain Sotoing Taïwe, Florine Lecerf-Schmidt, Ahcène Boumendjel, Michel De Waard, Hanns-Ludwig Schmidt and Richard J. Robins, **2015**, June 21-26, Jerusalem, Israel, **ISOTOPES 2015**
2. *Isotope fractionation by methionine synthase – a cause of depletion of ^{13}C in O-methyl and N-methyl groups.*
   Katarzyna M. Romek, A. Krzemińska, A. Dybała-Defratyka, G. S. Remaud, P. Nun, M. Julien, R. Vanel, P. Paneth, R. J. Robins, **2016**, October 3-6, Nantes, France, **ISI 2016**

8.3.2.3 Posters

1. *Can site-specific ^{13}C isotope fractionation during (bio)synthesis help indicate precursor-product relationships?*
   Katarzyna M. Romek, Pierrick Nun, Gérald S. Remaud, Virginie Silvestre, Anne-Marie Brossard, Ahcéne Boumendjel, Michel De Waard and Richard Robins, **2014**, June 1-4, Manchester, United Kingdom, **EMBO Enzymes**
2. *Initial studies towards determining the origin of ^{13}C depletion in O-methyl and N-methyl groups of natural products by ^{13}C NMR spectrometry.*
   Katarzyna M. Romek, Pierrick Nun, Gérald S. Remaud, Virginie Silvestre, Piotr Paneth and Richard J. Robins, **2015**, June 21-26, Jerusalem, Israel, **ISOTOPES 2015**
3. *Intramolecular distribution of ^{13}C in amino acids measured by ^{13}C NMR spectrometry.*
   Katarzyna M. Romek, Gérald S. Remaud, Maxime Julien, Piotr Paneth and Richard J. Robins, **2016**, October 3-6, Nantes, France, **ISI 2016**

CAN SITE-SPECIFIC ^{13}C ISOTOPE FRACTIONATION DURING (BIO)SYNTHESIS HELP INDICATE PRECURSOR-PRODUCT RELATIONSHIPS?

Katarzyna M. Romek[1,2], Pierrick Nun[2], Gérald S. Remaud[2], Virginie Silvestre[2], Anne-Marie Brossard[2], Ahcène Boumendjel[3], Michel De Waard[4], Richard J. Robins[2]

1. *Laboratory of Isotope Effects Studies, Department of Chemistry, Institute of Applied Radiation Chemistry, Technical University of Lodz, Żeromskiego 116, 90-924 Łódź, Poland*
2. *Elucidation of Biosynthesis by Isotopic Spectrometry Group, CEISAM, University of Nantes CNRS UMR6230, France*
3. *University Joseph Fourier, Grenoble, CNRS UMR5063, Department of Medicinal Chemistry, Grenoble, France*
4. *Grenoble Institute of Neuroscience Unit Inserm U836, 38700 La Tronche, France*

E-mail address: katarzyna.romek@univ-nantes.fr; romek.katarzyna @gmail.com

1-4 July, Manchester

Tramadol – synthetic worldwide-prescribed analgesic drug marketed as a racemic mixture of *1R,2R* and *1S,2S* stereoisomers, because of complementation of each other's analgesic activity. Tramadol is a typical opioid because it is a serotonin-norepinephrine reuptake inhibitor. Recently, it has been discovered[1] that the tree *Nauclea latifolia* ("pin cushion"), commonly used in natural medicine pain relief, contains Tramadol in the root bark, obtained to date only by synthesis.

SAMPLE TREATMENT

- Purification – TLC, column chromatography, crystallization
- NMR tubes – 200 mg of tramadol + 600 µL acetone-d_6 + 10 µL H_2O
- EA-IRMS – 1 mg of tramadol per capsule for carbon and nitrogen analysis

A key question was whether the isolated compound was indeed natural or whether contamination of the plant sample had occurred. Amongst a number of approaches taken to verify that the isolate was of biological origin, we are using the $^{13}C/^{12}C$ and $^{15}N/^{14}N$ isotope ratios. The phenomenon of isotopic fractionation during reactions is well known as a means to characterize reaction mechanisms and has a well-proven record in distinguishing different natural sources and different synthetic origins.

Figures 3 & 4. Carbon numbering in ferulic acid (*Fig. 3*) and tramadol (*Fig. 4*)

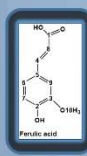

Figure 3

Figure 4

Figure 5. Potential origins of the $^{13}C/^{12}C$ ratios in natural tramadol

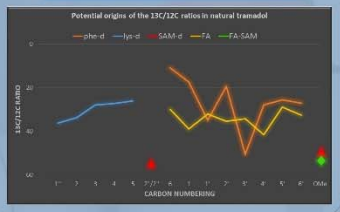

Figure 1. Commercial Tramadol ^{13}C NMR spectrum

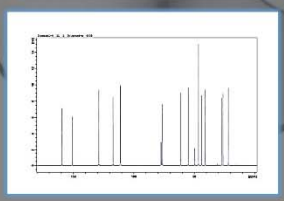

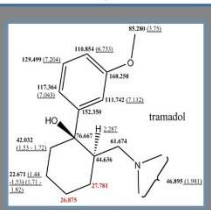

Figure 2. Assignment of peaks to the respective carbons and protons. Values for carbons marked in red indicate a problem with assignment

- significant depletion of OMe and N(Me)$_2$
- depletion of C3' – strong normal isotope effect
- C1 relatively enriched – possibly an inverse effect associated with the formation of a C–C bond
- relative depletion at C1'' and C2'' – due to the use of a more impoverished source of methylamine

Figure 6. Variation of $^{13}C/^{12}C$ ratios in natural and synthetic tramadol.

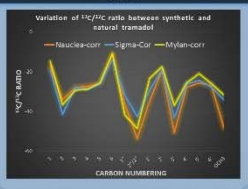

CONCLUSIONS

- Confirmation of the natural origin of tramadol in *Nauclea latifolia*
- Isotope patterns observed in synthetic tramadol can be related to the reactions involved
- Hypothetical biosynthetic pathway from the phenylalanine and lysine pathways can be proposed
- Isotope patterns observed can be related to the enzyme mechanisms proposed for key steps of the pathway

REFERENCES

1. Boumendjel A. et al. 2013 *Angewandte Chemie Int. Ed.* **52** 11780-11784
2. Gilbert A. et al. 2012 *Proc. Natl. Acad. Sci.* USA, **109** 18204-18209
3. Botosoa E. P. et al. 2009 *Anal. Biochem.* **393** 182-188
4. Silvestre V. et al. 2009 *J. Pharm. Biomed. Anal.* **50** 336-341

INITIAL STUDIES TOWARDS DETERMINING THE ORIGIN OF ^{13}C DEPLETION IN *O*-METHYL AND *N*-METHYL GROUPS OF NATURAL PRODUCTS BY ^{13}C NMR SPECTROMETRY

Katarzyna M. Romek[1,2], Pierrick Nun[2], Gérald S. Remaud[2], Virginie Silvestre[2], Piotr Paneth[1], Richard J. Robins[2]

1. *Laboratory of Isotope Effects Studies, Department of Chemistry, Institute of Applied Radiation Chemistry, Lodz University of Technology, Łódź, Poland*
2. *Elucidation of Biosynthesis by Isotopic Spectrometry Group, CEISAM, University of Nantes-CNRS UMR6230, France*

E-mail : katarzyna.romek@univ-nantes.fr; 146665@edu.p.lodz.pl

Methionine is a non-polar amino acid essential in all metozoa. With cysteine, it is one of the two sulfur-containing proteinogenic amino acids. It also plays a major role via its derivative *S*-adenosylmethionine (SAM) as a cofactor which serves as a methyl donor. Most *O*-methyl and *N*-methyl groups are derived from SAM. These methyl groups are typically relatively depleted in ^{13}C. Three steps during methionine metabolism could account for this. First, a cobalamin-independent methionine synthase catalyzes the transfer of a C1 unit from 5-methyl-tetrahydrofolate to the thiol of L-homocysteine. Second, SAM synthase couples methionine to adenine to make SAM. Finally, a range of methyl transferases transfer the methyl group to N- and O- receptors. Our aim is to define the steps introducing the relative depletion of ^{13}C in *O*-methyl and *N*-methyl groups.

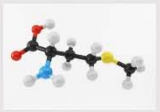

^{13}C NMR

In order to measure the ^{13}C isotope fractionation at each position in methionine, we are exploiting isotope ratio monitoring by ^{13}C NMR. This technique gives access to a quantitative measurement of $\delta^{13}C_i$ (‰).

Sample treatment

1. Derivatization with 2,2-dimethoxypropane and HCl
2. Extraction from aqueous ammonia (1M) solution with trichloroethylene
3. Drying in vaccuo

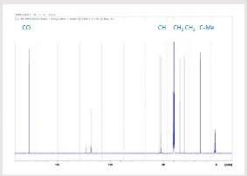

Figure 2. ^{13}C NMR spectrum for methionine methyl ester. 214 mg of D,L-methionine ester + 100 µL $Cr(Acac)_3$ + 500 µL DMSO.

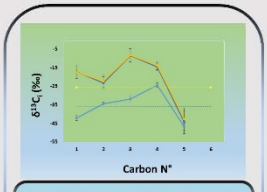

Figure 3. Distribution of $\delta^{13}C_i$ values in two commercial samples of D,L-methionine after derivatisation. Broken lines show the $\delta^{13}C_n$ values for the two samples

Bacterial fermentation

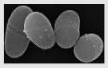

To study the ^{13}C composition of the *S*-methyl group of natural L-methionine the overproducing bacterium *Corynebacterium glutamicum* MH 20-22B/homFBR/ΔthrB is being used. This strain accumulates high levels of methionine and lysine during the fermentation of glucose [1].
Then, further micro-organisms that efficiently convert L-methionine to SAM will be used to study the activation of the methyl group donor.

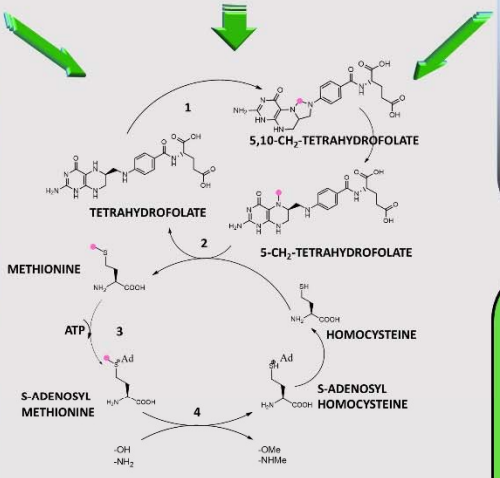

Figure 1. Simplified methionine and SAM metabolism showing the possible steps at which isotope fractionation occurs.
1 Serine hydroxymethyltransferase
2 Methionine synthase
3 *S*-Adenosyl methionine synthetase
4 Methyl transferases

Theoretical calculations

Simple theoretical models are being constructed to investigate the isotope fractionation associated with the catalytic reactions involved in methionine and SAM metabolism.
Using Gaussian, we are employing semi-empirical methods such as PM6 that should provide data to help explain the experimental data.

Figure 4. Crystal structure of the cobalamin-independent methionine synthase enzyme in a closed conformation.

Figure 5. Structure of the active sit, 10Å sphere from the Zn atom (catalyst) of homocysteine with visible folate structure.

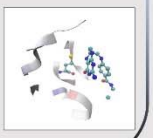

Conclusions

- Establishment of conditions for culture growth and validation of GC method for quantification.
- Establisment of derivatizatioin conditions.
- Establishment and validation of ^{13}C NMR method for commercial samples of DL-Methionine.

Perspectives

- Extention of the ^{13}C NMR of the position-specific $^{12}C/^{13}C$ ratios measurements in methionine to other amino acids.
- Establishment of adequate fermentation conditions of glucose to L-Methionine using the bacteria.
- Measurements by ^{13}C NMR a range of *O*-methyl and *N*-methyl groups of natural products.
- Calculations of the isotopic effects.

Methionine is not well-adapted to irm-^{3}C NMR due both to its insolubility and the poor resolution of the C3 and C4 positions. To overcome this we have made the methyl ester, which shows improved solubility and resolution (Fig. 2). As shown in Figure 3, L-methionine from different sources shows different position-specific ^{13}C isotope ratios.
This methodology can be applied to methionine metabolism in suitable micro-organisms over-expressing pertinent enzymes.

References:

1. Park S-D., Lee J-Y., Sim S-Y., Kim Y., Lee H-S. 2007 *Metabolic engineering* **9** 327-336
2. Ubhi D.K., Robertus J.D. 2015 *Journal of Molecular Biology* **427** 901-909

Intramolecular distribution of ^{13}C in amino acids measured by ^{13}C NMR spectrometry

Katarzyna M. Romek[1,2], Gérald S. Remaud[1], Maxime Julien[1], Piotr Paneth[2], Richard J. Robins[1]

1. *Elucidation of Biosynthesis by Isotopic Spectrometry Group, CEISAM, University of Nantes-CNRS UMR6230, France*
2. *Laboratory of Isotope Effects Studies, Department of Chemistry, Institute of Applied Radiation Chemistry, Łódź University of Technology, Łódź, Poland*

E-mail : katarzyna.romek@univ-nantes.fr; 146665@edu.p.lodz.pl

ISI NANTES 2016, *3 – 6 October 2016*, FRANCE

Although amino acids are best known as the monomer building blocks of proteins, several perform other tasks within living cells. Examples include the role of L-arginine as a precursor of polyamines and alkaloids, and L-methionine which acts as methyl group donor.
On the basis of their biosynthesis, amino acids can be classified into 5 groups taking their origin from pyruvate, oxaloacetate, 3-phosphoglycerate, shikimate and α-ketoglutarate (Fig. 1). In the case of pyruvate there are two subgroups leading to the formation of alanine, leucine and valine. We have developed a protocol to investigate their position-specific $^{13}C/^{12}C$ isotope ratios by ^{13}C NMR and investigated whether the values obtained can be related to the biosynthesis. This is illustrated for L-valine.

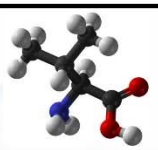

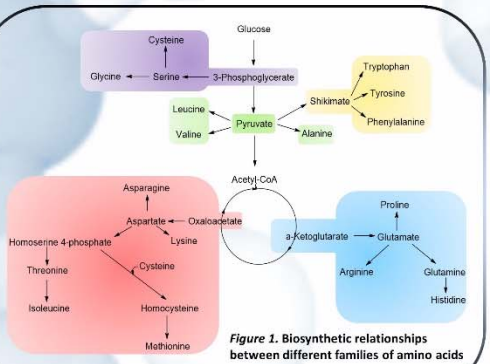

***Figure 1.* Biosynthetic relationships between different families of amino acids**

Target amino acids

Representatives of the families were selected (Fig. 2):
serine, valine, alanine, methionine, isoleucine, glutamic acid and tyrosine.
These amino acids possess a range of functional groups:
hydroxyl, amine, carboxylic acid, phenolic, *S*-methyl.

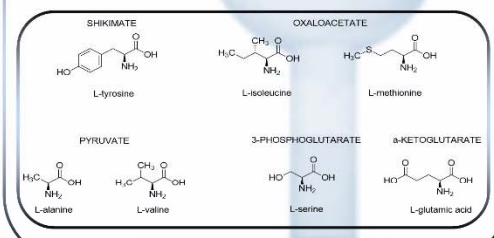

***Figure 2.* Structures of target amino acids**

Sample preparation

Amino acids are structurally not amenable to isotope ratio monitoring by ^{13}C NMR. By methylating the carboxyl function they are made less polar and more soluble in organic solvents that have good properties for NMR spectrometry.
Methylation with trimethylchlorosilane/MeOH[1] proved the most efficient approach (Fig. 3).

1. Derivatization with TMSCl/methanol
2. Washing methanol and diethyl ether (3x)
3. Drying in vaccuo

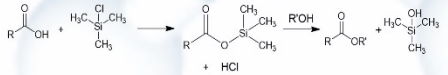

***Figure 3.* Methylation reaction scheme**

^{13}C irm-NMR measurements

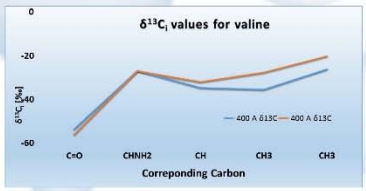

***Figure 4.* Distribution of $\delta^{13}C_i$ values in two samples of natural L-valine after derivatization.**

Biosynthesis of valine - interpretation

In the biosynthesis of valine (Fig. 5), acetohydroxy acid isomeroreductase catalyses the shift of the methyl of α-acetolactate to the adjacent carbon forming 2,3-dihydroxyisovalerate.

***Figure 5.* Scheme of the biosynthesis of valine**

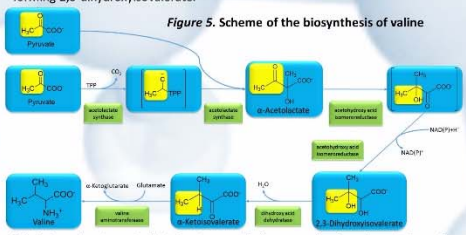

It is interesting to note that the two methyl groups of valine do not show the same $\delta^{13}C$ values (Fig. 4), one being approx. 9‰ more impoverished than the other. We suggest that this is due to fractionation in the shifted group associated with the transfer: selection being against ^{13}C.

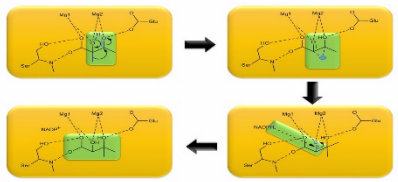

***Figure 6.* Proposed mechanism of acetohydroxy acid isomeroreductase[2]**

The mechanism of the enzyme has been carefully investigated and the implied breaking of sp^3 bond followed by the creation of an sp^3 bond would be expected to select against ^{13}C at both events (Fig. 6). This fits well with the isotopic data.

References:

1. Li J., Sha Y., 2008 *Molecules* **13** 1111-1119
2. Thomazeau K., Dumas R. 2000 *Acta Crystallographica* **56** 389-397

Acknowledgements:

K. M. Romek thanks the French Research Ministry for financial support. R. J. Robins thanks the CNRS for financial support. The authors thank Anne-Marie Schiphorst and Mathilde Grand for help with irm-MS and Virginie Silvestre for help with irm-^{13}C NMR.

8.4 Additional materials

8.4.1 NMR spectra

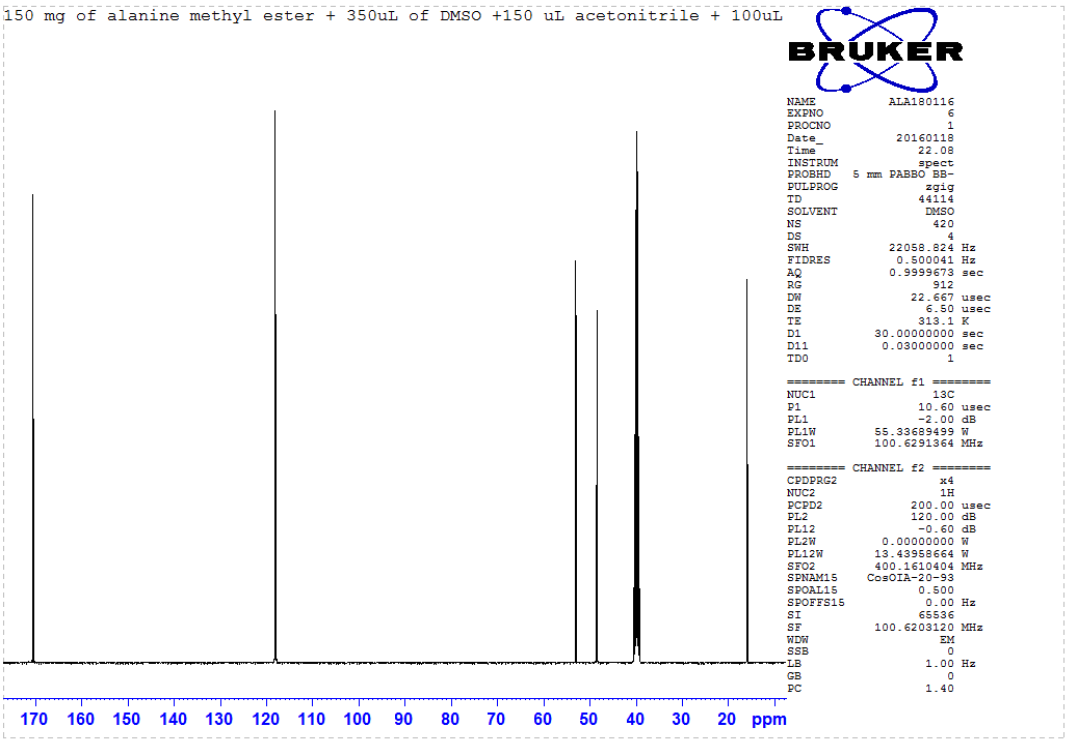

Figure 64. L-alanine irm-^{13}C NMR spectrum with acquisition conditions. Line broadening (lb) used for PERCH data treatment is equal to 1

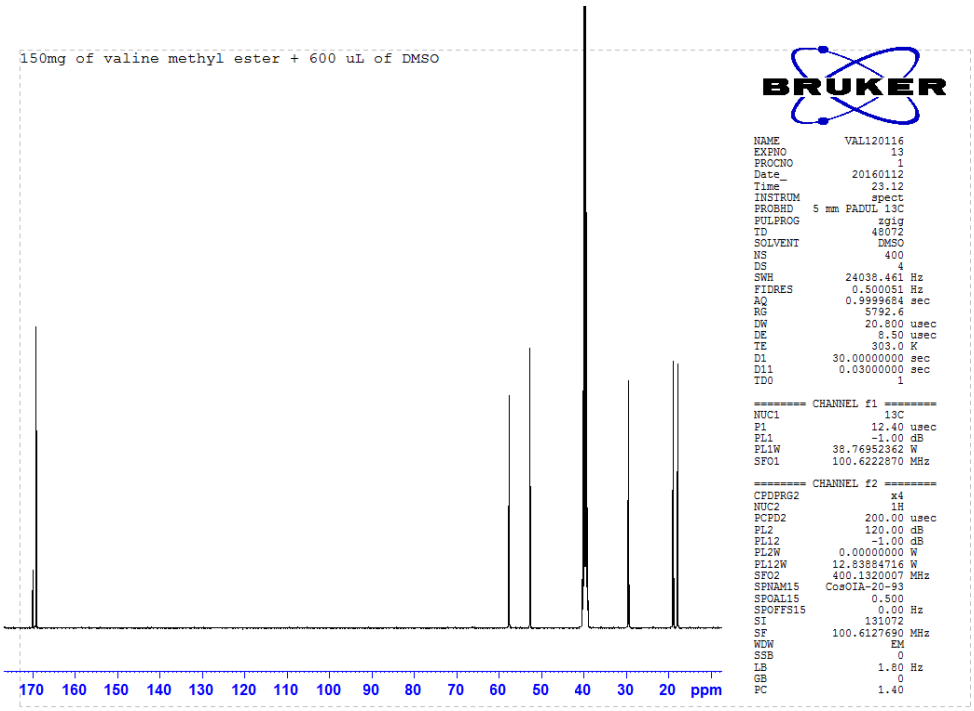

Figure 65. L-valine irm-^{13}C NMR spectrum with acquisition conditions. Line broadening (lb) used for PERCH data treatment is equal to 2

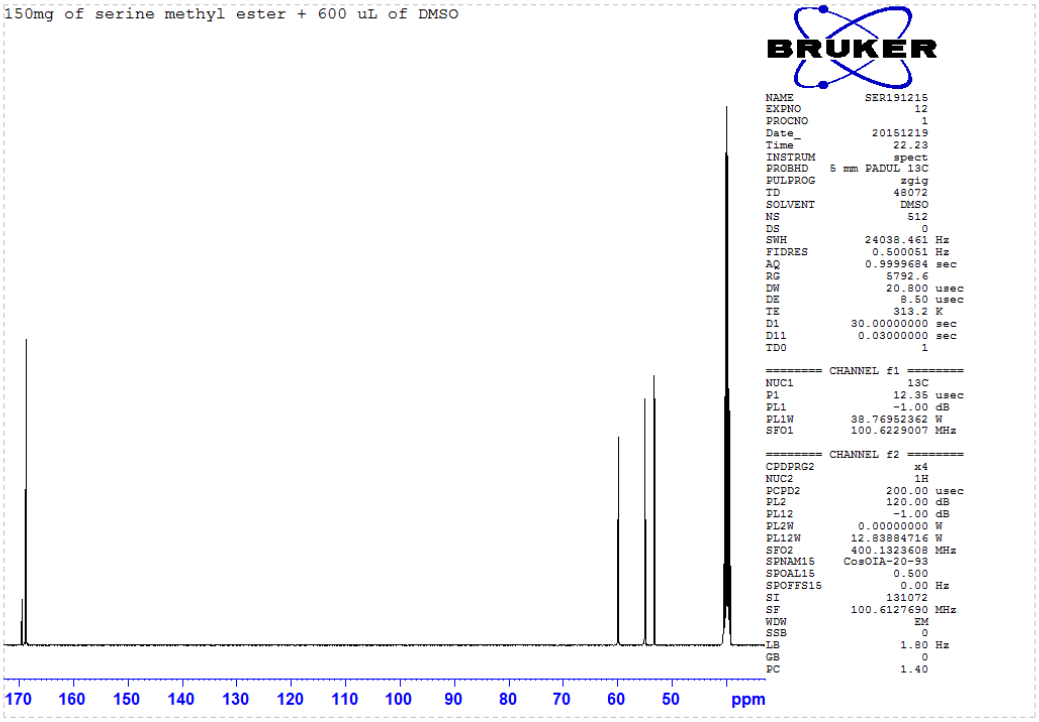

Figure 66. L-serine irm-^{13}C NMR spectrum with acquisition conditions. Line broadening (lb) used for PERCH data treatment is equal to 1.8

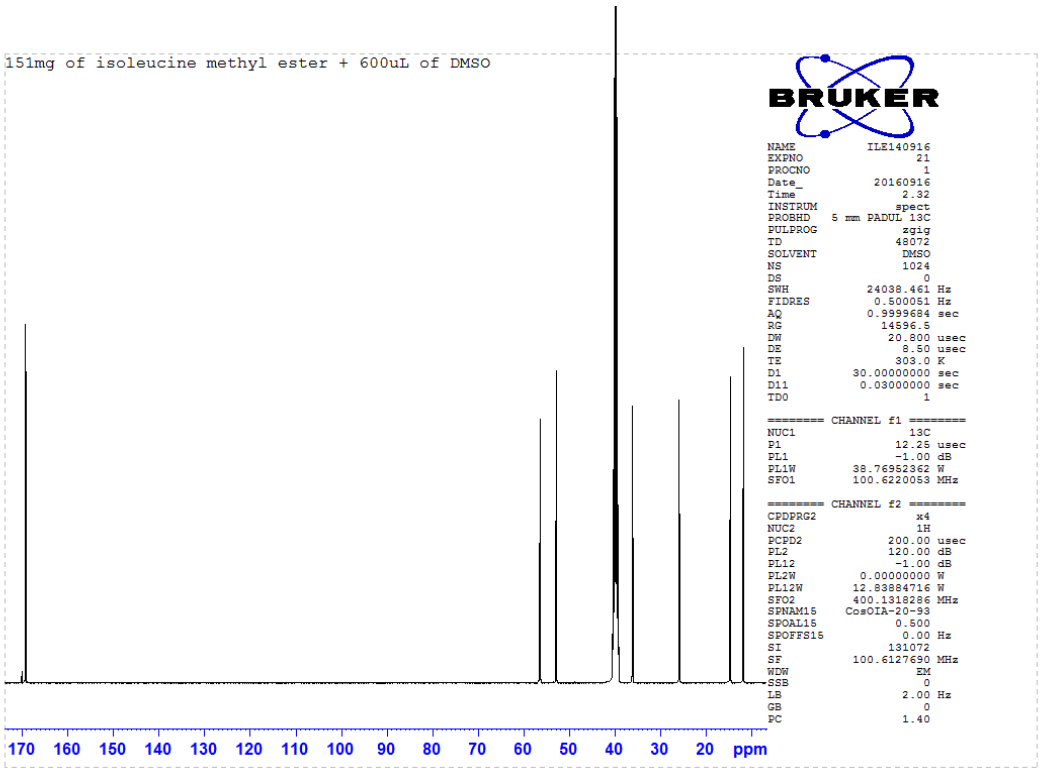

Figure 67. L-isoleucine irm-^{13}C NMR spectrum with acquisition conditions. Line broadening (lb) used for PERCH data treatment is equal to 1.2. Derivatization protocol for the sample was changed; 48h of reaction time and doubled solvent and reagent to achieve almost complete derivatization of the molecule

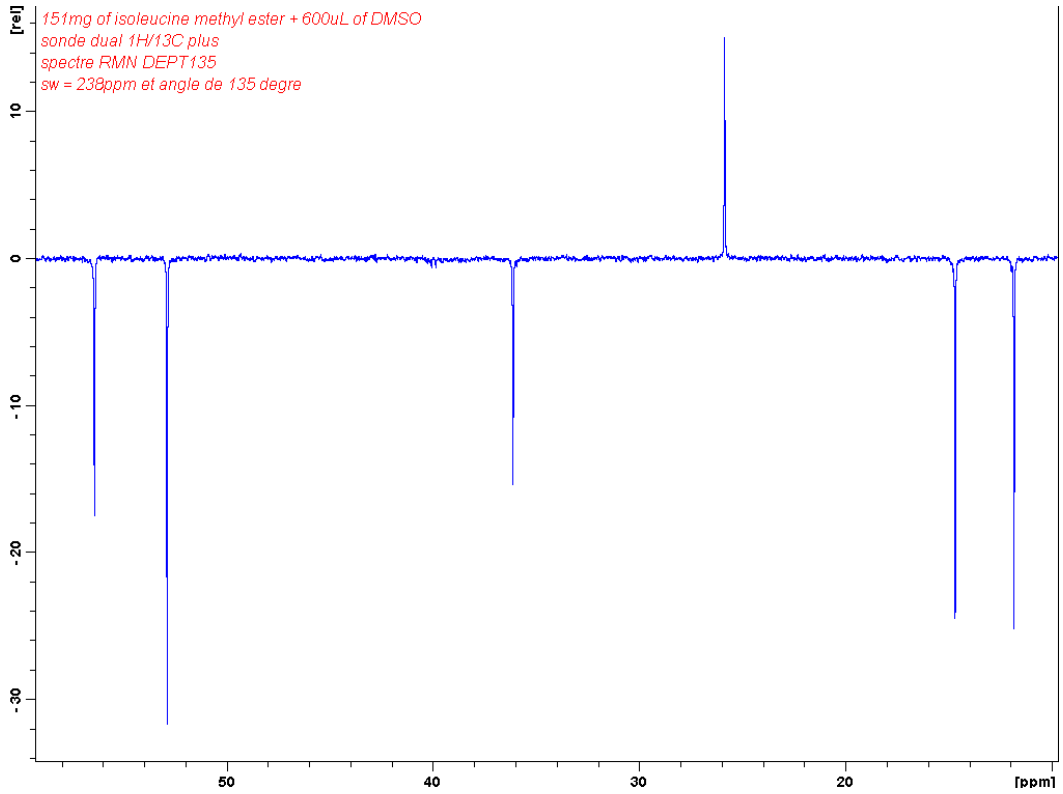

Figure 68. DEPT135 spectrum of L-isoleucine making possible the assignments for the CH_2 and CH_3 groups

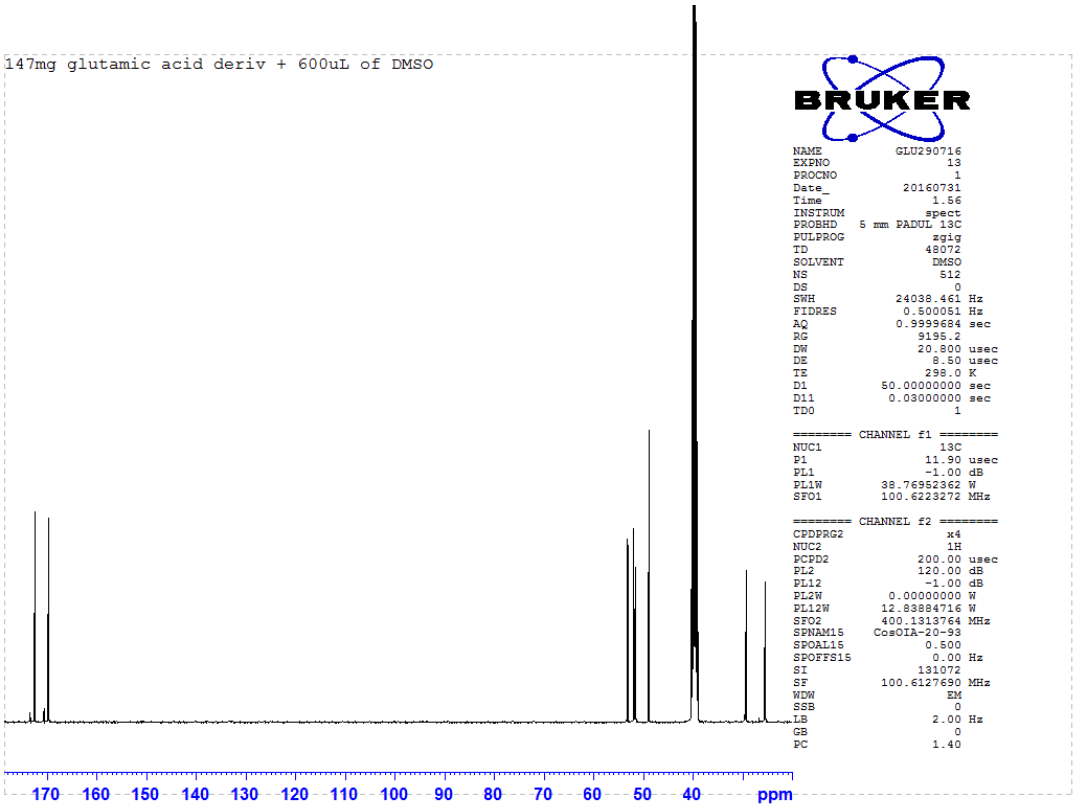

Figure 69. L-glutamic acid irm-^{13}C NMR spectrum with acquisition conditions. Line broadening (lb) used for PERCH data treatment is equal to 2

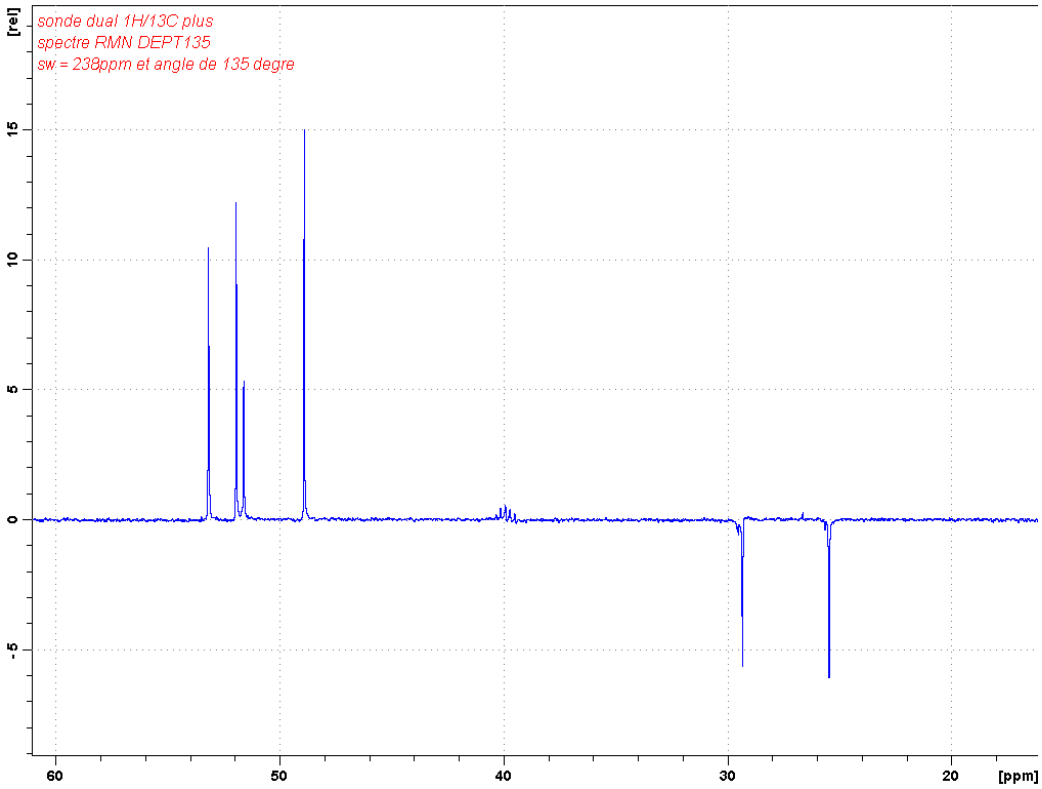

Figure 70. DEPT135 spectrum for L-glutamic acid

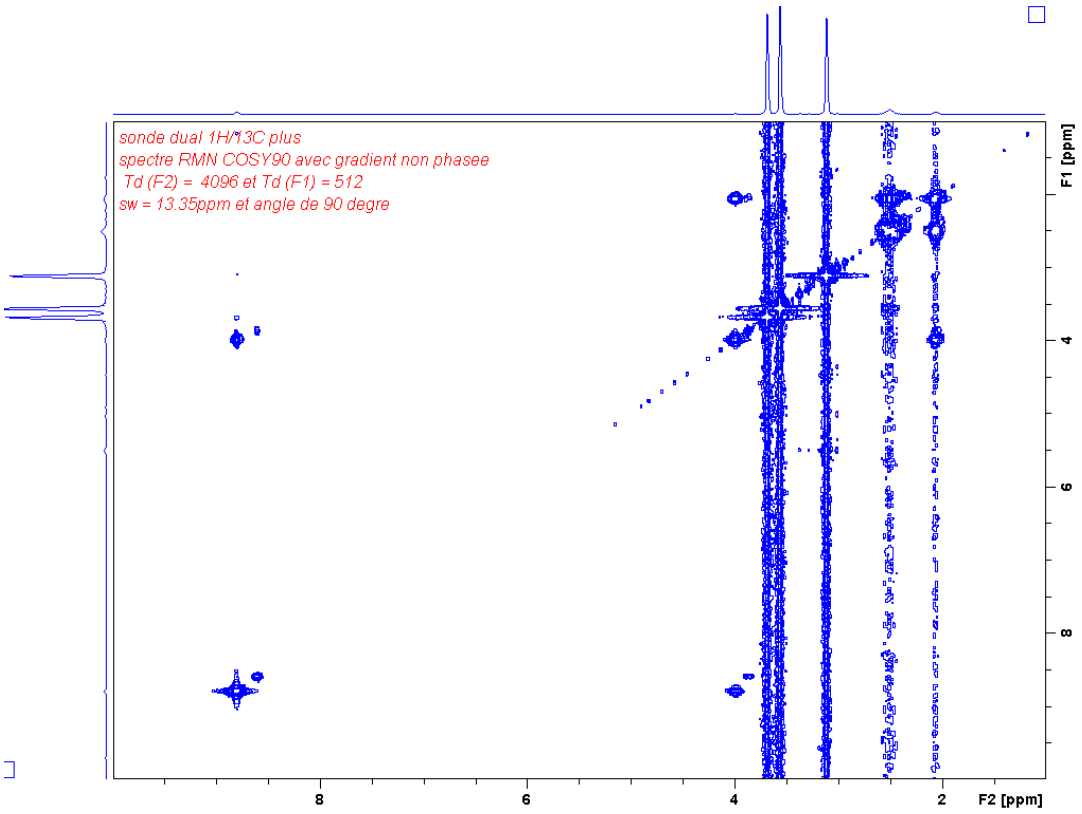

Figure 71. COSY spectrum for L-glutamic acid

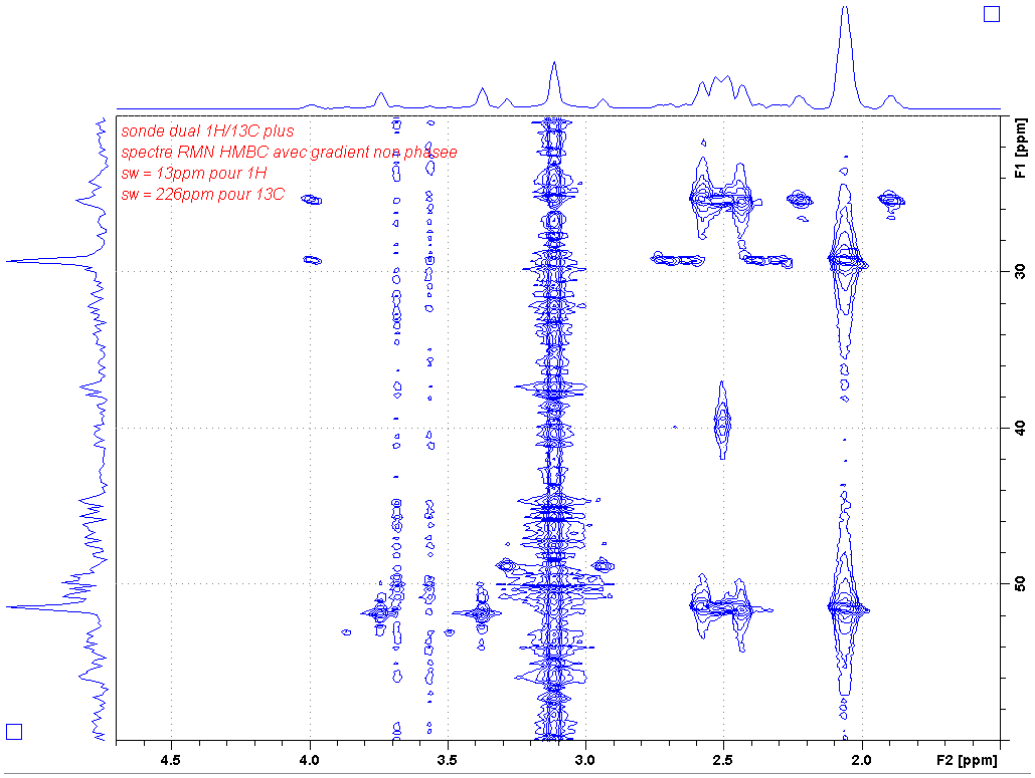

Figure 72. HMBC spectrum for L-glutamic acid

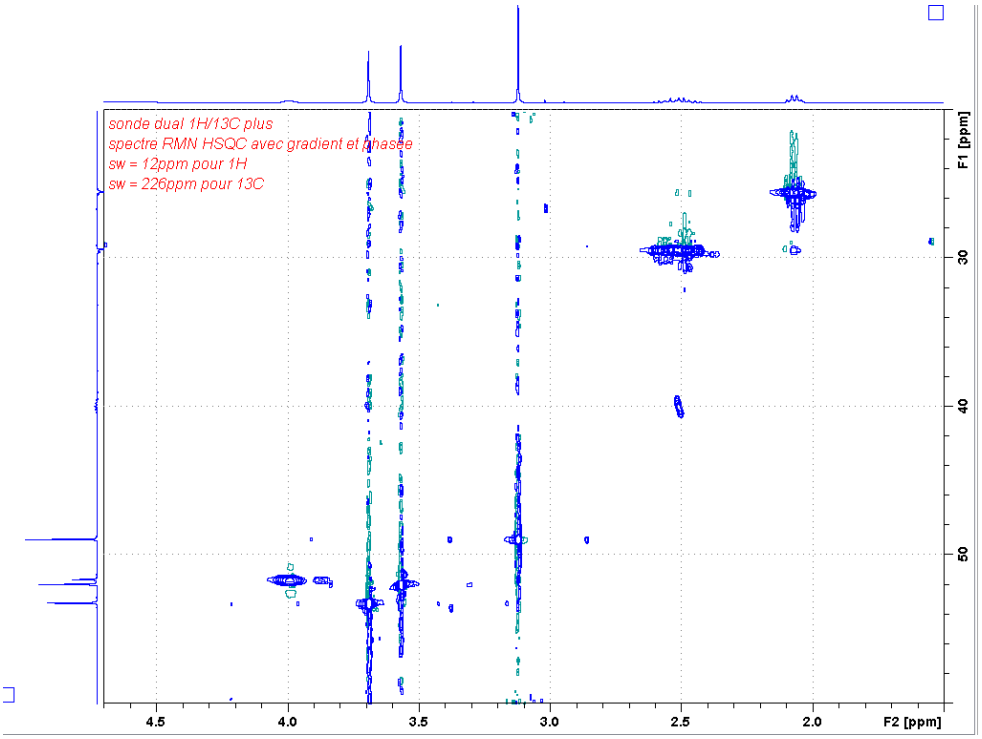

Figure 73. HSQC spectrum for L-glutamic acid

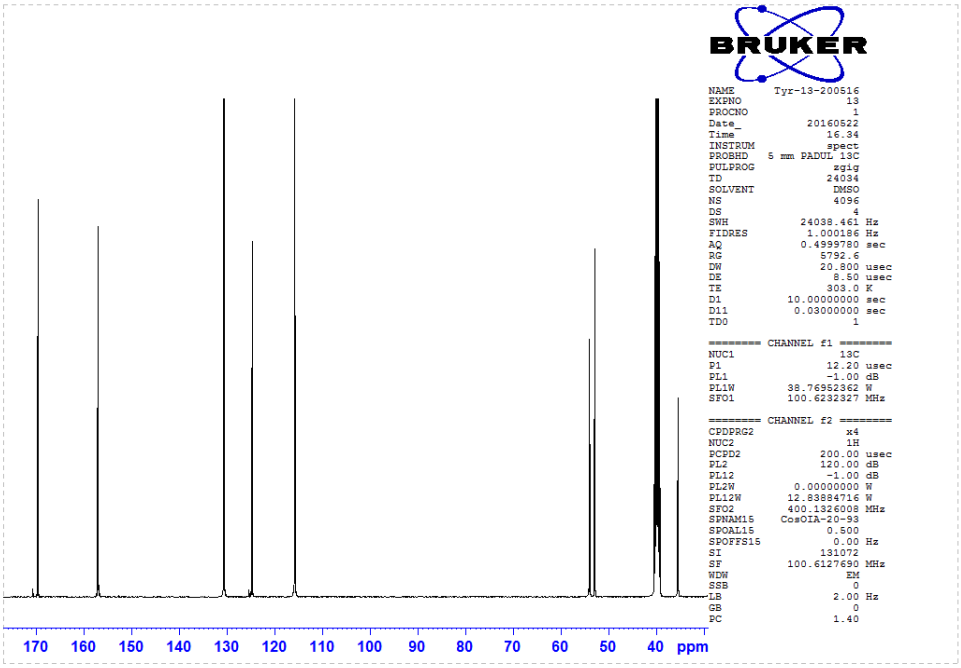

Figure 74. L-tyrosine irm-^{13}C NMR spectrum with acquisition conditions. Line broadening (lb) used for PERCH data treatment is equal to 2

8.4.2 irm-EA/MS

Table 8. $\delta^{13}C_g$ values for the amino acids used in this study obtained by irm-EA/MS

Sample name	$\delta^{13}C_g$	*mean*
Natural methionine	-34.73	-34.72
	-34.79	
	-34.66	
Commercial methionine	-25.61	-25.56
	-25.59	
L-serine	-13.45	-13.50
	-13.54	
	-13.51	
L-alanine	-22.60	-22.62
	-22.66	
	-22.61	
L-glutamic acid	-27.29	-27.25
	-27.20	
L-valine	-32.43	-32.49
	-32.41	
	-32.63	
L-tyrosine	-24.44	-24.36
	-24.28	
L-isoleucine	-13.80	-13.64
	-13.47	

8.4.3 Theoretical supplementary data

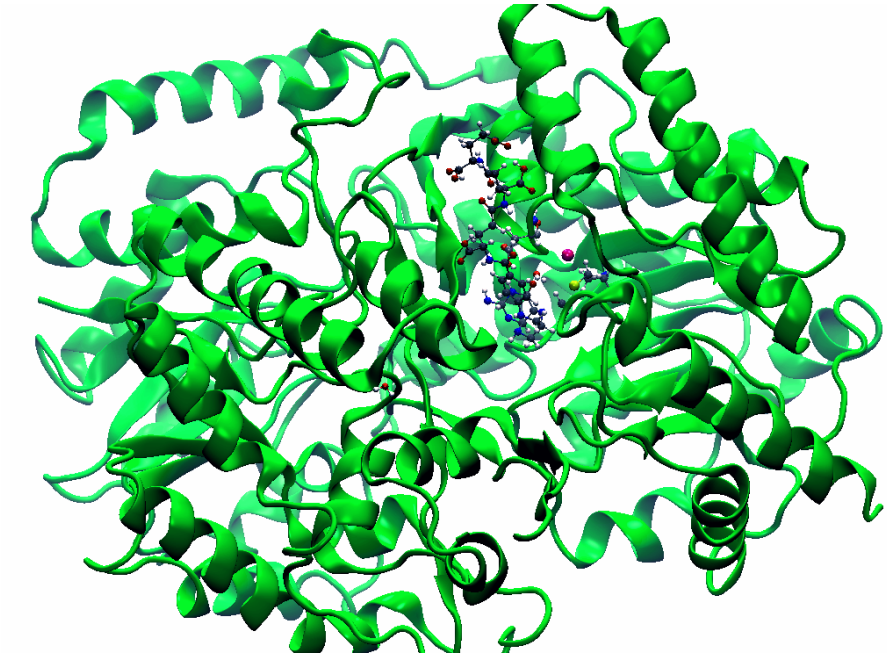

Figure 75. Cobalamin-independent methionine synthase with visible rate-limiting step in the active site of an enzyme

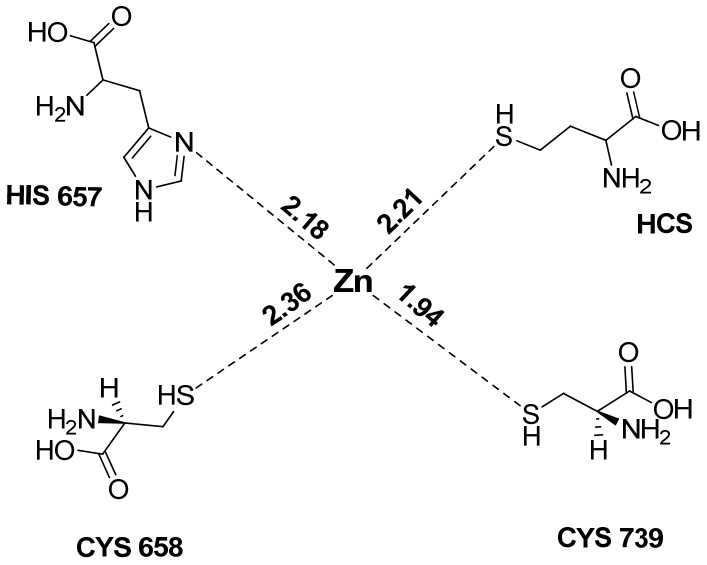

Figure 76. Zinc coordination bonds with the distances expressed in Å

Table 9. Parameters for ligands obtained by using GAFF program (as implemented in AMBER tools)

5-*N*-methyltetrahydrofolate - THF	**Zinc - Zn**
MASS BOND ANGLE n -c3-h3 49.780 109.500 same as hc-c3-n DIHE IMPROPER c3-n -c –o 10.5 180.0 2.0 General improper torsional angle (2 general atom types) c3-ca-nh-hn 1.1 180.0 2.0 Using default value c -ca-ca-ca 1.1 180.0 2.0 Using default value ca-ca-ca-ha 1.1 180.0 2.0 General improper torsional angle (2 general atom types) ca-ca-ca-nh 1.1 180.0 2.0 Using default value ca-n -c -o 10.5 180.0 2.0 General improper torsional angle (2 general atom types) NONBON	Zn coordination sphere parameters MASS Zn 65.41 BOND NB-Zn 70.0000 2.06000 ANGLE Zn-NB-CV 50.0000 126.7000 Zn-NB-CR 50.0000 126.7000 NB-Zn-NB 10.0000 110.0000 DIHE X-NB-Zn-X 1 0.0 180.000 NONBON Zn 2.20 0.200

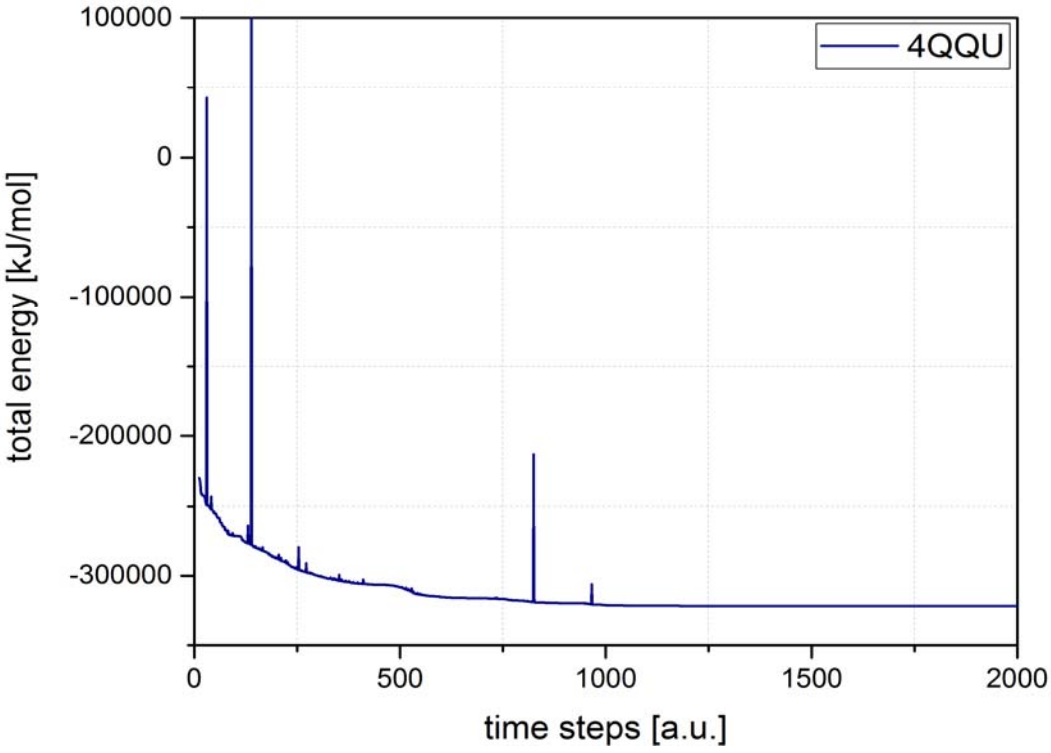

Figure 77. Energy minimization in 2000 steps

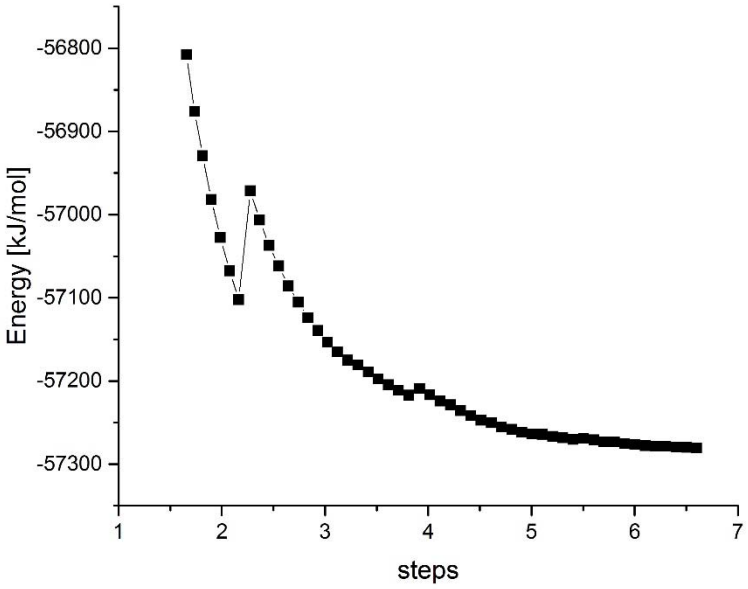

Figure 78. One-dimensional scan after dynamics for the starting structure

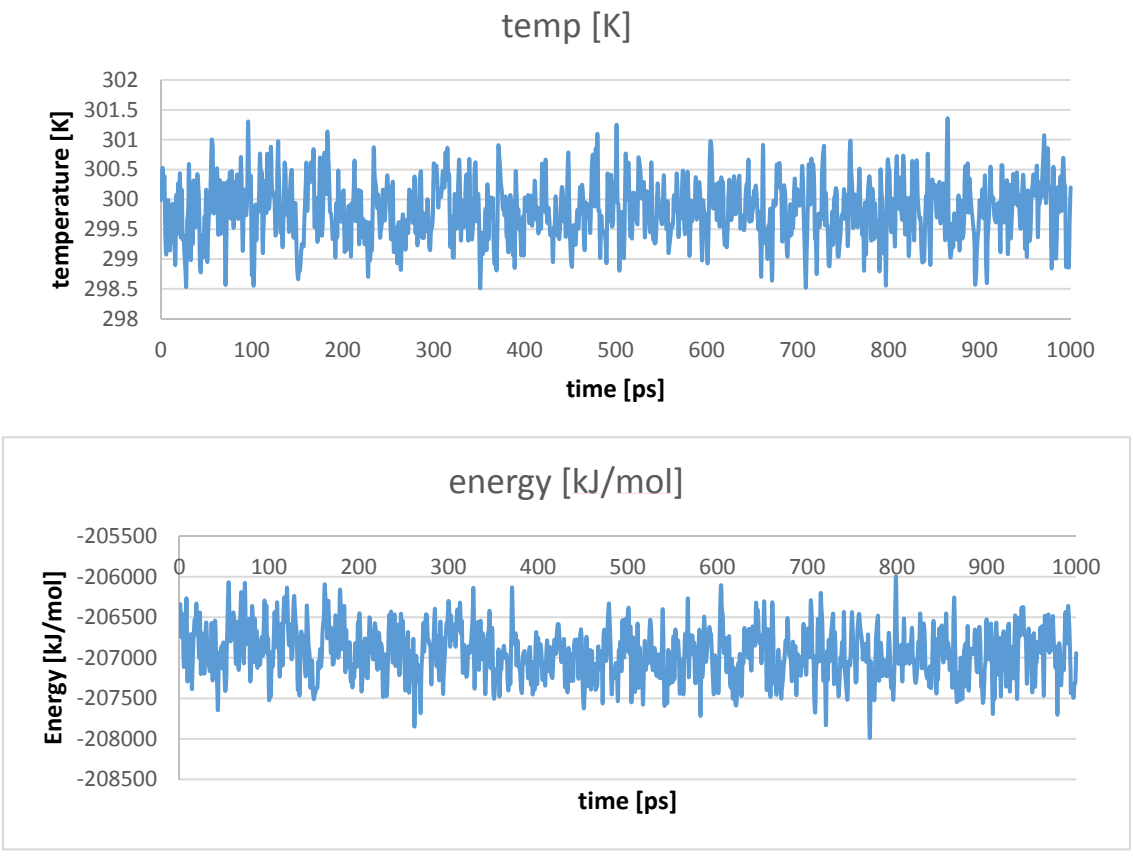

Figure 79. Energy and temperature in 1 ns. NVT MM MD 1 ns

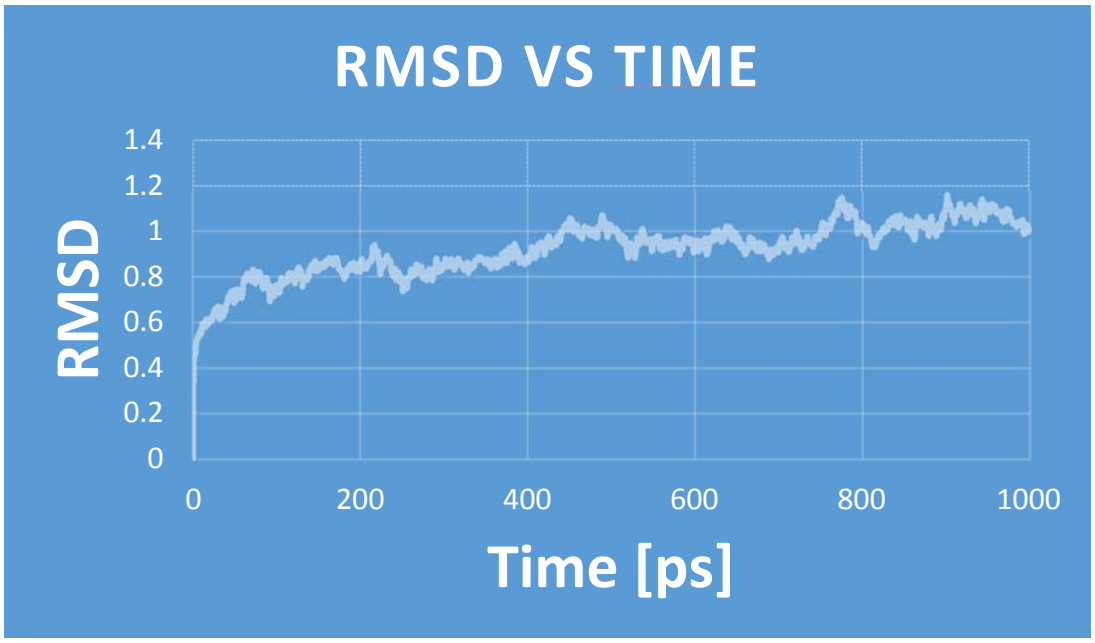

Figure 80. Root-mean-square deviation of atomic positions in 1 ns

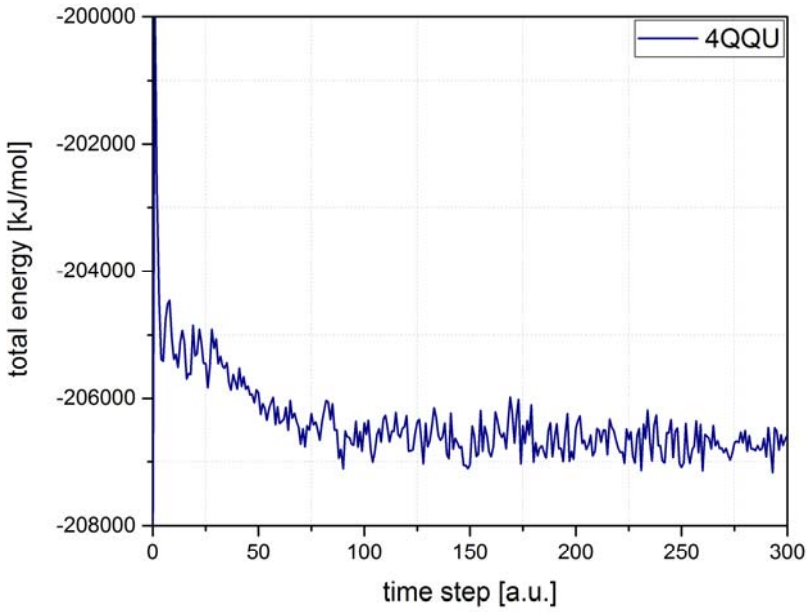

Figure 81. Energy equilibration in 300 K during 300 ps

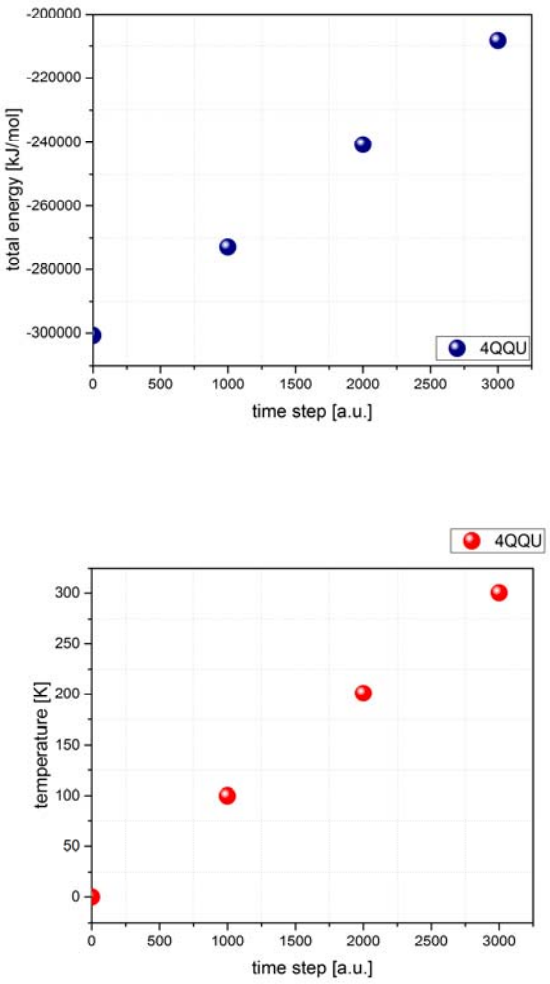

Figure 82. Heating in 3000 steps with 0.1 increment from 0 to 300K. Figure in blue shows the total energy values changes during the process and figure in red shows the temperature growth

9 Résumé en français

9.1 Contexte et Objectifs

La capacité à effectuer la surveillance du rapport isotopique par spectrométrie RMN ^{13}C (irm-^{13}C NMR) donne un accès direct à des distributions d'isotopes spécifiques positionnelles dans des molécules entières. Dans cette thèse, cette approche a été développée dans le but d'étudier les causes du fractionnement isotopique intramoléculaire dans une gamme de produits végétaux spécialisés. L'objectif principal était d'étudier si l'appauvrissement observé dans les groupes *O*-méthyle et *N*-méthyle de nombreux composés naturelles pouvait être lié à une étape du métabolisme de la méthionine. Le deuxième objectif spécifique était d'évaluer dans quelle mesure la variation isotopique intramoléculaire peut être liée à des voies biochimiques de formation de produits spécialisés.

9.1.1 Spectrométrie RMN ^{13}C pour étudier l'appauvrissement dans les groupes *O*-méthyle et *N*-méthyle

Les groupes *O*-méthyle et *N*-méthyle trouvés dans une large gamme de produits naturels proviennent de l'acide aminé, la L-méthionine, et montrent en commun un appauvrissement en ^{13}C. Nous avons donc sondé le fractionnement isotopique intramoléculaire de la L-méthionine par rapport à son rôle de donneur de groupe méthyle. L'hypothèse mise en avant est que l'appauvrissement isotopique se produit dans la formation du groupe *S*-méthyle au cours de la biosynthèse de la méthionine et est ainsi conservé dans tous les composés qui contiennent des groupes méthyle qui ont pour l'origine la méthionine.

La méthionine occupe une position centrale dans le métabolisme cellulaire, impliquée dans les processus de synthèse des protéines, le transfert du groupe méthyle par la *S*-adénosylméthionine (AdoMet), les polyamines et la synthèse d'éthylène. La synthèse des protéines, parmi ces voies, est la seule qui utilise toute la molécule de méthionine. Cependant, le métabolisme majeur de la méthionine est la synthèse de l'AdoMet: dans les plantes, environ 80% sont engagés pour des réactions de transfert de groupe méthyle dans lesquelles le groupe -CH_3 est délivré à divers accepteurs. Comme produits finaux importants, la choline et ses dérivés (ainsi que la phosphatidylcholine – le principal lipide polaire) doivent être mentionnés. Avec ces réactions, le recyclage de la fraction homocystéine (Hcy) se produit et régénère la méthionine. En bref, la *S*-adénosyl-L-homocystéine (AdoHcy) produite pendant la réaction de transfert de méthyle est convertie en Hcy via une réaction catalysée par AdoHcy hydrolase, puis la méthionine est régénérée par méthylation de Hcy.

Ainsi, la méthionine synthase sert non seulement à catalyser la dernière réaction en synthèse *de novo*, mais participe dans la régénération du groupe méthyle d'AdoMet. Dans certains tissus végétaux, l'utilisation de la fraction 4-carbone d'AdoMet pour la synthèse des polyamines et de l'éthylène est également servie par le recyclage du résidu méthylthio de la méthionine.

La méthionine synthase fabrique de la L-méthionine à partir du Hcy et du 5-méthyltétrahydrofolate (5-Me-THF) durant le cycle AdoMet et peut donc être identifiée comme l'enzyme clé de ce cycle métabolique. L'enzyme existe dans deux isoformes: une dans les plantes et les levures qui est indépendante de la cobalamine (EC 2.1.1.14), tandis que les mammifères utilisent dans le « cycle de récupération Met » une enzyme dépendante de la cobalamine (EC

2.1.1.13) génétiquement non apparentée. En dépit d'une homogénéité structurelle minimale au niveau primaire, les deux enzymes nécessitent Zn^{2+}, qui est impliqué dans la liaison de Hcy, une stratégie exploitée par un certain nombre d'enzymes impliquées dans l'alkylation des groupes thiol. La réaction, qui implique le transfert d'un groupe partant faible (le CH_3 lié au 5-N du 5-Me-THF), est complexe et, jusqu'à présent, seulement décrite en relation avec les complexes de liaison probables.

AdoMet sert alors de donneur de groupe méthyle pour une gamme de méthyl transférases. Ceux-ci forment une classe importante d'enzymes, car ils sont impliqués dans diverses voies dans le métabolisme primaire et secondaire. Le rôle de cette classe d'enzymes est de transférer des groupes méthyle à une variété de substrats cibles.

L'objectif principal était alors d'étudier si l'appauvrissement observé dans les groupes *O*-méthyle et *N*-méthyle pouvait être lié à cette étape du métabolisme de la méthionine. On a donc effectué une série d'expériences pour examiner les rapports $^{13}C/^{12}C$ du groupe *S*-méthyle dans la méthionine à partir d'un certain nombre de sources. En outre, la cause de l'appauvrissement du groupe *S*-méthyle a été étudiée par une étude théorique d'un petit modèle de la méthionine synthase indépendante de la cobalamine.

9.1.2 Spectrométrie RMN ^{13}C pour étudier le fractionnement dans les voies du métabolisme de produits spécialisés

Le deuxième objectif spécifique était d'évaluer dans quelle mesure la variation isotopique intramoléculaire peut être liée à des voies biochimiques de formation de produits spécialisés. En particulier, pour sonder l'utilisation du fractionnement isotopique intramoléculaire observé pour prédire des étapes inconnues des voies des produits spécialisés. Cet aspect a porté sur le fractionnement isotopique observé au cours des voies de biosynthèse dans les plantes d'un certain nombre d'alcaloïdes (nicotine, tropine et tramadol) qui ont certaines caractéristiques de leur biosynthèse en commun.

Il ya des milliers d'alcaloïdes différents trouvés dans les plantes, montrant une grande diversité de structures. Malgré que la plupart des alcaloïdes sont obtenus à partir de plantes, mais des alcaloïdes se produisent également dans certains organismes marins et les insectes. Tous les alcaloïdes sont des composés basiques qui contiennent un ou plusieurs atomes d'azote hétérocycliques qui, dans la plupart des cas, proviennent d'un acide aminé. En ce qui concerne leur origine biosynthétique, un grand nombre d'alcaloïdes sont dérivés partiellement d'un acide aminé plus des carbones supplémentaires provenant d'une autre source tels que les terpènes ou les aromatiques, en fonction des détails spécifiques de la structure alcaloïde. Dans de nombreux cas, ils sont obtenus à partir des acides aminés aromatiques, la tyrosine, le tryptophane ou la phénylalanine. Toutefois, les cycles aromatiques des alcaloïdes ne proviennent pas nécessairement de ces acides aminés aromatiques. Par exemple, dans l'alcaloïde du tabac, la nicotine, qui s'accumule dans des plantes telles que le tabac (*Nicotiana tabacum*), il a été montré qu'une partie de la structure provient de l'acide aspartique qui se combine avec le glycerylaldéhyde-3-phosphate dans la production d'acide nicotinique, Tandis que l'autre partie de la molécule de nicotine provient de l'acide aminé non protéique, l'ornithine.

Bien que pendant de nombreuses années, les alcaloïdes dans les plantes aient été considérés comme des déchets de métabolisme végétal, il est maintenant reconnu qu'ils ont de nombreux rôles importants, notamment comme agents chimioprotecteurs et antiherbivores dans les

plantes. L'utilisation d'alcaloïdes par les personnes remonte à plusieurs milliers d'années. Ils étaient, et sont encore, exploités pour les poisons, les stimulants, les narcotiques bien que des fins médicinales. Il y a environ 150 ans, l'intérêt s'est manifesté autour de la structure des produits naturels et beaucoup de recherches ont porté sur les alcaloïdes - ou dits «alcalins végétaux». La capacité d'isoler des échantillons analytiquement purs était une étape cruciale pour l'exploitation de composés possédant des effets biologiques. De nombreux médicaments courants - utilisés et maltraités - sont d'origine alcaloïde ou basés sur des alcaloïdes naturels. Les exemples les plus connus comprennent la caféine, la nicotine et la quinine. Des exemples plus dangereux pour la santé sont la cocaïne, la morphine et la strychnine. En général, bon nombre des alcaloïdes les plus connus sont pharmacologiquement actifs et ont des propriétés médicinales très importantes pour les humains.

9.2 Résumé des résultats et la discussion

9.2.1 Etude de l'appauvrissement en Méthionine

Des conditions appropriées ont été établies pour l'acquisition de spectres de RMN ^{13}C à partir desquels il est possible de calculer les valeurs spécifiques de $\delta^{13}C_i$ [‰] pour la L-méthionine. La plage de valeurs obtenue est de -12,6 à -48,2 ‰, avec des écarts-types acceptables pour la spectrométrie RMN-^{13}C (~1 ‰, plage de 0,7 à 2,7 ‰). Ces valeurs de $\delta^{13}C_i$ [‰] se situent dans la gamme des produits naturels.

Qu'est-ce que la distribution spécifique de position du ^{13}C dans la L-méthionine naturelle nous parle de l'origine de l'appauvrissement du ^{13}C ? La caractéristique la plus frappante de la distribution est la mesure dans laquelle le groupe *S*-méthyle est épuisé par rapport aux autres atomes de carbone dans la molécule. Les atomes de carbone dérivés de L-Hcy ont une moyenne $\delta^{13}C$ de -22 ‰, tandis que le groupe méthyle à -41 ‰ est appauvri 19 ‰ par rapport à ces autres positions. Par conséquent, il est évident que le carbone *S*-méthyle est fortement appauvri en L-Met. Cela implique que le phénomène général d'appauvrissement en atomes de carbone dérivé de ce S-méthyle peut être essentiellement expliqué par la sélection contre ^{13}C au niveau de la biosynthèse de L-Met. Le codicille qui doit être ajouté est celui de la situation improbable dans laquelle des effets à la fois forts et inverses sont manifestes dans les réactions ultérieures.

Dans la première de ces réactions, la synthèse d'AdoMet par l'enzyme ATP: L-méthionine *S*-adénosyltransférase, EC 2.5.1.6), la chaîne polyphosphate entière de MgATP est remplacée par la L-méthionine, avec formation concomitante d'un sulfonium. Bien que cette réaction montre un KIE de ^{14}C normal fort de 1,128 ± 0,003 (équivalent à un effet de 1,08 pour ^{13}C) au niveau du carbone 5' de l'unité ribosylique de l'ATP, on n'a pas observé de KIE de ^{35}S. De plus, aucun KIE secondaire ^{3}H significatif n'a été trouvé sur le *S*-méthyle (1,009 ± 0,008), ce qui indique que le groupe *S*-méthyle ne subit aucun fractionnement isotopique associé à cette réaction.

L'étape suivante, le transfert du groupe méthyle de l'ion sulphinium n'a pas été largement étudié du point de vue isotopique. Dans une étude du KIE de ^{13}C dans la méthylation du substrat non naturel 3,4-dihydroxyacétophénone à partir de l'AdoMet catalysé par la catéchol *O*-méthyltransférase de foie de rat, lorsque le ^{13}C était présent dans le groupe *S*-méthyle, un KIE de ^{13}C normal de 1,09 ± 0,05 ont été trouvé. Cela indique qu'un appauvrissement supplémentaire se produit probablement à ce deuxième transfert de méthyle et que le transfert de méthyle est

l'étape de limitation cinétique de la voie de réaction. De plus, ces auteurs concluent que l'état de transition a une structure serrée, le groupe méthyle étant symétriquement situé entre le donneur d'atome de soufre et le récepteur d'atome d'oxygène, compatible avec la valeur élevée (proche du maximum) du KIE de ^{13}C déterminée. Ces calculs ont montré une barrière énergétique élevée pour le transfert de groupe méthyle et un important effet isotopique cinétique de ^{13}C.

Deux points intéressants sont vus. Tout d'abord, on observe un KIE de ^{34}S négligeable pour l'atome de soufre de l'homocystéine (0,998), ce qui indique que ni la fission de la liaison S-H ni la formation de la liaison S-CH_3 n'influence la vitesse de la réaction. Deuxièmement, on calcule des effets isotopiques normaux forts pour le carbone du groupe méthyle (1,087) et l'azote (1,028) du 5-*N*-méthyltétrahydrofolate, ce qui indique que la rupture de cette liaison est l'événement clé dans le mécanisme réactionnel.

Un bon accord est trouvé entre les valeurs expérimentales pour KIE pour le groupe méthyle de transfert dans la formation de méthionine et le KIE prédit sur la base d'un traitement théorique de l'enzyme. Tout d'abord, on peut conclure que les calculs théoriques servent de résultats complémentaires aux données expérimentales obtenues par RMN de ^{13}C. Ensemble, ces données et calculs corroborent fortement l'hypothèse selon laquelle l'appauvrissement observé dans les groupes méthyle des produits naturels peut être attribué à la formation de la méthionine par l'enzyme méthionine synthase. Cependant, il reste à montrer dans quelle mesure une sélection supplémentaire contre ^{13}C a lieu dans les *O*- et *N*-méthyltransférases individuelles.

9.2.2 Etude du fractionnement isotopique au cours de la biosynthèse des acides aminés

La technique développée pour la méthionine a été appliquée à un certain nombre d'autres acides aminés. La compréhension des causes du fractionnement isotopique intramoléculaire au cours des processus globaux de métabolisme des acides aminés est utile pour l'élucidation des voies biosynthétiques dans les plantes. Plusieurs études se sont concentrées sur la distribution de ^{13}C dans les acides aminés obtenus à partir d'organismes photosynthétiques. Dès 1961, il a été trouvé que les acides aminés dans les protéines des microalgues photosynthétiques possédaient une gamme de valeurs de $\delta^{13}C_g$ [‰]. Depuis lors, des données similaires ont été obtenues pour les plantes supérieures, y compris une indication claire que le fractionnement dans les plantes C_3 et C_4 n'est pas le même. On a également observé une variation spécifique des tissus au sein d'une plante, et également qu'elle diffère entre les feuilles et les graines d'une même plante. La variation de $\delta^{13}C_g$ [‰] dans un acide aminé donné est étonnamment indépendante de la saison et dans cette étude, les auteurs ont pu montrer que les valeurs de $\delta^{13}C_g$ des acides aminés provenant de la protéine foliaire pouvaient dans une certaine mesure être liées à leur biosynthèse et à leur métabolisme. Il a été conclu que les valeurs de $\delta^{13}C_g$ sont influencées dans une plus grande mesure par le partage différentiel du flux métabolique à des points de ramification que le fractionnement en lui-même associé à la biosynthèse de novo.

Un bon exemple en est les données obtenues pour l'acide aminé L-tyrosine. Ici, un excellent accord de la disposition positionnelle en ^{13}C est observé avec le phénylpropanoïde, acide ferulique. Ces deux composés ont la même origine, la voie shikimate, et clairement le motif fondamental établi lors de la formation du chorismate est retenu dans ces différents composés dérivés de cette origine commune.

9.2.3 Etude du fractionnement isotopique au cours de la biosynthèse des alcaloïdes

On a montré que la technique de spectrométrie RMN de ^{13}C permet d'obtenir des informations générales de base sur la façon dont le ^{13}C est fractionné pendant des voies de biosynthèse pour une gamme de composés naturels et synthétiques. Il est désormais clair que le fractionnement isotopique intramoléculaire par position spécifique peut donner un aperçu des voies métaboliques, et que des caractéristiques communes du métabolisme peuvent être identifiées et décrites. Il est démontré au cours de ce projet et présenté dans cette thèse qu'il est possible d'obtenir des indices quant à la biochimie probable en interprétant le fractionnement isotopique intramoléculaire observé par rapport aux effets isotopiques connus, même lorsque la biochimie de la voie est inconnue. Cette technique de « rétro-biosynthèse » s'est avérée capable de donner des indications quant à un mécanisme de réaction possible pour des étapes non définies dans la biosynthèse de la nicotine, et d'indiquer une voie probable pour l'alcaloïde tramadol.

Dans le cas de la nicotine, la réaction par laquelle le sel de *N*-méthyl-Δ^1-pyrrolinium est condensé avec l'unité dérivée de l'acide nicotinique a résisté à un certain nombre de tentatives de caractérisation, malgré son rôle central dans la voie. Dans cette réaction, « nicotine synthase », une condensation décarboxylative stéréospécifique se produit. Une activité extrêmement faible de cette enzyme a été signalée, mais d'autres auteurs n'ont pas pu répéter cette découverte. Bien qu'il ait été suggéré que cela est éventuellement catalysé par une enzyme du type berbérine-pont, aucun détail de la nature de cette enzyme clé ni de son mécanisme n'est disponible. Cependant, certaines indications quant au mécanisme peuvent être obtenues à partir de la disposition isotopique observée.

Comme le précurseur, *N*-méthyl-Δ^1-pyrrolinium, est une molécule symétrique, l'une ou l'autre des positions en α de l'azote pourrait réagir. Cependant, les valeurs observées aux C2' et C5' de la nicotine ne sont pas équivalentes: le C2', le carbone auquel la liaison C-C avec la fraction nicotinée est faite, se trouve être ~4‰ enrichi par rapport à la C5'. Il est proposé que cette différence observée soit due à un KIE inverse de ^{13}C associé au mécanisme de la réaction de le « nicotine synthétase », pour laquelle le mécanisme de réaction n'est pas connu. Cependant, certaines suggestions peuvent être faites sur la base du fractionnement isotopique, d'où le KIE intrinsèque de la réaction. Il est proposé que le C2' subisse un changement d'état à partir d'une nature semi-aromatique avec des électrons délocalisés en carbone aliphatique tertiaire. Nos données indiquent que cette réaction favorise le $^{13}C{=}N^+$ sur le $^{12}C{=}N^+$, comme connu pour les transformations $sp^2 \rightarrow sp^3$. Un tel KIE conduira à un enrichissement relatif dans la position devenant le C2' et un appauvrissement relatif équivalent dans le C5'. En outre, la position C3, l'autre atome impliqué dans la nouvelle formation de liaison est fortement appauvri, ce qui indiquerait une sélection contre ^{13}C à cette position, compatible avec un mécanisme dans lequel le C3 subit une conversion $sp^3 \rightarrow sp^2$ avec limitation cinétique.

L'autre exemple est le tramadol. L'extraction du tramadol à partir des racines de *Nauclea latifolia* a suscité un grand intérêt dans le monde entier. C'était la première fois qu'une drogue synthétique largement commercialisée était considérée comme un produit apparemment naturel à forte abondance. Le 2-[(diméthylamino) méthyl]-1-(3-méthoxyphényl) cyclohexanol, commercialisé sous plusieurs noms y compris « Tramadol », a été synthétisé pour la première fois en 1967 par Grunenthal G.m.b.H. en Allemagne. Il a breveté la synthèse des 1-(*m*-substitué phé-

nyle)-2-aminométhylcyclohexanols, qui sont utiles comme médicaments analgésiques. Il a suscité un grand intérêt, car la plupart des produits pharmaceutiques opioïdes couramment connus (comme la morphine) présentent un risque élevé d'effets secondaires potentiellement dangereux, y compris la dépendance à ces substances. Même si le tramadol ne présente ni un degré élevé de tolérance ni de toxicomanie, il est encore considéré comme plus sûr que les autres alcaloïdes de la morphine.

Comme une approche classique exploitante un marquage en isotope pour étudier ses précurseurs biosynthétiques probables ainsi de caractériser les étapes enzymatiques et les métabolites intermédiaires n'est pas actuellement réalisable, la proposition du concept de « rétrobiosynthèse » en examinant la distribution isotopique positionnelle spécifique dans la molécule a été avancée. Interpréter les données obtenues en termes de procédés biochimiques connus des plantes peut aider identifier les étapes présentes dans la biosynthèse du tramadol. Il est prouvé que le schéma des valeurs de $\delta^{13}C_i$ obtenues par RMN de ^{13}C peut être utilisé pour différencier entre des schémas biosynthétiques putatifs. En travaillant à partir d'un schéma de biosynthèse plausible, la distribution isotopique spécifique de la position fournit des preuves cruciales qui soutiennent la biochimie proposée, tout en laissant inévitablement quelques questions sans réponse. Un examen attentif des valeurs de $\delta^{13}C_i$ met en évidence des différences de position significatives qui peuvent en grande partie être interprétées rationnellement en termes de réactions biochimiques connues. Les preuves convaincantes présentées par les groupes méthyle, qui montrent des valeurs de $\delta^{13}C_i$ apparentées, sont particulièrement intéressantes, comme on peut s'y attendre pour les groupes méthyle introduits à partir de l'AdoMet. En outre, les données isotopiques indiquent fortement qu'une voie de L-Lys via L-2-amino-adipic-6-semialdéhyde et la voie d'acides aminés aromatiques est crédible et qu'une origine pour le cycle aromatique à partir d'acétyl-CoA n'est pas.

9.3 Conclusions et Perspectives

La technique de la spectrométrie RMN de ^{13}C s'est révélée être apte à obtenir des informations générales de base sur la façon dont le ^{13}C est fractionné pendant les voies de biosynthèse pour une gamme de composés naturels et synthétiques. Il est désormais clair que le fractionnement isotopique intramoléculaire par position spécifique peut donner un aperçu des voies métaboliques et des caractéristiques communes du métabolisme peuvent être identifiées et décrites. Un bon exemple en est les données obtenues pour l'acide aminé L-tyrosine. Ici, une bonne concordance de la répartition positionnelle de ^{13}C spécifique est observée avec l'acide férulique. Ces deux composés ont la même origine, la voie shikimate, et clairement le motif fondamental établi lors de la formation du chorismate est retenu dans ces différents composés dérivés de cette origine commune.

Egalement, au cours de ce projet et présentées dans cette thèse il est prouvé que les données obtenues en ^{13}C spécifique peuvent servir comme indices à la biochimie probable en interprétant le fractionnement isotopique intramoléculaire observé par rapport aux effets isotopiques connus, même lorsque la biochimie de la voie est inconnue. Cette technique de «rétrobiosynthèse» s'est avérée capable d'indiquer une voie probable pour l'alcaloïde du tramadol et de donner des indications quant à un mécanisme de réaction possible pour des étapes non définies de la biosynthèse de la nicotine.

Ces aspects sont à poursuivre pour d'autres molécules d'intérêt. Une étude plus profonde sur les acides aminés sera très souhaitable.

La technique de la RMN de ^{13}C est bien établie comme une méthode puissante pour distinguer les produits chimiques d'origines différentes. Dans cette thèse, je n'ai pas mis l'accent sur cet aspect de l'application de cette technique, puisque l'objectif principal était d'appliquer la méthode pour étudier les causes du fractionnement isotopique. Cependant, une petite étude a été faite sur la nicotine. Cet exemple montre les difficultés inhérentes à l'étiquetage des composés comme «synthétiques» ou «naturels» et nous amène à remettre en question l'étiquetage de certains d'entre eux. Ceci est évidemment le cas de la *S*-nicotine, pour laquelle un échantillon étiqueté « synthétique » montre une correspondance étroite avec des échantillons naturels authentifiés mais est très éloigné d'un échantillon de la *R, S*-nicotine fabriqué en laboratoire. Ajoutez à cela que la préparation de la *S*-nicotine par synthèse est laborieuse et prend beaucoup de temps, alors que la purification de la *S*-nicotine de la plante *Nicotiana tabacum* est relativement peu coûteuse et directe, il semble improbable que cet échantillon soit fait par synthèse.

Pourquoi est-il donc étiqueté comme «synthétique»? Il me semblerait que ce soit un exemple de cas où le fournisseur est obligé ainsi nommer des composés parce que le procédé utilisé pour les fabriquer impliquait un ou plusieurs traitements chimiques exigeant que l'étiquetage ne soit pas «naturel». Néanmoins, dans ce cas, on peut raisonnablement proposer que le composé soit, à tous intenses et à des fins, extrait d'une plante.

Une situation similaire peut également exister avec les acides aminés de différentes origines examinés par irm-^{13}C-RMN, bien que le nombre d'analyses effectuées jusqu'ici soit insuffisant pour tirer des conclusions spécifiques. Par exemple, la L-alanine étudiée présente un profil compatible avec celui-ci étant d'origine naturelle, bien qu'elle soit marquée comme "synthétique".

Ce paradoxe est à poursuivre dans les études ultérieures.

UNIVERSITE BRETAGNE LOIRE

Politechnika Łódzka

UNIVERSITÉ DE NANTES

Thèse de Doctorat

Katarzyna M. ROMEK

Des études de fractionnement isotopique ^{13}C pendant la biotransformation et dans les réactions enzymatiques

Studies of isotopic fractionation of ^{13}C during biotransformation and in enzymatic reactions

Résumé

La capacité de mesurer les rapports isotopiques par spectroscopie RMN du ^{13}C (irm-^{13}C NMR) donne un accès direct à la distribution d'isotopes possédant une position spécifique au sein de molécules. Dans cette thèse, cette approche a été développée dans le but d'élucider le fractionnement isotopique au cours de la biosynthèse dans des plantes de différents alcaloïdes (nicotine, tropine, tramadol) qui ont certaines caractéristiques communes lors de leurs biosynthèses.

L'une des caractéristiques clés de ces composés est la présence de groupes *O*-méthyle et/ou *N*-méthyle. En général, le rapport $^{13}C/^{12}C$ dans les groupes *O*-méthyle et *N*-méthyle de produits naturels est exceptionnellement faible comparé aux autres carbones dans la molécule, ces travaux ont été axés sur l'explication de ce phénomène.

La grande majorité de ces groupes méthyles dans les produits naturels proviennent du transfert d'un groupe *S*-méthyle de L-méthionine (L-Met) *via* la S-adénosylméthionine (AdoMet). Il a été prouvé par irm-^{13}C NMR que, dans la molécule donneuse, L-Met, le groupe *S*-méthyle est appauvrit. La cause de ce phénomène a été explorée par le biais de l'étude de petit modèle théorique pour la cobalamin-independent méthionine synthase, l'enzyme responsable du transfert du groupement méthyle durant la biosynthèse de L-met. Ces calculs ont montré une barrière d'énergie élevée pour le transfert du groupe méthyle et un fort effet isotopique cinétique du ^{13}C y associé.

De plus, une méthodologie générique de l'étude du ratio $^{13}C/^{12}C$ dans les aminoacides a été développée, ce qui permet une meilleure compréhension du fractionnement isotopique intervenant durant la biosynthèse d'acides aminés.

Une caractéristique supplémentaire de ces travaux est que les données permettent : (i) une comparaison entre les produits naturels et commerciaux, permettant de distinguer ces deux sources, et (ii) une interprétation du modèle isotopique en terme d'origine biosynthétique de composés naturels. Pour le tramadol, il a été possible de proposer un chemin hypothétique pour ce produit naturel récemment découvert.

Mots-clés : Fractionnement isotopique, irm-^{13}C NMR, KIE théorique, produits naturels, plantes, alcaloïdes, acides aminés.

Abstract

The ability to carry out isotope ratio monitoring by ^{13}C NMR spectrometry (irm-^{13}C NMR) gives direct access to position-specific isotope distributions in whole molecules. In this thesis this approach has been developed with the aim of elucidating isotopic fractionation during the biosynthetic pathways in plants of a number of alkaloids (nicotine, tropine and tramadol) that have certain features of their biosynthesis in common.

One key common feature of these compounds is the presence of *O*-methyl and/or *N*–methyl groups. As it is generally found that the $^{13}C/^{12}C$ ratio in the *O*-methyl and *N*-methyl groups of natural products is exceptionally low relative to the other carbon positions in the molecule, the work focused on explaining this phenomenon.

The vast majority of these methyl groups in natural products are derived by the transfer of the *S*-methyl group from L-methionine (L-Met) via *S*-adenosyl methionine (AdoMet). It is shown by irm-^{13}C NMR that in the donor molecule, L-met, the *S*-methyl group is impoverished. The cause of this was investigated by the study of a small theoretical model for the cobalamin-independent methionine synthase, the enzyme responsible for methyl group transfer in L-met biosynthesis. These calculations showed a high energy barrier for methyl group transfer and an associated large ^{13}C kinetic isotope effect.

In addition, a generic methodology to study the $^{13}C/^{12}C$ ratios in amino acids has been developed, which allows insight into the isotopic fractionation occurring during amino acid biosynthesis.

A further feature of the work is that the data allow: (i) a comparison of natural and commercial products, which enables distinguishing between sources, and (ii) an interpretation of the isotopic pattern in terms of the biosynthetic origin of natural compounds. For tramadol, this made it possible to propose a hypothetical pathway for this newly-discovered natural product.

Keywords: isotopic fractionation, irm-^{13}C NMR, theoretical KIE, natural products, plants, alkaloids, amino acids

L'Université Nantes Angers Le Mans